

The
University
Of
Sheffield.

Whole Life Cost Modelling For Railway Drainage Systems Including Uncertainty

by
Yiqi Wu

Thesis
submitted to the Department of Civil and Structural Engineering
University of Sheffield
for the degree of
Doctor of Engineering

Supervised by
Dr Andrew Nichols, Prof. Simon Tait

June 5, 2023

Acknowledgement

First of all, I would like to acknowledge and give my warmest thanks to my supervisors Dr Andy Nichols and Professor Simon Tait who made this work possible. Their guidance and support were very much appreciated; without them I would get lost so many times on this challenging 5 year journey.

Secondly, I would like to thank Engineering and Physical Sciences Research Council and Network Rail for their financial contributions to this study. Also, I would like to give thanks to all Network Rail staff who have shown me great kindness and helped me in many ways.

I would also like to thank my friends Fei, Huan, Pat and Wendy who have been with me through ups and down, and provided me with emotional support in difficult times. Next would be a big thanks towards my cat Orange, she has brought me so much joy and life wouldn't be the same without her.

Last but not least I would like to thank my parents Juying Zhou and Hongzhen Wu, their unconditional love and continuous understanding make me feel safe and belonged, which gives me great strength to face any challenges in life.

Abstract

The UK railway drainage system is facing significant asset management challenges due to the presence of large numbers of assets with long asset life cycles. Maintaining the required asset performance economically and efficiently, while complying with the relevant legislation and regulations is a major concern for Network Rail's asset managers.

The whole life cost (WLC) approach has been developed and implemented in many industries and has proven its usefulness in the management of assets, particularly for assets with long life spans and in situations of uncertain future expenditure. WLC involves estimating the present value of the total cost of ownership over any asset's likely operational life. It is often integrated with decision support tools to enable a more robust decision making process. This has significant benefits in regulated industries in which all expenditure requires clear justification.

This project developed a whole life cost model suitable for railway drainage systems, considering the uniqueness and complexity of costs associated with railway business operations. This WLC model can offer prediction of the transitions of drainage assets condition grades; assessments of drainage system operational performance; and provide realistic estimates of financial requirements in order to achieve desired operational performance; and evaluate the financial consequences due to loss of performance. This WLC model provides the information to build decision support tools that can help Network Rail prioritise drainage maintenance and refurbishment based on available and anticipated budgets and operational risks. This work demonstrated that the whole life cost modelling approach can provide an ideal solution for sustainably maintaining drainage systems while optimising the total cost of ownership and minimising operational, social and environmental impacts.

The developed WLC approach enables asset managers to make decisions both on a strategic and operational level. Strategically, WLC approaches can forecast the overall budget and workload needed to maintain an infrastructure system over its assets' lifetime or a predefined financial period. Tactically, it can provide the asset owner with an optimum renewal, maintenance and utilisation plan under a given risk/cost requirement. This project provides WLC approaches that operate at both a strategic and tactical level for the UK railway drainage system. The methods developed in this thesis are now being implemented by NR into operational practice.

Contents

1	Introduction	9
1.1	Background	9
1.2	Aim	11
1.3	Novelty	12
2	Literature review	15
2.1	Whole life cost model	15
2.2	Decision support tool	20
2.3	Degradation model	25
2.4	Performance model	32
3	Model Framework	37
3.1	Overview	37
3.1.1	Whole Life Cost Framework	38
3.1.2	Model summary	40
3.2	Degradation	42
3.3	Performance	43
3.3.1	Hydraulic performance model	43
3.3.2	Failure modes analysis	44
3.4	Intervention	45
3.5	Penalty	46
3.6	Whole life cost simulation process	47
3.7	Uncertainties	50
4	Drainage Asset Service and Structural Degradation Modelling	51
4.1	Introduction	51
4.2	Methodology	52
4.2.1	The Markov model framework	52
4.2.2	Verification of the Markov Property	53
4.2.3	Development of Transition Rate Matrices	55
4.2.4	Condition degradation Simulation	55
4.2.5	Determine the minimum sample size required	56
4.2.6	Model calibration and validation	56
4.3	Data Processing	57
4.3.1	Condition historical records	57
4.3.2	Data cleansing	58
4.3.3	Further data processing	59
4.4	Case Study	60
4.4.1	Verification of the Markov Property	60
4.4.2	Cohort analysis	62
4.4.3	Estimate condition transition matrices	64
4.4.4	Condition score trajectory simulation	67

4.4.5	Determine the minimum sample size required	68
4.4.6	Minimum Sample Size Required with shorter timeframe	72
4.4.7	Model validation	73
4.4.8	Uncertainty analysis	75
4.5	Discussion	78
4.6	Conclusion	80
5	Hydraulic Performance Model	81
5.1	Methodology	82
5.1.1	Overview	82
5.1.2	SWMM	84
5.1.3	Data sourcing and processing	85
5.1.4	Catchment analysis	87
5.1.5	Model calibration	92
5.1.6	Asset criticality analysis	96
5.2	Case Study	98
5.2.1	Digital replica	99
5.2.2	Catchment analysis	102
5.2.3	Rainfall data	105
5.2.4	Sensor proposition	106
5.2.5	Sensor installation and data collection	110
5.2.6	Model calibration	119
5.3	Conclusion	131
6	Integrated Model Combining Hydraulic Performance Model and Degrada-	
	tion Model	133
6.1	Methodology	133
6.1.1	Rainfall time series construction	135
6.1.2	Selection of simulation number	138
6.2	Case Study	138
6.2.1	Assumptions	140
6.2.2	Scenarios	141
6.2.3	Number of simulations	141
6.2.4	Cases study results	142
6.2.5	Sensitivity testing	143
6.3	Conclusion	147
7	Whole life cost model using hydraulic performance measures	149
7.1	Methodology	149
7.2	Case Study	151
7.2.1	Assumptions and model inputs	151
7.2.2	Results	154
7.2.3	Sensitivity testing	157

7.3	Conclusion	162
8	Whole life cost model using data driven approach	165
8.1	Methodology	165
8.1.1	Failure mode analysis	165
8.1.2	Whole life cost optimisation	167
8.2	Case Study	169
8.2.1	Failure Mode Analysis	169
8.2.2	Whole life cost optimisation	172
8.2.2.1	Inputs and assumptions	173
8.2.2.2	Calculations steps	175
8.2.2.3	Optimisation problem summary	176
8.2.3	Results	176
8.3	Conclusion	183
9	Discussion	185
10	Conclusion	191
	Reference	193
	Appendix	207

1 Introduction

1.1 Background

An important component of a railway's infrastructure is railway drainage assets, which in the UK are designed and maintained by NetworkRail(NR). The purpose of railway drainage is to collect the surface and groundwater that enters and issues from the railway, and transport it to a suitable outfall without causing damage to other assets or causing a risk to the safe operation of the railway. Railway drainage assets consist of the following parts:

- Earthworks drainage
- Track drainage
- Tunnel drainage
- Structures drainage
- Stations, depots and other building drainage
- Third party connections to and from the NR drainage assets

As stated in Spink et al. (2014): “The effective management and maintenance of the drainage asset require knowledge of the asset inventory, its condition, capacity, performance and status”. However, like many other infrastructure owners such as the Water and Sewerage Companies, the Highways Agency, London Underground, Transport for London and other highway authorities, drainage assets are often the least known compared with the other principal asset types. One major reason for this is that the significance of the drainage system in preventing performance reduction of other assets has been overlooked in the past. Drainage assets are often below ground so not clearly visible. Also, for NR, drainage drawings are patchily available across the network and the accuracy and authenticity of the drawings are difficult to verify. This situation has begun to change within the last 10 years with an increase in the acknowledgment of the importance of drainage; NR is in the process of improving its drainage asset knowledge by scheduling surveys and inspections to verify the existing data record and identifying unrecorded assets. NR is carrying out an Integrated Drainage Project to organise and migrate all data into a centralised database, where drainage assets are classified into 39 asset types which are then simplified into 13 inventory groups compatible with CIRIA RP941 (2013) *Transport infrastructure drainage: condition appraisal and remedial treatment*.

The railway network is divided into 14 strategic geographical routes which are supported by five regions (see Figure 1.1). Each route is responsible for its own day-to-day operations. In this way, the routes can work more closely with the relevant train and freight operating companies to better meet the needs of passengers and businesses(*Our routes - Network Rail*, n.d.). 99% of decisions will be made by route teams, while the central strategic departments provide them with advice and guidance. In the UK rail industry, every five years is defined as a Control Period; NR drafts a Strategic Business Plan that is agreed with the regulator and this agreed plan contains the goals and objectives for

the Control Period. For drainage, asset management plans are created with the aim of providing a well-performing system that functions in the most economical and efficient way, whilst not compromising operational safety.

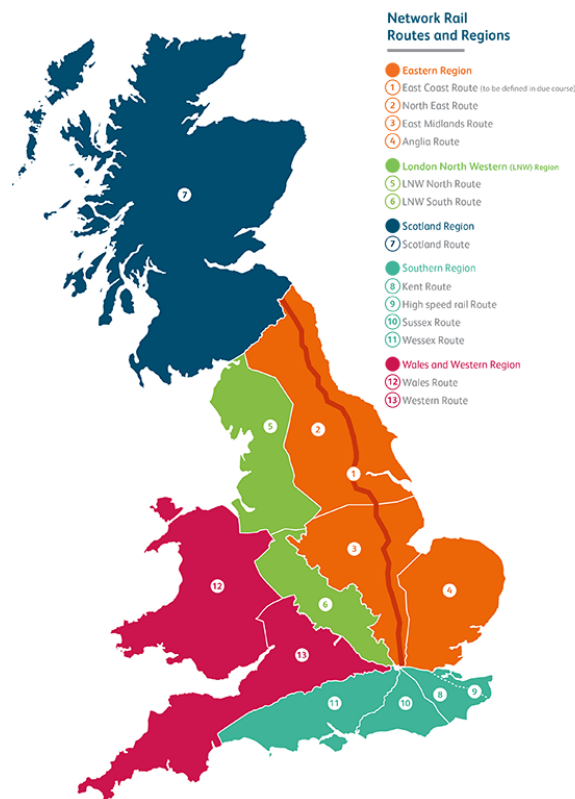


Figure 1.1: NetworkRail Routes

Effective control of water and proper understanding and maintenance of drainage assets is fundamentally important for the safe operation of the rail network (Haines, 2020). It is increasingly recognised that an effective drainage system plays a vital role in the resilience and safe performance of the railway. Inadequate hydraulic capacity will cause unexpected flooding which leads to temporary speed restrictions or temporary closures of railway lines. In the year 2021 alone, there are 3067 hours of delay recorded due to flooding, leading to a compensation cost of 11.7 million pounds. This not only presents safety risks for staff and passengers but also brings severe financial and reputational impacts for NR. Control of water is also important to the management and maintenance of other railway infrastructure (Track, Earthworks and Structures). This is because water plays a crucial role in many degradation mechanisms that affect infrastructure, such as the long-term softening of materials that form the track support system and earthworks (NetworkRail, 2017). An impaired drainage system can result in damage to other NR assets, and disruption to train operations as well as risk to human safety.

Most of the drainage assets are buried underground and are often difficult or very costly to examine, so it is hard for NR to understand the true condition of these assets. Drainage assets can become reduced in capacity or blocked due to gradual accumulation of silt,

debris or vegetation in anywhere from 0.5 to 10 years, as well as unexpected large debris entering the system; so a regular inspection and maintenance scheme is needed to keep the performance of the system at an adequate level. However the majority of drainage assets are composed of hard assets (pipes, channels, chambers etc. made of concrete, brick, stone, earthenware), which typically have a long structural life, in the order of 50 to 150 years, before the physical integrity of the structure is likely to fail and will need to be renewed (Spink et al., 2014). A regular proactive inspection and maintenance regime over a long life span means overall a higher operational cost, which is often limited by budgetary constraints; on the other hand, minimising maintenance expenditure can cause asset life expectancy to be shortened, which could lead to much a larger spending on capital investment. Hence it is important for asset managers to understand the balance between capital renewal and operational maintenance of the assets, and make the most economical decisions considering both the organisation's short-term and long-term objectives. It is both NR's short-term and long-term goal to mitigate operational, environmental, performance, and reputational risks due to drainage asset failure. However, the ability to achieve that goal in the short term is often limited by the available budget and workforce. Hence finding a feasible solution under conflicting constraints is vital for NR's operation.

1.2 Aim

The overall aim of the project is to provide a framework of models that help NR understand and manage its existing railway drainage system. It is NR's objective to maintain a sustainable drainage system while optimising the total cost of ownership and minimising operational, social and environmental impacts. By considering the whole life cost (the total cost of managing an asset over its life) and incorporating it into decision support tools, NR will be able to derive a more effective and economical asset management strategy.

The whole life cost (WLC) approach has been developed over the past 20 years and has been widely used in many industries. To develop a whole life cost model suitable for railway drainage systems, a deeper understanding of its composition and design must be established, as well as an understanding of the unique and complex costs associated with the railway business operation.

The research objectives will therefore be:

1. Provide a framework of WLC that can be applied across the railway drainage network.
2. Analyse the residual asset life and deterioration patterns of existing assets in order to assist maintaining aged drainage assets.
3. Develop a drainage system performance assessment regime so that NR can have a thorough realisation of the impact of poor drainage.
4. Identify high risk / critical drainage assets within the system. This will provide the foundation of a more robust and economic maintenance scheme.

5. Build a decision support tool that can help NR prioritise drainage work based on budgets and risks.

After achieving the objectives, anticipated outcomes & benefits for the stakeholders are:

- Increase asset knowledge — gain in depth understanding of the drainage system’s capacity and performance.
- Budget planning – with a WLC model, the lifetime expenditure is taken into consideration, which will help with overall budget forecasting and allocation.
- Decision support – WLC approach helps asset managers to make comprehensive and robust strategic management decisions for NR’s drainage system.
- Reduce risk – studying the railway drainage system in detail will allow NR to understand its weakness and control, if not eliminate, the risks associated with drainage failure.
- Improve service – maintaining the drainage system at a desired performance level will reduce disruption to train operators and increase the reliability of the railway network for passengers.
- Improve reputation — relationship with neighbours would be improved if there were fewer flooding events, which can be achieved with a better designed maintained drainage system.

1.3 Novelty

The key novelty of our study lies in the development of a framework for the objective examination of different railway drainage asset management strategies. The framework allows for the WLC of drainage asset management to be minimised over different time periods (single or multiple control periods), at different scales and under long-term uncertainties such as climate change. WLC approaches have been adopted in many industries including construction, transportation, and manufacturing. It has not been applied to the railway drainage systems hence this study also addresses this application gap in the field of asset management.

The WLC approach with its supporting sub-models helps NR’s railway drainage asset managers to better understand the performance of their assets, identify assets at higher risk of failure and hence offer the opportunity to use proactive maintenance regimes. This work has the potential to be adopted by drainage stakeholders of other linear transport infrastructure such as highway operators and railway owners in other countries in which piped drainage systems are used to manage rainfall induced runoff.

Due to the complex interlinks in other piped systems such as for water distribution and wastewater disposal, it can be extremely costly to simulate the hydraulic performance of the whole system. However, for rail drainage systems it is relatively simple, as they are often only composed of two or three parallel pipelines alongside the track, and hence require less computational power to be analysed. Hence, this study has the opportunity

to show the full potential of incorporating a complex hydraulic model within a WLC model which is not yet computationally realistic for other piped industries.

Furthermore, the scope of the WLC model developed in this study is both strategic and tactical, providing wide usage across national and route level asset management. On a strategic level, it can forecast the expenditure and amount of works needed for the drainage systems nationally, and prioritise the works based on the risks and/or financial costs of failure associated with the part of the system where the work is carried out. It can help asset managers make national level operational decisions while facing short term budget constraints to work out the optimum budget allocation strategy that best achieves the company's goal. On a tactical level, it can provide WLC calculations for a small portfolio of asset and assess its performance under a range of renewal, maintenance and utilisation option scenarios. This can be used by Routes engineers in their day to day work planning.

2 Literature review

This chapter comprises several sections, providing a literature review of existing research related to whole life cost concepts and the relevant model types that could be integrated to form the Whole Life Cost model. A state-of-the-art review of studies on whole life cost models for infrastructure assets was conducted. This was then followed by a review of the decision support tools used in asset management, some of which are developed based on the whole life cost concept. As the degradation process and the performance of railway drainage assets are crucial aspects (which will be explained in detail in Chapter 3), this chapter also presented a comprehensive review of degradation and performance models for infrastructure assets including drainage and other piped systems.

2.1 Whole life cost model

Whole life cost is the total cost of ownership over the life of an asset. It is also known as life cycle cost (LCC), lifetime cost, through-life-costing, total-life-costing, total-cost-of-ownership, and total cost. LCC was originally designed for procurement purposes in the US Department of Defence in the mid-60s of the twentieth century (Korpi and Ala-Risku, 2008). Since then, the WLC models continue to be developed and deployed in many industrial sectors over the years, with the first attempts made in the construction industry in the mid-1980s (Wieczorek et al., 2019). The WLC approach involves examining and determining all the costs, either direct or indirect, of designing, building and management (operating, maintenance, support and replacement) throughout an infrastructure asset's entire service life including the disposal cost (El-Haram et al., 2002).

In the railway industry, the WLC approach has been used to assist better management planning for various railway assets. Rama and Andrews (2016) proposed a framework for conducting whole system lifecycle cost analysis on railway infrastructure, providing support to asset management decisions in a whole-system context. A whole life cost model was also built for the Overhead Line Equipment underbridge project to provide decision makers with cost estimates for both the installation phase and over the entire service life of such systems, so that they can make more informed management decisions (Kirkwood et al., 2016). For ballasted railway track, maintenance strategies are compared and prioritised with the WLC analysis under uncertainty approach considering all costs associated with ballasted track construction; namely maintenance, de-commissioning, track use, mode change and the environment (Sasidharan et al., 2020a). Various railway ballast tamping and renewal policies were investigated from a whole life cost point of view to better understand their effectiveness (Zhao et al., 2006).

Beside the use in other types of railway infrastructure, the WLC model is also widely appreciated in the UK water industry. Interest in WLC in the water sector first began in the mid 1990s, especially in its potential application to the rehabilitation of underground assets in a regulated sector (Skipworth, 2002).

Skipworth (2002) presented the use of WLC in water distributing systems, and provided

a unique and robust solution to the problems faced by operators aiming to maintain the quality of service with continuously deteriorating assets. The Whole Life Costing Methodology consists of two major themes: “Whole Life Cost Accounting” and “Network Performance”. The WLC accounting framework draws on activity based costing and life cycle analysis to draw out all cost elements and link these to cost drivers (Skipworth, 2002). The drivers are mostly based on aspects of the performance of the distribution network such as bursts and leakage measured by the regulator and which are then quantified by the Network Performance model. The model also quantifies the effect on system performance of different interventions, where an intervention is any action carried out on the network, such as a pipe rehabilitation or replacement. (Skipworth, 2002) then showed how WLC models could help in the decision making process. Information generated by these two themes (“Whole Life Cost Accounting” and “Network Performance”) are consolidated in the decision support tool to simulate management scenarios with limited capital budgets. By testing various strategies with pre-defined intervention options, the solution with the lowest cost can be found using an optimisation technique namely the genetic algorithm.

Fuchs-Hanusch et al. (2011) investigated the calculation of whole life costs for individual pipes. A proportional hazards model was used to make failure predictions at the pipe level and it was amended to fit the requirements of WLC and pipe rehabilitation prioritisation. It was tested on data from three Austrian utilities, along with some sensitivity analysis. Rehabilitation prioritisation with WLC calculations was also discussed.

Shepherd et al. (2004) showed the possibility of using WLC in sewer systems. COST-S methodologies and tools were developed based on the WLC concept to assist management decisions in order to provide acceptable performance at a minimum cost over the whole life of the sewerage system (Savic et al., 2005). Similar to the approach of Skipworth (2002), it is composed of three modules: Network Definition; Whole Life Cost Accounting; and Decision Support Tool. The Network Definition concerns the characteristics of the sewer system and its performance, which is quantified via Key Performance Indicator (KPI) values. The Whole Life Cost Accounting module links the costs with the range of activities required to maintain the provision of the service using an activity based costing approach. Finally the Decision Support Tool links the performance based cost drivers to the KPIs as well as the cost of rule based management intervention strategies that can be adjusted over different time periods, allowing different scenarios to be investigated and compared.

A report on whole life costing for sustainable drainage was produced by *Whole Life Costing for Sustainable Drainage* (2004). It provided a brief background of sustainable drainage in England and Wales, and introduced a Whole Life Costing approach suitable for evaluating the costs and benefits associated with sustainable drainage systems, followed by a case study of a SUDS scheme in Worcestershire, UK. The whole life cost framework accounted costs including planning costs, capital costs, land-take costs, residual costs, environmental benefits, operation and maintenance, and disposal costs. It is

noted that not only the conventional monetary costs that contribute to the cash flow of the drainage system owner are counted, non-monetary costs such as environmental and social costs due to flood and pollution events are also included in the calculation. This was designed to enable sustainable concepts to be fully incorporated at the design stage.

Whole life cost framework

In order to build a whole life cost model, it is important to establish a framework of the WLC that identifies all the cost elements associated within the lifetime of the assets. While there are existing studies on WLC for railway assets, there is a lack of literature specifically focused on WLC frameworks for railway drainage assets. However, it would be valuable to explore how WLC frameworks have been designed for other infrastructures such as different railway asset systems (e.g. embankment, track and signalling). These WLC frameworks can potentially be adopted to form the foundation of building a WLC framework that is tailored for the railway drainage assets.

Usually, elements of whole life costs arise from different stages of a product’s life cycle, which are often divided into three or four phrases based on the individual assets/product’s perspective (Korpi and Ala-Risku, 2008). Fabrycky and Blanchard (1991) used a four-step division to categorize the costs of an individual product as shown in Figure 2.1.

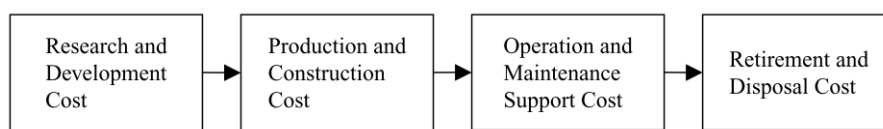


Figure 2.1: Life cycle cost categories

Expanding upon the fundamental four stages, additional cost components can be included to cater to the requirements of specific industries being studied. The elements of whole life cycle and life cycle cost for the building industry were established and presented by (Wieczorek et al., 2019). A list of the cost elements and their linkages are shown in Figure 2.2, such definitions are adopted from *ISO 15686-5:2008 - Buildings and constructed assets — Service-life planning — Part 5: Life-cycle costing* (2008).

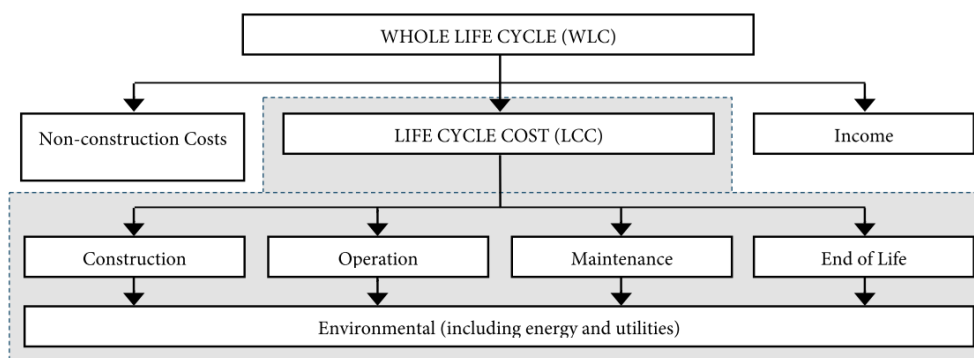


Figure 2.2: Elements of whole life cycle and life cycle cost of a building

Similarly, a flow chart of the Whole Life Cycle Costs of ballasted railway track was also adapted from *ISO 15686-5:2008 - Buildings and constructed assets — Service-life planning — Part 5: Life-cycle costing* (2008) by (Sasidharan et al., 2020b), as presented in 2.3

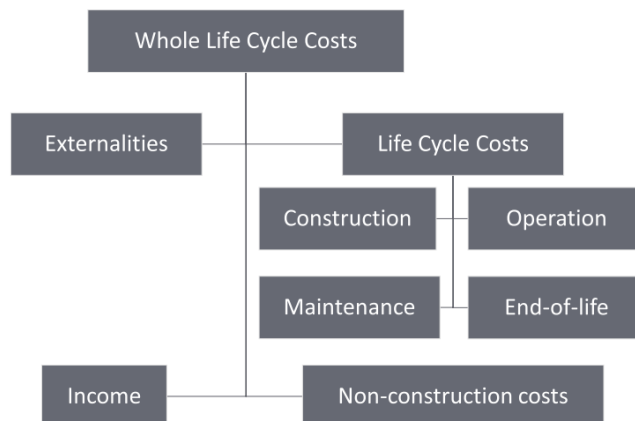


Figure 2.3: Elements of whole life cycle and life cycle cost of railway track

Rama and Andrews (2016) developed a LCC model for the railway infrastructure assets adopting the methodology proposed in IEC (2004). Figure 2.4 presented the generic framework for modelling infrastructure LCCs, which consists of the state model and the cost model. Performance of the infrastructure assets is estimated using the state model, considering the effects of changes in individual asset on other assets and subsequently on the infrastructure as a whole. The outputs of the infrastructure state model are then fed into the costs model to evaluate the LCCs.

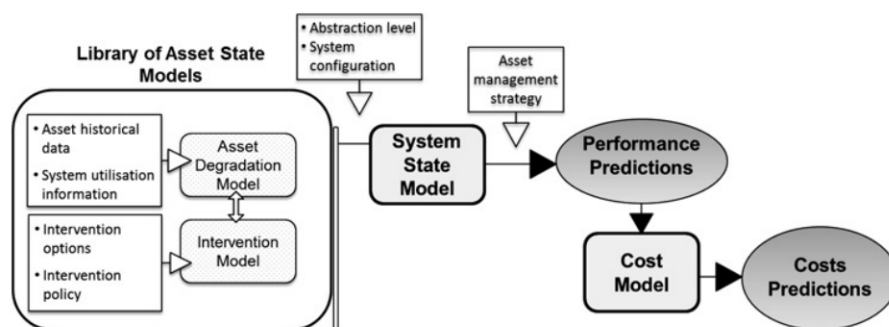


Figure 2.4: Overview of the Whole life cost framework for railway infrastructure asset

A more detailed framework tailored for the assets under investigation is presented in Figure 2.5, namely the superstructure and individual assets (sleepers and rails). Individual LCC cost elements are identified and the breakdown of the system to lower indenture levels, cost categories (e.g. labour, materials) and lifecycle phases are also specified. The

cost elements are then aggregated to form the LCC in accordance with the cost breakdown structure.

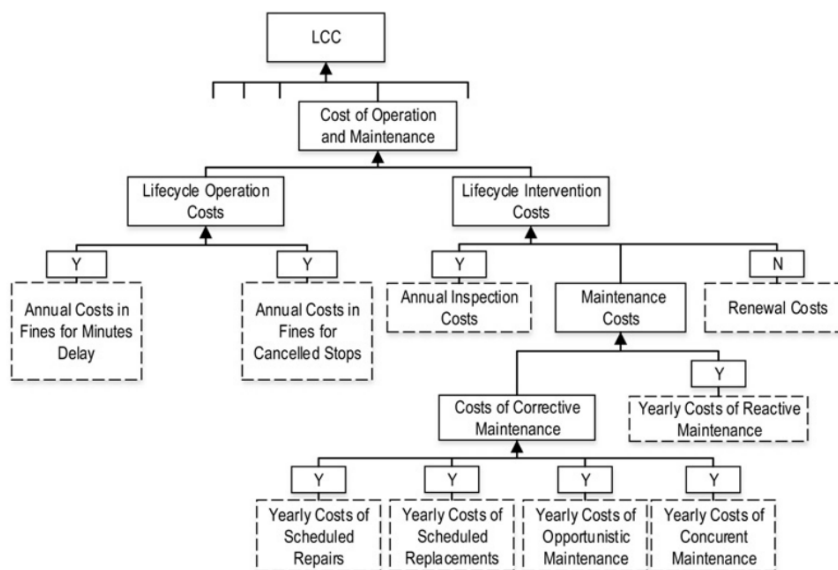


Figure 2.5: LCC breakdown structure used for railway infrastructure asset

Although Rama and Andrews (2016) established the whole life cost framework for railway infrastructure assets, the technical aspects of railway drainage assets were not discussed in the paper. This may be because the importance of the railway drainage assets was overlooked, and/or the effect of impaired drainage assets on the performance of other railway assets and the whole infrastructure system was not fully understood. There is a gap in the study which would be addressed in this study. The WLC framework presented for other railway infrastructure systems can also be potentially adopted for the railway drainage assets.

Activity based costing (ABC) was developed in the 1980s Harvard Business School Professors Kaplan and Cooper (Skipworth, 2002), and suggested to be brought into the life cycle cost analysis by (Emblemsvag, 2001) as a substitute of the alternative to conventional costing systems. ABC establishes links between activities and products by allocating activity costs to activities to products based on an individual product's consumption or demand for each activity (Korpi and Ala-Risku, 2008). This approach enables a better understanding of the nature of indirect, overheads and general cost items and what drives them as they are often not directly tied to the production volume. For some industries, ABC may be hard to adopt due to the complexity of business and difficulties in obtaining an extensive activity-cost databases. However, it would be useful when analysing assets with a long life span such as pipes. These assets are less likely to be replaced in a short time interval, hence the drivers of the whole life cost elements are more likely to be tied up to operational activities rather than the construction and disposal of assets.

For the water distribution industry, an activity based whole life costing framework was

developed, the links between the actions, their effect on the system and its subsequent impact on costs are shown in Figure 2.6. For every action, its resultant cost is calculated and its impact on performance is evaluated. These connections allow each element to be treated as a variable, so that their corresponding influences can be observed and analysed (Engelhardt et al., 2003). The same methodology has also been adopted for sewer systems (Shepherd et al., 2004). Similar to the water distribution systems and the sewer networks, the majority of the railway drainage systems are also composed of buried piped systems, but usually with a less complicated design, hence, it is proposed that it is reasonable for a similar WLC framework to be adopted for the railway drainage assets.

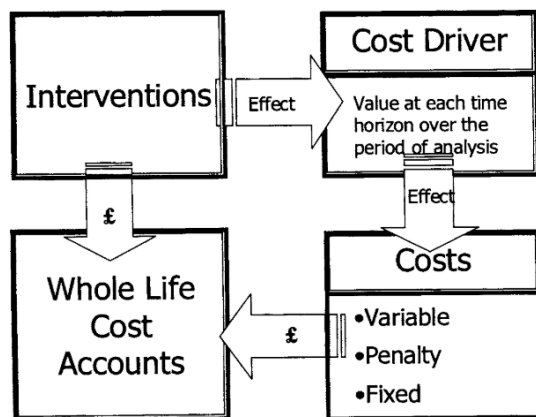


Figure 2.6: The linkage within the WLC methodology of water distribution system

2.2 Decision support tool

The aim of the decision-making process is to identify the course of action that will most benefit the asset system’s state and performance within pre-determined economic, time, and resource constraints (Allouche and Freure, 2002). Asset managers are seeking optimum management strategies that maintain acceptable network-level performance while reducing operational costs (Luque and Straub, 2019; Balekelayi and Tesfamariam, 2021). They bear the responsibility of making tough decisions that frequently have long-term, potentially critical impacts on their organization and/or its stakeholders. Hence, the need of decision-support tools has emerged, as they can help enhance the precision and validity of these decisions (Ana and Bauwens, 2007).

For railway track infrastructure, Sasidharan et al. (2022) presented a risk-informed decision support tool that can provide economical justifications for asset management strategies, taking into account the infrastructure maintenance costs, train operating costs, travel time costs, safety, social and environmental impacts over the assets’ life cycle. The risk-informed capability of the tool enables asset managers to deal with uncertainties associated with forecasting costs and the effects of track maintenance, and the unavailability of data. In the process of resolving real-world issues, one might encounter both imprecision and uncertainty. Monte Carlo simulation combined with the Fuzzy logic algorithm, enabled the use of less precise linguistic expressions, capturing expert opinion for

evaluating the impacts/severity of train derailments. Data from three different routes of the UK's railway network were used as a case study. Results illustrated that this method can aid both strategic and tactical railway asset management, providing plausible design and optimal maintenance tactics within a given budget.

For buried piped systems such as sewer networks, a review of selected decision-support tools was presented by Ana and Bauwens (2007). Figure 2.7 illustrates the tools discussed and the steps they addressed within the infrastructure asset management system.

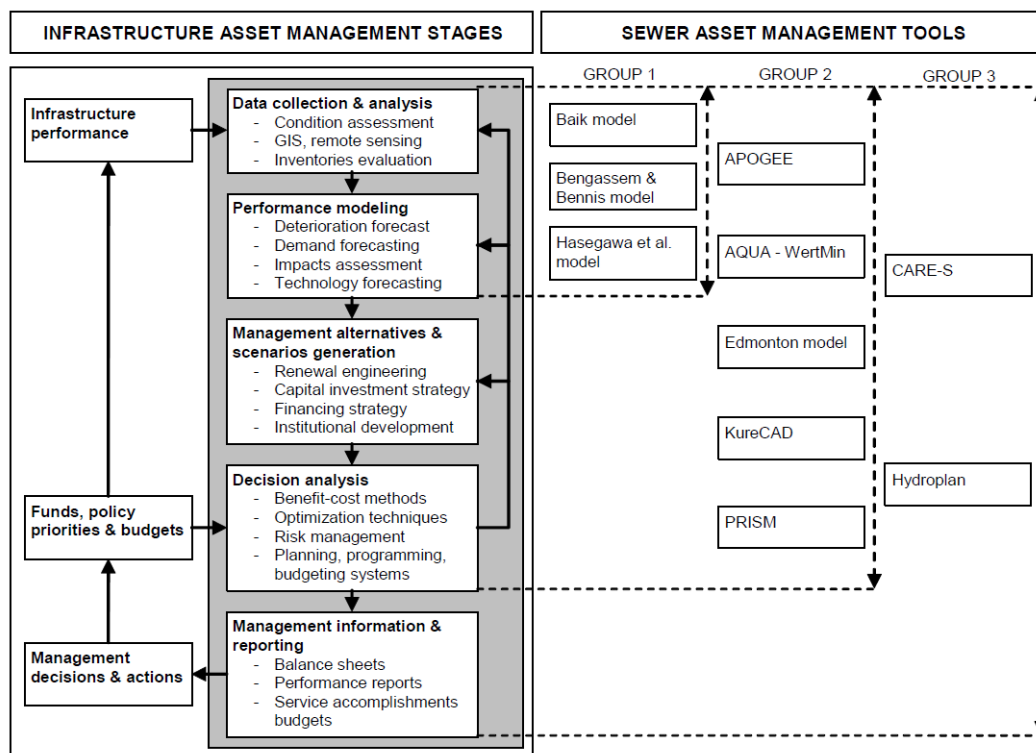


Figure 2.7: The generic infrastructure asset management system with the corresponding sewer asset management tools applicable at different stages (Ana and Bauwens, 2007).

As Group 1 tools mainly model asset deterioration/performance, they can not provide a review of the management options available. They can only be used as part of the decision making process to evaluate the asset status under a given assumption and without intervention. Whereas group 2 tools provide certain levels of decision making analysis based on performance calculated from the collected asset data. Group 3 tools are the most comprehensive ones that cover all aspects of the asset management system. The two group 3 tools reviewed are CARE-S (Computer-Aided Rehabilitation of Sewer Networks) and Hydroplan.

CARE-S is a decision-support tool developed by Sægrov and Schilling (2002) that helps determining the best strategies for rehabilitating sewer networks, considering all crucial influencing factors such as anticipated structural failures, hydraulic performance, and pollution discharges. The method incorporates the existing condition of the sewer and

storm water networks, as well as forecasts of their long-term functionality on both a comprehensive network scale and an individual pipe scale. This procedure also provides visualization of the economic and non-monetary implications of any selected rehabilitation strategy.

Hydroplan is a sewer asset management approach proposed by Gueldre et al. (2007) based on structural, hydraulic and environmental risk assessments carried out on the strategic elements of the sewerage network. The procedure starts with building an asset inventory of the existing conditions and historical data, followed by a pipe-level strategic analysis where pipes are evaluated based on the potential damage they might cause if they were to fail. This assessment includes financial, social, and environmental damage factors. Weighting factors are then applied to these scores to assign an overall strategic level to each sewer. Subsequently, failure probabilities of sewers are calculated based on the structural condition (using aging models like Herz distribution and inspection outcomes) and hydraulic and ecological factors (employing calibrated hydrodynamic models such as InfoWorks). The results of the strategic analysis and the failure probabilities are then integrated to generate an overall risk score. The most critical assets are highlighted and tailor-made solutions are proposed to decrease the risk. This provided a short to medium term action plan that would take the network to a higher performance level. For long-term management plans, software was developed (Hades), which uses total life cycle modelling with Monte Carlo simulations and integrates all costs by monetising the risks and preventive investments.

Although it would be ideal to develop a stand-alone software for the railway drainage asset management decision support tool, similar to the ones developed for the sewer system. In practice, integrating all modules of a whole life cost model into one software can be complex, especially when dealing with data sourcing issues as the asset data and failure records are fragmented. However, a framework for the decision support tool could be established in this study to provide guidance for further studies and software development.

Another example of the application of decision support tools in asset management of sewer networks is demonstrated by Tran et al. (2010) with a case study Australia. The study proposed a proactive management methodology for sewer assets through decision support tools. The paper reviewed several models which addressed various issues in sewer asset management, including condition prediction, risk ranking, selection of repair methods, and cost-benefit analysis. In addition to conventional modelling methods like Markov chain and statistical regression, novel artificial intelligence-based models such as artificial neural networks and support vector machine has also been brought to attention. These models can be helpful in prioritizing sewer network inspections, justifying budget distributions, and conducting asset evaluations for financial analysis. A conceptual framework was proposed for the effective and efficient management of the sewer network asset, as shown in Figure 2.8. The database is the centerpiece of the framework, storing all the physical and operational data related to the network. These data are used

in a variety of decision support models to provide multi-dimensional information that is critical for making management decisions. Decisions then can be made to meet the prescribed network performance measurements such as the serviced volume and number of service failures. It is suggested that an additional data collection step be made after the decision-making process to enhance and validate models. Although the case study in the paper mainly focused on the structural degradation of cement-based sewers and manholes, the discussed modelling techniques could be adopted for other infrastructure assets and a more comprehensive list of performance measurements.

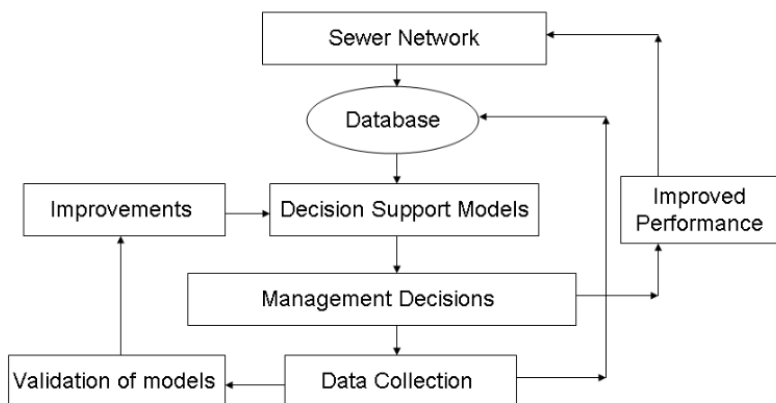


Figure 2.8: Conceptual framework for the application of decision support models for sewer system asset management

A survey exploring municipal infrastructure asset management needs in Canada indicated that a significant 91% of respondents acknowledged a need for decision support tools to manage their assets; 24% specifically pointed to Life cycle cost analysis (LCCA) as a potentially useful tool for decision support; and 70% of those surveyed believed that the LCCA process could assist in decreasing the substantial backlog of deferred maintenance (Rahman and Vanier, 2004).

Life cycle cost approach has already been applied in the railway industry to assist asset management. Rama and Andrews (2016) employed life cycle cost as a tool to guide well-informed decisions in railway infrastructure asset management. Choices regarding asset management were driven by monetary criterion alongside infrastructure performance objectives. A generic framework for decision support in infrastructure asset management is proposed, as shown in Figure 2.9. The framework consists of two major models namely the system state model and the cost model. The infrastructure system state model estimates performance parameters, taking into account the impact of individual asset's condition degradation on other assets and the entire infrastructure. The condition degradation may be influenced by specific actions including inspection, testing, servicing, repair, renewal, and upgrade, which will consequently affect the performance parameters. These actions are determined by the asset management strategies chosen. These outputs from the system state model are then incorporated into the cost model to assess the life cycle costs.

The use of the modelling framework was illustrated in a case study examining track superstructure performance over a 60-year period under varying intervention strategies. The resulting infrastructure performance and life cycle cost indicated that a combination of opportunistic and concurrent maintenance strategies yields the most substantial benefits in terms of cost savings, reduced overall downtime of the line, and a minimised duration of speed restrictions. However, this is a generalised model and the case study mainly focused on the track superstructure. In order to adapt it for the railway drainage system, a detailed discussion of deterioration mechanisms and performance measurements specific to the railway drainage assets is required.

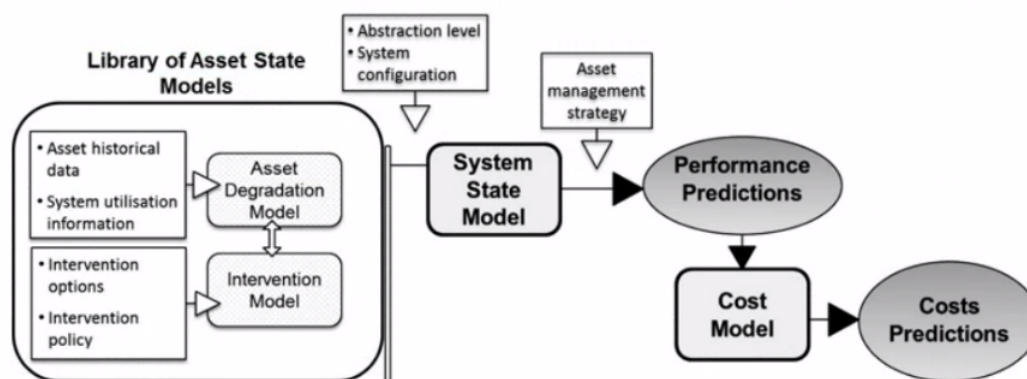


Figure 2.9: Generic framework for decision support in infrastructure asset management

Maharjan et al. (2009) developed a whole life (staged) cost optimisation tool based on the hydraulic performance of the urban storm drainage system. A one dimensional hydraulic model is combined with a genetic algorithm based optimization tool to determine optimal intervention timings and responses over a simulation period. Storm Water Management Model (SWMM) is used as the hydrologic/hydraulic simulator to evaluate the hydraulic performance of the drainage network. The objective function of the optimization scheme is the minimisation of the whole life cost. The whole life cost component and the hydraulic simulator are integrated using interfacing code written in C. The conceptual diagram of the model is presented in Figure 2.10 (Maharjan et al., 2009). The model was applied in a case study area in the city of Porto Alegre, Brazil, to determine staged intervention strategies for urban storm water systems subjected to gradually changing external factors like climate change, demographic and land use changes, etc. The detention storage implementation schedule is optimised using an objective function of the total cost which consists of the cost of interventions and residual flood damages. The results showed that significant financial savings and enhanced flood safety could be realised by approaching the design problem as a staged plan, rather than a one-time scheme. This provided a basis for proactive decision making in a changing environment.

The methodology developed by Maharjan et al. (2009) is quite suitable to be adopted in the railway drainage system as they share some similarities. This is because the

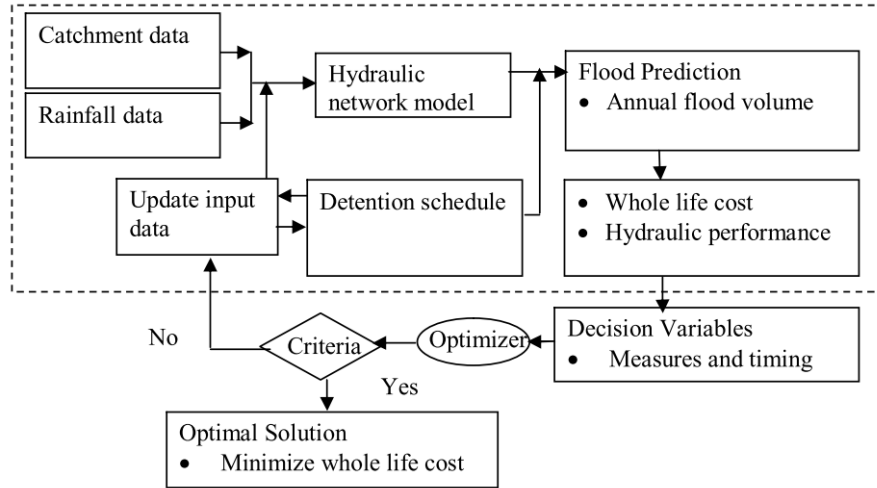


Figure 2.10: Conceptual diagram of whole life cost optimisation model for urban storm drainage systems

main purpose of the storm water systems is to drain excess rain and ground water from impervious surfaces, whereas the the main purpose of the railway drainage systems is to drain excess rain and ground water from other railway assets (NetworkRail, 2017). Since they share the similar function, the way their performance is evaluated may also be similar.

2.3 Degradation model

Drainage assets degrade over time due to various reasons such as debris, aging, corrosion and pressure, which can lead to a loss of performance and even worse, a loss of functionality. Deterioration models are built to simulate the degradation process of assets. They can be split into service deterioration models and structural deterioration models according to the different causes of decline in serviceability. Structural deterioration of pipes is the continuing reduction of hydraulic load bearing capacity, which can be characterized through structural defects (Tran et al., 2009a), whereas service deterioration is the reduction in serviceability for other reasons such as accumulation of debris. In order to forecast future degraded conditions, predictive models are developed incorporating various factors such as pipe size, age, and soil type (Tran et al., 2007).

Deterioration models can be divided into three categories: physical, statistical, and machine learning (ML) based models (Aljafari et al., 2022). Physical models are derived from mathematical relationships based on the understanding of the physical phenomenon of deterioration; whereas statistical deterioration models are built on relationships between deterioration observations and factors that influence the deterioration process, where one or more of these factors are treated as random variables (Rokstad and Ugarelli, 2015). Although physical models may be scientifically more robust, insufficient understanding of the physical deterioration process and scarcity of the data has limited the development of the physical models (Kleiner and Rajani, 2001). Another limitation of the physical

models is that they require relatively large amounts of specific types of data that are often difficult to obtain due to time and financial constraints (Kimutai et al., 2015). In cases where a large number of assets is to be examined but there is not enough manpower to carry it out, or the low likelihood of failure does not justify the expensive data acquisition expenditure, statistical models could provide a more economical and efficient solution.

For both the physical and statistical models, they can be classified into deterministic and probabilistic models (Rajani and Kleiner, 2001). Deterministic models produce the same exact results for a particular set of inputs, whereas stochastic models analyse input data and then give predictions that account for certain levels of unpredictability or randomness. In practice, for deterministic models, the assets analysed are partitioned into groups to form a homogeneous cohort with respect to other factors that might influence the asset deterioration rate, such as operational and environmental parameters (Kleiner and Rajani, 2001). This enables the model to give more accurate predictions based on a small set of input parameters.

Physical Models

One example of the physical deterministic models is the linear model developed by Randall-Smith et al. (1992). It estimates the remaining residual life of water mains, assuming that the corrosion pit depth has a constant growth rate. However, The assumption of a constant corrosion rate over the life of the pipe is questionable (Rajani and Kleiner, 2001). Rajani and Makar (2000) developed a methodology to predict the lifespan of grey cast iron water mains considering both the influence of corrosion pits on the structural resistance capacity of water mains and changes in anticipated corrosion growth pit rates. When there is a lack of historical corrosion rate data, it is suggested to take measurements of the dimensions of corrosion pits using non destructive technology, and then use these measurements to approximate the corrosion rates with a Rossum-like (Rossum, 1969) power model. However, the main drawback of this model is that it relies on corrosion pit data that may not be easily obtained due to economic or operational reasons. The model's dependence on corrosion rate measurement from direct pipe inspection makes the model expensive to implement (Wilson et al., 2017).

Probabilistic physical models have also been developed over the years to capture the randomness in the physical deterioration process. (Davis et al., 2007) developed a model to predict the failure of polyvinyl chloride (PVC) pipes due to cracking caused by inherent defects in the pipe wall. The model makes predictions of time to brittle fracture for pipes with internal defects subject to combined internal pressure and soil deflection loading together with through-wall residual stress. To include uncertainty in the failure process, the inherent defect size is treated as a stochastic variable, which is modeled by the Weibull probability distribution function. As PVC is a relatively recent pipeline material and typically decays slowly, its long-term deterioration mechanisms remain poorly understood. Davis et al. (2007) made the first attempt to fill this knowledge gap. The probabilistic structure of the model is beneficial as it factors in the uncertainty associated with inherent defect sizes. However, the use of the Weibull distribution for defects

is based on Australian data, hence it would require validation when applying the model to other locations (Wilson et al., 2017).

Wang et al. (2022) studies the corrosion degradation of pipelines using a physical model and a probabilistic method. The natural metal loss characteristics of corroded surfaces are modeled with random fields. The corrosion growth is also captured using a probabilistic framework by combining Bayesian inference and Markov Chain Monte Carlo. However, in line inspection data is required to update the failure probability of corroded pipelines, which is not always possible to obtain.

However, all these physical models require a very thorough understanding of assets' current physical status and detailed measurements of the asset's physical characteristics which are not present in NR's drainage asset database. Although physical deterioration might be simulated accurately using the deterministic models in a controlled environment, the asset deterioration process may have a high level of uncertainty associated with "external conditions" (Aljafari et al., 2022), and the asset condition degradation may vary widely and is generally not captured by available data (Korving and van Noortwijk, 2008). Therefore, statistical models may be used to incorporate many more possible factors that might relate to the asset degradation process.

Statistical Models

A statistical model that gives deterministic predictions for pipe breakage was developed by Shamir et al. (1979). Non-linear regression analysis was performed to obtain the pipe break prediction model that relates a pipe's breakage to the exponent of its age (Yamijala et al., 2009). Enhanced time exponential models were sequentially developed by the following researchers: Walski and Pelliccia (1982), Clark et al. (1982) and Yamijala et al. (2009). Additional factors were added to the set of deterioration equations to improve model accuracy, such as asset installation date and asset historical failure records. These models are simple and relatively easy to implement, but their simplicity requires additional data pre-processing where data are segmented carefully into homogeneous groups (Kleiner and Rajani, 2001). Also, this type of model usually simulates a specific type of asset failure that is unique to a particular industry and hence may not be suitable for railway drainage asset failures. They also do not indicate the impact of deterioration on specific assets, but on assets within a defined group or type.

König (2005) presented a computer software package ExtCorr, which estimates the external corrosion of concrete pipes with a linear model, considering asset characteristics such as age, diameter and wall thickness, as well as the environmental parameters such as soil type and groundwater depth. However, drainage asset failure mechanisms can be very complex as they are the result of interaction among numerous factors with randomly occurring damage propagation (Aljafari et al., 2022). Such randomness and uncertainties in the degradation process may be better explained with a probabilistic model.

A probabilistic, statistical model to predict the breakage patterns of individual pipes was developed using the non-homogeneous Poisson process (NHPP) (Constantine and

Darroch, 1993; Jarrett et al., 2003; Kleiner and Rajani, 2010). In particular, the NHPP model developed by Kleiner and Rajani (2010) not only considered the static factors (i.e., pipe-intrinsic) but also the dynamic factors (e.g., climate, cathodic protection, breakage history). The model was trained on 40 years of historical breakage data and forecasted for the next 5 years. While the prediction of the total number of breaks per year was good, it tends to overestimate the break numbers for pipes with a few historical breaks and underestimated those with a high history of breaks (Kleiner and Rajani, 2010). The model is designed for the breakage of pipes in the water distribution system, since the failure type and failure mechanism would be different for railway drainage systems, it would not be suitable to be adopted in this study. Also, the model requires a good, sizeable record of the failure incidents which might not exist for the railway drainage system. This is because not all railway drainage failures are recorded as an incident, for example, if a section of the railway was flooded due to a collapsed pipe but the flooding happens at a time when no train was running on that section, the flooding will unlikely to be spotted, and even if it is observed, it does not qualify as an incident as it won't affect business operation.

Among the existing statistical models used to predict sewer pipe deterioration, many are designated as survival models (Baur and Herz, 2002; Bruaset et al., 2018; Duchesne et al., 2013). Herz (1996) proposed a lifetime probability distribution density function to model the life span of pipes, which is based on the principles that had originally been applied to population age classes or cohorts. For better prediction results, it is proposed to divide the pipes into homogeneous groups (cohorts) with respect to their material type and environmental/operational stress class. The model is hence called the cohort survival model and the estimation of parameters was done using historical data where the time of pipe replacement was considered to be the time of its "death" (Kleiner and Rajani, 2001). In the absence of historical data, a Delphi process was proposed by Deb and Foundation (1998) to estimate the parameters in the cohort survival model. The model's application is weakened by the assumption that the replacement of an asset by the asset owner represents the end of its lifespan, as the decision can be influenced by operational factors rather than objective technical assessments (Kleiner and Rajani, 2001).

The proportional hazard model (PHM) was first proposed by Jeffrey (1985) to be used for the prediction of water main breakages by examining the probability of the time duration between consecutive breaks. The method has then been improved and implemented by other researchers (Andreou et al. (1987), Le Gat and Eisenbeis (2000), Fuchs-Hanusch et al. (2011), Xie et al. (2017) and (Xu and Sinha, 2020) amongst others) to predict pipe failures. Fuchs-Hanusch et al. (2011) used the Proportional Hazards Model (PHM) to forecast the annual number of water supply pipe failures, which then provided means for calculating the failure costs in the whole life cost calculations. Xie et al. (2017) used PHM approach to model the risk of blockage for clay pipes considering not only established parameters such as pipe age, length, diameter and soil type, but also new explanatory variables such as proximity to roads, land use code and road type. The study was carried out with blockage data from 43,976 vitrified clay pipes spanning seven

years in Australia. The Weibull proportional hazards model was adopted by Xu and Sinha (2020) to analyse pipes' mean time to failure using historical pipe break records (Aljafari et al., 2022). The duration that an asset remains in a certain condition until it moves to a worse condition category was presented by a survival curve. Xu and Sinha (2020) identified the main limitation of the model is the missing data points in historical records which would also pose a major concern when applying to railway drainage assets. The proportional hazards model is valued for its robustness, versatility, and ability to incorporate multiple variables. However, the model would assume that all asset types are equally affected by environmental and operational stresses which is not always valid. Hence, it is best to segregate the assets into groups that share the same aging process through careful analysis.

Nevertheless, the Markov approach is a common probabilistic statistical model for simulating infrastructure deterioration. Markov models operate on the assumption that the present state of the asset encompasses all relevant information impacting its future conditions. Therefore, the future state of the asset depends solely on its present condition (Aljafari et al., 2022). There Markov models categorised into two types: the homogeneous Markov model, which are time independent, and the non-homogeneous Markov model, which are time dependent, i.e. the transition probabilities relate to the age of the asset, so older assets are believed to deteriorate faster (Ana and Bauwens, 2010).

The homogeneous Markov model has been widely used for modelling pipeline asset deterioration process, such as sewers (Wirahadikusumah et al., 2001; Baik et al., 2006) and stormwater pipes (Wirahadikusumah et al., 2001; Meegoda et al., 2004). Wirahadikusumah et al. (2001) proposed a Markov model to capture the deterioration of Indiana sewers. They have applied a nonlinear optimization-based approach to derive the transition probabilities, minimizing the absolute distance among the condition data and the expected value obtained from the Markov model. As age was the only considered predictor of the sewer condition, pipes have to be classified matching the groups with the same deterioration behaviours. 16 sewer categories were defined but reliable data were only available for 4 groups, limiting the scope of the modelling.

A study was performed by Baik et al. (2006) to explore sewer deterioration in the city of San Diego, California using a Markov model. They have derived the transition probabilities using an ordered probit model approach, based on sewer age and condition data and covariates like pipe physical properties. In comparison to the nonlinear optimization-based approach for transition probabilities estimation, they have claimed that their approach was both theoretically and statistically more robust. However, to ensure the accuracy of the model, it is essential to get panel data spanning over multiple time periods. Also, information such as the groundwater level, the soil condition, the depth of the installation, and the frequency of sewage overflows need to be collected and properly evaluated. Such information is often not available in current inspection practices which could be a major limiting factor.

Micevski et al. (2002) demonstrated a similar application on the stormwater pipes in an

Australian network. In this analysis, they have used the Metropolis–Hastings algorithm to estimate the transition probabilities from sewer condition and age data. Like Wirahadikusumah et al. (2001), pipes are divided into categories according to pipe diameter, material, and soil type. The model was validated using the Chi-square goodness-of-fit test and results have confirmed its suitability to model the deterioration of stormwater pipes at 5% significance level. A similar methodology may be adopted for the railway drainage assets.

An example of the non-homogeneous Markov model is presented by Le Gat (2008), modelling the deterioration of urban drainage infrastructures with a case study of Dresden sewer network in Germany. The time dependent transition probabilities of the multi-state deterioration process are derived from condition data using Gompertz distribution. The transition probabilities were dependent on the values of a set of covariates (e.g. pipe diameter, type of effluent), and a pipeline specific random frailty factor. The advantage of the model is that by incorporating pipe specific covariates, the model is able to predict directly the deterioration of individual pipes without the need to divide the assets into homogeneous groups like Wirahadikusumah et al. (2001). Despite this, the methodology still suffers major challenges due to the scarcity of data and the effect of selective survival bias (Ana and Bauwens, 2010).

In contrast to the assumption of Markov chain models, where the time in one state before transitioning to another follows an exponential distribution for continuous time, semi-Markov models can apply any continuous-time distribution to represent the time (Thomas and Sobanjo, 2013). Semi-Markov processes have been developed and used in deterioration models for piped systems as well as many other infrastructure assets such as flexible pavements (Thomas and Sobanjo, 2013) and bridges (Ng and Moses, 1998; Sobanjo, 2009). In Liang et al. (2023)’s paper, the fatigue degradation of the piping was described by a homogeneous time-continuous Semi-Markov process, which allows accounting for generic distributions of the holding times of the system states. Kleiner (2001) proposed the use of Semi-Markov models for simulating the deterioration process of large infrastructure assets such as water transmission pipes and trunk sewers. The possible conditions of the asset were categorised into condition states and the waiting times between each state were modelled using a two-parameter Weibull distribution. Kleiner (2001) presented the model with a case study of five hypothetical large-diameter water mains. The mean time-to-failure was determined to be approximately 60 years, with most failures occurring between 40–90 years. The method was also adopted by Altarabsheh et al. (2016) to estimate the transition probability of the sewer pipes as a function of time. The model is capable of dealing with uncertainty in the deterioration process from the beginning of the asset cycle using age-dependent transition probabilities. However, Kleiner (2001) pointed out that currently there is insufficient deterioration data to determine the parameters of the waiting time probability distributions. Although a procedure was proposed to determine the parameters based on expert opinion, further studies in this area are required (Wilson et al., 2017).

Although Markov models have not been applied to railway drainage assets before, their usefulness has been proven in modelling the deterioration of other railway infrastructure. Moghtadernejad et al. (2021) used Markov chains for the estimation of deterioration curves of railway bridges and retaining walls, and addressed the challenges that normally exist when dealing with real-world data. Le and Andrews (2013) presented a Markov modelling approach for predicting the condition of individual railway bridge elements. The degradation process is analysed using maintenance records and the duration it takes for each element to degrade to a level where maintenance of a certain severity classification is required. The deterioration process created by the irregularities in sections of the track was analyzed in the form of a Markov stochastic process by Bai et al. (2015).

Machine learning models

Machine learning (ML) and artificial intelligence (AI) techniques offer an alternative modelling strategy, particularly when the inherent bias and scarcity of inspection datasets hinder the development of statistical models (Tavakoli et al., 2019). Examples of pipe deterioration modelling with AI methods include neural networks (Najafi and Kulandaivel, 2005; Tran et al., 2006, 2009b; Khan et al., 2010), Bayesian networks (Jung et al., 2012), support vector machine (Mashford et al., 2011) and random forests (RF) (Jung et al., 2012; Harvey and McBean, 2014; Tavakoli et al., 2019).

A random forest model was developed by Harvey and McBean (2014) to predict individual sanitary sewer pipe conditions in Guelph, Ontario, Canada; achieving a satisfactory true positive rate of 82% and true negative rate of 73%. The model facilitates the identification of uninspected pipes in a sewer network that are most likely to be structurally defective, thereby guiding decisions about potential future inspections. Similarly, Tavakoli et al. (2019) used the random forest model to predict sewer pipe conditions for a dataset from the City of Los Angeles, California. The model demonstrated 99.99% in-sample accuracy and 94.06% out-of-sample accuracy. Although the results of the random forest models are good, their applicability to different datasets was not tested. The absence of crucial asset characteristic data may limit the model's ability to predict asset conditions.

Neural networks are particularly effective in dealing with data that has high volatility and non-constant variance. Tran et al. (2006) used neural networks to predict the condition of stormwater pipes and Najafi and Kulandaivel (2005) used them on sewer problems. The probabilistic neural network model developed by Tran et al. (2006) is tested with snapshot-based sample data and compared with a traditional parametric model using discriminant analysis. Results show it slightly outperforms others in terms of prediction performance, however the accuracy of the model is still not high and the key factors for prediction are difficult to interpret.

Aljafari et al. (2022) developed data-driven models for predicting the condition of drainage pipe assets using machine learning algorithms. Four ML algorithms are tested and compared, namely neural networks, decision trees, bagged trees, and k-nearest neighbour. Predictions were performed for both the structural and service condition of the UK rail-

way drainage assets. Results showed that bagged trees outperformed the other algorithms on a balanced dataset, yielding an overall accuracy of 87% for structural condition prediction and 72% for service condition prediction. Out of the nine influencing factors examined using connection weight analysis, pipe length, prior condition, years since last condition assessment, and maintenance history were found to be the most significant factors in condition prediction. While this model was developed specifically for UK railway drainage systems, it is exclusively focused on analysing the condition of railway drainage pipes. The degradation process of other types of railway drainage assets, such as chambers, culverts, channels, and structures, remains to be examined.

There are many factors influencing the rate of deterioration such as age, size, material, soil characteristics, etc. In Ana et al. (2009), an analysis on identification of the important factors affecting sewer deterioration in the sewer network of Leuven (Belgium), is carried out using logistic regression. It revealed that out of the 10 variables considered, age, material and length are the only three that significantly affect the deterioration process. However, by comparing results with similar studies in the UK and Canadian networks, they found that each of them has a slightly different set of significant factors, and thus conclude that there is no single set of factors that can explain sewer deterioration and it will vary from one network to another.

As condition assessment can be very subjective, knowledge of senior experts can be very valuable in the determination of asset status. Korving and van Noortwijk (2008) developed a stochastic model for sewer deterioration, incorporating expert opinion and visual inspections using Bayes' theorem. Dirichlet distribution is used to model 'subjective' prior knowledge, i.e. expert knowledge, while the likelihood function of condition states changing is updated by way of inspections.

2.4 Performance model

Performance is a measure of accomplishment for a given task. It is important for the asset operator/owner to maintain performance at a given standard. Poor performance often leads to financial expenditure as compensation for damage and/or improvement of the underperforming asset. It is hence logical to link the costs with the performance in the WLC model. A performance model is developed to quantify the performance of the concerning assets with the underlying purpose of numerically connecting it to the whole life costs.

Performance criteria vary across different industries, and are mainly defined based on the purpose of the asset and the objectives of the owner/operator. For example, in water distribution, the companies' main focus is to meet the customers' water demand without disruption, while ensuring the water quality meets the required standard. As stated in the book *Whole life costing for water distribution network management* (Skipworth, 2002), there are six performance sub-modules in the framework: Leakage, Demand Patterns and Projections, Structural Performance, Customer Interruption, Water Qual-

ity, and Hydraulic Capacity; which are split into three groups: Supply and Demand, Structural Performance, and Water Quality. Each group coincides with one aspect of the business goal: Supply and Demand modules examine whether customer's demand is satisfied, Structural Performance modules measure service disruptions due to physical damage of the system, and Water Quality modules test the water quality supplied. Urban stormwater drainage systems serve as another example. They are designed to drain excess rain and groundwater from impervious surfaces in order to prevent flood-related disruptions and property damage. Therefore, the performance of these systems can be assessed by the frequency, extent, depth, and duration of flooding incidents (Kolsky and Butler, 2002).

Ashley and Hopkinson (2002) reviewed the current framework for measuring and assessing the performance of UK water service providers (WSPs). In the UK sector, the three critical areas of performance judged by the regulatory bodies are: value for money, service delivery, environmental and social impacts. In England and Wales, the performance objectives and targets are produced jointly by the Companies, the Government and the Water industry Regulator; whereas in Scotland, the Water Industry Commissioner covers economics and customer service regulation and the Scottish Environmental Protection Agency deals with emissions into the environment. The performance of the English and Welsh WSPs is evaluated by the Office of Water Services (OFWAT) against different 'levels of service'. OFWAT's annual reports outline the quality of services delivered to customers by each company and compared their performance with the industry average. The report also sets out an overall performance assessment for each company, considering four key categories: water supply, sewerage service and flooding, customer service, and environmental impact (Ashley and Hopkinson, 2002). Besides regulatory bodies, various stakeholder has also taken the initiative to enable performance evaluation of WSPs. An important example is the International Water Association's publication of Performance Indicators (PI) for WSPs (Alegre et al., 2016). PI can be a value or characteristic, commensurate or non-commensurate, used to measure relevant aspects of the industry's performance in a true and unbiased way Cardoso et al. (2004). The PI for water supply and wastewater consists of the following six areas: Natural resources (water supply)/environmental (wastewater), Operational, Personnel, Physical, Quality of service, and Financial (Alegre et al., 2016; Matos et al., 2003; Cardoso et al., 2004).

Cardoso et al. (2004) discussed the performance assessment in water and wastewater systems, reviewed the concept of PI, and presented the use of the Performance Assessment System (PAS). PAS was suggested by Alegre and Coelho (1995) as a tool to measure the performance of water supply or wastewater systems. This system is designed for engineering applications and considers numerous factors and perspectives, such as hydraulics, water quality, reliability, and social impact. The performance areas explored for water supply are:

- hydraulics - nodal pressure, nodal pressure variation, link velocity, system energy consumption;

- water quality - chlorine residual concentration, travel time;
- reliability - nodal path entropy is used as a measure of supply path redundancy.

For wastewater systems, the following performance domains were identified (Cardoso et al., 2004):

- hydraulics - water level, flow velocity, overflow volume, overflow peak and duration, ratio between maximum wet weather flow and maximum dry-weather flow;
- environmental - concentration of pollutants, polluted overflow discharges, septicity;
- structural - damage rate, leakage;
- economic - maintenance costs, power costs;
- social - disruption to public activities, complaints, odours.

(Cardoso et al., 2004) applied the PAS, combining water level and flow velocity metrics, to evaluate the hydraulic performance of the sewer system. Case studies were conducted on a combined sewerage system and a separate domestic sewerage system in Portugal, under various scenarios of different load factors and weather conditions. The hydraulic model was built using the MOUSE package. Records from 2 flow metering points were used to analyse the performance.

The performance of sewer systems was also studied in Shepherd et al. (2004)'s paper and quantified using Key Performance Indicators (KPIs). Sewer systems transport sewage from houses and commercial buildings through pipes to treatment facilities or disposal. As it is wastewater in the pipes, factors such as sedimentation and severity of sewer overflows are taken into consideration and evaluated as one of the measurements of performance. Other factors such as hydraulic capacity and asset structure integrity, which affect the capability of delivering the asset's intended purpose, are also included as KPIs. The performance model was composed of two parts: hydraulic modelling and asset performance modelling. The hydraulic modelling is simulation-based via 3DNet software, whereas the asset performance modelling is derived from historical data. Figure 2.11 demonstrated the flow chart of sewer KPIs. KPIs analysed with hydraulic modelling are: Sewage Available to Transport (SATT), wet weather performance, sedimentation and CSOs. SATT was calculated by the available volume in the sewer divided by the design volume, measuring hydraulic inadequacy in dry weather environment. In wet weather environment, performance was evaluated with either water level or discharges, using the method proposed by Cardoso et al. (2005). Sedimentation had a similar performance function, built upon the time aggregated velocities in the sewer in relation to the self-cleansing velocity. For combined sewer overflows (CSOs), the KPI was calculated based on the consent conditions for the CSO in terms of number of spills. Asset performance modelling was divided into three areas, blockage, collapse and pump station. Predictive modelling for blockage and collapse was developed by analysing incident records and the corresponding asset databases. Whereas, for pump stations, analysis of operational data was performed to identify the regularity of failures that were related to physical characteristics and maintenance regimes (Shepherd et al., 2004).

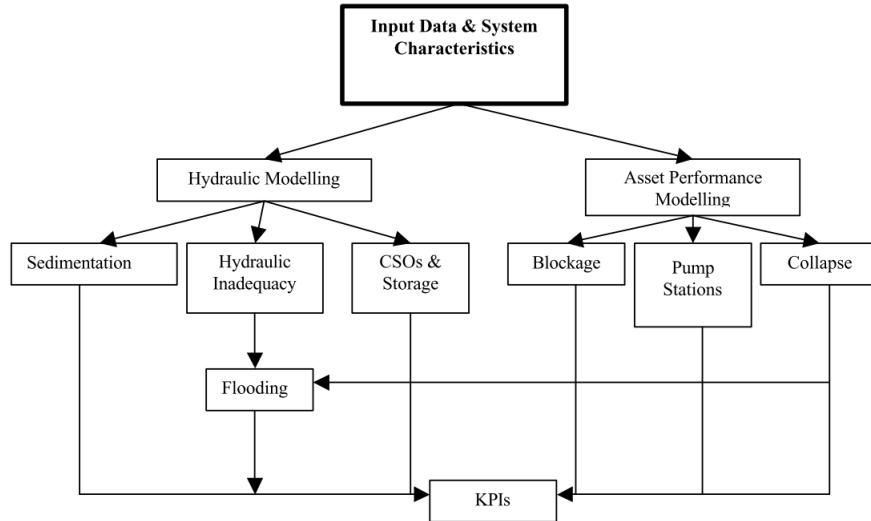


Figure 2.11: Sewer system KPIs

To build a performance model for railway drainage, it is useful to learn from other buried piped systems as many are designed to direct stormwater from one location to another through buried pipes, but it is also necessary to consider the unique performance indicators relating to the railway sector. The major concern of the railway drainage system is not just the successful delivery of stormwater to a designated discharge point, but also eliminating water related disruption to railway operation and protecting other railway assets from water damage.

The uncertainties in the performance model were not often discussed in the existing literature. Most of the uncertainties typically arise from the quality of input data, such as inaccurate or missing asset characteristics. There are also other significant factors to consider, such as the impact of climate change. For instance, drainage assets/systems that previously met performance requirements might fail to maintain satisfactory standards due to more frequent and/or heavier rainfall events brought on by climate change. Additionally, regulations and standards set by the country's railway industry regulatory bodies can affect the performance criteria used in the model. These effects also need to be considered and incorporated into the whole life cost framework. The performance model proposed in this study is designed to identify and evaluate the performance indicators specific to the railway drainage system, taking into account the model's uncertainties.

3 Model Framework

Railway drainage assets include several types of components designed to collect surface and groundwater which runs towards, falls onto or issues from the railway corridors, and then deliver it to a suitable outfall (with sufficient capacity), whether that be a natural watercourse such as a river, a public sewer or a soakaway. Effective management of the drainage system is essential for safe operation, because the drainage system plays an important role in protecting rail network infrastructure assets from the damage caused by moving water as well as eliminating water related service disruption to train operators. Almost all of NR's drainage assets are of unknown age and design but were most likely built before the 1950s. Many may date from the Victorian times (NetworkRail, 2017). Due to the long life span of drainage assets, it is only reasonable to expect a much higher future expenditure in maintenance and operation as they continue to degrade. Currently the maintenance and renewal of the drainage assets are carried out and financially accounted as an integral part of the renewal and maintenance of the track, earthworks, structures and buildings assets. However, with increasing attention on the importance of railway drainage asset developed in the past few years, Network Rail is in need of developing an asset management tool that could assist them with future asset maintenance regime planning and expenditure projection calculation for drainage assets. It is suggested that NR to take a whole of life costing approach, as this will allow them to take all the costs of owning and maintaining the asset into account at an appraisal stage.

In the past, while considering the provision of assets, it was usual to focus on minimising the initial construction costs of the assets in order to achieve a shorter payback period. However, it was soon discovered that for capital expenditure with a long life span, initial costs are only a small part of the investment required throughout the assets' life time (Engelhardt et al., 2003). Undue attention to minimising initial costs without taking other costs into consideration can thus potentially lead to a higher overall cost. The whole life cost concept is hence cultivated on the realisation of the importance of costs which occur after an asset has been constructed, such as maintenance, operation and disposal, acknowledging their power to influence decision-making.

3.1 Overview

In this study, a methodology has been developed to facilitate the understanding and calculation of the whole life cost of the UK railway drainage systems. The construction of the WLC framework begins with identifying all costs that contribute to the WLC accounts and the drivers behind these costs. The objectives that the potential model users wish to achieve have also been considered. User objectives were found to be the need for a better understanding of the asset degradation process which enables accurate forecasting of drainage asset conditions, as well as the ability to build tools that provide justifications for proactive maintenance decisions which would mitigate the risks of drainage asset failure before they occur.

As described by NR drainage asset managers, the major concern and main cost driver of managing the railway drainage system is the effect of drainage asset condition degradation. Hence a degradation model was developed to help analyse the remaining useful life and patterns of deterioration for existing drainage assets. The model also provided the knowledge to further investigate the potential future costs that may arise due to asset condition degradation.

The two main sources of costs that arise from the operation, maintenance and management of drainage assets are determined to be the cost of intervention and the cost incurred due to the future failure of the asset. Intervention is defined by NR as actions taken on drainage assets in order to prevent the worsening of the current condition level or improve the asset condition level to a better state. Hence, intervention is naturally linked with asset degradation, as asset conditions deteriorate, intervention will be carried out to maintain the assets in a desirable state. Therefore, intervention is deemed as an important module in the whole life cost framework.

The cost arising from asset failure is usually consequential, so it is defined as a penalty cost paid out after incidents. A detailed list of possible cost drivers behind the penalty is discussed in Section 3.5. The root cause of all penalty cost drivers is the loss of functionality in drainage assets due to deterioration. In order to investigate the potential penalty costs, it is important to build a performance model that can measure the capability of the drainage system and hence quantify the loss of functionality. A performance model needs to be embedded in the whole life cost framework, providing a tool for the estimation of the impact of degraded drainage systems.

The whole life cost account is formed by consolidating the two sources of costs listed above: intervention cost and penalty cost. Combining the two cost drivers with the degradation and performance models that are essential to assist better realisation of the drainage assets and enables the calculation of the whole life costs, a comprehensive WLC framework for UK railway drainage was developed in this study as described in Section 3.1.1. The Railway Drainage WLC framework consists of four modules: asset performance, asset degradation, intervention and penalty, as well as the WLC accounts.

To help NR make proactive and robust management decisions, a decision support tool was developed within the whole life cost framework. A proactive and cost effective management regime can then be derived from the whole life cost account by minimising the total cost while complying with budget constraints and at an agreed tolerance to failure risk.

3.1.1 Whole Life Cost Framework

The developed Railway Drainage WLC framework is composed of four modules: asset performance, asset degradation, intervention and penalty. Figure 3.1 indicates links between the four modules and their subsequent impact on the whole life accounts. Degradation influences the intervention decision, as high levels of degradation mean the performance

of the asset will be jeopardised, and consequently lead to disruption of normal business and increase in safety risk; vice versa intervention can influence degradation as it will lower or stabilize the severity of degradation, or reset the degradation none. When the performance is weakened due to degradation, the likelihood of failure is increased, hence higher penalty cost is expected to be paid out as a financial consequence which feeds into the whole life cost accounts. On the other side, if intervention is performed to prevent degradation and loss of performance, it also generates capital/operational expenditure that goes to the whole life cost accounts. The optimum intervention strategy can be found by solving the optimising problem with the objective of minimising the whole life cost account, while complying with risk tolerance and budget constraints. This framework helps asset managers to build an asset management plan that is cost efficient, evidence based and that also mitigates any undesired risks due to drainage asset failure.

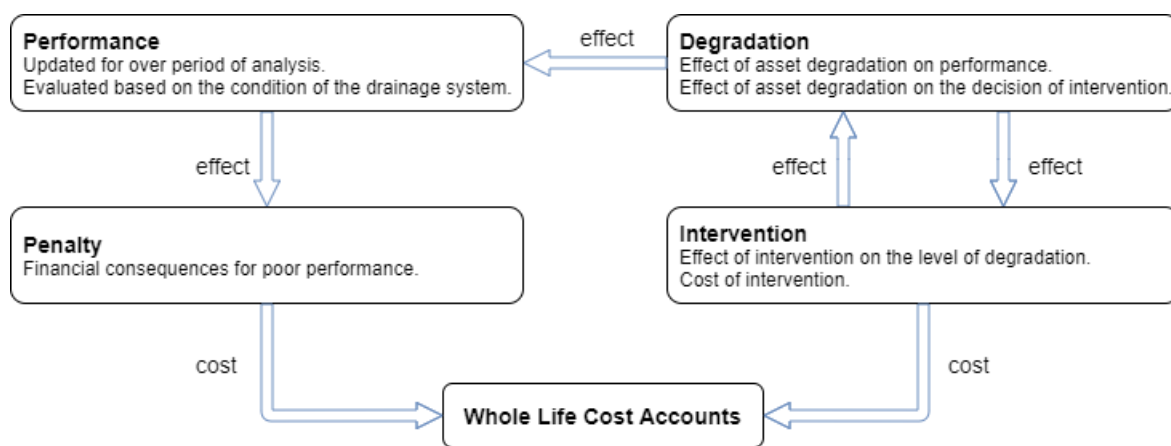


Figure 3.1: WLC framework showing the linkage between the four modules (performance, degradation, penalty and intervention) and the WLC accounts

The WLC framework developed by the author can be configured to operate at both a strategic level and a tactical level. This flexibility will provide asset managers with a robust model that fits all aspects of management needs, generating both top-down strategic plans to assist national/regional budget planning and bottom-up tactical plans to assist building day-to-day maintenance workbank.

On a strategic level, the author has developed tools that can forecast the expenditure and amount of works needed for the railway drainage assets nationwide to maintain a desired level of performance over a long period of time. This can help asset managers to establish a financially sustainable drainage policy, making proactive investment decisions that will prevent risks in advance and are more cost effective.

On a tactical level, the author has developed tools that can provide route engineers with WLC calculations for local drainage systems and assess the site specific performance under a range of renewal, maintenance and utilisation option scenarios. This can be used by route engineers in their day to day work planning. They will be able to prioritise their works based on the risks/financial costs of failure associated with the part of the system

where the work is carried out. It can help asset managers making decisions while facing short term budget constraints to work out the optimum budget allocation strategy that best achieves the company’s goal.

Figure 3.2 presents the various models developed by the author based on the different components of the WLC framework; and the dynamic relationships between the models which form two flowcharts of the WLC model on the two different levels of application. The orange arrows indicate the strategic level WLC framework, whereas the blue arrows indicate the tactical level WLC framework. For each module, a model specific to the two levels was developed. The models listed in blue boxes are models developed by the author in this study, whereas the models listed in green boxes are models developed in other NR funded projects and have been applied for the first time in a WLC framework by the author. Each model will be discussed separately in the following sections.

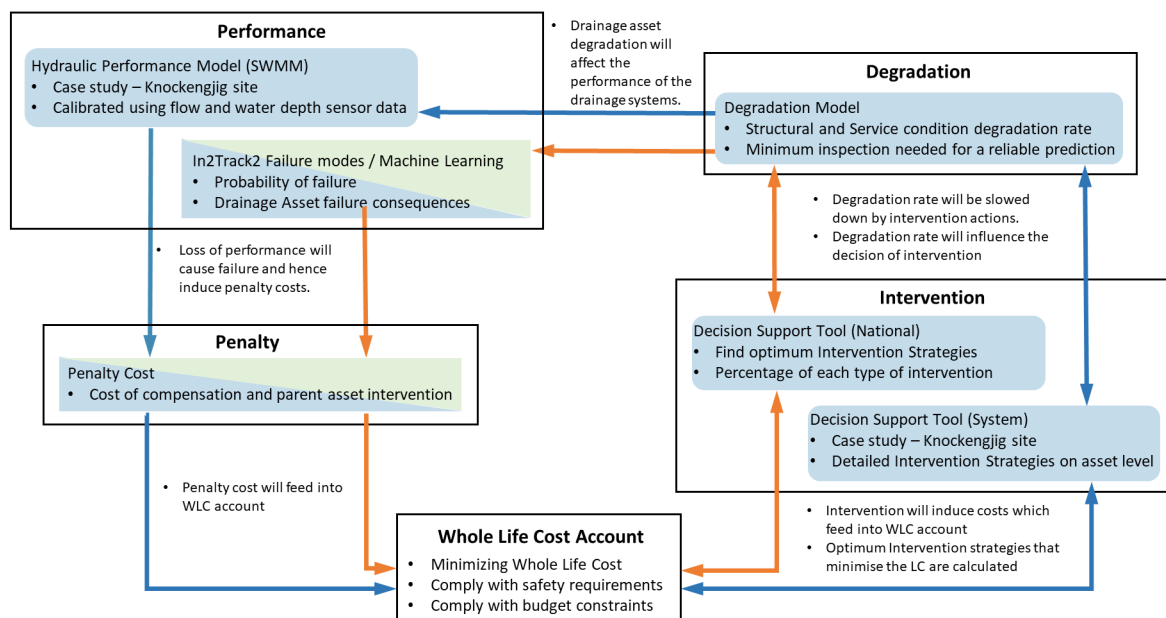


Figure 3.2: WLC model flowchart

3.1.2 Model summary

Figure 3.3 presented a flow chart of how the models shown in the Figure 3.2 are utilised in the work described in this thesis. The objectives achieved by completing the development of each stage of the models are listed on the right hand side of this figure.

First, a service and structural condition degradation model was built in this study to analyse the degradation process of UK railway drainage assets. This provides a tool that enables the realisation of an asset’s current condition grade and provides a prediction of future condition grade. The degradation model is described in Chapter 4, and case studies were performed on selected UK railway drainage asset groups.

Performance models to simulate the performance of the drainage systems were also built

in this study. A hydraulic performance model was built to enable the quantification of the hydraulic capacity of a single or a small number of linked systems. This type of performance model requires detailed information of the local drainage system, it is used within a tactical level WLC model. The model is described in Chapter 5, followed by a case study of a real-life drainage system in Scotland. The hydraulic performance model was then integrated with the degradation model to enable simulation of future drainage system performance with estimated future asset degradation. This is described in Chapter 6, presented with a case study of the same drainage system used in Chapter 5. For the strategic level WLC model, a data driven machine learning performance model was used to quantify the risk of drainage failure induced failure. This type of model, which was developed in a previous project, was trained and validated using data collected for UK railway drainage assets in this study. The validated model was then employed to provide performance predictions for the WLC model. Details of the data driven performance model were described in Chapter 8.

For both the strategic and tactical levels, whole life cost models were developed using the same degradation model but the hydraulic performance model and data driven approach were linked to the tactical and strategic levels respectively. At the same time, decision support tools are built based on the WLC model using the simulation process stated in Section 3.6. The two whole life cost models (tactical and strategic) are described in Chapter 7 and Chapter 8.

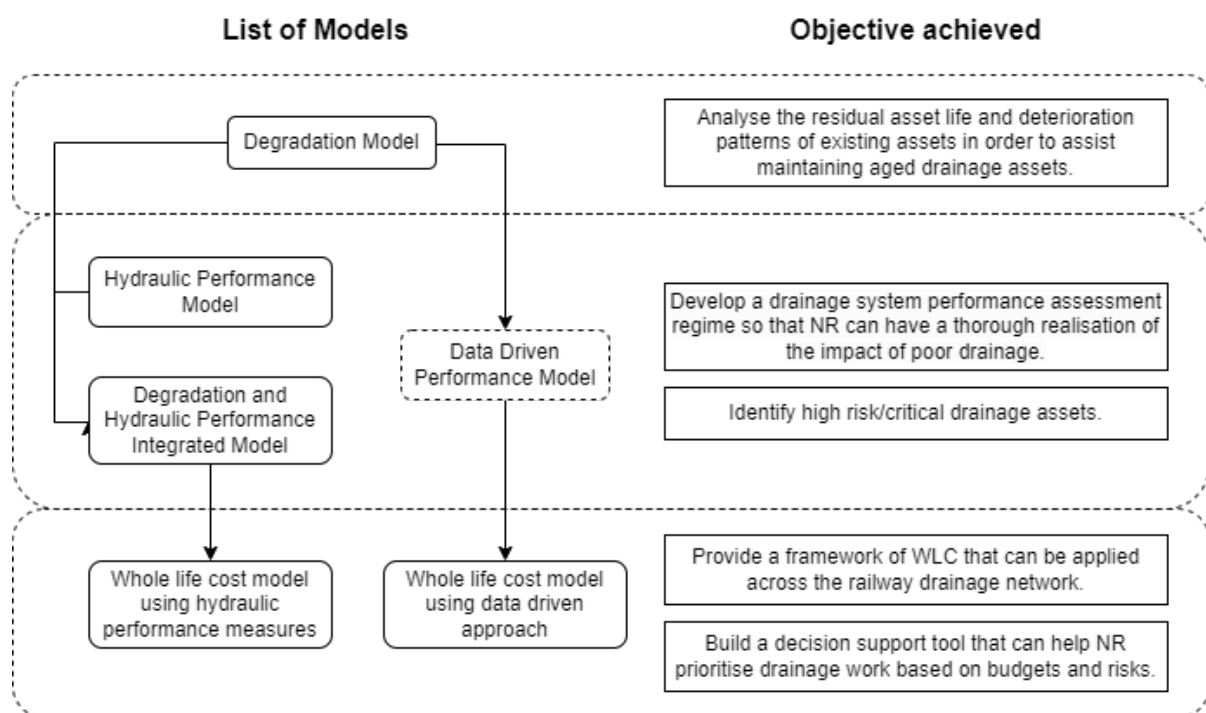


Figure 3.3: Model list

3.2 Degradation

Asset degradation is reflected by changes in the asset condition grade. Asset condition grading is split into two parts: the structural condition grade and the service condition grade:

- Structural condition: relates to the fabric of the asset and the severity of the structural defects that affect its integrity. Structural defects can be addressed by repairing or replacing the asset;
- Service condition: relates to aspects of the condition of the asset that can impact on the water carrying capacity of the asset and the severity of the defects that reduce its capacity below its original design level, but is independent of the structural condition. Service defects can normally be addressed by maintenance of the asset and are related to defects such as sediment deposits and blockages, and vegetation.

In NR, the Service and Structural condition are both defined on a 1 to 5 grading system as shown in Table 3.1. The system adopted is compatible with guidance from Spink et al. (2014).

Service Condition	Description
1	Clear
2	Superficial deposits with no loss of capacity
3	Capacity slightly reduced
4	Capacity severely reduced
5	Blocked or unsafe condition

Structural Condition	Description
1	No defects
2	Superficial defects
3	Minor defects
4	Major defects
5	Blocked or unsafe condition

Table 3.1: Description of Service and Structural Condition Score (NetworkRail, 2017)

Degraded assets could cause reduction in the drainage system performance and in the worst case loss of functionality, so it is important for NR to understand the degradation process and inspect the assets' condition at appropriate intervals. NR is in the process of improving its drainage asset knowledge by scheduling surveys and inspections to verify the existing data record and identify unrecorded assets. The Integrated Drainage Project (IDP) is being carried out to address the current shortfall in drainage asset knowledge (NetworkRail, 2017). In order to develop better inspection regimes, appropriate degradation modelling tools are required to enable a better understanding and estimation of the current condition grade of drainage assets. Degradation behaviour can be analysed

using the historical condition scores and the asset characteristics; and prediction of the future structural and service scores can be made based on the past degradation pattern.

In this study, as shown in Chapter 4, a degradation model using Markov Chain was built. A case study of the UK railway drainage system service and structural condition was performed using existing historical asset condition records.

3.3 Performance

Degradation of drainage asset condition will reflect on the performance of the drainage assets. For example, siltation of a pipe reduces its cross-sectional area as well as increases its hydraulic roughness, hence reducing its hydraulic capacity; a structural defect in a syphon could reduce water transferring from one side of a cutting to another under the track. In order to efficiently manage the drainage assets, both an understanding of the current asset performance (in its current condition state) and a forecast of the future asset performance (in its future condition state) is required.

3.3.1 Hydraulic performance model

In NR, the purpose of drainage assets is to conduct surface and subsurface water away from sensitive assets such as tracks and earthworks. Hence it is sensible to say that the performance of any drainage asset can be measured by its hydraulic capacity (the maximum volumetric flow rate it is able to convey before becoming surcharged). However, it is worth noting that the hydraulic capacity of a single asset cannot be assumed to be its true hydraulic capacity, as it will diminish if the upstream and downstream assets have inadequate hydraulic capacity. Hence, the whole NR drainage network is considered as a group of sub-systems, where each sub-system is defined as a series of drainage nodes and links connected to carry water from an inflow to an outflow.

Lack of hydraulic capacity can be caused either by asset degradation or inadequate designed capacity. As stated in Section 3.2, both asset service and structural condition change can be simulated using the degradation model. However, it is harder to determine whether the existing drainage assets lack the capacity to withstand the current and future precipitation levels. There might also be places where drainage infrastructure is missing, which can also be considered as a lack of designed capacity. In order to determine whether the existing drainage system will serve its purpose, it is also important to perform a catchment analysis as part of the performance model, as this informs the size of the flow volumes that the drainage system must have the capacity for.

Catchment Analysis

Although drainage assets are normally designed to cope with rainfall events with certain return periods following the company design standards as shown in Appendix A (NetworkRail, 2011)). NR's drainage systems consist of large amounts of historical assets where the original design plan is unknown. Also, with climate change, changes in the

surrounding catchment including any changes in geography and land use, the original designed capacity may not be sufficient anymore, which will reduce the current system performance.

Hence it is necessary to identify contributing catchment areas for the sub-systems and understand their characteristics. Although it is difficult to predict the future change in geography of the surrounding catchment; due to the increase of extreme weather in recent years, it can be assumed that a certain rate of increase in the rainfall return period is expected, and hence a predicted increase in the hydraulic capacity demand can be simulated based on such assumptions. Moreover, with a detailed catchment analysis alongside all railway lines, it is also possible to identify potential locations where drainage systems are required but not installed.

In this study, as shown in Chapter 5, a hydraulic performance model is developed using Storm Water Management System (SWMM) to enable the simulation of rainfall-runoff from the field adjacent to the railway and routing of runoffs through the railway drainage system into the outfall. A detailed methodology is also demonstrated to help locate and analyse the catchments that served by the railway drainage system.

3.3.2 Failure modes analysis

A detailed hydraulic model for all railway drainage sub-systems could provide an asset performance evaluation both on a strategic and a tactical level. However, given the current incompleteness of the drainage asset inventory, adequate hydraulic models cannot be built for all sub-systems. Hence, on the strategic level, a data-driven failure modes analysis has been adopted as a substitute.

The In2Track2 failure modes analysis project took a data driven approach to explore the linkage between drainage asset condition and failures using several Machine Learning (ML) techniques. The In2Track2 is an EU-funded project that addresses the topic of “Research into optimised and future railway infrastructure”, aiming to reduce lifecycle costs, improve reliability and punctuality, whilst increasing capacity, enhancing interoperability and improving the customer experience (*In2Track2*, 2018). An unsupervised ML technique Self-Organising Maps (SOMs) was employed to qualitatively investigate and identify any plausible linkages between various input parameters that could cause failure of drainage assets. The plausibility of the identified linkages was further investigated by conducting interviews with experienced members of NR staff, and probable failure mechanisms were identified and presented in the form of failure pathways (Kazemi et al., 2021). The failure pathways are then used to help build a data-driven model that enables simulating number of incident caused by drainage failures based on the weather and asset condition parameters. The model is developed and demonstrated as part of the WLC model using data driven approach in Chapter 8.

3.4 Intervention

There are various intervention options that can be carried out on drainage assets in order to prevent the worsening of the current condition grade or improve the asset condition grade to a better state, and hence maintain their current performance or remedy their unsatisfactory performance. Interventions can be categorised into the following six general groups: Inspect, Survey, Maintain, Refurbish, Renew and New Build. Definitions of each category are listed in Table 3.2 (NetworkRail, 2017).

Intervention category	Definition
Inspect	Routine inspection of the asset to assess its performance and identify locations requiring further intervention.
Survey	Periodic detailed surveying of the asset to assess its condition, capacity, inventory and physical attributes.
Maintain	Maintaining the performance of the asset by cleaning and minor repairs.
Refurbish	Restoring the performance of the asset by major repair, local replacement or re-profiling.
Renew	Wholesale replacement of the asset. May also include an element of asset improvement.
New Build	Installation of new assets to address a shortfall in drainage performance where there is currently no or insufficient drainage.

Table 3.2: Definition of drainage intervention categories

After each intervention is applied, it is believed that the intervention will affect condition grade of any drainage asset as follows:

- Renew and New Build will reset the condition grade to 1.
- Refurbish will improve performance and bring the asset to a lower condition grade.
- Maintain will make any asset stay in the current condition grade for a certain period of time, or will bring the asset to a slightly better condition state.
- Inspect & Survey will not have a direct impact on the asset condition grade, but will help improve asset knowledge and better monitor the asset condition level change. Hence, it will potentially shorten the reaction time between asset condition degradation and intervention actions.

Each intervention group contains various intervention methods, and they each have different levels of impact on asset structural and service condition. Some methods will have a larger effect on condition than the others, whereas some intervention methods that are intended to remedy one type of degradation will also have a collateral effect on other types of degradation. For example, methods of repair or refurbishment aimed at improv-

ing the structural condition will also result in an improvement in the service condition as the asset has to be cleaned in order to carry out the repair or refurbishment (NetworkRail, 2017). Detailed discussion on the intervention effects will be given later in Section 7

Interventions are made to maintain assets' functionality, and costs arising from these actions will feed into the whole life cost account. These costs are classified as direct costs since they are directly related to the life cycle of the asset itself, i.e. the costs of design, construction and maintenance over its whole life to its disposal (Ambrose et al., 2008).

Decision support tools were developed using the WLC approach to assist asset managers in establishing proactive and cost-effective drainage asset management policies. On the strategic level, a tool was developed to evaluate long-term intervention strategies that minimize the whole life costs. This tool allows for the comparison of different long-term strategies under various input conditions such as rainfall, budget, and resource constraints. On the tactical level, the developed tool enables testing for shorter-term solutions that prioritise drainage work at a single asset level, thus helping the route asset manager in making day to day plans that minimize WLC and the risk of system failure.

In this study, as shown in Chapter 7 and Chapter 8, intervention costs are calculated as part of the WLC model and are used in the decision support tool. In both chapters, it is demonstrated that decisions of which assets should be intervened and the frequency of intervention to be carried out can be optimised by minimising WLC using the decision support tool. This was demonstrated through application to several case studies.

3.5 Penalty

A penalty arises when a drainage asset does not reach its desired functionality, consequently financial costs are incurred, such as repair costs for damages to third party properties, compensation cost for train disruption and human accident/fatality. These costs are classified as indirect (or consequential) costs since they arise as a 'consequence' of owning or operating an asset (*Whole Life Costing for Sustainable Drainage*, 2004). The possible cost drivers are listed in Table 3.3. Consequential costs are divided into short term and long term costs. The short term costs arise when there is a rapid failure, for example, track flooding; whereas long term costs arise when repeated lack of water carrying functionality causes damage to other railway assets (e.g. earthworks, signaling) which then leads to disruption of the train operations and outside entities which result in financial, environmental, reputational and social costs.

The probability of drainage related failures can be modelled by linking the historical failure records with impaired drainage performance, where drainage performance can be simulated using the hydraulic performance model. Short term failures are expected to occur when the hydraulic performance model indicates there is flooding from the trackside drainage system with water levels above the railway track level. Long term failures are harder to examine since they will be the cumulative result of minor flooding losses which may not disrupt normal railway operation.

Short term drivers	Long term drivers
<ul style="list-style-type: none"> • Accident due to flooding • Delay due to flooding • Damage other railway assets & third party assets due to flooding • Flood damage to surrounding area 	<ul style="list-style-type: none"> • Long term damage to other railway assets & third party assets (e.g. wetbed) • Accident due to other railway asset failure • Delay due to other railway asset failure • Derailment due to other railway asset failure • Environmental damage

Table 3.3: Consequential Cost Drivers

Hence, when analysing frequency of failure on a strategic scale, the failure mode analysis mentioned in Section 3.3 can be used to provide a generalised prediction for areas where there is insufficient quantity of specific failure records and/or historical asset inventory. This type of model is able to quantify linkages between rainfall, drainage asset condition, and historical failure records nationwide. Such relationships can hence be applied to simulated future asset conditions in combination with rainfall to generate a failure probability prediction of individual assets.

Unit costs associated with each failure are examined using both historical data and market price. For some consequences that are hard to assign a monetary value, such as fatality, environmental damage and reputation damage, a pseudo value can be given to reflect the severity of their consequences.

In this study, the calculation of penalty costs is discussed in both the Chapter 7 and Chapter 8. In the case studies of the WLC models, only the flooding unit costs are considered since the linkage between drainage asset failure to other incidents are complicated and still required further studies to be fully understood.

3.6 Whole life cost simulation process

The whole life cost simulation process is developed in the study and the Figure 3.4 illustrates the flow chart of the simulation process to calculate the whole life costing of the drainage system. The whole life cost is the “womb to tomb” costs which include all costs from construction to disposal. However in real life, since a drainage network has a long structural life, it may have been built a long time ago. Therefore, if at the start of accounting time, there are existing drainage assets, the acquisition costs will be calculated instead of design & construction cost. The process starts by evaluating the performance of the system. If there are existing assets, asset condition scores will be extracted from historical records or current survey reports. Whereas if the assets are newly built, it is assumed to have condition score 1. It is then modelled over the service time of an asset,

or over an appropriate accounting period as the assets may have a very long life-cycle, by iterating through a predefined time-step (normally one year).

A decision support tool has been developed as part of the simulation algorithm. The tool generates a set of feasible intervention strategies based on user defined constraints, such as a total budget constraint, risk constraint (e.g. maximum number of failure allowed), and a labour constraint (e.g. maximum number of interventions can be carried out during one time step due to limited in house manpower). It compares the results of the tested intervention strategies after each step to decide the next one to be feed into the model. At the end of the simulation, it indicates the optimum intervention strategy that minimise the whole life cost account while complying with the defined constraints. On a tactical level, besides finding the overall amount of intervention to be carried out, asset managers can also potentially use the decision support tool to prioritise the intervention to towards the asset that has the largest effect on performance loss when degraded.

The steps of the simulation process are described as follows over an asset service life time of n time-steps:

1. At $t = 1$, Calculate the acquisition costs or design & construction cost.
2. Apply the degradation model to forecast the condition state changes of assets.
3. Carry out interventions on the assets based on the intervention decision made using decision support tool.
4. Change asset condition based on intervention executed.
5. Calculate the costs of the interventions to be carried out.
6. Evaluate performance using a performance model based on current asset condition (for that time step).
7. Calculate the cost of penalties based on the asset's performance.
8. If $t \neq n$, let $t = t + 1$, repeat steps 2 to 7.
9. At $t = n$, the loop stops and disposal cost is calculated.
10. Aggregate the present value of all the costs throughout all time-steps.
11. Compare the total cost generated with previous simulations (compare with 0 on the first iteration). If the WLC is minimal, end simulation and export the optimal intervention strategy; if not, rerun the simulation with a new intervention strategy generated by the decision support tool.

In this study, the WLC models were developed and the calculation of the WLC account were both stated in Chapter 7 and Chapter 8 as part of the model development. For both the WLC model using hydraulic performance measurements and the WLC model using data driven approach, the WLC simulation process follows the same principle as described in this section.

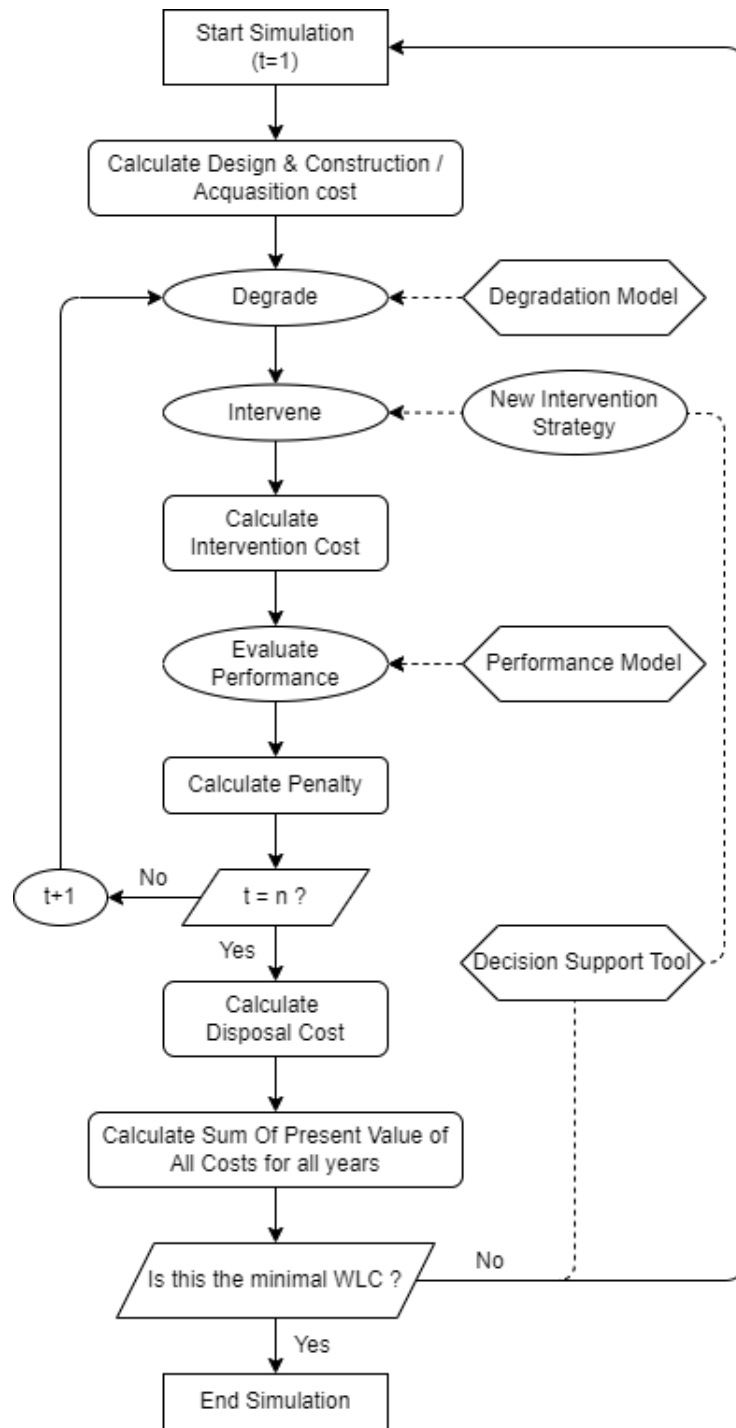


Figure 3.4: WLC simulation process

3.7 Uncertainties

The whole life cost model would incorporate a wide range of input parameters, each associated with various degrees of uncertainty. To address the challenge that arise from the uncertainties in the data, an uncertainty analysis is required to be carried out as part of the model (Skinne et al., 2011). The uncertainties of the degradation model primarily revolve around the lack of asset condition data and unstable data quality. Whereas for the performance model, besides the asset data quality, uncertainties also arise from the simulation of runoff processes as the railway drainage system typically serves a small catchment compared to the water distribution or sewer system, whose hydraulic model has been frequently explored in the literature. Also, the failure criteria/performance indicators might be affected by the local railway industry's regulator, hence can be country-specific; this also imposes a source of uncertainty in the model. Nevertheless, climate change is a major factor, as it will lead to more frequent and/or heavier rainfall, which might cause drainage assets or systems that once satisfied performance standards to fail to cope with the more extreme weather condition. For the whole life cost calculation, uncertainties arise from data deficiencies of unit cost and penalty cost, as well as the unpredictability of interest rates. In this study, these uncertainties are discussed and evaluated for all the models in each Chapter.

4 Drainage Asset Service and Structural Degradation Modelling

A degradation model is constructed using a Markov Chain to evaluate the degradation process of the railway drainage assets. This model serves as a tool for assessing the present state of assets and forecasting their future condition. In this Chapter, a detailed methodology of the Markov model is presented, describing how the transition rate matrix can be constructed, how to simulate future asset condition based on the transition rate matrix, and how to determine the minimal number of samples required in order to obtain a stable transition rate matrix. The applicability of the model for both drainage assets' service and structural condition are tested. A case study of UK railway drainage asset service and structural condition degradation is presented. The transition rate matrix was calculated for all asset groups. The model is tested and validated with 300mm diameter pipes and an uncertainty analysis is carried out.

4.1 Introduction

As railway drainage assets deteriorate, their capability may be compromised and they could fail to fulfill their designed purpose, which is to direct water safely away from other railway assets. A loss in capability would lead to obstruction to train operations as well as potential damage to other NR assets. Hence it is vital to develop an appropriate model that could simulate the degradation process of railway drainage assets, which would help better understand the current asset state as well as provide estimation of the future asset condition.

As mentioned in Section 3.2, in NR two grades are recorded to reflect the condition of any drainage asset: service condition grade and structural condition grade. Service condition is often affected by the probability of siltation at a particular location, which can be subject to different factors such as the asset geometry, soil content, pipe slope and water discharge. All these factors are relatively stable as the surrounding environment is unlikely to change in short periods of time; and the position of the asset is not going to move unless an incident happens or replacement is required. Hence, it is sensible to presume that the service condition of the assets is going to follow the same pattern as before. As for the structural condition, the status of the asset is most likely affected by the age of the asset as well as the surrounding geometry and track loading. Since the age of the railway drainage assets can be dated back to Victorian ages and are scarcely recorded, most asset ages are unknown; and the surrounding environment is not expected to change significantly in a short period of time. It is hence to assume that the structural condition also follows the same pattern as exhibited in the historical condition database.

Service Condition	Description
1	Clear
2	Superficial deposits with no loss of capacity
3	Capacity slightly reduced
4	Capacity severely reduced
5	Blocked or unsafe condition

Structural Condition	Description
1	No defects
2	Superficial defects
3	Minor defects
4	Major defects
5	Blocked or unsafe condition

Table 4.1: Description of Service and Structural Condition Score (NetworkRail, 2017)

As stated in the NetworkRail (2017), the Service and Structural condition grades are both defined on a 1 to 5 grading system as shown in Table 4.1.

4.2 Methodology

4.2.1 The Markov model framework

In this study, a Markov chain approach is used to model the degradation rate, which gives an estimation of transition probability from one state to a lower state. This decision is made under the assumption that the probability of degradation depends only on the current condition of the asset. Such an assumption is made based on expert opinion and will be verified later. Since drainage assets could degrade to a worse state any time during the year, in order to correctly estimate the adverse effect of degradation on the drainage capacity throughout the year, a Markov model with continuous time steps is chosen as it is believed to better reflect the degradation process of railway drainage assets. A continuous time Markov chain (CTMC) is described by a stochastic process $X = \{X(t) | 0 \leq t\}$ with discrete state space $S = \{s_1, s_2, \dots, s_n\}$, that satisfies the following for any time $s, t \geq 0$ and $i, j \in S$.

$$\mathbb{P}(X(s+t) = j | X(s) = i, \{X(u) : 0 \leq u < s\}) = \mathbb{P}(X(s+t) = j | X(s) = i) \quad (1)$$

In other words, CTMC is a stochastic process having the Markovian property: the conditional distribution of the future $X(s+t)$ given the present state $X(s)$ and the past states $X(u)$, $0 \leq u < s$, depends only on the present and is independent of the past (Ross, 2014).

In the case of modelling railway drainage asset service and structural condition degradation, the $X(t)$ the is condition score of the modelled asset at time t , and the state space $S = 1, 2, 3, 4, 5$ represents the 1 to 5 grading system mentioned above. The matrix

Q shown below is the transition rate matrix, or infinitesimal generator, of the Markov Chain,

$$\mathbf{Q} = \begin{pmatrix} -q_1 & q_{12} & q_{13} & q_{14} & q_{15} \\ 0 & -q_2 & q_{23} & q_{24} & q_{25} \\ 0 & 0 & -q_3 & q_{34} & q_{35} \\ 0 & 0 & 0 & -q_4 & q_{45} \\ 0 & 0 & 0 & 0 & -q_5 \end{pmatrix} \quad (2)$$

where $q_{ij} = \lim_{\Delta t \rightarrow 0} \frac{\mathbb{P}(X(\Delta t)=j|X(0)=i)}{\Delta t}$, representing the transition rate from condition i to condition j given that the asset is currently in condition i , assuming that the limit exists in $[0, \infty]$. The diagonal of the matrix is defined as q_i , where $q_i = \sum_{j=1, j \neq i}^n q_{ij}$. The holding time of an asset in rating i is exponentially distributed with parameter q_i . It is assumed that the assets' condition cannot improve without human intervention, hence $q_{ij} = 0 \forall i < j$. Although degradation is a gradual process, it is not always possible to monitor the status of an asset continuously, so the condition of an asset may have degraded by more than one state before the next inspection; thus, transition from state i to state j where $j > i + 1$ is also included in the model.

Given matrix Q, a transition probability matrix for a small time interval Δt can be expressed as:

$$\mathbf{P}(t, t + \Delta t) = \mathbf{I} + \Delta t \mathbf{Q} + o(\Delta t) \quad (3)$$

where I is an identity matrix. Let s denote $t + m\Delta t$. Then,

$$\mathbf{P}(t, s) \approx (\mathbf{I} + \Delta t \mathbf{Q})^m = \left(\mathbf{I} + \frac{(s - t)}{\mathbf{Q}} \right)^m \quad (4)$$

Taking the limit $m \rightarrow \infty$, the probability matrix P for any arbitrary time interval t to s can be obtained by

$$\mathbf{P}(t, s) = \exp((s - t)\mathbf{Q}). \quad (5)$$

The Markov model used in this study is time-homogeneous, which means the transition probability is time-independent. Although in reality, an asset's deterioration rate may be affected by the age of the asset (Ana and Bauwens, 2010; Kleiner et al., 2006), without any data related to the age of the railway drainage asset currently available in NR's database, it is not possible to explore the effect of age on transition rate in this study. Hence, the transition probability is assumed to be stationary over time. As drainage assets normally have a long life span, the effect of age on the transition probability would be minimal for short period simulations (i.e. 5-year Control Period); however, for simulations over longer time periods, such an assumption could lead to underestimation of the degradation rate.

4.2.2 Verification of the Markov Property

For the Markov property to stand, it is required to prove that the probability of an asset degrading into score j with a given current score i is not related to its previous conditions.

This can be done by analysing the three state transition sequence $(X_t|X_{t-1}, X_{t-2})$ of the historical data set, where $(X_t = i|X_{t-1} = j, X_{t-2} = k) = (i|j, k)$ represents an asset condition jump from j to i , given that the previous condition before j is k , i.e. the condition transfer from state k to state j and then state i . If the Markov property holds, for any given i and j , there would be no difference in the probability of the sequence $(i|j, X_{t-2})$ to exist, for all $X_{t-2} < j$.

The Chi-square Test (χ^2 test) is one of the most widely used statistical hypothesis tests for independence and goodness of fit, testing whether two or more categorical variables are related in some population. Hence it is adopted here to test whether the pre-condition of an asset is related to its current condition. A similar method has also been used in water distribution networks (Sempewo and Kyokaali, 2016) and other infrastructure such as pavements (Surendrakumar et al., 2013).

For a given current condition i and previous condition j , the null hypothesis is that the past condition X_{t-2} has no effect on the probability of the asset jump from condition j to i . The contingency table for the given current condition i and previous condition j is constructed by listing all possible sequences $(i|j, X_{t-2})$ as rows, then calculating under the given past condition j and X_{t-2} , the number of occurrences that the current condition is i and the number of occurrences that the current condition is not i . The contingency table is shown as Table 4.2.

Sequence	Number of sequence occurrence $X_t = i$	Number of occurrences of all other sequences with same past condition $X_t \neq i$
$(i j, 1)$	$N(i j, 1)$	$\sum_{s=j, s \neq i}^{s=5} N(s j, 1)$
$(i j, 2)$	$N(i j, 2)$	$\sum_{s=j, s \neq i}^{s=5} N(s j, 2)$
\vdots	\vdots	\vdots
$(i j, j - 1)$	$N(i j, j - 1)$	$\sum_{s=j, s \neq i}^{s=5} N(s j, j - 1)$

Table 4.2: Contingency Table for sequence $(X_t = i|X_{t-1} = j, X_{t-2})$

where $N(i, j|k)$ is the number of occurrences of the sequence $(i|j, k)$.

The test statistic for this table is:

$$\chi^2 = \sum \frac{(O - E)^2}{E^2} \quad (6)$$

where O is the observed value and E is the expected value for each scenario. For example, for the sequence $(i|j, 1)$, the observed value $O = N(i|j, 1)$, and the expected value:

$$E = \sum_{x=1}^{x=j-1} N(i|j, x) \times \frac{N(i|j, 1)}{\sum_{s=j+1}^{s=5} N(s|j, 1)} \quad (7)$$

The null hypothesis is normally rejected at a 5% significance level, meaning that if the χ^2 statistic with $j - 2$ degree of freedom is less than 0.05, the Markov property holds as the current condition is independent of past conditions.

4.2.3 Development of Transition Rate Matrices

Estimation of generator matrix is possible given complete asset condition score history, ie. for any asset $x \in \{x(t)|0 \leq x \leq n\}$ is available. Consider the likelihood of observations with a transition from i to j at time τ_1 followed by a subsequent transition from j to k at time τ_2 and etc. Assuming that an initial state probability is known, the likelihood can be expressed as

$$\begin{aligned} L(\mathbf{Q}) &= \exp(-q_i(\tau_2 - \tau_1)) q_{ij} \exp(-q_j(\tau_2 - \tau_1)) q_{jk} \dots \\ &= \prod_{i=1}^n \prod_{i \neq j} q_{ij}^{N_{ij}(T)} \exp(-q_i R_i(T)) \end{aligned} \quad (8)$$

where $R_i(T) = \int_0^T 1_{x(s)=i} ds$ which is the total value of the holding time at rating grade i by the time t ; $N_{ij}(T)$ is the number of times for ij transition by the time T . The log-likelihood is

$$\log L(\mathbf{Q}) = \sum_{i=1}^n \sum_{j \neq i} \log(q_{ij}) N_{ij}(T) - \sum_{i=1}^n \sum_{j \neq i} q_{ij} R_i(T) \quad (9)$$

Solving $\frac{\partial \log L(\mathbf{Q})}{\partial q_{ij}} = 0$, the maximum likelihood estimator for the element of the generator matrix is

$$\hat{q}_{ij} = \frac{N_{ij}(T)}{R_i(T)} \quad (10)$$

(Inamura, 2006)

4.2.4 Condition degradation Simulation

After obtaining the transition rate matrix, the potential future condition grade of the drainage system can be simulated using the stochastic simulation algorithm (SSA), also known as the Gillespie algorithm (Banks et al., 2011). The detailed procedure is described below:

1. Initialize the state of the system x_0 at time $t = 0$, which is the current condition score of the asset.
2. For the given state $x_0 = i$, find the transition rate λ_{ij} from state i to all other states, i.e. generator matrix elements $\lambda_{ij} = \hat{q}_{ij}$, $\forall j \in s, j \neq i$.
3. Calculate the sum of all transition rates, $\lambda_i = \sum_{j \neq i} \lambda_{ij}$.
4. Simulate the time, τ , until the next transition by drawing from an exponential distribution with mean $1/\lambda_i$. Generate a pseudo random uniform variable u_1 from the interval $[0, 1]$, $\tau = \frac{(-\ln(u_1))}{\lambda_i}$.
5. Simulate the transition type by drawing from the discrete distribution with probability $Prob(\text{transition to state } j) = \frac{\lambda_{ij}}{\lambda_i}$. Generate a pseudo random uniform variable u_2 from the interval $[0, 1]$, and choose the transition as follows: if $0 < u_2 < \frac{\lambda_{i1}}{\lambda_i}$, choose transition 1; if $\frac{\lambda_{i1}}{\lambda_i} < u_2 < \frac{\lambda_{i1} + \lambda_{i2}}{\lambda_i}$ choose transition 2, and so on.
6. Update the new time $t = t + \tau$ and the new system state x_t .
7. Iterate steps 2-6 until t is larger than the designed simulation period.

4.2.5 Determine the minimum sample size required

As drainage assets are often buried underground, they are difficult and more costly to inspect than other assets in the railway system. It is in the interest of asset managers to minimise such inspection costs whilst obtaining sufficient data to build a robust transition rate matrix for subsequent use in a degradation model. Hence, a study is performed to determine the number of samples required to obtain a stable transition rate matrix in which the rate values would not alter more than 5% by including more calibration data. Procedures are as follows:

1. Randomly select n samples (assets) from the whole asset database, calculate transition rate matrix $Q_{n,1}$ using the condition scores of these n samples.
2. Repeat previous step m times, giving a sample of m transition rate matrices $\{Q_{n,1}, Q_{n,2}, \dots, Q_{n,m}\}$.
3. Calculate sample mean \bar{Q}_n and standard deviation $\bar{\sigma}_n$, where $\bar{Q}_n = \frac{\sum_{s=1}^{s=m} Q_{n,s}}{n}$ and $\bar{\sigma}_n = \sqrt{\frac{\sum_{s=1}^{s=m} (Q_{n,s} - \bar{Q}_n)^2}{n}}$.
4. Increase the number of samples in steps of n , repeating steps 2-3 to obtain matrices $\{\bar{Q}_n, \bar{Q}_{2n}, \dots\}$ and $\{\bar{\sigma}_n, \bar{\sigma}_{2n}, \dots\}$.
5. Find the critical sample number r where \bar{Q}_r is within 5% of the actual transition rate calculated using all assets.

4.2.6 Model calibration and validation

To examine the performance of the degradation model, test is performed using the entire data set and through a split sample analysis. The split sample analysis is a more rigorous test because it uses data independent of that used in the model calibration (Micevski et al., 2002). the asset datasets were randomly split into two groups: a calibration group

and a validation group. The calibration data set was used to build the model and the predicted analysis results were compared with the validation data set to verify the model (Wellalage et al., 2015). After finding the minimal sample size n that is required to generate a stable transition matrix, n assets were randomly selected from the dataset to form the calibration group, whereas the remaining assets in the dataset belong to the validation group. The transition matrix Q was calculated using the calibration dataset then applied to the validation set to predict the number of transitions in each condition category. Observed and expected percentage of transitions were then compared to test the accuracy of the Markov Model proposed.

4.3 Data Processing

The robustness of the degradation model simulation results highly depends on the quality of the input data. It is hence important to perform data cleansing and data processing before inputting and using them in the model. This involves detecting and removing false or inaccurate records from the dataset, and identifying duplicates, incomplete or irrelevant parts of the data and then modifying, replacing or removing them accordingly. The detailed data processing steps are described in the following subsections. As a result, around 59.5% of the assets have remained in the service condition analysis and 57.8% of the assets have remained in the structural condition analysis; 68.5% of the service condition records and 65.5% of the structural condition records remained in the analysis respectively.

4.3.1 Condition historical records

Historical condition records are extracted from the Network Rail drainage asset database (Ellipse). With the oldest asset condition records dated in 2007. As dated on 19/02/2020, there are in total 445,584 drainage assets recorded in the Ellipse database. The assets stored in Ellipse are categorized into 13 asset groups which are further divided into 39 asset types. A full list of the asset groups and asset types can be found in Appendix B. Each asset has several general and asset specific attributes associated with it, namely asset number, asset type, location, condition scores and asset characteristics such as pipe diameter and size.

As the importance of the drainage assets is gaining more attention, NR has made efforts to attempt to complete the asset register. The Integrated Drainage Project was undertaken in Control Period 4 (01/04/2009 – 31/03/2014), the project consisted of:

- A review of available drainage data held centrally and with the routes from previous systematic surveys, which comprise around 35% of all the drainage assets.
- A national walkover survey of the remaining 65% of the NR drainage networks.
- Establish a national drainage database within the Ellipse maintenance system.
- Migrate the data from the previous databases into Ellipse (NetworkRail, 2017).

The number of assets recorded is plotted in Figure 4.1. To be noted that the date of recording is missing for 99,498 assets, so the year of first recording can only be found for the 346,086 assets. The act of data migration and asset survey is recognised in the sudden jump in the number of drainage assets on record from 60,489 in 2011 to 235,805 in 2012 in Figure 4.1. It is hence decided to use condition scores taken after 2012 to ensure the standard of condition assessment is consistent throughout the dataset.

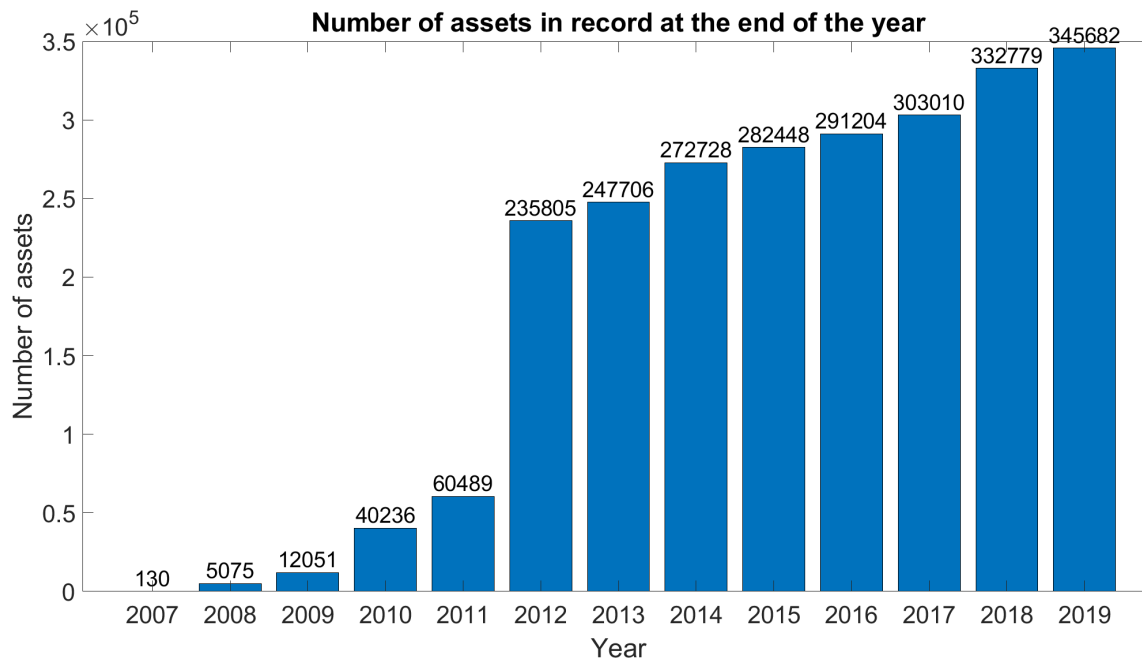


Figure 4.1: Number of asset in record at the end of the year

4.3.2 Data cleansing

In this study, the NR asset condition dataset was examined in detail and the following data cleansing procedures were developed to remove data points considered "invalid" and so prepare a data set that can be used in the degradation analysis carried out in the case study. If an asset condition score is missing or is deemed invalid, such a data entry is removed from any further analysis. A condition score is considered invalid if it is not a number, or if it is not one of the defined condition scores, e.g. the score is set to 0. After the initial data cleanse, it was found that out of all assets, 264,933 has at least one service condition score record, and 257,514 has at least one structural condition score record. That means, for both service and structural condition data, around 60% of the total assets has been inspected at least once in the 8 years' period (2012-2020).

It is noticed that for some of the assets, some of their condition data are recorded on the same date. If these condition scores are the same, then they are treated as duplicates and are merged into one data entry. If these condition scores are different, with no additional information provided, there is no way to determine whether these data are in error in NR's asset database system or a real condition improvement and/or degradation that

happened on the day of inspection. Therefore, these assets are removed from the dataset and not used in further analysis to maintain the validity of the data. As a result, 1,102 assets are removed from the service condition dataset and 995 are removed from the structural condition dataset.

After the data cleanse, the percentage of assets remaining in each asset groups are indicated the Table 4.3. As shown, most asset groups have 74-87% of assets that have a valid service and structural condition record that can be used to calibrate and validate the degradation model except for the pipe and granular drain asset group, which only has less than 50% of these assets with valid condition data after the data cleansing. This may be due to the fact that pipes are buried assets and granular drains are also covered or buried, hence they are more difficult to access and inspect.

Asset group	Service Condition	Structural Condition
Chamber	74%	74%
Pipe	43%	38%
Channel	87%	86%
Structure	82%	80%
Culvert	79%	77%
Outfall	82%	82%
Inflow	87%	87%
Covered Channel	79%	78%
Granular Drain	47%	47%
Pond	81%	81%
Syphon	75%	76%

Table 4.3: Percentage of assets remaining in each asset group with valid condition scores after data cleansing

4.3.3 Further data processing

The number of assets in each asset group was then examined to see whether there was enough data to produce a reliable transition rate matrix. The number of assets with valid conditions scores in each asset group is shown in Table 4.4. As Granular Drain, Syphon and Pond have less than 1,500 assets recorded with condition scores, it was assumed that there are not enough historical data points to produce a reliable probability prediction, so they were not taken into consideration in the following analysis.

It is noted that for some assets the recorded condition scores can go both higher and lower over time. As the condition score of an asset improves (goes lower), it would be assumed that there has been either an unknown intervention has taken place or there is an inspection error. Since this study is focused on the degradation of drainage asset condition, only the transitions where the condition is degraded (score has increased) has been considered to calculate the transition matrix. However, in order to eliminate the

Asset group	Service Condition	Structural Condition
Chamber	120982	121696
Pipe	57642	50337
Channel	30821	30645
Structure	18139	17866
Culvert	15760	15434
Outfall	10134	10081
Inflow	7726	7737
Covered Channel	2204	2187
Granular Drain	1072	1078
Pond	400	399
Syphon	53	54
SUM	264933	257514

Table 4.4: Number of all assets of each asset group after data cleanse

effect of score improvement on the assets without affecting the total holding time $R_i(T)$ used to calculate the transition matrix (as stated in equation 10), for all the transitions where the score is decreased (condition is improved) the end condition is substituted by the start condition, which means the asset is assumed to have stayed in the starting condition score until the moment that the asset's service condition is improved. The subsequent transition is unaffected as the next transition will be separate out from the previous one with a start condition of the original improved condition. Nevertheless it is assumed that the asset remains in their current condition until the data cutoff date of 19/02/2020.

Although in reality the degradation is unlikely to be observed immediately after a transition and the change of score is therefore recorded some time after the asset deteriorates. Such knowledge can only be obtained if all assets are constantly monitored. As this is practically and economically impossible, it is decided to make the assumption that the degradation happens on the day of the change of condition score. The possible uncertainty caused by such an assumption will be discussed later in Section 4.4.8.

4.4 Case Study

4.4.1 Verification of the Markov Property

As explained in the Methodology Section 4.2.2, the Markov property can be tested with the Chi-squared Test to verify that the net transition from the current condition is independent of past conditions. The test has been carried out for all asset groups and for both service and structural condition. Examples of the contingency table for Channel, Chamber, Culvert and Pipe asset categories are shown in Table 4.5. A full list of contingency tables is presented in Appendix C.

All test statistics are above the significance level of 5% except the transition from condition 3 to 4 for Channel structural condition. For all other asset groups, it can be concluded that there is no evidence to reject the null hypothesis of the independence for each asset group under 5% significance level. Hence, they are proven to possess the Markov properties, so the Markov methods described in the above Methodology section may therefore be applied.

The dependence of Culvert structural transition from 3 to 4 on the previous condition status may be due to several reasons. The precondition for transition from condition 3 to 4 is either 1 or 2; since the difference between condition 1 and 2 is very minor, there may be a chance that this condition transition exhibits some degree of dependence on the pre-condition. Also, for structural condition, it is possible that a new-build asset that is graded with condition 1 has a slower degradation rate than condition 2. However, with no information on the asset age profile, it is hard to accurately predict the age related factor of the structural degradation rate. Hence, in this analysis, it is assumed that the Culvert structural condition degradation also follows a Markov process.

Channel				Culvert			
sequence	$X_t = i$	$X_t \neq i$	χ^2	sequence	$X_t = i$	$X_t \neq i$	χ^2
(4, 3 1)	13	153	0.80	(4, 3 1)	65	372	0.72
(4, 3 2)	65	706		(4, 3 2)	124	668	
(5, 3 1)	3	163	0.31	(5, 3 1)	48	389	0.89
(5, 3 2)	7	764		(5, 3 2)	85	707	
(5, 4 1)	0	6	0.30	(5, 4 1)	43	68	0.97
(5, 4 2)	6	54		(5, 4 2)	75	124	
(5, 4 3)	9	173		(5, 4 3)	60	101	

Chamber				Pipe			
sequence	$X_t = i$	$X_t \neq i$	χ^2	sequence	$X_t = i$	$X_t \neq i$	χ^2
(4, 3 1)	15	48	0.04	(4, 3 1)	4	31	0.28
(4, 3 2)	19	131		(4, 3 2)	36	154	
(5, 3 1)	3	60	0.43	(5, 3 1)	2	33	0.17
(5, 3 2)	4	146		(5, 3 2)	27	163	
(5, 4 1)	2	6	0.49	(5, 4 1)	2	6	0.88
(5, 4 2)	6	23		(5, 4 2)	8	17	
(5, 4 3)	4	31		(5, 4 3)	11	30	

(a) Chi-squared test contingency table for Channel, Chamber, Culvert and Pipe service condition

Channel				Chamber			
sequence	$X_t = i$	$X_t \neq i$	χ^2	sequence	$X_t = i$	$X_t \neq i$	χ^2
(4, 3 1)	11	115	0.004	(4, 3 1)	15	114	0.30
(4, 3 2)	22	662		(4, 3 2)	26	138	
(5, 3 1)	0	126	N/A	(5, 3 1)	0	129	N/A
(5, 3 2)	0	684		(5, 3 2)	0	164	
(5, 4 1)	0	7	0.73	(5, 4 1)	1	48	0.39
(5, 4 2)	0	23		(5, 4 2)	0	31	
(5, 4 3)	1	47		(5, 4 3)	1	16	

Culvert				Pipe			
sequence	$X_t = i$	$X_t \neq i$	χ^2	sequence	$X_t = i$	$X_t \neq i$	χ^2
(4, 3 1)	2	16	0.39	(4, 3 1)	0	3	N/A
(4, 3 2)	5	84		(4, 3 2)	0	94	
(5, 3 1)	0	18	N/A	(5, 3 1)	0	3	N/A
(5, 3 2)	0	89		(5, 3 2)	0	94	
(5, 4 1)	0	5	N/A	(5, 4 1)	0	2	N/A
(5, 4 2)	0	10		(5, 4 2)	0	1	
(5, 4 3)	0	5		(5, 4 3)	0	0	

(b) Chi-squared test contingency table for Channel, Chamber, Culvert and Pipe structural condition

Table 4.5: Chi-squared test contingency table for Channel, Chamber, Culvert and Pipe service and structural condition

4.4.2 Cohort analysis

Each asset group is further divided into several asset types based on their function or characteristic as shown in Appendix B; for example, pipes are divided into three asset types based on the type of water they carry: surface water, foul water or combined. For all assets, other characteristics such as size and material are also recorded in the database. To decide whether the transition rate matrix should be produced based on these groups and characteristics, a correlation between each of these parameters and the service or structural condition was explored with linear regression using a least squares approximation. As the characteristics of Inflow, Outflow and the Structure are scarcely recorded, they are not further divided into smaller cohorts. Tests were therefore performed for Channel, Chamber, Culvert and Pipe, as they are the majority groups with asset characteristics such as material and shape recorded. The resulting significance level of each characteristic is listed in Table 4.6, of which below the 5% (0.05) critical level would be deemed as influential.

Channel	
Characteristics	Significance
Channel Material	1.9×10^{-48}
Channel Shape	0
Route	1.2×10^{-32}
Asset Type	2.3×10^{-5}

Chamber	
Characteristics	Significance
Chamber Material	7.6×10^{-26}
Chamber Shape	0.46
Route	2.3×10^{-16}
Asset Type	5.6×10^{-50}

Culvert	
Characteristics	Significance
Culvert Material	2.9×10^{-5}
Culvert Shape	1.2×10^{-12}
Route	1.4×10^{-17}

Pipe	
Characteristics	Significance
Pipe Size	2.1×10^{-117}
Pipe Material	0.63
Pipe Shape	0.39
Route	1.3×10^{-20}
Asset Type	0.19

(a) Linear regression result of the asset characteristics with service condition score

Channel	
Characteristics	Significance
Channel Material	3.07×10^{-31}
Channel Shape	0
Route	5.4×10^{-109}
Asset Type	1.4×10^{-20}

Chamber	
Characteristics	Significance
Chamber Material	0
Chamber Shape	3.9×10^{-5}
Route	1.2×10^{-234}
Asset Type	5.6×10^{-8}

Culvert	
Characteristics	Significance
Culvert Material	0.03
Culvert Shape	2.6×10^{-130}
Route	1.1×10^{-123}

Pipe	
Characteristics	Significance
Pipe Size	4.5×10^{-7}
Pipe Material	4.9×10^{-60}
Pipe Shape	7.1×10^{-8}
Route	0
Asset Type	5.7×10^{-80}

(b) Linear regression result of the asset characteristics with structural condition score

Table 4.6: Linear regression results of the significance coefficient of different characteristics for channel, chamber, culvert and pipe

The results can be summarised as follow:

- Channel: both service and structural condition are correlated with its material, shape, route and asset type.
- Chamber: service is correlated with its material, route and asset type; structural condition is correlated with its material, shape, route and asset types
- Culvert: both service and structural condition are correlated with its material, shape and route.
- Pipe: service condition is correlated with its size and route; structural condition is correlated with its size, shape and asset type.

The construction material of the assets may affect the rate of deterioration, and hence a higher chance to form cracks and collapse, which means a higher rate of structural condition degradation. It can also lead to a higher possibility of increase in surface roughness and hence an increase in the probability of lower hydraulic capacity, lower flow velocities, and higher likelihood of sediment derived blockage and hence a higher rate of service condition degradation. With different size, assets are expected to enable different flow rates to pass through. Higher flow rates without an adequate slope gradient could bring more debris and cause sedimentation which can then lead to loss of hydraulic capacity and decline in service condition. Also, smaller pipes may more easily become blocked by large debris at lower flow velocities. For an asset's structural integrity, size and shape would also be influential as they could affect the strength and load bearing ability. If any particular size or shape is more vulnerable to the load from railway trains, asset with these characteristics will have a faster structural condition degradation. The dependence of service and structural score on location may be due to different local hydrological characteristics, as all drainage assets are designed to withstand rainfall events with a certain return period depending on route classification following the company design standards (as stated in Appendix A). It may also be due to the way each route inspects and records the score, which could warrant a future study on uncertainty in condition scoring.

4.4.3 Estimate condition transition matrices

As shown in the last Section 4.4.2, dividing the asset groups into smaller cohorts based on asset characteristic would produce cohorts that have more cohesive asset behaviour. The transition rate matrix of generated by these cohorts will hence potentially give better prediction of the asset degradation process of the assets in each cohort. Although the asset groups can be divided based one or more influential characteristics, the resultant cohort may not have enough data to generate a stable matrix. Hence, as requested by NR, transition matrices are calculated for a selection of asset cohorts which has more than 1,500 assets, and results are available upon request from NR.

For demonstration of the developed methodology, 300mm diameter pipes were chosen, as it has the largest population among all pipe sizes, 78% of pipes that a diameter record

of 300mm. After the data cleanse process described in Section 4.3, the total number of assets used in the analysis for service condition is 33,472 whereas for structural condition it is 30,493. The service condition transition rate matrix for pipes with 300mm diameter is given by the Markov Chain degradation model as:

$$\mathbf{Q}_{service} = \begin{pmatrix} -0.1484 & 0.1295 & 0.0120 & 0.0028 & 0.0041 \\ 0 & -0.0372 & 0.0302 & 0.0041 & 0.0030 \\ 0 & 0 & -0.0342 & 0.0231 & 0.0111 \\ 0 & 0 & 0 & -0.0496 & 0.0496 \\ 0 & 0 & 0 & 0 & 0.0000 \end{pmatrix};$$

the structural condition transition rate matrix is:

$$\mathbf{Q}_{structural} = \begin{pmatrix} -0.0483 & 0.0447 & 0.0033 & 0.0002 & 2.28 \times 10^{-5} \\ 0 & -0.0215 & 0.0209 & 0.0007 & 0.0000 \\ 0 & 0 & -0.0027 & 0.0027 & 0.0000 \\ 0 & 0 & 0 & 0 & 0.0000 \\ 0 & 0 & 0 & 0 & 0.0000 \end{pmatrix}.$$

The one year transition probability can be calculated by taking the exponential of the transition rate matrix \mathbf{Q} ,

$$\mathbf{P}_{service,1} = e^{1 \times \mathbf{Q}_{service}} = \begin{pmatrix} 86.21\% & 11.81\% & 1.28\% & 0.29\% & 0.41\% \\ 0\% & 96.34\% & 2.92\% & 0.42\% & 0.32\% \\ 0\% & 0\% & 96.64\% & 2.21\% & 1.15\% \\ 0\% & 0\% & 0\% & 95.16\% & 4.84\% \\ 0\% & 0\% & 0\% & 0\% & 100.00\% \end{pmatrix}.$$

The structural condition one year transition probability matrix is:

$$\mathbf{P}_{structural,1} = e^{1 \times \mathbf{Q}_{structural}} = \begin{pmatrix} 95.29\% & 4.32\% & 0.37\% & 0.02\% & 0.002\% \\ 0\% & 97.87\% & 2.06\% & 0.07\% & 0.00\% \\ 0\% & 0\% & 99.73\% & 0.27\% & 0.00\% \\ 0\% & 0\% & 0\% & 100.00\% & 0.00\% \\ 0\% & 0\% & 0\% & 0\% & 100.00\% \end{pmatrix}.$$

As seen in the service condition transition matrix, for 300mm pipes in all service condition states except condition one, less than 5% of the assets degrade to a worse condition state; whereas for structural condition, less than 5% of pipes in all condition states degrade into a worse condition state. Although the number does not seem large, this small number of degraded pipes can still have a large effect on the performance of individual drainage systems. Railway drainage systems usually consist of a series of drainage nodes and links, that are interconnected to form several drainage pipelines alongside tracks to bring water from a series of inflows to an outfall. If one of the assets fails, for example one of the pipes is blocked or collapsed, it will not only affect its own water carrying ability, but also diminish the upstream hydraulic capacity and potentially cause the whole drainage sub system to fail.

It is also important to look at the condition transitions to the worst state, as a blocked or collapsed pipe would cause shut down for the whole drainage system whereas assets in other condition states would still preserve some functionality. For service conditions, the transition rate to score 5 is the highest from condition 4, which is anticipated as assets that are failing will have a higher chance of losing their functionality entirely. However, for structural condition scores, such a pattern is not observed, this is mainly due to the fact that there are not many 300mm pipes that failed structurally in the period of time. More precisely, there is only one transition from structural condition 1 to 5 and no transition from other condition states to 5. This does not mean that pipes with 300mm diameter do not transit into condition 5. It may simply have a very small probability of collapse in a short time period as pipe usually has a very long life span. The accuracy of the matrix can be improved over time with additional condition observations that provide more information on the degradation rate. Alternatively, statistical models built for other piped systems in other industries might be used as a substitute, however, the uncertainty of such substitution would need to be examined as pipe might degrade with different rates based on their functionality.

It is noted that, for both service condition and structural condition, the likelihood of transition from condition 1 to condition 2 is very high compared to other state transitions. The reasons behind such phenomenon could be varied. The high transition rate could be due to both how condition 1 and 2 are classified and interpreted. Condition 1 is described as no defects/clear, which is only expected to be seen in new build assets; any new build will soon show superficial defects and have potentially small amounts of deposits which have negligible effects on its hydraulic capacity but warrants escalation to condition 2. Hence, a transition from condition 1 to 2 is expected to be easily identified and promptly recorded which will lead to a higher transition rate. However, on the other hand, the definition of whether superficial defects are present can be vague and could vary across inspectors and may be affected by the weather condition on the day of inspection. A superficial defect in one inspector's opinion may seem unnoticeable to another. The subtle difference between service condition 1 and 2 might cause extra fluctuations in condition scores between 1 and 2, and hence induce an increase in N_{12} and hence a higher transition rate from 1 to 2.

It is worth mentioning that all condition scores are purely examined by visual inspection and based on expert knowledge. Without a clear quantification method, human subjectivity is inevitable. A similar 1 to 5 grading system is also being used in the sewer drainage system but with more complex inspection rules (Water Research Centre (Great Britain), 2001). Adopting this more complex systems for railway drainage systems in the future may lead to better condition classification, but is more time consuming and so more costly.

4.4.4 Condition score trajectory simulation

While the above section estimated the probability of transitions for the whole asset cohort, if individual asset degradation is to be simulated, the stochastic simulation algorithm is used as explained in Section 4.2.4 to simulate condition state change. A few exemplar assets' simulated status transitions are presented assuming the asset followed the historical transition rate of the cohort and no intervention will take place in the simulated period (i.e. no improvement in asset condition). The simulation process is forecasted for a period of 50 years from the data cut-off date (19/02/2020). To be noted that the sample trajectories presented are probabilistic, which means that the predicted date of asset degradation is not an absolute certainty. To obtain a more accurate prediction in real-life scenarios, it is recommended to take an average of an ensemble of simulations to represent the most probable time and likelihood of degradation.

Asset Number	Service Condition	Date Of Transition
17344381	2	23/01/2018
17344381	3	04/05/2019
17344381	4	01/08/2026
17344381	5	08/04/2031

Asset Number	Service Condition	Date Of Transition
18911409	2	22/09/2018
18911409	3	15/10/2050

Asset Number	Service Condition	Date Of Transition
17344381	2	23/01/2018
17344381	3	04/05/2019
17344381	4	01/08/2026
17344381	5	08/04/2031

Asset Number	Service Condition	Date Of Transition
18940379	1	06/02/2019
18940379	2	27/10/2033

(a) Service condition simulation for exemplar assets from 19/02/2020 to 18/02/2070

Asset Number	Structural Condition	Date Of Transition
6769394	2	11/09/2019
6769394	3	05/09/2032
6769394	4	03/02/2050

Asset Number	Structural Condition	Date Of Transition
18911409	2	22/09/2018
18911409	3	19/09/2040

Asset Number	Structural Condition	Date Of Transition
17344381	1	23/01/2018
17344381	2	30/06/2022

Asset Number	Structural Condition	Date Of Transition
18940379	1	06/02/2019
18940379	2	18/12/2020
18940379	3	30/08/2046

(b) Structural condition simulation for exemplar assets from 19/02/2020 to 18/02/2070

Table 4.7: Examples of asset service and structural condition degradation trajectory simulation

Four 300mm pipes are randomly chosen as examples, their service and structural condition scores are simulated and the results are shown in Table 4.7. Each sub-table shows the condition transition simulated in the 50 year time period. The first row of each table is the start condition and the date of that condition state measurement was taken, i.e. the last inspected condition score before the simulation start date 19/02/2020. Then the rest of the rows listed have the forecasted condition and the predicted date of transition taken place.

4.4.5 Determine the minimum sample size required

In order to reduce the costs of inspection for buried assets, a method has been proposed in the Section 4.2.5 to determine the minimum number of samples that could provide sufficient data to obtain a stable transition matrix for the degradation model. With any pre-divided cohorts from the above linear regression test, the transition rate matrix will be calculated with various numbers of randomly selected samples. Such results are then to be compared with the transition rate matrix generated from all assets in the cohort, in order to investigate what is the critical number of assets that can represent the whole cohort.

The pipes with 300mm diameter is tested below as an example, following the procedure listed in Section 4.2.5 with chosen value $n=100$ and $m=100$. Results are shown in the Figure ; in the figures, the left-hand y-axis of each sub-plot represents the change of

one element \bar{q}_{ij} in the estimated transition rate matrix \bar{Q}_s with increasing number of samples. For better clarity of the comparison of elements q_{ij} in transition rate matrix Q , all figures of \bar{q}_{ij} are shown as $\frac{\bar{q}_{ij}}{q_{ij}}$. The right-hand y-axis demonstrates the change in standard deviation for each sample size.

Service condition

As shown in Figure 4.2, the sample mean \bar{Q}_s graphs for all elements in the transition rate matrix start to flatten out after around 5,000 samples. Also, the standard deviation decreases dramatically first and then slows down after 5,000 samples, which makes sense because as sample size gets larger, there is less error in estimating the true transition rate matrix. Although for each element \bar{q}_{ij} of \bar{Q}_s the rate of convergence is different, their difference with the q_{ij} in transition matrix Q all converge below 5% after 7,000 samples.

Hence it can be said that for this cohort a 7,000 sample will be able to provide a stable transition rate matrix with a five-year historical data record. Although the transition rate matrix produced with the minimum required sample size is a sound estimation of the whole cohort, a certain degree of uncertainty will always be present, which the asset managers should take into consideration while interpreting the results of this method.

Structural condition

For structural condition, more asset samples are required to generate a stable matrix. Although the standard deviation drops around a 5000 sample size, although high fluctuations in the sample mean still exists until around 20,000 sample size. The highest sample size required for elements \bar{q}_{ij} of \bar{Q}_s to converge within 5% difference of the transition matrix Q is 28,700.

This large value is mainly due to the fact that there is many fewer transitions in the structural condition, and hence whether a particular asset is selected as a sample could make a large difference in the transition rate. For example, there is only one transition from condition 1 to condition 5 recorded throughout the whole time period, when sample size is small, the likelihood of that asset is chosen would be much less, and hence a large sample size is required to ensure this particular asset is included in the dataset used to estimate the transition matrix.

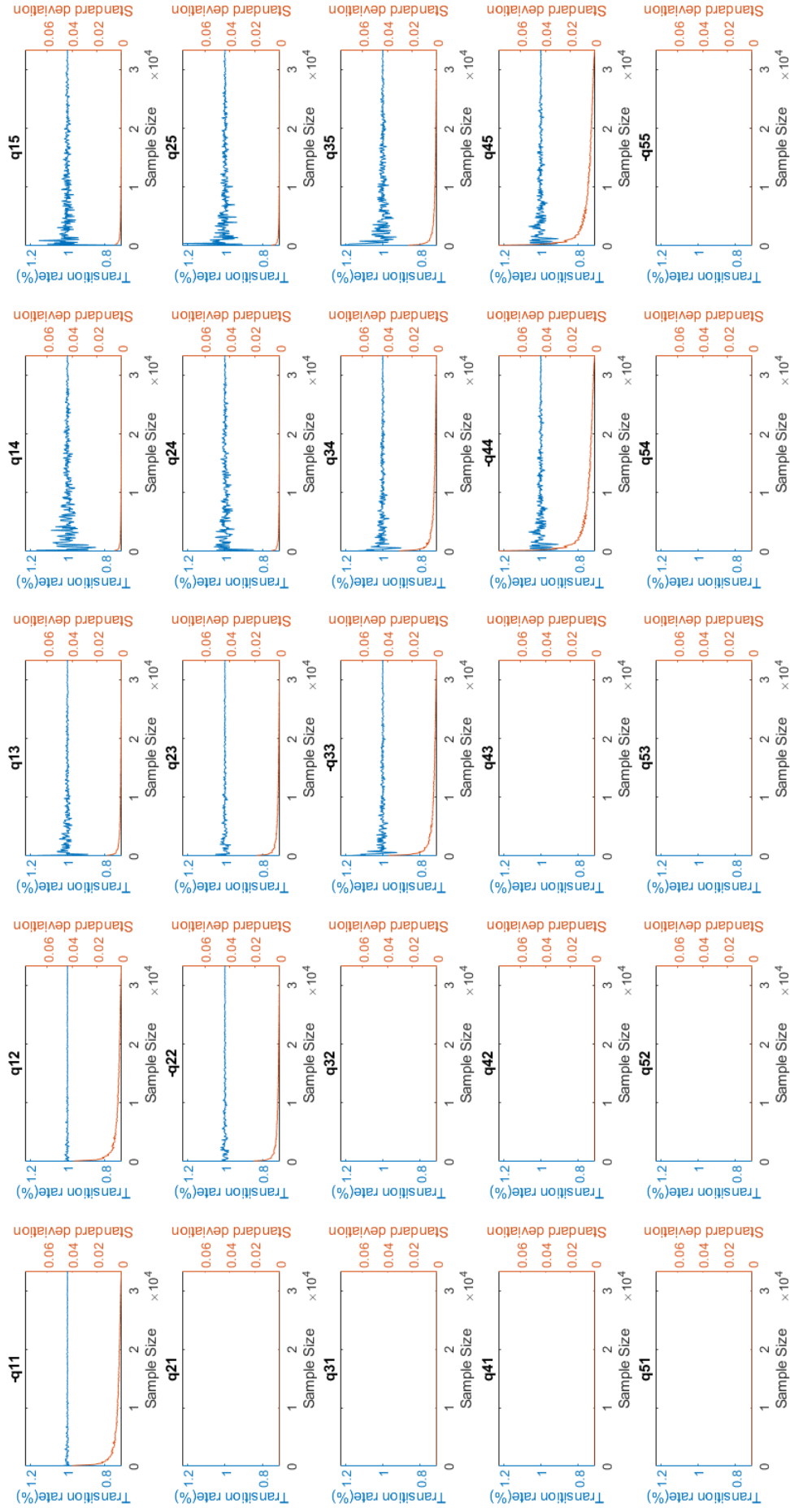


Figure 4.2: Mean and standard deviation of service condition transition rate matrix Q as sample number increases

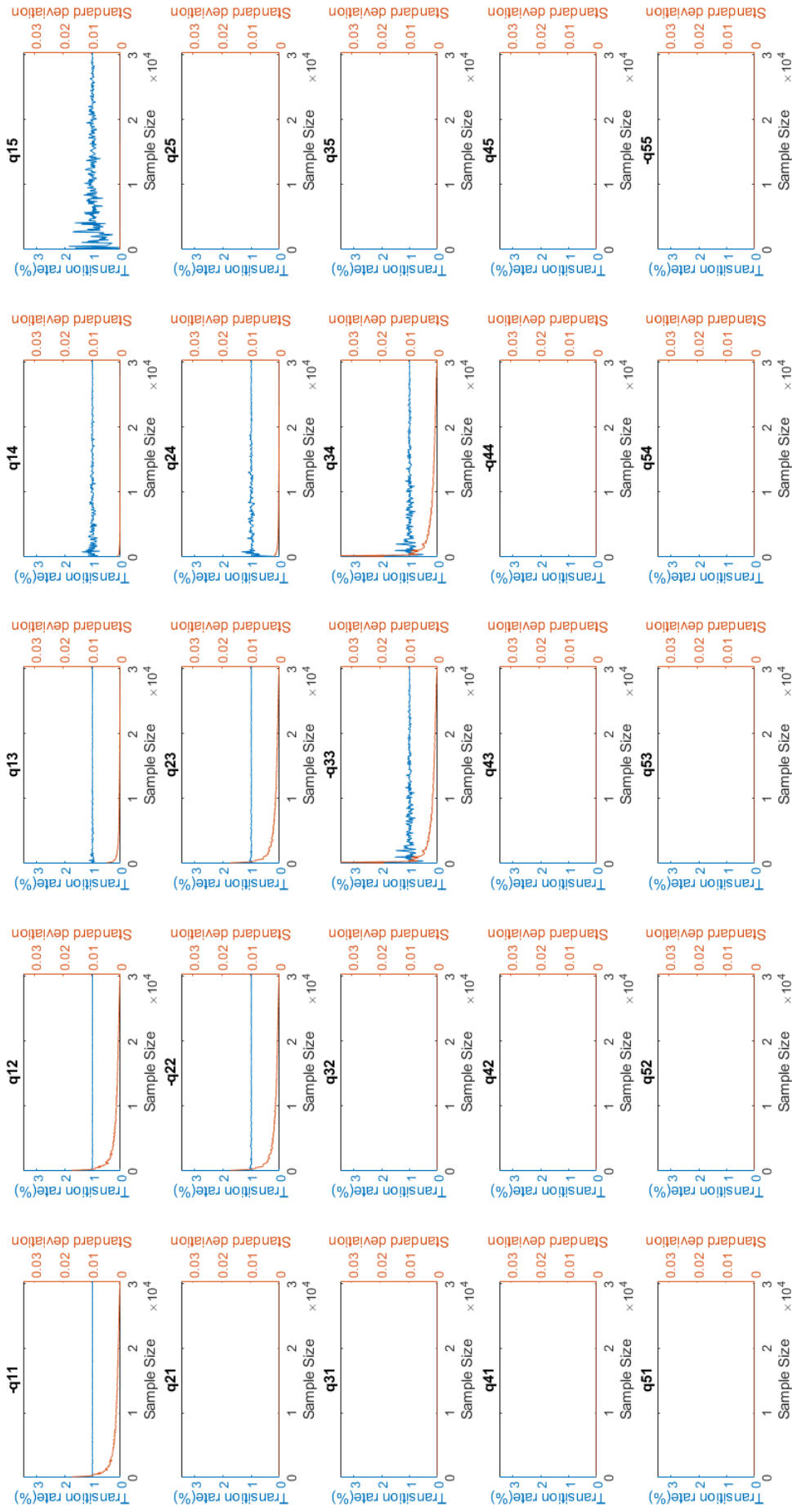


Figure 4.3: Mean and standard deviation of structural condition transition rate matrix Q as sample number increases

4.4.6 Minimum Sample Size Required with shorter timeframe

Although there exists a quite sizable historical condition data record ranging from 2007 to present nationwide, there are some areas that have fewer years of past data and hence it is important to understand how that could affect the number of samples that are required to obtain an accurate matrix.

Number of years	Total number of assets	Number of assets required for a stable matrix	Percentage of Assets Required
5	33,434	5,500	16%
4	32,583	9,300	29%
3	30,441	10,400	34%
2	24,406	11,900	49%
1	14,753	13,300	90%

(a) Number of assets required for a stable service condition transition rate matrix

Number of years	Total number of assets	Number of assets required for a stable matrix	Percentage of Assets Required
5	30,437	27,800	91%
4	29,693	28,200	95%
3	27,765	26,200	94%
2	22,045	19,100	87%
1	13,791	12,400	90%

(b) Number of assets required for a stable structural condition transition rate matrix

Table 4.8: Number of assets required for a stable condition transition rate matrix with 1 to 5 years' historical condition record

The same analysis was performed to investigate the number of assets required to obtain a stable matrix for 300mm diameter pipes (see Table 4.8). For service condition, the percentage of samples required to provide a stable matrix increases as the number of years' data collection decreases. This is because in a shorter period, fewer condition transitions occur, and hence the behaviour of asset degradation would appear to be more volatile, and therefore the degradation matrix over a smaller time window may be less easy to extrapolate into the future. Whereas for structural condition, the number of assets required for a stable matrix does not vary much with the duration of the condition record used. This may be due to the fact that the amount of particular condition status transition is very low (e.g. transition 1 to 5), and this will affect the speed of convergence for the particular element in the transition matrix, and hence lead to a high sample size requirement for all tested datasets.

4.4.7 Model validation

Service Condition

The degradation model is validated with 300mm diameter pipe asset data. The data is randomly split into two groups; one is the calibration group, consisting of 7,000 assets which are shown to be the minimum amount required to generate a stable transition rate matrix for asset service condition; the other contains the remaining assets and is the validation group. The split was done once by randomly selecting 7,000 assets using Matlab function 'randsample'. Although validation may be performed multiple times, it is generally believed that any random split can adequately represent the model validation process. The transition rate matrix is calculated using the calibration dataset assuming no intervention is performed between inspections. This matrix is then applied to the validation set to predict the number of transitions in each condition category. The observed and expected percentage of the condition state transitions are shown in the Table 4.9 below, while the differences between observed and expected percentages are shown in Table 4.10. The number of expected values are on average within 2% of the observed value, which provides sound evidence that prediction of possible transitions in a given period is possible. The only transition with a high difference in transition rate is the transition from condition 1 to 2. This is due to the high variability of the data for transitions from condition 1 to 2, which is also reflected in the Figure 4.2, where the standard deviation of q_{11} and q_{12} with 7,000 samples has one of the highest standard deviation value among all element values. Hence it is more likely that the randomly selected sample groups have a higher difference in their transition rate than the others. Moreover, the difference between condition 1 and condition 2 are minimal, hence there might exist more uncertainty in determining the transition from 1 to 2 purely due to the subjectiveness of different inspectors. Some inspectors may think condition 1 is only designated to newly build assets and mark the asset to condition 2 once on the subsequent visit, whilst other inspectors may continue to use condition 1 if no noticeable defect is observed.

Start Condition		End Condition				
		1	2	3	4	5
1	Observed	77.70%	19.40%	1.87%	0.41%	0.62%
	Expected	80.35%	16.74%	1.83%	0.48%	0.60%
2	Observed		95.53%	3.65%	0.46%	0.36%
	Expected		95.91%	3.16%	0.55%	0.37%
3	Observed			94.84%	3.48%	1.68%
	Expected			96.18%	2.47%	1.35%
4	Observed				92.92%	7.08%
	Expected				93.46%	6.54%
5	Observed					100.00%
	Expected					100.00%

Table 4.9: Observed and expected percentage of service condition transition in validation dataset

Start Condition	End Condition				
	1	2	3	4	5
1	-2.65%	2.66%	0.04%	-0.07%	0.01%
2		-0.38%	0.48%	-0.09%	-0.01%
3			-1.35%	1.02%	0.33%
4				-0.54%	0.54%
5					0.00%

Table 4.10: Difference between observed and expected percentage for service condition validation set

Structural condition

For Structural condition a similar validation process was performed, where the samples dataset containing randomly picked 28,700 assets and the validation set contains the remaining assets. The split was done once by randomly selecting 28,700 assets using Matlab function ‘randsample’. The results are shown in the Table 4.11 and 4.12. For all transitions, the expected and observed percentages have a less than 2% difference. The largest difference appears in the transition from condition 3 to 4. As shown in Figure 4.3, q_{33} and q_{34} are both higher in the variance. The high variance would be due to the fact that the structural condition of buried assets such as pipes is often difficult to visually examine. The change from 3 to a worse condition state might not be noticed until severe obstruction to water flow is observed as a result of structural failure. As a result, the variation of time between condition change from 3 to 4 has high volatility, which leads to the high variability in the observed and predicted transitions.

Start Condition		End Condition				
		1	2	3	4	5
1	Observed	93.88%	5.76%	0.36%	0.00%	0.00%
	Expected	94.01%	5.43%	0.53%	0.03%	0.00%
2	Observed		97.59%	2.41%	0.00%	0.00%
	Expected		97.23%	2.67%	0.10%	0.00%
3	Observed			98.33%	1.67%	0.00%
	Expected			99.71%	0.29%	0.00%
4	Observed				100.00%	0.00%
	Expected				100.00%	0.00%
5	Observed					N/A
	Expected					N/A

Table 4.11: Observed and expected percentage of structural condition transition in validation dataset

Start Condition	End Condition				
	1	2	3	4	5
1	-0.12%	0.33%	-0.17%	-0.03%	0.00%
2		0.35%	-0.26%	-0.10%	0.00%
3			-1.38%	1.38%	0.00%
4				0.00%	0.00%
5					N/A

Table 4.12: Difference between observed and expected percentage for structural condition validation set

4.4.8 Uncertainty analysis

The reliability of the transition matrix is dependent on the quality of the historical asset condition records. The methods used to preprocess the asset condition before input into the degradation model were explained in Section 4.3. The analysis described below has been carried out to understand how various assumptions and data cleanse criteria could affect the degradation transition probability. In this section, different assumptions will be tested to quantify the variability of the output matrix that is due to the uncertainty of the input data. The following analysis are performed with the 300mm diameter pipe cohort.

Case 1

In the above sections, assets that have at least one condition score are included in the study. Assets with only one record are assumed to stay in that condition until the data cut-off date. However, there is a possibility that these data do not provide valid information on the true condition state transitions, as they may have been only inspected once and then forgotten. Lack of frequent inspections for these assets could give a false

illusion that these assets have always stayed in a stable condition whilst they may have already been degraded, or that these assets have stayed in a bad condition while they have been intervened and brought to a better condition. Hence, it is suggested to remove the assets with only one condition record and investigate the effect of such data filtering. The result one-year probability matrices are as follows:

$$\mathbf{P}^*_{service,1} = \begin{pmatrix} 71.82\% & 23.83\% & 2.81\% & 0.64\% & 0.89\% \\ 0\% & 94.09\% & 4.64\% & 0.72\% & 0.55\% \\ 0\% & 0\% & 93.60\% & 4.13\% & 2.27\% \\ 0\% & 0\% & 0\% & 91.20\% & 8.80\% \\ 0\% & 0\% & 0\% & 0\% & 100.00\% \end{pmatrix},$$

$$\mathbf{P}^*_{structural,1} = \begin{pmatrix} 88.95\% & 10.07\% & 0.92\% & 0.02\% & 0.01\% \\ 0\% & 96.86\% & 3.04\% & 0.10\% & 0.00\% \\ 0\% & 0\% & 99.53\% & 0.47\% & 0.00\% \\ 0\% & 0\% & 0\% & 100.00\% & 0.00\% \\ 0\% & 0\% & 0\% & 0\% & 100.00\% \end{pmatrix}.$$

The difference between the new matrix and the matrix composed with all assets in the cohort in Section 4.4.3 are as follows:

$$\mathbf{P}_{service,1} - \mathbf{P}^*_{service,1} = \begin{pmatrix} 14.39\% & -12.02\% & -1.54\% & -0.35\% & -0.48\% \\ 0 & 2.25\% & -1.72\% & -0.30\% & -0.24\% \\ 0 & 0 & 3.04\% & -1.91\% & -1.13\% \\ 0 & 0 & 0 & 3.96\% & -3.96\% \\ 0 & 0 & 0 & 0 & 0.00\% \end{pmatrix},$$

$$\mathbf{P}_{structural,1} - \mathbf{P}^*_{structural,1} = \begin{pmatrix} 6.33\% & -5.75\% & -0.55\% & -0.04\% & 0.00\% \\ 0 & 1.02\% & -0.98\% & -0.04\% & 0.00\% \\ 0 & 0 & 0.21\% & -0.21\% & 0.00\% \\ 0 & 0 & 0 & 0.00\% & 0.00\% \\ 0 & 0 & 0 & 0 & 0.00\% \end{pmatrix}.$$

As expected, there is an increase in the probability of staying in the current status for all condition states, this is due to the fact that assets with only one condition score do not contribute to any of the condition transitions count N_{ij} , whilst they contributed to the holding time R_i since they are assumed to stay in the observed condition from the date of inspection to the data cut-off date. It is noted that for both service and structural condition, the probability of staying in condition 1 has the biggest decrease after the data filtering. This indicated that the assets with only one condition record spend the longest time in condition 1, and this is because the majority of these assets have a condition score 1. This suggests that assets with only one data record do bias the transition matrix.

By removing the assets with one condition score, it could prevent the underestimation of asset degradation rate due to infrequent asset condition inspection. However, on the other

hand, it could also exclude the portion of the asset whose service/structural condition that are genuinely unchanged, and hence cause overestimation in the degradation rate. It can be concluded that the true degradation rate would fall in between the P and P^* . With no additional information, it is impossible to accurately quantify the influence of infrequent inspection. It is hence suggested to the asset manager to appreciate the impact of these data assumptions while making the decision on which data to use for asset management planning. The filtered dataset can be used as an indication of the worst degradation scenario; whereas the unfiltered dataset can be used as a bottom line case. Such differences in results can also be used to support any recommendation to promote a more frequent and regular inspection regime.

Case 2

In the above case, one assumption is made without pre-justification which is that condition transitions happen at the time of inspection. In reality, it is impossible to observe the condition change immediately, hence such assumption should be challenged and there should exist a time lag between the time of degradation and the time of inspection. Without constant monitoring of the asset degradation process, it is hard to define the how long the time lag should be. Therefore, it is assumed in this section that such transition happens half way between inspections and test the difference such an assumption would make to the degradation transition matrix. The resulting one-year probability matrices are as follows:

$$\mathbf{P}^*_{service,1} = \begin{pmatrix} 86.42\% & 11.63\% & 1.27\% & 0.29\% & 0.40\% \\ 0\% & 96.19\% & 3.04\% & 0.44\% & 0.33\% \\ 0\% & 0\% & 96.69\% & 2.18\% & 1.12\% \\ 0\% & 0\% & 0\% & 95.46\% & 4.54\% \\ 0\% & 0\% & 0\% & 0\% & 100.00\% \end{pmatrix},$$

$$\mathbf{P}^*_{structural,1} = \begin{pmatrix} 95.32\% & 4.29\% & 0.37\% & 0.02\% & 0.00\% \\ 0\% & 97.84\% & 2.09\% & 0.07\% & 0.00\% \\ 0\% & 0\% & 99.74\% & 0.26\% & 0.00\% \\ 0\% & 0\% & 0\% & 100.00\% & 0.00\% \\ 0\% & 0\% & 0\% & 0\% & 100.00\% \end{pmatrix}.$$

The difference between the new matrix and the matrix composed with all assets in the cohort in Section 4.4.3 are very minimal: less than 0.3% difference for service condition and less than 0.03% difference for structural condition. This may be because the effect of early transition is averaged out across the various condition transitions. It may also suggest that a more frequent inspection regime may not impose a big improvement in the accuracy of the degradation prediction. The example shows that an additional transition inspection placed in the middle of the original two inspections, which provides a more accurate time of condition transition, will not bring much change to the original degradation probability.

4.5 Discussion

As shown above, the continuous Markov Chain model can provide a robust prediction of the service degradation process of the railway 300mm diameter drainage pipes with only 21% randomly selected samples from the entire cohort; and provides a sensible prediction of the structural degradation process with 94% randomly selected samples. Such analysis would help asset managers to justify the overall inspection costs while maintaining a sufficient understanding of degradation process for different asset classes, which would further contribute to objective budget planning of potential maintenance and renewal schemes. Also to be noted, as shown in Section 4.4.6, is that with a longer duration of historical record, fewer asset samples may be required to simulate the whole cohort's service condition degradation behaviour. However, this may not apply to structural condition, at least not for the 300mm pipe cohort chosen in the case study. This may be due to the fact that structural condition transitions have a slower speed and hence more asset samples are needed to simulate the whole asset group. These results would provide asset managers with quantitative evidence of the advantages of maintaining a consistent and continuous inspection regime, and guide the extent of such a regime.

Moreover, by combining the degradation estimation with a hydraulic model of the drainage system, there is possibility of estimating the frequency and scale of drainage failure under different maintenance strategies over long time periods. This could allow asset managers to weigh the cost of intervention against the loss of performance quantitatively, hence bringing stronger arguments when producing budget estimations for future asset management purpose.

This Markov Model forms a cornerstone of the decision support tool developed to assist the route managers in prioritising works on drainage assets. For assets that have a detailed track record of condition scores, by comparing the degradation rate of different asset groups and different routes, asset managers will be able to identify the type of asset and the location of the system that is more prone to degradation. Hence they may objectively justify decisions to increase the inspection frequency and prioritise maintenance/renewal works of these assets.

Impact of Intervention

In this study, the effect of apparent historical interventions is removed by disregarding any upgrading incidents in the historical database. Although in this way the effect of intervention is minimised, the interference to the estimation of the degradation rate caused by this data processing process cannot be fully eliminated. It is assumed that if an asset has been upgraded due to an intervention, it stayed in the previous condition until intervention happened. Without intervention, the particular asset may have stayed in its current condition for a further amount of time before degrading, hence this may cause an underestimation of the possibility of remaining in the same condition state, and hence an overestimation of the possibility of degradation. This problem cannot be rectified without establishing a model that could simulate the intervention activities. However,

slightly overestimating the degradation rate may not be a shortcoming in real life, as degradation can always be accelerated due to unforeseen events such as extreme adverse weather conditions; hence it can prepare asset managers with a worst case scenario.

As stated in Section 3.4, there are various intervention options that NR carries out on drainage asset in order to slow down, stop or reset the condition of degraded assets; and hence remedy any unsatisfactory system performance. Each type of intervention is believed to affect condition level as follows and will be implemented in the WLC model using these rules:

- Renew and New Build will reset the condition score to 1.
- Refurbish will improve performance and brings the asset to a certain low condition score with no defect or only superficial defect that does not affect serviceability (ie. condition 1 or 2).
- Maintain will make assets stay in the current condition score for a certain period of time, or brings the asset to a slightly better condition state (lower condition score).
- Inspect & Survey will not have a direct impact on the asset condition level, but will help improve asset knowledge and better monitor the asset condition level change. Hence, it will potentially shorten the reaction time between asset condition degradation and intervention actions.

Besides resetting the asset condition score to 1, renewal of an asset might have other effects on the degradation rate. The degradation rate of a new-build asset might be slower than the older assets in the same condition score category. Such a difference in rate can only be examined if there is information about the age of drainage assets. However, almost all railway drainage assets are of unknown age, many may date from as early as Victorian times. Until additional age related data is provided, this will remain as one of the limitations of the model.

Routine maintenance will defer the rate of degradation in service condition. If routine maintenance is applied to all assets nationwide with the same schedule, its effect will be normalised and will not cause bias in the degradation rate. However, in real life the frequency of maintenance for a particular asset can depend on many terms such as the criticality of the asset failure, the budget allocation of the region and the current condition of the asset. The effect of routine maintenance is to be quantified in further studies and is assumed negligible in this study.

There are currently limited studies on how interventions are affecting the rate of degradation of different types of drainage assets. The effect of intervention is to be investigated by linking the intervention records to the improvement of condition score. Analysis of NR asset database during this study indicated such data are scarce and unorganised. It is uncertain whether the asset owner always updates asset condition data once an intervention is made. Also, drainage asset interventions can be carried out as part of the work order of other railway assets such as earthwork or track, and hence make the linkage to condition score improvement harder to locate. Since all these questions cannot

be answered conclusively given the current quality of NR's asset data, it was decided to overlook the effect of interventions in this study.

4.6 Conclusion

This chapter presented a continuous Markov chain model to quantify the degradation process of the service and structural condition of railway drainage infrastructure in the UK. The model was informed by condition data of the UK railway drainage assets collected by Network Rail. The characteristics influencing the degradation process were studied so that the drainage assets could be divided into homogeneous groups. Hence, the transition matrix derived from each group could predict the probability of the degradation process of individual assets in the group. Methodologies were performed on the case study with NR drainage assets to verify the Markov property of the data set, compute the transition rate matrix, and find the minimum number of samples needed for any cohort of assets in order to get a stable transition matrix that can represent the whole cohort. The model was applied and validated for the service and structure condition degradation of pipes with 300-mm diameter, and the results showed that the difference between the observed and predicted percentage of asset degradation is within 2%.

5 Hydraulic Performance Model

As explained in Section 3.3, in this study models are developed to simulate current railway drainage system performance and forecast the risks of failures under potential future weather conditions and possible asset condition degradation. Two complimentary models were designed, that could accommodate asset management scenarios aligned at a tactical and a strategic level. With a tactical approach, individual route can use the model to find the optimum maintenance schedule that ensures acceptable system performance while minimising the total expenditure for a local area or a particular problematic site, whereas at the strategic level asset managers can make decisions on a national scale by ensuring adequate performance while taking into account the economics of the whole of NR drainage assets over a long time period.

For regions with detailed and complete asset databases, a comprehensive hydraulic model could be built to represent the performance of individual drainage systems. Whereas places with insufficient asset inventory and/or limited recordings of asset characteristics, a data driven failure mode analysis can be used as a substitute. Also, on a strategic level, it would be more cost efficient to estimate the performance of the national drainage assets' performance with a data driven approach than the hydraulic modelling as they are usually more time consuming.

In this chapter, the methodology for the hydraulic performance model to be used in the tactical approach is presented with a case study of a historically frequently flooded site in Scotland. The methodology consists of the following sections:

- Overview: This section provides an outline of the methodology section, including a flow chart of how each subsection is linked and presented.
- SWMM: Introduction of the storm water management model used in the study, listing and describing the steps taken to construct a hydraulic performance model for railway drainage systems using SWMM.
- Data sourcing and processing: This section described the data required to build the hydraulic performance model, including the datasets acquired for this study and the data processing methods used to prepare the data for use in the performance model.
- Catchment analysis: This section described a methodology for determining the catchment area served by any railway drainage system. This methodology helps to prepare the data required for the SWMM model and provides NR with a way of defining the catchment area associated with their railway drainage systems.
- Model calibration: This section described a methodology for calibrating the hydraulic performance model with field collected data such as flow rate and water depth within the drainage system.
- Asset criticality analysis: This section described a methodology for identifying the most vulnerable assets in a railway drainage system using the hydraulic performance model. This helps asset managers locate high-risk or critical drainage assets. In this study, it also helped to optimize sensor placement for field measurements when

monitoring resources are limited.

The case study was then carried out following the methodologies introduced. The case study section consists of the following subsections:

- Digital replica: The exemplar railway drainage system was built into the hydraulic performance model, creating a digital replica of the system in SWMM.
- Catchment analysis: Catchment analysis was carried out for the exemplar system using the methodology described in Section 5.1.4.
- Rainfall data: This section states how the rainfall data used in the case study were acquired and prepared following the methodology described in Section 5.1.3.
- Sensor proposition: Sensors were planned to be placed in the field to collect data for the model calibration. The locations of the sensor placement were decided based on preliminary tests with the hydraulic performance model using historical rainfall time series and the critical asset analysis following the methodology described in Section 5.1.6. Locations of flooded site in the preliminary test and weak links determined in the critical asset analysis are chosen.
- Sensor installation and data collection: This section described the sensor installation procedure, and analyzed the data collected using the implemented sensors.
- Model calibration: This section describes the process of calibrating the hydraulic performance model of the exemplar railway drainage system using the data processed in Section 5.2.5.

5.1 Methodology

5.1.1 Overview

The performance of a railway drainage system could be measured by its available hydraulic capacity due to the nature of its designed purpose, which is transporting water away from other railway assets to protect them and maintain normal operations of NetworkRail. The hydraulic capacity can be modelled using EPA's Storm Water Management Model (SWMM), simulating water flow in the drainage system according to asset conditions, surrounding catchment characteristics and imposed rainfall. When the hydraulic capacity of the system is inadequate, water is expected to come out of the catchpits and accumulate above ground. If the level of the ponded water is higher than the level of the rail, it is defined as a flooding event that could cause obstruction to train operations. The level of flooding can hence be used as the indicator of drainage system failures.

SWMM is a dynamic rainfall-runoff simulation model used for single event or long-term (continuous) simulation of runoff quantity and quality from primarily urban areas (Rossman, 2015). It comprises a rainfall-runoff component and a routing module. The rainfall-runoff component represents the transformation of rainfall into runoff through the user defined catchment areas. Then the routing module transport the runoff through a drainage

system that is composed of pipes, channels, storage/treatment units, pumps, and regulators, into an outfall. It is used throughout the world for planning, analysis, and design related to stormwater runoff, combined and sanitary sewers, and other drainage systems (Rossman, 2015). The railway drainage system can be deemed as a simplified urban storm sewer system with small and elongated catchments, and is well suited to be modelled by SWMM.

The workflow of the methodology section is displayed in the flow chart in Figure 5.1. The general methodology for building a hydraulic performance model with SWMM is described in Section 5.1.2. Data required for constructing the model is listed in the Section 5.1.3 and the methodology of processing the data is also described. In order to obtain the catchment related input parameters, a catchment analysis methodology is developed as shown in the Section section:CathMethod. The developed model using the data prepared can be used in the asset criticality analysis to inform the location of vulnerable assets and hence suggest the locations where field measurement should be taken for model calibration. The methodology of the asset criticality analysis is presented in Section 5.1.6. Once the model is calibrated with sensor data using the methodology explained in Section 5.1.5, the resultant model can be used to provide an accurate evaluation of the railway drainage system performance. It can also be used in the asset criticality analyse to provide a more accurate prediction of the level of risk for drainage assets in the systems.

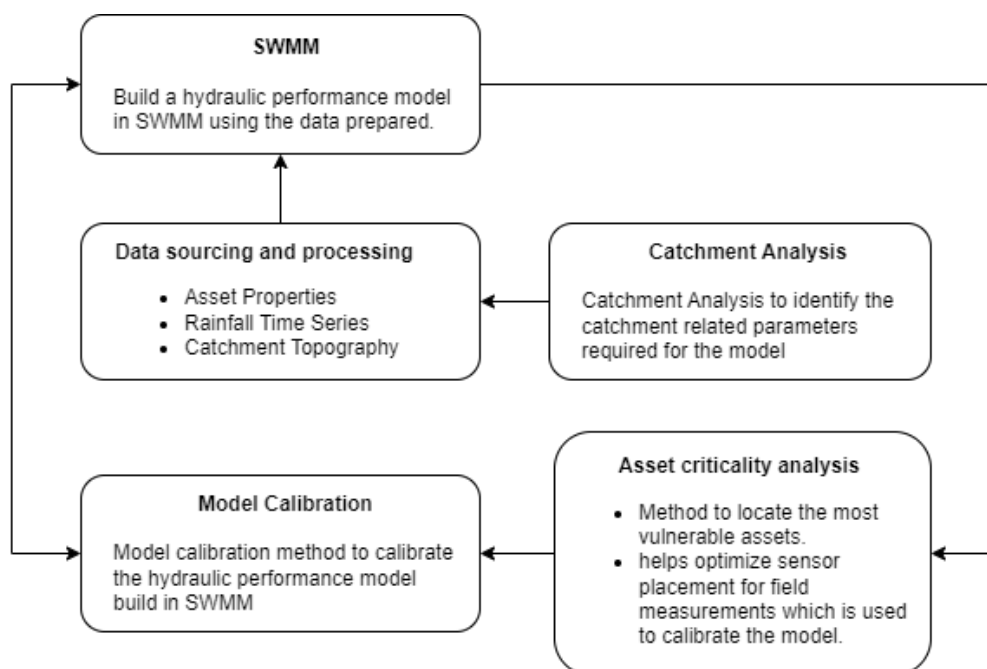


Figure 5.1: Workflow of the hydraulic performance model methodology

5.1.2 SWMM

Water transportation from precipitation into a drainage system is simulated in SWMM as a series of flow exchange between several major environmental compartments. The compartments and their objects used in this study are listed as below:

- The Atmosphere compartment.
It generates precipitation and deposits pollutants onto the land surface compartment. SWMM uses Rain Gauge objects to represent rainfall inputs to the system.
- The Land Surface compartment.
It is represented through one or more subcatchment objects. It receives precipitation from the Atmospheric compartment in the form of rain or snow; it sends outflow as surface runoff to the Transport compartment.
- The Transport compartment.
It contains a network of conveyance elements (channels, pipes pumps, and regulators) and storage/treatment units that transport water to outfalls. Inflows to this compartment can come from surface runoff or from user-defined hydrographs. The components of the Transport compartment are modelled with Node and Link objects. Nodes are points of the system that connect links together, consisting of Junctions, Outfalls, Flow Dividers and Storage Units. Links are the conveyance components of a drainage system that lie between a pair of nodes. Types of links are Conduits, Pumps and Regulators (Rossman, 2015).

The following steps outline the procedure to create a hydraulic performance model for any railway drainage system in SWMM:

1. Build a digital replica of the physical components of the study drainage system using the SWMM objects.
2. Adjust each object properties according to the corresponding drainage asset characteristics and condition information.
3. Perform catchment analysis to find the subcatchments that are served by the drainage system, and analyse their characteristics.
4. Draw the subcatchments in SWMM.
5. Prepare the rainfall time series for each subcatchment.
6. Choose appropriate modelling options.
7. Run the simulation.
8. Extract modelling results from output file.
9. Calibrate Model by comparing field collected sensor data and calibrated results.
10. Use the calibrated model to predict future drainage system performance.

5.1.3 Data sourcing and processing

Prior to building any model, it is important to explore and analyse the data required. For each type of object in SWMM, the properties to be inputted in SWMM are listed in Table 5.1.

Object	Properties
Node (Junctions, Outfalls, Flow Dividers, Storage Units)	All Nodes X-Coordinate, Y-Coordinate, Invert Elevation, Maximum depth, Pondered Area
	Category Specific Flow Divider: Diverted Link, Type of divider and corresponding parameters Storage Unit: Storage Curve and corresponding coefficients
Link (Conduits, Pumps)	Conduits Inlet Node, Outlet Node, Shape, Maximum Depth of Cross Section, Length, Roughness (Manning's n), Inlet Offset, Outlet Offset, Initial Flow, Loss Coefficient
	Pumps Inlet Node, Outlet Node, Pump Curve and corresponding coefficients
Rain Gauge	X-Coordinate, Y-Coordinate, Rain Format, Rain Interval, Data Source
Subcatchment	X-Coordinate, Y-Coordinate, Rain Gage, Outlet, Area, Width, Slope, Percentage of Impervious Area, Manning's n for overland flow over the pervious and impervious area, Depth of depression storage on the pervious and impervious area, Infiltration coefficients

Table 5.1: List of SWMM object properties

Asset Properties

The properties of the Nodes and Links are expected to be found in the drawings and design documents of the study drainage system from the NR drainage databases (Ellipse). Each type of asset in Ellipse is linked to one object in SWMM, for example a Chamber is defined as a Junction in SWMM. In cases where there are insufficient recordings of the study drainage system, or the data quality of the existing asset database is inadequate; field surveying is recommended to obtain the most accurate levelling measures and detailed asset condition information. If surveying could not be performed due to operational difficulties such as restricted accessibility to specific sites, digital terrain models can be

used as a substitute to find the elevation level of the top of the Nodes. However, in this case, the accuracy of the model will be undermined as there is no way to verify the invert level of the Junctions and which will increase the uncertainty in the gradient of the conduits, which is thought to be one of main influence of the hydraulic capacity of the drainage system (Spink et al., 2014).

Rainfall Time Series

Rainfall used in SWMM can be real life data (collected using rain gauges or estimated from radar data), or user selected design rainfall events based on expected return periods. In this study, when real life rainfall data is required, rainfall time series that are produced from rainfall radar data operated by the UK Meteorological Office and processed by the Met Office's Nimrod system is used in the simulations. Data are downloaded from CEDA (Center for Environmental Data Analysis) Archive site. Nimrod is a fully automated system for weather analysis and nowcasting based around a network of C-band rainfall radars located throughout the UK. Four or five radar scans at different elevations at each site are processed to give the best possible estimate of rainfall intensity at the ground (*Met Office (2003): Met Office Rain Radar Data from the NIMROD System*, n.d.). Data files are available at a time resolution of 5 or 15 minutes, on a 1 km and 5 km Cartesian grid, dating from late 2002. For higher accuracy in the performance model simulations given the small contributing areas of railway drainage systems, rainfall time series on a the finer temporal and spatial scale of 1 km grids with a 5 minutes' interval is used.

After downloading the raw rainfall time series data, it is to be cleaned and processed to remove the anomalies such as negative values and repetitive data points. To be noted that subcatchments in the model could cover more than 1 km grid, or span over a few adjacent 1 km grids. Hence, rainfall time series for the catchments should be calculated based on the size of area belongs to each kilometer square grid. It is decided to make the distance between the centroid of the subcatchment and the centroid of each 1 km grid as the indicator of the proportion of rainfall contributed by each grid. The reciprocal of the distance is used as part of the weighting factor to calculate the weighted average rainfall time series for the subcatchment, so that the contributing rainfall amount of each grid is inversely proportional to the distance.

If a subcatchment is to span over n 1 km grids, namely C_1, C_2, \dots, C_n . Let $X_{C_1}, X_{C_2}, \dots, X_{C_n}$ and $Y_{C_1}, Y_{C_2}, \dots, Y_{C_n}$ to be the X and Y coordinates of the centroid of the 1 km grid C_1, C_2, \dots, C_n ; and let $R_{C_1}, R_{C_2}, \dots, R_{C_n}$ to be the rainfall data of each grid. Let X_s, Y_s, R_s to be the X, Y coordinates and rainfall data of the subcatchment. The distance D_{C_i} between the centroid of 1km grid C_i and the centroid of the subcatchment is equal to:

$$D_{C_i} = \sqrt{(X_{C_i} - X_s)^2 + (Y_{C_i} - Y_s)^2} \quad (11)$$

The rainfall data of the subcatchment can be computed as:

$$R_s = \sum_{i=1}^{i=n} W_{C_i} \times R_{C_i} \quad (12)$$

where W_{C_i} is the rainfall weighting factor calculated based on the distance D_{C_i} .

For each grid C_i , W_{C_i} is evaluated by solving the following equation:

Find constant k such that:

$$W_{C_i} = \frac{k}{D_{C_i}}$$

$$\sum_{i=1}^{i=n} W_{C_i} = 1 \quad (13)$$

Catchment Topography

In order to construct the subcatchments in SWMM, topographical catchment analysis is required to identify the boundaries of the contributing subcatchment of the linked railway drainage system. Topographic information can be analysed using Open source data available at DigiMap ¹. The dataset used in this study are:

- OS OpenMap: OS OpenMap is a digital map dataset provided by Ordnance Survey, the national mapping agency of the UK, offering high-quality, vector-based mapping providing geographic information.
- Aerial Image: Aerial Image provides high quality aerial photography of a bird's-eye view over Great Britain. It is ideal for looking at the reality of a location in great detail.
- LIDAR Composite DTM (Digital Terrain Model): A LIDAR Composite DTM is a 3D representation of the earth's surface created from LIDAR (Light Detection and Ranging) data. The data is captured by firing very rapid laser pulses at the ground surface. laser energy reflected back from the ground the surface is examined and captured as a dense cloud of 3D points, which are then converted into highly detailed terrain models of the surface of the earth.

DTM data are available in resolution of 25 cm, 50 cm, 1 m and 2 m. All LIDAR data has a vertical accuracy of +/-15cm RMSE. Highest possible resolution is preferable as higher resolution will enable analysis of more detailed minor drainage features. OpenMap and Aerial Image are used to observe the land use and any minor drainage feature that could not be identified automatically by using the DTM.

5.1.4 Catchment analysis

Catchment Analysis is performed using ArcMap with LIDAR Composite DTM. DTM is converted into raster, which consists of a matrix of cells each containing a value representing the average elevation level of the area in that cell. The size of the cells is determined by the resolution of the DTM data, data with 25cm spatial resolution will produce cells with areas 25x25 cm.

¹<https://digimap.edina.ac.uk/>

After obtaining the topography of the surrounding land, the next step is to investigate the hydrologic characteristics of the surface. In the study of Jenson and Domingue (1988), it demonstrated that algorithms in their computer-based tools could transfer vector-based geographic information systems to drainage lines and watershed polygons and pour point (outlet) linkage information. The algorithm consists of two phases:

1. Conditioning phase that generates three data sets:
 - Original DTM with depressions filled.
 - Flow direction data set which contains the direction of flow for each cell.
 - Flow accumulation data set in which each cell receives a value equal to the total number of cells that drain to it.
2. Application phase that processes the original DTM and these three derivative data sets to delineate drainage networks, overland flow paths, watersheds for user-specified locations, sub-watersheds for the major tributaries of a drainage network, or pour point linkages between watersheds.

A procedure is developed for the small catchments found in this study and performed using several tools within ArcMap to help understanding how water flows across the surface and analysing the subcatchments served by the drainage system. Below listed the steps of using ArcMap tools to determine the contributing area of each subcatchment.

1. Use Fill tool to fill depressions in the surface raster to remove small imperfections in the data.
2. Apply Flow Direction tool to the DTM raster to find the direction of flow from every cell in the raster.
3. Apply Flow Accumulation tool to the Flow Direction raster to calculate accumulated flow and identify streams by locating areas of concentrated flow. vFind points where streams intersect with railway drainage systems.
4. Perform Watershed tool on the Flow Direction raster to find the area that contributes flow to the designated points, which are the junctions of streams and the drainage system determined in step 3.

Once watersheds are determined, they are used as subcatchments in the SWMM model. The following subcatchment characteristic can also be computed using ArcMap tools: Area, Average slope, Flow width, Impermeability. The Slope tool identifies the steepness at each cell of the DTM raster. Average slope is calculated by finding the average of the slope within a subcatchment. An estimate of the subcatchment width is given by the subcatchment area divided by the average maximum overland flow length (Rossman, 2015). Flow length can be computed using ArcMap Flow length tool. Impermeable area is estimated by manual detecting and aggregating the area of building and road in ArcMap using OS OpenMap and Aerial Image.

The details of the algorithm behind each ArcMap tools used are explained below.

Fill

DTMs almost always contain depressions (sinks) that obstruct flow routing (Jenson and Domingue, 1988), hence they should be filled to ensure accurate delineation of watersheds and streams. These sinks are often caused by errors due to the resolution of the data or rounding of elevations to the nearest integer value. The Figure 5.2 shows how the cross section of the landscape changes after Fill is performed (*How Fill works—ArcGIS Pro*, n.d.).

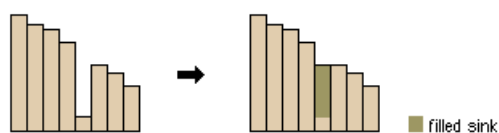


Figure 5.2: Profile view of a sink before and after running Fill

Fill of sinks are performed in the following steps:

1. Identify sinks inside the DTM raster data. A sink is defined as a cell in the DTM raster that has an undefined flow direction, i.e. no cells surrounding it has a lower elevation level.
2. Identify the contributing area of each sink by computing the flow direction of all cells and hence find the watershed of the sink; and then locate the pour point of that area. The pour point is defined as the cell with the lowest elevation on the boundary of the area.
3. If a z-limit is specified, sinks with a maximum difference between the depth of the sink and the pour point of its contributing area that is larger than the z-limit will be filled. Otherwise, all sinks found in step on will be filled.
4. Elevation of the sinks to be filled will be changed to the elevation level of their pour points.
5. As existing sinks are filled, additional sinks may form at the boundaries of the filled areas. Step 1-4 are repeated until all sinks are removed.

Flow Direction

The Flow Direction tool analyses the direction of flow out of the cell. For any given cell, there are eight cells that are spatially adjacent to it in the raster. A unique value is assigned to the processing cell, each representing the orientation of one of the eight directions that the flow could travel in. The procedure is developed by Jenson and Jenson and Domingue (1988) and is usually known as the eight-direction (D8) flow model. The output of the tool is an integer raster whose values range correspond to the orientation of one of the eight cells that surround the cell (x) as follows:

64	128	1
32	X	2
16	8	4

The methodology is presented below:

1. The direction of flow is determined using the maximum drop from one cell to its surrounding cells. The maximum drop is calculated as following:

$$\text{maximum drop} = \frac{\text{change in } z \text{ value}}{\text{distance}} \times 100$$

The z value for this model would be the elevation value of each cell and the distance is calculated between cell centers.

2. Find the adjacent cell/cells with the highest maximum drop, or the steepest descent, and apply one of the following:
 - (a) If the largest maximum drop is less than zero, that cell is given the value of its lowest neighbour, and flow is defined toward this cell.
 - (b) If the largest drop is drop is less than zero, and if multiple neighbours have the lowest value, assign the flow direction as the sum of those directions.
 - (c) If the largest maximum drop is greater than or equal to zero and occurs at only one neighbour, assign the flow direction to that neighbour.
 - (d) If the largest maximum drop is greater than zero and occurs at more than one neighbour, the flow direction is assigned with a lookup table defining the most likely direction. See Greenlee (1987).

Flow Accumulation

The Flow Accumulation tool uses flow direction information evaluated by the Flow Direction tool to calculate accumulated flow for each cell of the DTM raster. Accumulated flow is computed by adding up the weight of all cells flowing into the downstream cell. If no weight raster is provided, a weight of 1 is applied to each cell, and the accumulated flow of any given cell is the total number of cells that flow into it (*How Flow Accumulation works—ArcGIS Pro*, n.d.).

Figure 5.3 demonstrates the conversion of an exemplar flow direction raster into the flow accumulation master. The left two squares illustrate the direction of flow travel from each cell in the graphic way (arrow pointed to the flow direction), and in the numerical format as stored in the flow direction raster file. The right image shows the result flow accumulation raster.

Cells with a high value of flow accumulation are areas where water would concentrate and can be used to identify streams across the land surface.

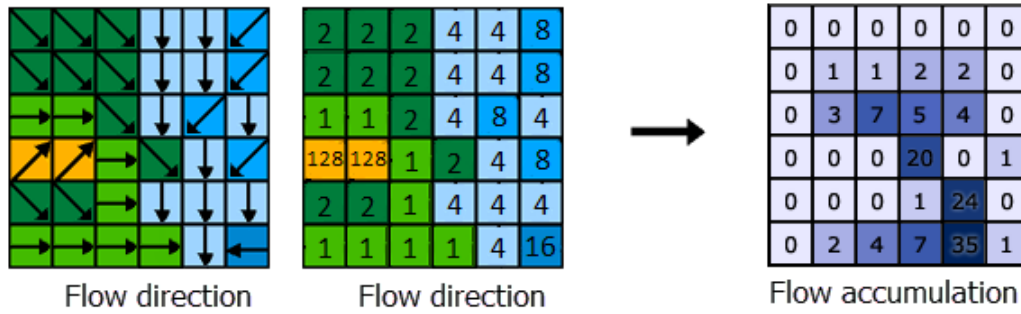


Figure 5.3: Computing the accumulation of flow from flow direction

Watershed

A watershed is the land area that contributes flow to an outlet point where water is assumed to flow out of the area. After the flow direction raster file is computed from DTM using the Flow Direction tool, it can be used by the Watershed tool to delineate the watershed of a designated pour point. The pour points in this model are the points where the overland flow stream intersect with the railway drainage system, and are identified by manual detection on the map. During the watershed generation procedure, the flow direction data set is used iteratively to examine whether each cell will eventually flow into the pour point. Cells contributing to the pour point will be grouped together and form a watershed.

Slope

Slope of a cell is measured as the maximum rate of change in elevation level from the cell to adjacent cells in a 3 by 3 cell neighbourhood. The calculation is performed on a projected flat plane using a 2D Cartesian coordinate system using the average maximum technique as described by (Burrough and McDonnell, 1998)(*How Slope works*, n.d.). The slope is computed using the rates of change of the surface in the horizontal $\left[\frac{dz}{dx}\right]$ and vertical $\left[\frac{dz}{dy}\right]$ directions from the the cell for which the slope is being calculated. Formula of slope calculation in degrees in as follows:

$$\text{slope} = \text{atan} \left(\text{sqrt} \left[\left[\frac{dz}{dx} \right]^2 + \left[\frac{dz}{dy} \right]^2 \right) \right) \times \frac{180}{\pi} \quad (14)$$

Figure 5.4 illustrated the surface scanning window when calculating the slope of the middle cell e. Cells in this 3 x 3 window are labelled by letters from a to i.

a	b	c
d	e	f
g	h	i

Figure 5.4: Profile view of a sink before and after running Fill

The rate of change in the x direction $\left[\frac{dz}{dx}\right]$ and the rate of change in the y direction $\left[\frac{dz}{dy}\right]$ for cell e is calculated with the following algorithm:

$$\left[\frac{dz}{dx}\right] = \frac{(c + 2f + i) \times 4/wght1 - (a + 2d + g) * 4/wght2}{8 \times \text{cellsize in } x \text{ direction}} \quad (15)$$

$$\left[\frac{dz}{dy}\right] = \frac{(g + 2h + i) \times 4/wght3 - (a + 2b + c) * 4/wght4}{8 \times \text{cellsize in } y \text{ direction}} \quad (16)$$

Where wght1, wght2, wght3 and wght4 are weighted counts of valid cells in the bracket beforehand. For instance, if cells c, f and i all has a valid value of elevation level, $wght1 = (1 + 2 \times 1 + 1) = 4$.

Flow Length

By selecting the Upstream direction, the Flow length tool will use flow direction data to find the flow paths from the top of the subcatchment to each cell, calculate the upslope distance along these flow paths and output the longest distance.

5.1.5 Model calibration

Since the rainfall-runoff model of SWMM relies on a number of site specific parameters to simulate the catchment runoff, and some of these parameters such as infiltration levels are not easily obtainable without field studies. These parameters are normally estimated using existing experimental data of sites under similar geographical conditions. However, whenever possible, it is encouraged to calibrate the model using field-measured observations, such as water depth in catchpits and flow discharge volume at the outlet.

The general calibration process is described below:

1. Select a section of the sensor monitored time period as the calibration sample data set.
2. Adjust the model calibration parameters to produce simulations that have the best match for the real life sensor data (water level and flow rate) for defined objective functions.
3. Use the remaining sensor monitored period as a validation data set. Run SWMM model with the selected calibration parameter values for rainfall events in the validation period.

4. Compare simulated results to the sensor data to validate model prediction against defined objective parameters.

SWMM model calibration presents significant challenges since a SWMM model may consist of hundreds of sub-catchments, each having over 20 parameters (Shahed Behrouz et al., 2020). Manual calibration can be labor intensive, hence automatic parameter estimation and calibration methods have been explored to address this challenge (Chamani et al., 2011).

Baffaut and Delleur (1989) developed an automated parameter estimation and calibration procedure that used expert system technology. The system analyses the simulation results and offers recommendations for parameter modifications, hence reducing the user's time and effort. Liong et al. (1991) described a knowledge based system for automating the calibration of the SWMM's runoff block. The proposed method first derives functional relationships using the response surface method and then estimates the optimal set of parameters using a probabilistic approach. Later, Liong et al. (1995) proposed a method of calibrating SWMM using genetic algorithms, which is a search method based on the principles of natural evolution. It selects individuals from the existing population to be the parents and use them to create mutation children by randomly changing the genes of the parent. Population hence can gradually "evolves" towards an optimal solution over various generations. Zaghoul and Kiefa (2001) used an artificial neural network for sensitivity calibration of the SWMM model. However this research was limited to models with impervious areas. An optimization procedure using the complex method was incorporated to estimate runoff parameters, and ten storms were used for calibration and validation (Chamani et al., 2011). The main idea of the complex method is to replace the worst point with a new point obtained by reflecting the worst point through the centroid of the remaining points in the complex. However, all these methods listed above are limited to the calibration of the hydrologic parameters of the Runoff block of SWMM and the Transport compartment was not incorporated due to the complexity of the model, lack of data, and limited resources.

An SWMM calibration method with multi-objective optimisation approach was developed by Herrera et al. (2006) using Non-dominated Sorting Genetic Algorithm (NSGA-II). The model was also originally used to calibrate the hydrologic parameters, it is later used by Arriero Shinma and Ribeiro Reis (2014) to model both the hydrologic parameters (roughness coefficient for impervious areas and pervious areas, min and max infiltration rate, decay coefficient) and the hydraulic parameters (conduit roughness coefficient).

Optimisation is one of the most commonly used approaches to address the problem of model calibration. An optimization problem involves finding the best solution from all feasible solutions. The optimization problem has two core components: (1) Objective Function: This is the function that needs to be optimized (either minimized or maximized), (2) Constraints: These are the restrictions or limitations that define the range of feasible solutions. The Multi-objective optimisation approach is based on the Pareto optimality or non-dominance concept (Herrera et al., 2006). For a multi-objective opti-

misation problem, the objectives may conflict with each other, which means the optimal set of parameters for one objective is different from the optimal set of parameters for one or more of the alternative objectives (Shahed Behrouz et al., 2020). In this situation, the Pareto optimality or non-dominance concept states that for a given set of solutions, there exists a subset of solutions, often referred to as the Pareto front or the non-dominated set, that outperforms the rest of the solution taking all objectives into account. The concept of Pareto dominance is illustrated in Figure 5.5 with an example of a hypothetical calibration problem presented by Herrera et al. (2006).

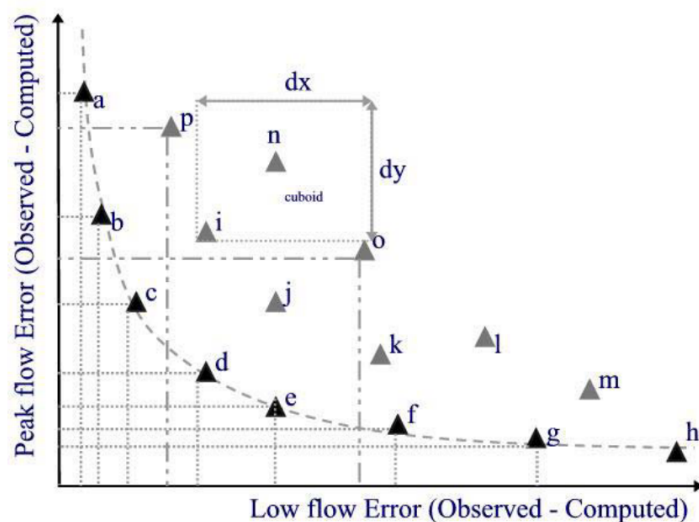


Figure 5.5: Set of Pareto optimal group of solutions for a two-objective hypothetical calibration.

The hypothetical calibration problem has two objectives: minimization of high and low flow model errors. The Pareto front is composed by solutions $\{a, b, c, d, e, f, g, h\}$ while $\{i, j, k, l, m, n, o, p\}$ are dominated solutions. Note that, although $k < f$ in terms of low flows, $e < k$ in both objectives, so k is a dominated solution. When comparing solution e with solution f , none of them are dominated as neither one is better than the other considering both objectives (Herrera et al., 2006).

Several other multi-objective SWMM calibration models were also developed and implemented. Awol et al. (2018) calibrated a selection of representative semi-distributed hydrologic parameters with a multi-objective optimisation approach using the Pareto Archived Dynamically Dimensioned Search algorithm. An automated calibration tool OSTRICH-SWMM was developed by Macro et al. (2019); Shahed Behrouz et al. (2020). SWMM was integrated with the Optimization Software Tool for Research Involving Computational Heuristics (OSTRICH) to enable both single-objective and multi-objective automatic calibration. The tool was tested with a case study catchment in Buffalo, NY and was calibrated according to two objectives: minimizing errors in simulated peak flow and minimizing errors in total flow volume. The Pareto front of the two competing objectives was examined and trade-offs between the two criteria were evaluated.

In this project, an automated multi-objective SWMM calibration model was built based on the similar concept using Matlab. The best fit (optimum) parameters were found by comparing the simulated results systematically. The Matlab-SWMM tool developed in this study is constructed using scripts that interact with the SWMM module and hence enable an automated parameter optimisation process. The tool uses parallel programming so that multiple simulations can run at the same time, which significantly reduces the computation time required. The methodology behind the tool is listed as following:

1. Define a reasonable range for all input SWMM parameters to be calibrated using expert knowledge.
2. Work through each combination of possible parameter values, alter the SWMM input accordingly.
3. Run SWMM simulations for all possible choices within the predefined parameter value range.
4. Extract the time series of SWMM object variables such as flow rate and water depth in each catchpits from the SWMM output files.
5. Use the extracted results and the sensor data to solve the objective functions and find the optimal value for the SWMM parameters.

In this study, the main objective of hydraulic model is to find the time and scale when the drainage system fails under heavy storms. Hence the calibration process should be focused on the peak of the water depth in catchpits, as these values are important to show whether water level will rise above ground level and potentially cause a track flooding failure. The end goal is to find a set of SWMM parameters that gives the best fit simulated peak water depth.

The calibration process is hence designed into two stages:

- Hydrology
The runoff volume will be calibrated by adjusting the infiltration parameters and comparing the simulated and sensor measured volume of discharge.
- Hydraulics
The condition of the drainage assets will be calibrated by adjusting the roughness of the pipes and comparing simulated and sensor measured catchpit depths as well as the flow rate.

Hence for each stage, one or more objectives have been considered. For the Hydrology part, the two objectives are:

1. Minimising the high flow rate error. The objective function is:

$$E_1(X) = \frac{100\%}{n \times m \times 10\%} \sum_{i=1}^n \sum_{top10\%Q_{sensor,i}} \left| \frac{Q_{sensor,i} - Q_{SWMM,i}}{Q_{sensor,i}} \right|, \quad (17)$$

where X is the set of hydrological parameter values such as infiltration rates; n is

the number of flow rate sensors; $Q_{sensor,i}$ is the flow rate recorded by sensor i , and $Q_{SWMM,i}$ is the simulated flow rate by SWMM at the location of sensor i .

2. Minimising the total flow volume error. The objective function is:

$$E_2(X) = \frac{1}{n} \sum_{i=1}^n \frac{\sqrt{\frac{1}{m} \sum_{j=1}^m (Q_{sensor,i,t_j} \Delta t_j - Q_{SWMM,i,t_j} \Delta t_j)^2}}{\frac{1}{m} \sum_{j=1}^m Q_{sensor,i,t_j} \Delta t_j}, \quad (18)$$

where n is number of flow rate sensors; Q_{sensor,i,t_j} is the observed flow rate at time j by sensor i ; Q_{SWMM,i,t_j} is the simulated flow rate at time j at the location of sensor i ; Δt_j is the length of time step, and m is the total number of time steps.

As mentioned above, the trade-off between the objectives in the multi-objective calibration model can be examined using Pareto front. Without additional criteria, all Pareto optimal solutions can be considered candidates for the “best fit” parameter set. The selection of the solution can be made based the asset manager’s objective. By choosing to prioritise minimising $E_1(X)$, asset managers will be able to eliminate more risks of flash flood due to high flow rate. However, this could potentially overestimate the total volume of runoff during a long period and less intense rainfall event and hence overestimate the potential track flooding risk.

For the Hydraulics part, the objective is to minimising the catchpit water depth error, and the objective function is:

$$E_3(Y) = \frac{1}{n} \sum_{i=1}^n \frac{\sqrt{\frac{1}{m} \sum_{j=1}^m (D_{sensor,i,t_j} - D_{SWMM,i,t_j})^2}}{\frac{1}{m} \sum_{j=1}^m D_{sensor,i,t_j}}, \quad (19)$$

Where Y represents the asset characteristic parameters such as roughness and pipe diameter, D_{sensor,i,t_j} is the observed water depth at time j by sensor i ; D_{SWMM,i,t_j} is the simulated water depth at the location of sensor i at time j ; n is the number of water depth sensors and m is the total number of time steps.

Mean absolute percentage error (MAPE) is used for high flow rate error $E_1(X)$ as it is a widely used measure for prediction accuracy and it is present in percentage format which is easier to understand. Also, MAPE is scale independent, hence it is a suitable indicator for evaluating errors of different locations as they are expected to have difference scales of readings. However, for total flow volume $E_2(X)$ and water depth error $E_3(Y)$, MAPE is not suitable since there are 0 values in the time series which cannot be divided, hence, percent root mean square error (%RMSE) (Li et al., 2013) is used as error indicator.

5.1.6 Asset criticality analysis

Once the hydraulic performance model is build, calibrated and validated, it can be used to identify the critical assets of the drainage system. Critical assets are defined as the weak link of the system, and the hydraulic performance will be more prone to changes in their

condition. The method proposed here is the Achilles Approach, since it is a straightforward approach which has been used for the identification of weak points during operation and emergency for the urban water infrastructure, as well as for the identification of most critical elements in a network of sewer system with respect to malfunctioning of the system as a whole (Meijer et al., 2018).

Figure 5.6 shows the flow chart of the steps in determining the criticality of an asset in the drainage system using the Achilles approach. For simulation run 0, all assets are assumed to be in the perfect condition. The simulation result of this run will set a baseline of the system performance. Then the simulation will run for n more times, where n is the total number of conduits in the system. In the run i , where $i \in [1, n]$, the roughness of conduit i is increased to mimic the loss of serviceability when conduit is degraded, whilst leaving the remaining assets under the perfect condition. The results of these simulations were then compared with the baseline performance. The conduit that has the biggest effect on the whole drainage system's hydraulic performance can be found by finding the one causing the highest volume and/or the longest duration of flooding. These conduits are the more vulnerable asset of the system and hence can be defined as critical assets.

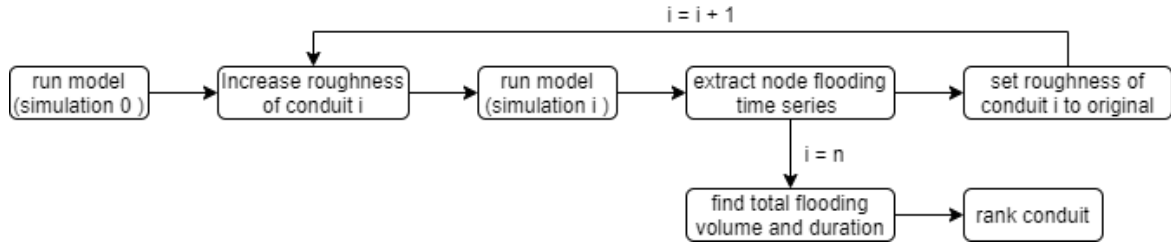


Figure 5.6: Process to determine criticality of individual conduit using Achilles approach

Two indicators are used to define the criticality of the assets. One is the total flooding volume out of all the nodes, as this will define how much water will be accumulated above the ground, which could potentially disturb the train operation. The second indicator is the total duration of flooding across the whole system. If multiple nodes are flooded at the same time, such period of time will only be counted once. The second indicator could measure the time scale of the flooding events, whereas the first indicator will give an overall severity valuation of the flooding event. The two criticality indicators can be expressed as below in $CI_{1,i}$ and $CI_{2,i}$.

$$CI_{1,i} = \sum_t \sum_{s=1}^S FV_{i,s,t} \quad (20)$$

$$CI_{2,i} = \sum_t I_t \quad \text{where } I_t = \begin{cases} 1, & \text{if } FV_{i,s,t} > 0 \\ 0, & \text{otherwise} \end{cases} \quad (21)$$

$CI_{1,i}$ and $CI_{2,i}$ are the two criticality indicators for simulation run i as explained above. $V_{i,s,t}$ is the flooded volume out of nodes s at time t for simulation run i . S is the total number of nodes.

The criticality indicators can be then used to rank the conduits, and hence find out which conduit is more critical for the whole drainage system. In addition, the degree of criticality of can be evaluated by comparing the $CI_{1,0}$ and $CI_{2,0}$, the baseline criticality for simulation 0. Furthermore, the effect of degraded pipe on the location of flooding, and severity of flooding on single locations can also be investigated. Comparing the time series of $FV_{i,s,t}$ and $FV_{0,s,t}$ for any given simulation run i can show the degraded conduit will cause additional flooding at which nodes. Comparing $\sum_t FV_{i,s,t}$ for a given node s across all conduit i will show which degraded pipe will cause the largest flooding volume at node s .

5.2 Case Study

In order to verify the practicality of the proposed method, a case study was performed on a real life functioning railway drainage system. Network Rail’s Scotland Route kindly offered an opportunity to collaborate and provided the Knockenjig Level Crossing site, which has a known history of frequent flooding. The mileage of the site is between GSW 63 m 0565 yards and 63 m 1298 yards, east to the Kirkconnel station. The drainage system starts around the easting and nothing of (274876, 611625). The location of the Knockenjig site is shown in the map in Figure 5.7, marked with a red dot. The site was chosen because it is one of the few available sites that is easily accessible. It is in a rural area with a relatively quiet train schedule, hence the installation of inspection of the site can be arranged without disruption of the train operation.



Figure 5.7: Map of the Knockenjig site location

Since there is limited availability of sensors, water depth sensors and flow rate monitors

were installed in locations identified as links in the system that would provide the most useful information. Asset criticality analysis was also performed before the installation to identify the optimum sensor locations. The proposed location was carefully presented to the installation technicians in detail. Due to restricted access to the site, the installation process was supervised remotely via phone. Once installed, the sensors remained in the test site for a minimum of 6 months. Sensor data were transmitted to the online platform eDas through the telemetry unit every day. The live data were constantly monitored to ensure data quality. At the end of the period, the collected sensor data was used to calibrate the hydraulic performance model and assist further model development.

The following steps are planned to carry out the case study:

1. Collect geometrical and catchment data required to build the model.
2. Build a digital replica of the Knockenjig drainage system in SWMM.
3. Perform catchment analysis for the designated drainage system.
4. Perform preliminary tests on the hydraulic capacity of the system.
5. Determine weak links in the system using asset criticality analysis.
6. Propose sensor locations to a monitoring contractor using analysis results.
7. Instruct a monitoring contractor to install sensors.
8. Collect data from sensors remotely and check for validity.
9. Calibrate and validate SWMM model using collected and checked data.
10. Use the validated model to evaluate Knockenjig drainage system's hydraulic performance against collected historical time series rainfall data.

5.2.1 Digital replica

The digital replica is the virtual replica of the physical drainage assets. Compared to using traditional visual inspections to determine when and where intervention needs to be scheduled, the digital replica provides asset managers with an opportunity to diagnose the root cause of a decline in drainage system performance and predict the potential performance loss due to asset degradation. The model would hence help reduce the costs incurred due to frequent inspections and also reduces the disruption of any unscheduled interventions.

Through discussions with NR asset managers and other European railway asset owners, it was agreed that using digital replicas in asset management would be advantageous. Although drainage systems in the UK are modeled in hydraulic models during the design phase to test whether they meet the design requirements, digital replicas of existing systems have not yet been implemented. French railway operators have begun to build digital replicas of their drainage assets to enhance their understanding of the drainage systems and help them make robust maintenance plans. Hence, I've proposed the method of building a digital replica as part of the hydraulic performance model as described in the Methodology Section 5.1 and demonstrated with this exemplar UK railway drainage

system in Knockenjig. This method can also be applied to other railway drainage systems in the future as it provides a robust tool for evaluating drainage system performance comprehensively. It is therefore suggested that NR carry out a national rollout of the model if sufficient resources and the required asset information are available.

The effectiveness of the digital replica relies on the accuracy and reliability of the data used to build the model. Higher precision of the asset location, characteristics and condition will help the asset manager to better mimic the real world situation. For the provided site at Knockenjig, since Network Rail Scotland is planning to renovate the drainage system to resolve the flooding issue in the next few years, a levelling survey was produced using high accuracy laser levels in order to provide a system design specialist with detailed information of the existing drainage system and surrounding topography.

Elevation data are all indicated in the CAD drawings, a snapshot of the drawing is presented in Figure 5.8. Essential elevation readings were extracted to be input into the digital replica, for example, the invert level of the pipes and culverts, elevation levels of the top and bottom of the catchpits, and contour lines in 50 cm scale covering the width of the rail. In the drawing, the surveyor also indicated important information of the asset characteristics such as the pipe diameter and structure material, which can be used to cross check with the NR Ellipse database to improve the accuracy of the asset property information. The survey also provides additional information such as the location and size of the vegetation, the presence of other NR infrastructure such as fences, elevation level of track and ballast. This additional information would help asset managers indicate any external obstruction that may impose a constraint onto the drainage system such as excess vegetation and potential debris accumulation due to leaf fall. Also, it would help asset managers assess the severity of the flooding as water ponded above ground would be less likely to affect train operation if it is below the top of the railway track.

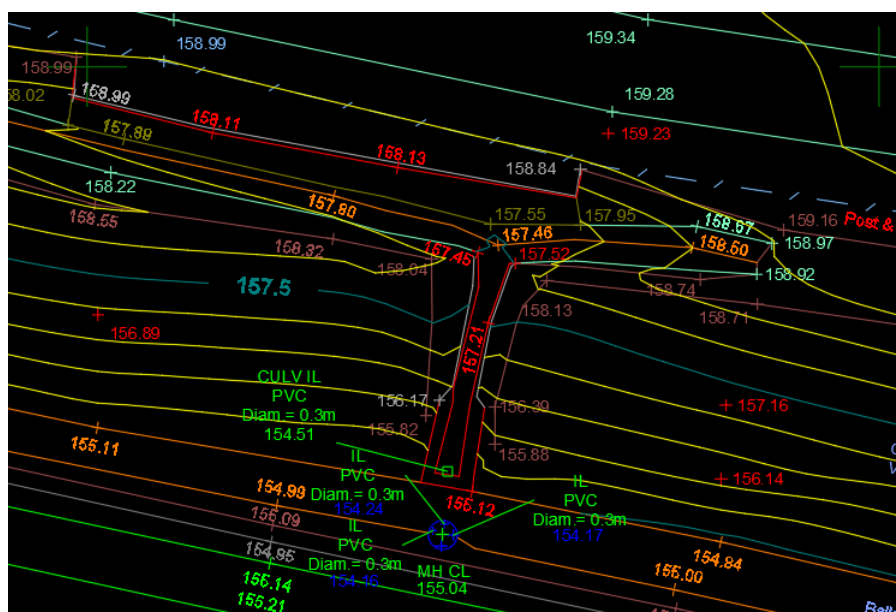
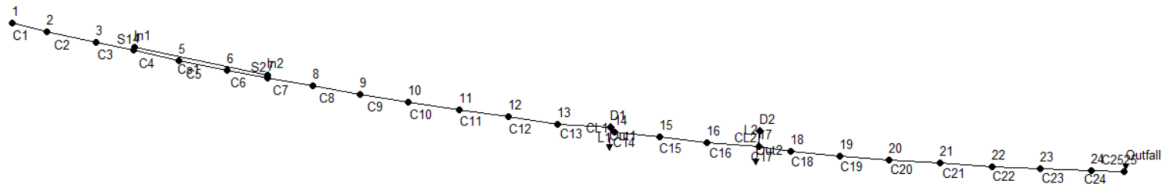
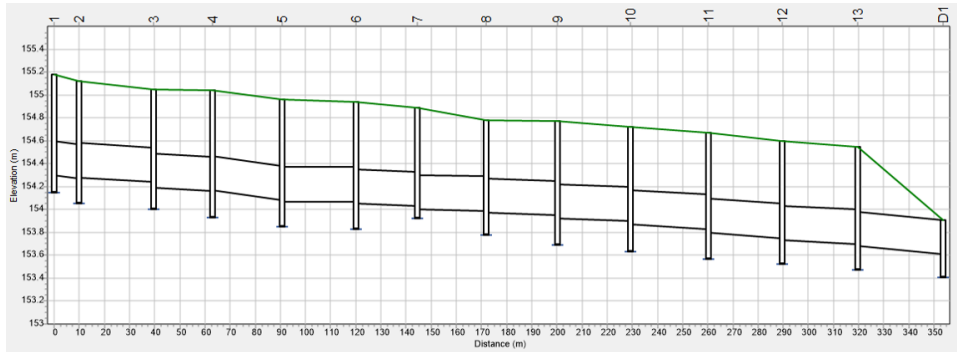


Figure 5.8: Snapshot of the Knockenjig levelling survey



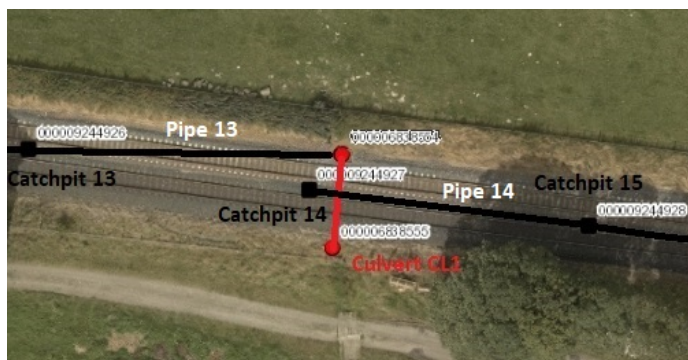
(a) Plan view of the Knockenjig drainage system



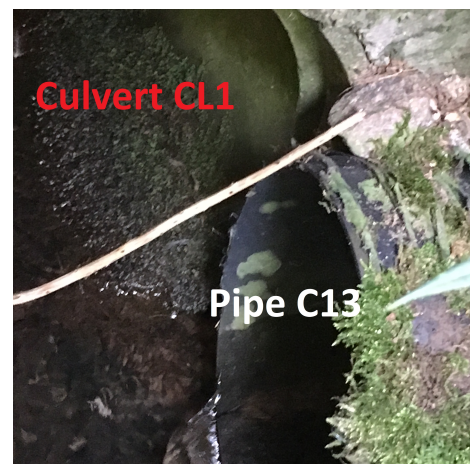
(b) Long section of the Knockenjig drainage system

Figure 5.9: Top view and long section view of the Knockenjig drainage system

A digital replica was built in SWMM from the ground and pipe elevation data. Figure 5.9(b) illustrates a plan view and a cross section view of the Knockenjig drainage system. Although relatively thorough survey data has been provided by the asset management team, some connections between assets are still remain uncertain. This is because in the current NR database, assets are recorded in isolation, interlinkage such as which pipe is connected to which catchpit or discharge point is not logged in the system. Relationships between assets can only be assumed based on the relative locations of them.



(a) Top view of the connection around catchpit 13



(b) Outlet point of pipe C13

Figure 5.10: Connection from catchpit 13 to culvert CL1 (photo taken on 23/08/2019)

Hence a field investigation was conducted by me, my supervisors and the Scotland drainage

asset manager on the 24/07/2019 to further clarify the uncertainties in building the digital replica. For instance, though catchpit 13 and 14 are next to each other, the downstream pipe leaving catchpit 13 does not connect to the catchpit; instead it is connected to the culvert underneath the track to discharge the water cross the railway into the natural stream nearby (photos of the discharging pipe are presented in Figure 5.10).

5.2.2 Catchment analysis

Catchment Analysis was performed using a Digital Terrain Model with 50cm spatial resolution to determine the catchment area serviced by the Knockenjig railway drainage system. The Digital Terrain Model was created from LiDAR data, and the 3D terrain model is illustrated in Figure 5.11. Water concentration features were then analysed and plotted using ArcGIS; the blue lines spanned over the surface in Figure 5.11 indicate the paths where water would flow and accumulate to form water features when precipitation presents. The darker the blue colour means a higher flow accumulation.

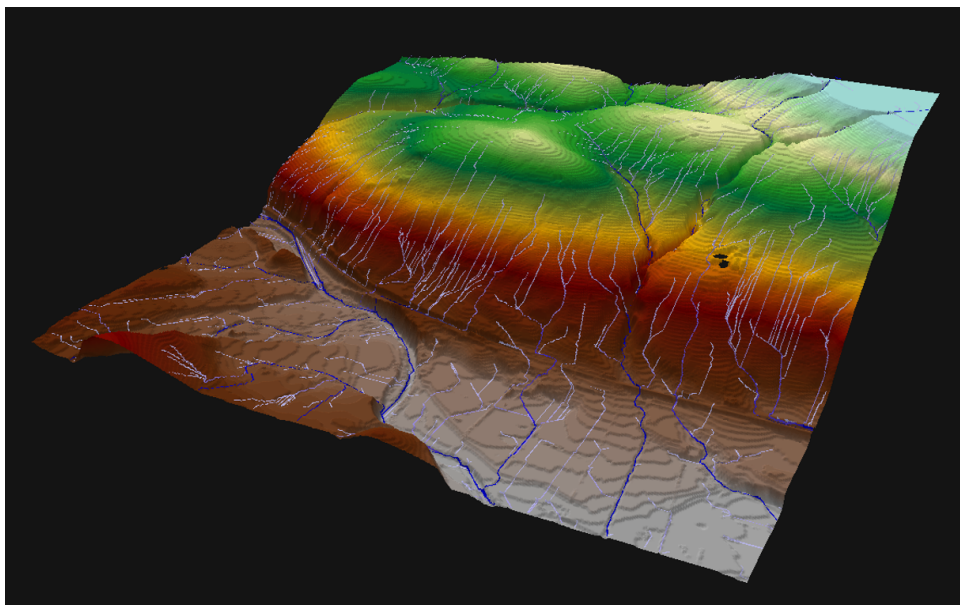


Figure 5.11: The DTM illustration of the topography at the Knockenjig site and the overland water concentration features

In order to find which and where water concentration features feed into the drainage system, drainage assets plotted into the ArcMap and DTM close to the track were investigated. Figure 5.9(a) shows a zoomed-in plot of the DTM model with the railway drainage system. Conduits are marked in light blue and nodes are marked in yellow. Intersection points where the water concentration lines meet the drainage system are marked out in the plot. These points were then used as pouring points in the watershed analysis. Catchments were drawn as the result of watershed analysis, 8 sub-catchments were determined as shown in Figure 5.12. Each colour block corresponds to one sub-catchment, where precipitation onto the land is expected to move across the land following the plotted water concentration paths into the NR drainage system.

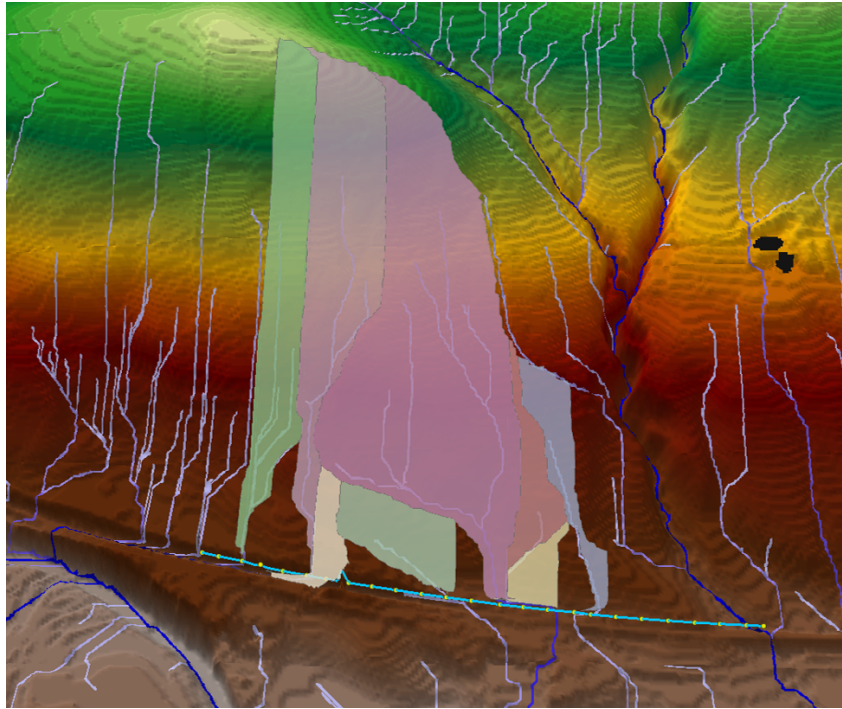


Figure 5.12: Watershed analysis of the Knockenjig site

Sub-catchments are then manually adjusted to include the small areas that have not been assigned an inlet point. The existence of these areas may be due to the fact that they are generally small in size, i.e. no bigger than 0.02 kilometer square, hence the concentration feature in that area is hard to determine or does not exist. Therefore, these areas are all assigned to the downstream sub-catchment. Also, since information from visual inspection and aerial maps indicates that for some adjacent sub-catchments, their water flow paths converge into one ditch above the track before it feeds into the system through one inlet point; these sub-catchments are hence combined into one.

Moreover, it was noticed that the surrounding sub-catchments are mainly composed of pasture land, and hence there are some man-made structures such as fences and paths that may create small water concentration features that affect the overland flow paths but may not be detected by the DTM. As shown in the aerial image in Figure 5.13, in the red circles are two fences parallel to the railway line, which divides up the subcatchments and could direct water to flow alongside them before flowing down the slope towards the track. Therefore, it was decided to split the left two sub-catchments into smaller catchments, since they are narrower and maybe more prone to the disturbance of the fences.



Figure 5.13: Man-made features that could disturb overland flow

After the adjustments of the sub-catchments, the adjusted sub-catchments were extracted and plotted into the SWMM model as shown in Figure 5.14. Area, flow length and slope of the sub-catchments were calculated using ArcMap. All physical characteristics of the sub-catchments required for the model are listed in Table 5.2.

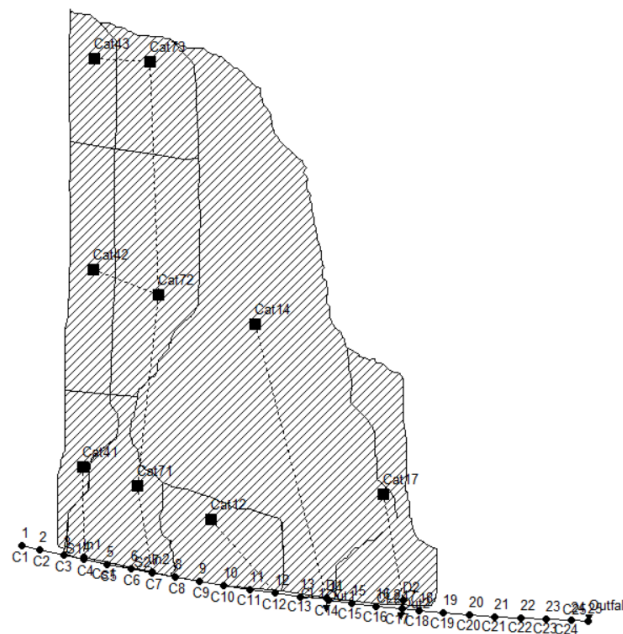


Figure 5.14: Sub-catchments of Knockenjig drainage system

Sub-Catchment	Area (m ²)	Flow Length (m)	Width (m)	Slope (%)
Cat41	6682.53	223.58	29.89	10.79
Cat42	15317.07	299.99	51.06	14.09
Cat43	7963.94	169.33	47.03	13.56
Cat71	14607.02	224.12	65.18	12.72
Cat72	24237.23	330.72	73.29	14.47
Cat73	12829.24	188.52	68.05	14.56
Cat12	13125.22	210.26	62.42	14.42
Cat14	98914.39	756.80	130.70	12.28
Cat17	16225.43	364.92	44.46	12.75

Table 5.2: Sub-catchment characteristics

5.2.3 Rainfall data

Radar derived rainfall data from 2007 to date were downloaded from the CEDA site. Since the rainfall data is produced over 1 km² in 5 minute intervals, the first step was to find out which grid squares the rainfall should be taken from. Figure 5.15 plotted the 1 km grid (yellow lines) on top of the sub-catchments of the Knockenjig system, it can be seen that the sub-catchments are located in the intersection of 4 kilometer squares, hence 4 rainfall time series were extracted to estimate each sub-catchment's rainfall intensity. As explained in the Methodology Section 5.1.3, the distance between the centroid of the sub-catchment and each 1 km grid was used as the weighting factor for the amount of rainfall contributed by that grid to the sub-catchment.



Figure 5.15: Kilometer grid of the rainfall data over the Knockenjig site

5.2.4 Sensor proposition

Water depth sensors and flow rate monitors were installed at locations identified as weak links in the system. The sensors remained in the test site over a minimum 6-month time period, and the collected data was then used to calibrate the hydraulic performance model and assist further model development. It is believed that once the model is fully developed, it will be able to forecast possible flooding events with a minimal number of sensors in a few critical points. Preliminary hydraulic performance analysis and critical asset analysis were performed to help decide how many sensors are needed and where the sensors should be installed.

For this case study, the preliminary hydraulic performance analysis and critical asset analysis was done at the early stage of the research study. At the time the available topographic data available was the OS Terrain 50, which has a lower resolution than the LIDAR Composite DTM used in Section 5.1.4 for catchment analysis, hence the catchment division would be expected to be less accurate. The resulting sub-catchments are demonstrated in the Figure 5.16.

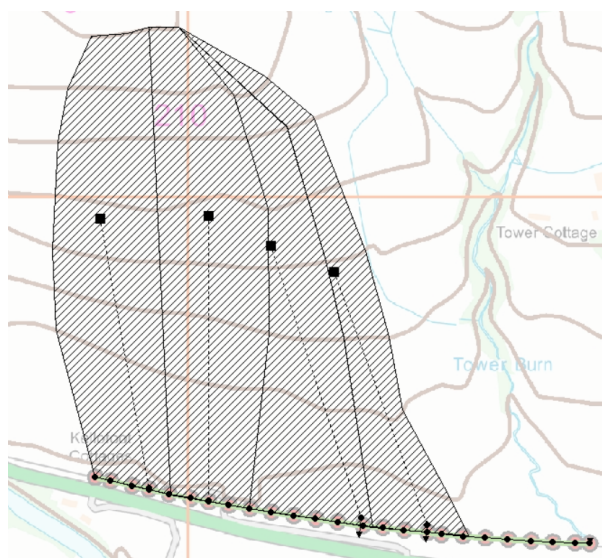


Figure 5.16: Sub-catchments for preliminary test at Knockenjig site derived using OS Terrain 50 data

Preliminary Hydraulic Performance Analysis

Preliminary hydraulic performance analysis was conducted to examine the hydraulic capacity of the Knockenjig system with the available data, and determine the potential locations of flooding.

The hydraulic capacity was tested with historical rainfall data of 2018, under the assumption that all assets have a service condition with no defects. Although rainfall time series is available from 2007, for the preliminary test, it is believed that one year of simulation should provide enough rainfall event samples to give an indication of how the drainage system might behave. Therefore, the year 2018 was chosen as it is the year before the

simulation was carried out, and hence is assumed to best reflect the current weather conditions. Horton’s model was chosen as it is a robust and commonly used infiltration model based on empirical parameters. Also, results from Rajasekhar et al. (2018)’s field tests showed that Horton’s model gives a better prediction than the Green-Ampt model for uncultivated land, which composes the majority of the catchment area. Moreover, tests have been carried out for the different infiltration models with designed rainfall events, and the results showed very similar/identical flow rate and water depth time series. The following simulation options were set for this analysis:

- Infiltration Model: Horton model was selected; default values are used for the four required parameters as listed below.
 - Maximum Infiltration Rate: 3 mm/hr
 - Minimum Infiltration Rate: 0.5 mm/hr
 - Decay Constant: 4
 - Drying time: 7 days
- Routing Model: Dynamic wave model
- Routing time step: 30 seconds
- Reporting time step: 5 minutes

Results show that the system is under capacity to drain runoff away from the track. There is a total of 21.07×10^6 litre flooding loss through catchpits over the whole year. There are 4 flooded catchpits, details of flooding are listed in Table 5.3. Locations of the flooded nodes are indicated with red circles in Figure 5.17.

Node	Hours Flooded	Maximum Rate (m^3/s)	Total Flood Volume ($10^3 m^3$)
4	80.56	0.506	9.232
5	112.56	0.015	4.405
7	91.53	0.162	7.078
D1	1	0.336	0.358

Table 5.3: Node flooding summary table

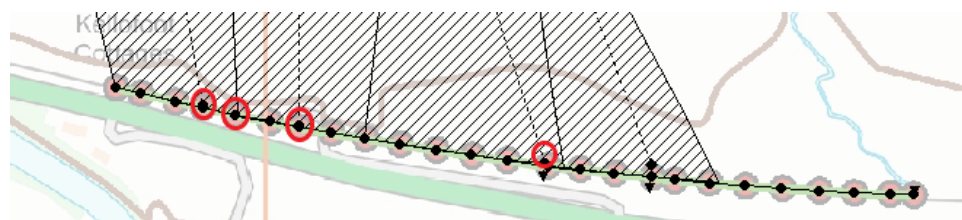


Figure 5.17: Location of Flooded nodes

Catchpits 4 and 7 floods often because they are inlet points of the drainage system, and catchpit 7 has a relatively short depth, which will affect its water storage capacity. Catchpit 5 floods because the pipe linking it with the downstream catchpit is a flat pipe (slope = 0) as shown in Figure 5.18, which will affect the speed of flow and hence the

depth. The node D1 is both the outlet from trackside drainage to the culvert CL1 and the inlet point of adjacent land runoff towards the culvert CL1, hence it would be stressed when experiencing high intensity of rainfall. However, there is very minor flooding (less than an hour) over the whole year, which means the culvert in general is functioning well under current weather conditions.

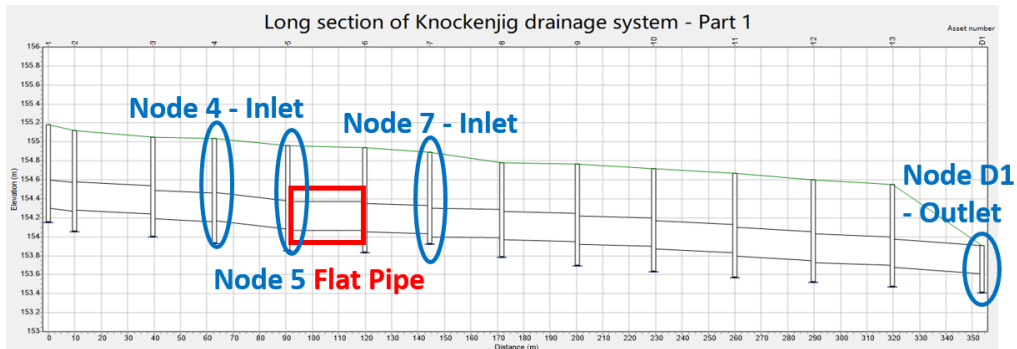


Figure 5.18: Long section view of the flooded nodes

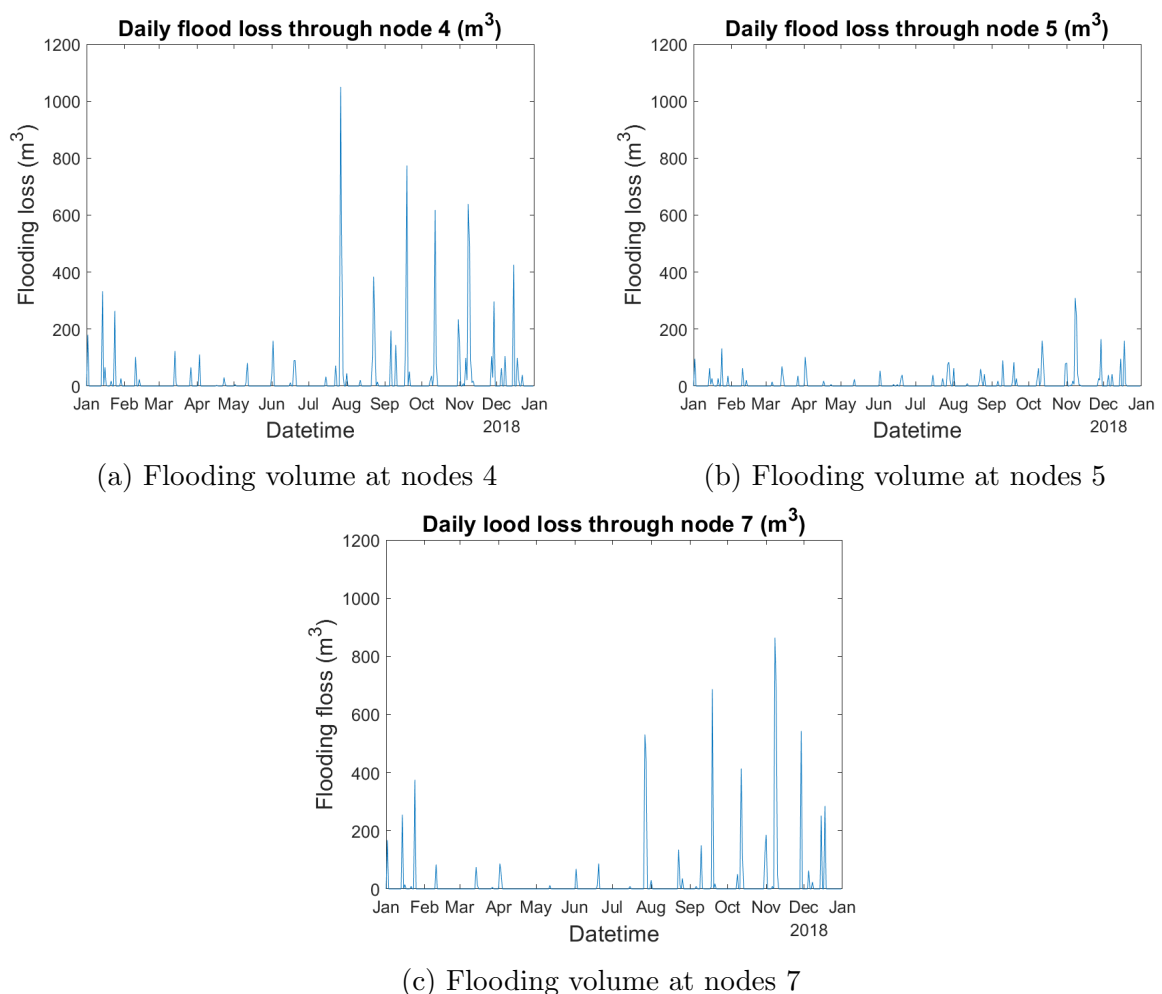


Figure 5.19: Flooding volume at nodes 4, 5 and 7

Figure 5.19 plots the simulated flooding events at the flooded nodes in the year 2018. As shown in the graph, there exists a major flooding event every month since July for nodes 4, 5 and 7.

Asset criticality analysis

Asset criticality analysis was performed to determine the weak links in the Knockenjig drainage system using the methodology explained in Section 5.1.6. Each pipe was individually set to its worst condition by changing its manning's n roughness coefficient to 0.05; then the system hydraulic performance as simulated with the hydraulic performance model to test the importance of each pipe over the whole drainage system. Two factors were used as a numerical validation: a) the total amount of flooding loss over the tested period (ie. aggregate amount of water that came out of all the catchpits); b) the total duration for which flooding occurred (ie. aggregate time whenever water came out of any of the catchpits). The full results are shown in Appendix D. The top 5 critical pipes are listed in Table 5.4. Conduit C8, C9, C10, C13 are in both lists, hence making them the most critical pipes in the system.

Pipe	Total Flooding Volume ($10^3 m^3$)
C13	40.04
C10	37.14
C12	36.54
C9	36.31
C8	35.78

(a) Top 5 Critical Pipes based on Total Flooding Volume

Pipe	Duration of Flooding Occurred (Hour)
C7	221.50
C9	174.00
C10	173.92
C8	173.92
C13	173.50

(b) Critical Pipes based on Total Duration of Flooding Occurred

Table 5.4: Top 5 critical pipes

After gaining an understanding the degradation in condition of which pipe would impose the largest effect on the drainage system hydraulic performance, it could also be in asset managers' interests to investigate the exact location of flooding under the influence of such pipe. In the next step, the time series of node flooding were extracted for each critical conduit, the aggregate flooding volume was calculated and is listed in Table 5.5. As shown in the table, pipe C13 has the largest impact on the flood volume at catchpit 8, whereas for the rest of the catchpits, all 4 critical pipes have a similar effect on the flooding severity. Such results show that the blocked pipe could be somewhere further upstream or downstream from the position of flooded catchpits, the severe flooding at Catchpit 8 is not caused by the worsening in pipe C8's condition which is next to the catchpit, but caused by pipe C13, which is the outlet pipe 160 metres from the catchpit. Therefore, this analysis could help an asset manager to gain better understanding of the cause and effect relationship between asset failure and flooding, and help detect the actual location of problematic assets when flooding occurs in order to give out the best

remediation advice.

Conduit \ Node	1	2	4	5	7	8	13	D1
C8	0.0000	0.0000	9.6972	5.8998	9.7278	10.2960	0.0000	0.2920
C9	0.0000	0.0000	9.6897	5.8869	9.7287	10.8543	0.0000	0.2910
C10	0.0000	0.0000	9.6891	5.8860	9.7293	11.6829	0.0000	0.2890
C13	0.0009	0.0045	9.6753	5.8647	9.7392	14.6343	0.0003	0.2830

Table 5.5: Flooding Volume ($10^3 m^3$) of each node (non-flooded nodes are hidden) when critical pipe is degraded

Sensor Deployment

Based on the results of the preliminary hydraulic performance analysis, a sensor deployment plan created had 4 water level sensors installed into the most frequently flooded catchpits to monitor potential flooding events. The catchpits expected to have more frequent flooding are 4, 5, 7 and D1. Since a water depth sensor will not give additional information of water leaving the system when the catchpit is already flooded, it was also suggested to put one sensor in the non-flooding catchpit as a baseline. It would also be a good idea to put a sensor in one of catchpit 10, 11 and 12; because though they may be unlikely to flood, they are the downstream catchpit of a critical pipe. The critical pipes should be monitored as they are the weak link of the system and the system hydraulic capacity is more sensitive to any changes in their condition. It was also decided to implement 2 flow rate sensors in one of the inlet points and the conduit C13 which is the outlet pipe from track drainage to the under track culvert. This would help to more precisely understand the amount of rainfall runoff entering and leaving the railway drainage system. The sensors were planned to stay in the test site over a minimum of a 6-month time period, and the collected data was used to calibrate the hydraulic performance model and assist further model development. The sensor deployment plan was communicated to a monitoring company, who installed the monitors based on the instructions in the plan.

5.2.5 Sensor installation and data collection

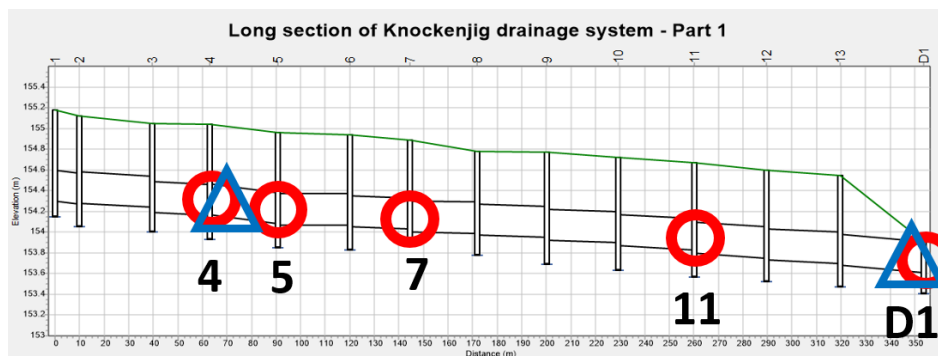
Sensor Implementation

The installation of the sensors was implemented by an experienced monitoring contractor on the 23rd April 2020. I was not able to attend on the installation day due to covid restrictions, however, I was communicating with the installation engineers throughout the whole process with photos and phone calls to check the installation status of each monitor. Live data were available to view online from the eDAS platform from 1st May 2020. Maintenance was scheduled on a quarterly basis to check the general physical condition of the sensor and change the battery when required. Monitor data was therefore continuously reviewed by me for range and noise.

Five water depth sensors and two flow rate sensors were installed; the locations of the sensors are shown in the Figure 5.20. The red circles indicate the locations of the water depth sensors; the blue triangles indicate the locations of the flow rate sensors. The water depth sensors were installed in the catchpits numbered 4, 5, 7, 11 and culvert entry D1. The flow rate sensors were installed in the pipe linking catchpit 4 and 5, i.e. the downstream pipe of the inlet point at catchpit 4; and the pipe linking catchpit 13 and the culvert entry D1, i.e. the outlet point of the system.

Appendix E contains several photographs from the installation team showing the sensor locations within the catchpits/pipes and the conditions of the asset at the time of installation. The detailed installation sheets for the level monitoring locations can be found in Appendix F; these show the depth of installed sensors, level of siltation, and invert level of the catchpits/pipes at the time of installation.

Sensors were set with a logging interval of 5 min and transmitted data to an online server once every 24 hours. These configurations were set to mimic the simulation settings in the drainage system hydraulic model. In the current model, both the rainfall interval and the reporting steps are set to 5 minutes, hence for easier comparison between the collected and simulated water depth/flow rate data, it is best to record the sensor data using the same interval.



(a) Long section of the Knockenjig drainage system



(b) Aerial map of the Knockenjig drainage system

Figure 5.20: Location of the sensors

Sensor Data Processing

Before using the sensor data collected for further model calibration, it is important to first review the data quality and perform a data validation/cleanse to remove any anomalies.

The sensor data were collected from 1st May 2020 to 28th February 2021. For clarity, the sensors are referred to using the abbreviations stated in Table 5.6.

Abbreviation	Sensor description
F1	flow meter sensor in pipe between catchpit 4 and 5 (inlet point)
F2	flow meter in the pipe linking catchpit 13 and the culvert entry D1 (outlet point)
L1	water depth sensor at Catchpit 4
L2	water depth sensor at Catchpit 5
L3	water depth sensor at Catchpit 7
L4	water depth sensor at Catchpit 11
L5	water depth sensor at culvert entry D1

Table 5.6: Sensor abbreviation

The first step of data processing is to look at the consistency of the data, check for any missing data points and identify outliers. Table 5.7 indicated the aggregate duration of the missing data in days, and in which month these missing data points are located. As shown, for most of the months, there is only a very limited number of missing data points, which may be present due to logging or transmission errors. The data in February 2021 for sensor F1 and October 2020 for sensor L4 are missing due the loss of battery power. There are also some missing data in July and August 2020 for L1, L2 and L3, which is due to a configuration issue in the telemetry unit, which had then been rectified in a subsequent maintenance visit.

Month/year	F1	F2	L1	L2	L3	L4	L5
05/2020	0.02	0.201	0.55	0.01	1.51	3.04	0
06/2020	0.52	0.01	1.51	1.01	2.99	1.50	0
07/2020	0.52	0	21.58	17.99	4.00	1.74	0
08/2020	0	0	26.76	17.66	1.51	3.10	0.06
09/2020	0.05	0.05	9.08	1.03	0.05	13.29	0.04
10/2020	0.06	0.03	2.56	1.35	1.32	31.00	1.24
11/2020	0.11	0.08	0.63	0.76	0.78	13.50	0.94
12/2020	0.50	0	0	0	0	0	0
01/2021	0	0	0	0	0	0	0
02/2021	26.88	0	0	0.50	0.003	2.00	0.50
Total	28.64	0.37	62.66	40.32	12.15	69.16	2.78

Table 5.7: Aggregate duration of missing data points in days

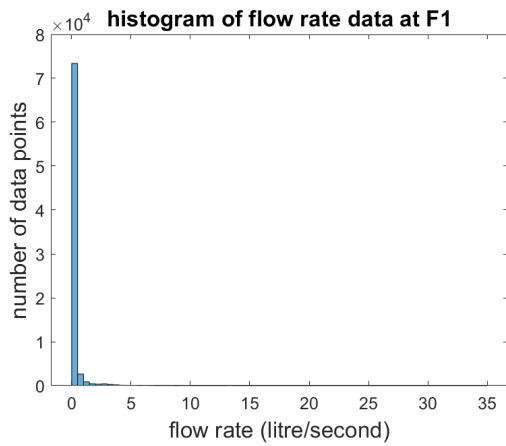
The negative values in the water depth datasets were investigated. Table 5.8 lists the number of negative values from each sensor dataset and the duration of these data.

Sensor	Number of negative values	Duration of negative data (days)
F1	431	1.50
F2	9	0.03
L1	0	0
L2	0	0
L3	1296	4.50
L4	1504	5.22
L5	16	0.06

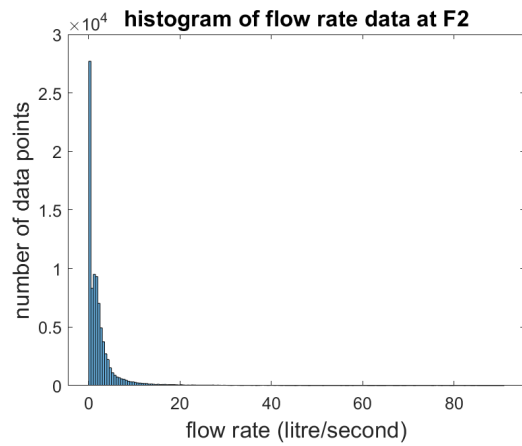
Table 5.8: Negative data points in sensor data

For the flow rate sensor, the flow rate is calculated using the water depth and velocity detected. Hence the negative values could be possible due to errors in the water depth measurement or velocity measurement. When water levels are low the doppler velocity sensor can have significant uncertainty due to the weak/poor reflected signal. For the water depth sensors, the negative values are usually clustered within one day, or a few consecutive days. Hence it can be assumed that the pressure sensor may be impacted by debris which are then resolved naturally as debris are washed away by subsequent inflows. Both issues obviously impact flow rate measurement.

After removing the negative values, the histogram of the sensor data is plotted to help visualise the distribution of the data, and this assists in observing the presence of any outliers. Figure 5.21 contains the histograms of the two flow rate sensor datasets and Figure 5.22 contains the histograms of five water level sensor datasets. After the initial data cleansing described above, all histograms exhibit a lognormal distribution shape, with no abnormal cluster of data at the lower tail of the distribution. For the flow rate distribution, the skewness towards the left is because there is believed to be a constant inflow from groundwater even when there is no rainfall event. Usually, this kind of inflow will have a small but consistent flow rate that may vary seasonally. For water level distribution, the skewness towards the left is due to the fact that there will always be a certain level of water stored at the bottom of the catchpits. Since there is an offset from bottom of the catchpit to pipe invert, designed to catch silt and debris flowing through pipes, it hence also provides a storage space for water causing a constant presence of water in the catchpits.

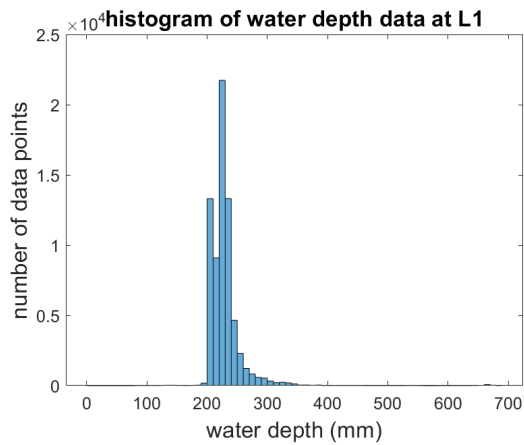


(a) Histogram of flow rate data at F1

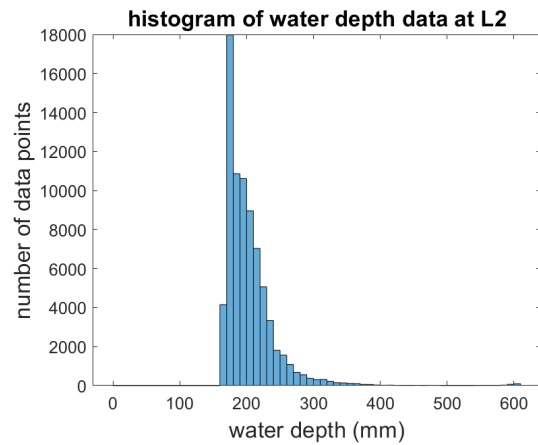


(b) Histogram of flow rate data at F2

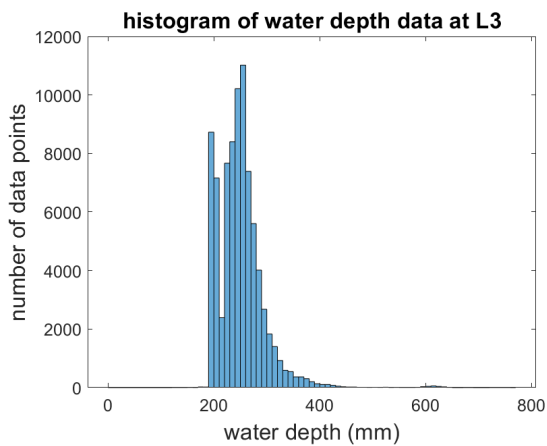
Figure 5.21: F1 and F2 flow rate histogram



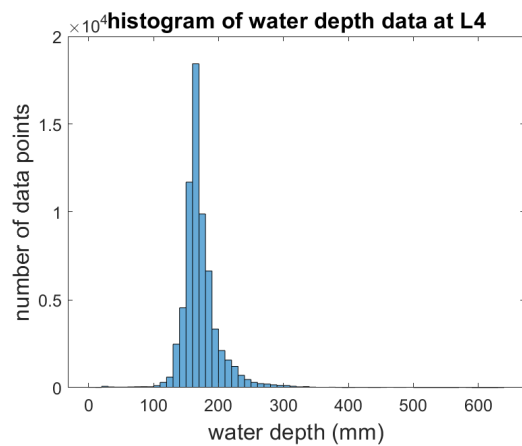
(a) Histogram of water depth data at L1



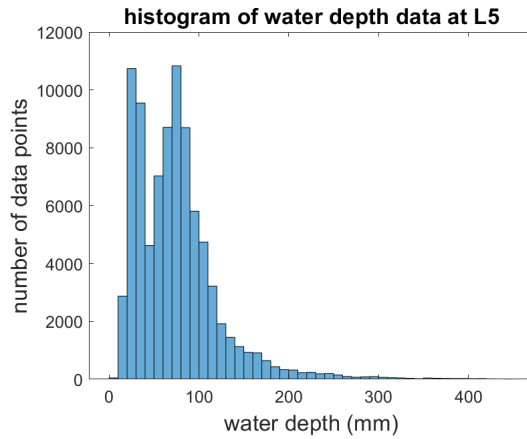
(b) Histogram of water depth data at L2



(c) Histogram of water depth data at L3



(d) Histogram of water depth data at L4



(e) Histogram of water depth data at L5

Figure 5.22: Water level histogram

Data Validation

Although there is no second source of flow volume or flow rate data to check against and verify the integrity of the sensor data, logic tests can be done among different sets of sensor data as they should exhibit correlations between each other. It is logical to assume that the time series of inlet and outlet flow volume are correlated; and the upstream catchpit water depth is correlated to the downstream catchpit water level. Once water enters the piped drainage system, it will not leave until the next catchpit or the outlet. Hence the total amount of water flowing into the system will equal to the volume flow out of the system through the outlet point. Also, the increase in the upstream water depth indicates there is an increase in the amount of flow into the system towards the downstream pipes and outlet point, which should be reflected in an increase in the water depth at the downstream catchpit as well.

The Pearson's linear correlation coefficient between flow rate from F1 and F2 is 0.8476 with a p-value of 0.0000, indicating a strong positive correlation, and the rejection of the hypothesis that no correlation exists between the two datasets. A linear regression test has also been performed and plotted in the Figure 5.23.

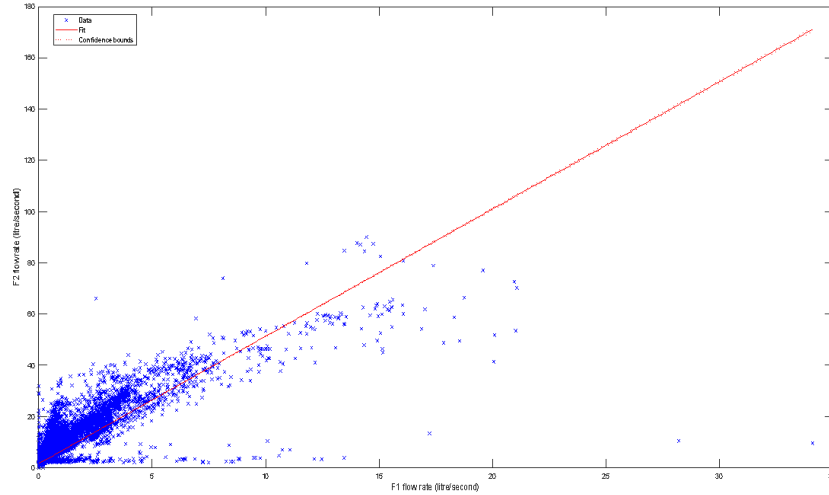


Figure 5.23: Linear regression between flow rate at F1 and F2

The Pearson’s linear correlation test results between water depth level in each of the 5 tested catchpits and their downstream catchpits are listed in Table 5.9. The P-value for all the correlation coefficients in the table 0.0000. Hence it can be concluded that upstream catchpit water level is strongly correlated to the downstream catchpit water level as expected, proving that the sensor data collected are reasonable and expected to be reliable.

	L2	L3	L4	L5
L1	0.9033	0.8564	0.3636	0.8094
L2		0.9662	0.4346	0.9593
L3			0.4181	0.9726
L4				0.4293

Table 5.9: Pearson’s linear correlation coefficient between catchpit water depth time series

Moreover, the amount of inflow is a result of runoff from the precipitation falling on the catchments serviced by the drainage system. Hence it is expected that the rainfall volume will also be correlated with the amount of inflows and outflow of the drainage system.

Therefore, expected correlations between the sensor time series and rainfall volume time series are investigated to examine the reliability of the sensor data collected. The rainfall time series used is the Met Office Rain Radar Data from the NIMROD System, recorded on 1 km grids with a 5 minute interval. Nimrod is a fully automated system for weather analysis and nowcasting based around a network of C-band rainfall radars. Data are downloaded from the CEDA (Center for Environmental Data Analysis) Archive site. The rainfall time series are then logged in the intensity format as millimetre per hour, it is then converted to the total rainfall volume contributing the runoff that enters the system by multiplying the intensity by the catchment area surrounding the drainage

system. Figure 5.24 indicates the area of the corresponding catchment for the inlet point at catchpit 4 and outlet point at culvert entry point D1. The area shaded yellow is served by the inlet point at catchpit 4, so the sensor F1 should recorded the flow rate of the runoff from this area. The area shaded by red is served by the whole drainage system that discharges at Culvert entry point D1, so the sensor F1 should reflect the flow rate of the runoff from this area.

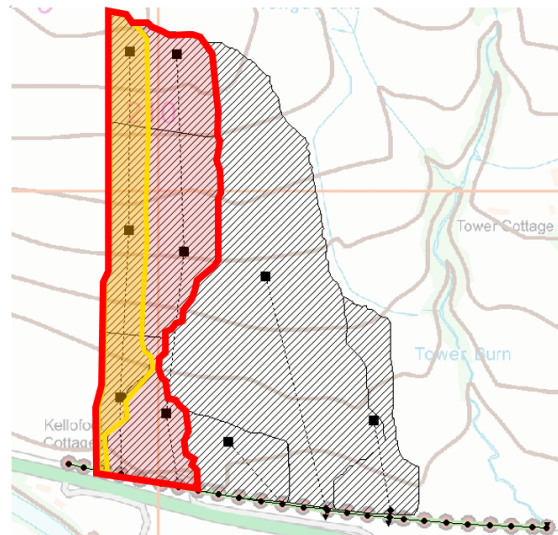
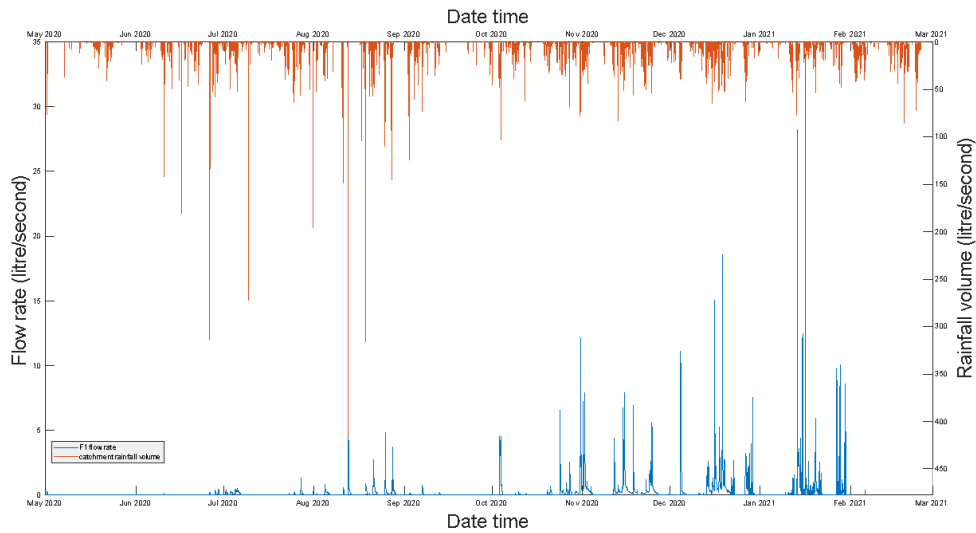


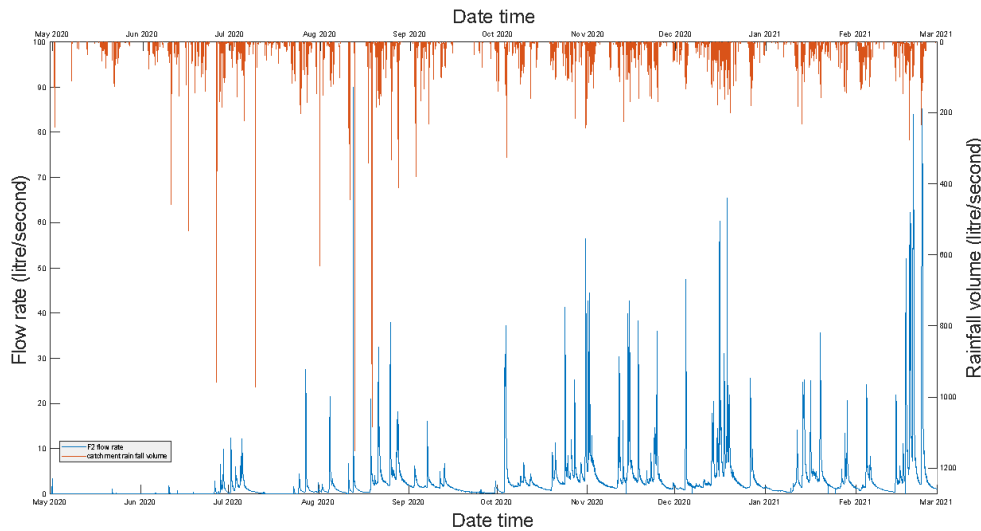
Figure 5.24: Catchments serviced by the drainage system

Figure 5.25 shows comparison plots between the flow rate time series of F4/F14 and rainfall volume from the corresponding catchment areas. As shown in the graph, the peaks of the rainfall coincide with the peaks of the flow rate quite well, indicating both data sets share a very similar pattern. This is expected as the vast majority of the water inflow is due to the rainfall, and higher rainfall volume will cause higher volume of runoffs and hence higher water flow rate collected by the drainage system.

It is noticed that the average magnitude of rainfall volume is higher from February to September 2020, than in the second half of the inspected period. This is due to the fact that there are more convectional storms in summer which provides rainfall events with higher intensity over a short period of time. However, the average magnitude of the flow rate exhibits the opposite behaviour; in general, it has a higher magnitude in the second half of the observed period than the first half. These could be caused by several reasons: the temperature in summer will be higher causing a higher level of evaporation; the soil moisture level could be lower in summer, which leads to higher soil infiltration levels and hence less runoff, and lower flows in the drainage system. Also, since convectional storms happen at a shorter time period and generally are more volatile than frontal driven rain events, the radar measurements of the rainfall intensity may be less accurate.



(a) Flow Rate at F1 and Catchment Rainfall Volume



(b) Histogram of flow rate data at F2

Figure 5.25: Flow Rate at F2 and Catchment Rainfall Volume

Table 5.10 shows the Kendall's Tau coefficient between the water flow rate at F1/F2 and their corresponding catchment rainfall volumes. Kendall's Tau correlation test is used here as the flow rate in the drainage system and the rainfall volume may not be linearly correlated, as the difference between them is caused by non-linearities in the runoff processes such as the soil infiltration process which is still unclear at the current stage. Kendall's Tau coefficient is more suitable here as it provides a non-parametric measure of the strength and direction of association that exists between the two datasets measured. As shown in Table 5.10, both coefficients are positive with p value much lower than 0.05. Therefore, it proves that although the magnitude of the rainfall and pipe flow rate may be affected by seasonality, their trends are still positively correlated with each

other.

	Kendall's Tau coefficient	p-value
F1 flow rate and catchment rainfall volume	0.1028	2.31×10^{84}
F2 flow rate and catchment rainfall volume	0.1189	2.55×10^{149}

Table 5.10: Kendall's Tau coefficient between flow rate sensor data and catchment rainfall volume

The positive correlations demonstrated above between all the listed datasets proves that the sensor data collected are reasonable and are expected to be reliable.

5.2.6 Model calibration

As explained in Section 5.1.5, two phases are involved in the model calibration process. The hydrology phase determines the best fitted hydrological parameters for the small catchments of the tested site, whereas the second hydraulics phase determines the most suitable asset condition parameters of the test railway drainage system at Knockenjig.

The data set is split into two parts, one is used for the calibration process, whilst the other is used for the verification process. Hydrological and hydraulic parameters that best mimic the real situation and best reproduce the sensor data will be found using the calibration methods stated in Section 5.1.5. This set of parameter values will then be verified with the second verification part of the data.

Previous studies have performed sensitivity analysis on SWMM parameters to understand the impact of each on model outputs. Given the considerable number of parameters in the SWMM model, to lessen computational strain, the influential parameters identified by sensitivity tests can guide the selection of key parameters for the calibration process. Based on the review of previous studies carried out by Shahed Behrouz et al. (2020), 7 SWMM parameters that were frequently reported as sensitive in the literature and are relevant to the case study were identified as: "Roughness": Manning's n for the conduits; "N-perv": Manning's n for overland flow over the previous portion of the subcatchment; "Width": Width of the overland flow path for runoff over the subcatchment; "%Slope": Average percent slope of the subcatchment; "MaxInfilRate": Maximum infiltration rate for Horton infiltration; "MinInfilRate": Minimum infiltration rate for Horton infiltration; "DecayConst": Decay rate constant for Horton infiltration. Since the geographic characteristics of the subcatchment ("Width", "%Slope") are determined through the detailed catchment analysis, they are believed to be accurate measurements. Also, Manning's n for subcatchment ("N-perv") has been tested in preliminary trials and shown to be less influential, as a $\pm 70\%$ change in "N-perv" made no change to the high flow error and peak flow error.

Therefore, the hydrological parameters to be calibrated are the three Horton infiltration parameters: the maximum and minimum infiltration parameters and the decay constant. It is difficult to determine the soil properties of the tested site due to the lack of geographical information, and little knowledge of the effect of agricultural use of the surrounding farm land. Hence, initial calibration of a few randomly selected rainfall events are performed to narrow down the range of the infiltration parameters to be tested. This calibration was done using the updated sub-catchment data described in Section 5.2.2. The SWMM simulation was run and the high flow error $E_1(X)$ was calculated to find the optimum solution that could best fit the real time sensor data.

In this study, rainfall events are defined as a continuous period of precipitation, where continuous means that there does not exist consecutive zero precipitation readings for over a period of three hours. Under such criteria, 291 rainfall events are found over the 10 months monitoring period. The histogram of the rainfall events duration and the total precipitation volume over the catchment areas shaded in red in Figure 5.24 are plotted in Figure 5.26. Events with very small rainfall volume (i.e. less than 1 mm rain which means roughly 2×10^5 litres in rainfall volume for the test catchments), and events with a short duration of less than an hour are excluded from the selection.

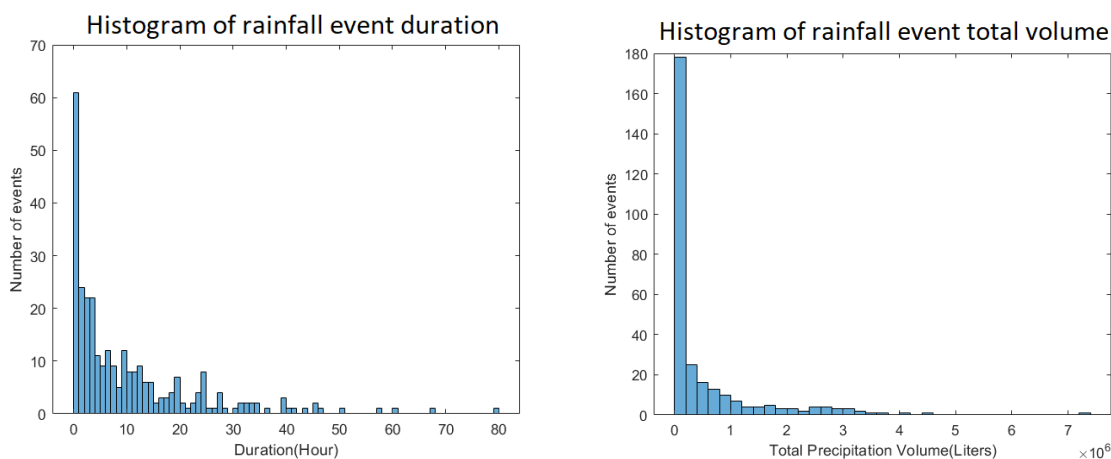


Figure 5.26: Rainfall events duration and total rainfall volume histogram for the test catchment

Seasonal changes in the infiltration rate have been noticed and discussed in many other studies (Horton, 1933, 1940*a*; Cerdà, 1997; Cerdà, 1999; Cerdà, 1996; Beven, 2004; Boddice et al., 2017). However, how the infiltration varies with seasonality is not fully understood, due to the lack of high-quality long-term seasonal field monitoring data of various soil conditions (Boddice et al., 2017). SWMM models were not usually calibrated based on seasonality mainly due to the lack of long period field data. Nonetheless, Shahed Behrouz et al. (2023) assessed the robustness of SWMM under dry and wet hydroclimatic conditions and discovered that the best fit estimates of SWMM parameters (including infiltration rate) differed significantly between dry and wet years. Considering the possible effect of seasonality on rainfall volume and other weather related conditions, in order to

exclude any possible bias in the initial parameter calibration process, three samples are randomly chosen, each from a different season (summer, autumn and winter). The date and time of these three events are listed in Table 5.11.

	Start Date Time	End Date Time
Event 1 - Summer	02/07/2020 22:35	04/07/2020 04:40
Event 2 - Autumn	03/10/2020 06:30	04/10/2020 09:00
Event 3 - Winter	27/01/2021 22:20	28/01/2021 14:40

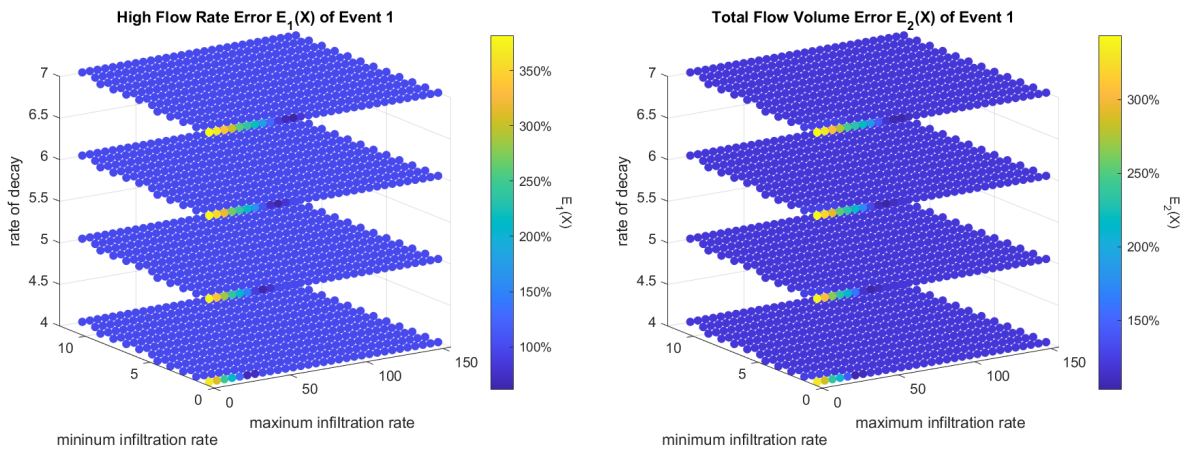
Table 5.11: Sample rainfall events date and start and end time

Simulations are run for these three events using a combination of parameter values as listed in Table 5.12. The range of these parameters are chosen based on the suggested values in the SWMM user guide; the interval is set to pick a moderate number of data points so that the preliminary tests would provide sufficient information to help locate the potential values for the best fit while not taking too much computational time.

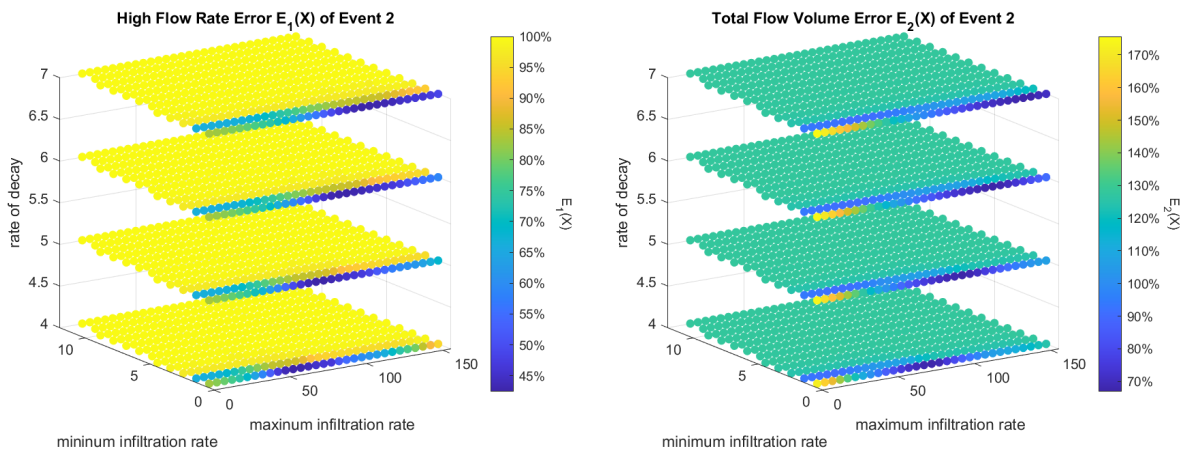
Parameter	Range (mm/hr)	Interval (mm/hr)
Maximum Infiltration Rate	(5,155)	5
Minimum Infiltration Rate	(1,12)	1
Decay Constant	(4,7)	1

Table 5.12: Range and interval of the test parameters

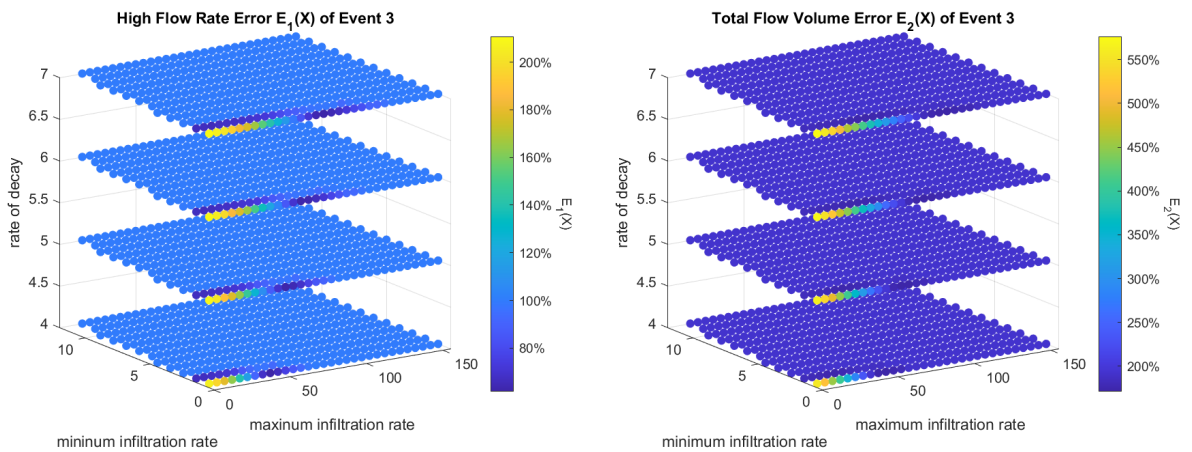
The resulting high flow error $E_1(X)$ and total flow volume error $E_2(X)$ are calculated with simulated flow rate time series and sensor data of F2 which is the outlet of the whole system. It is then plotted in Figure 5.27 and the value of errors are indicated with a colour map. As shown, for all three rainfall events, the colour pattern of the dots with each decay constant number are quite similar, which indicates that the decay constant does not have as much effect on the $E_1(X)$ and $E_2(X)$ as the other two parameters. With small minimum infiltration rates, $E_1(X)$ and $E_2(X)$ are more sensitive to any changes in maximum infiltration rate, as the colour changes rapidly along the maximum infiltration axis when minimum infiltration is 1 or 2 mm/hr.



(a) High flow error $E_1(X)$ and total flow volume error $E_2(X)$ of event 1



(b) High flow error $E_1(X)$ and total flow volume error $E_2(X)$ of event 2



(c) High flow error $E_1(X)$ and total flow volume error $E_2(X)$ of event 3

Figure 5.27: High flow error $E_1(X)$ and total flow volume error $E_2(X)$

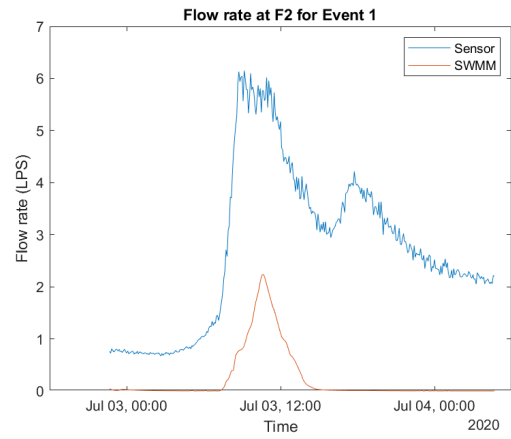
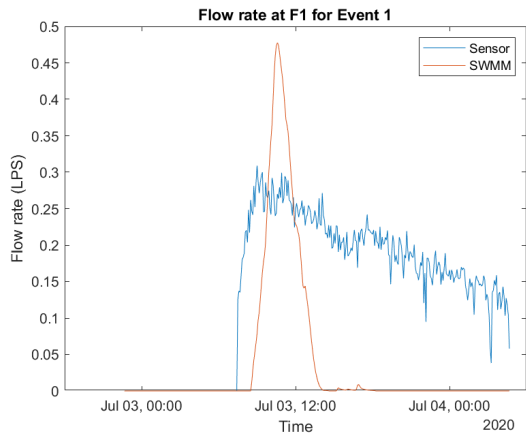
The set of parameters with the minimum value of $E_1(X)$ and $E_2(X)$ for each of the three samples are then found and listed in Table 5.13. The optimum minimum infiltration rate

is the same for all rainfall events, whereas the decay constant varies, but is an insensitive parameter. The optimum maximum infiltration rate is quite different for each event, this may be because the soil moisture level changes with the season. It is noted that, the optimum infiltration rate is higher in autumn and lower in summer, which is not as expected. The infiltration rate is generally expected to be greater in summer (dry season) (Horton, 1940*a,b*; Cerdà, 1997; Beven, 2004). The reason behind this may be due to the nature of summer rainfall events, which are mostly smaller scale convective storms. These storms typically have a shorter duration and tend to be more volatile than frontal driven rain events. As a result, the radar measurements of rainfall intensity might be less accurate, and hence the rainfall data used for calibration could be lower than what was actually received on-site (Schleiss et al., 2020). Such uncertainties that arise from the radar rainfall data can only be mitigated through the use of more accurate, site-specific data collection methods such as rain gauges.

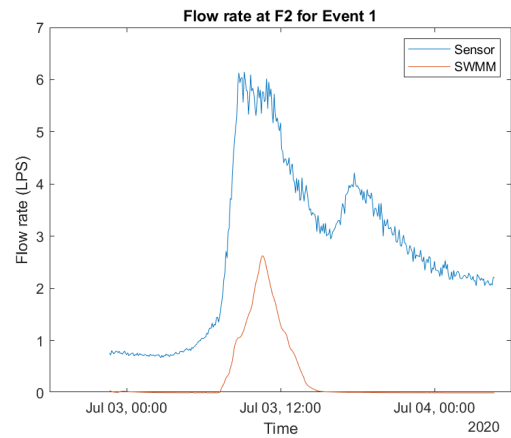
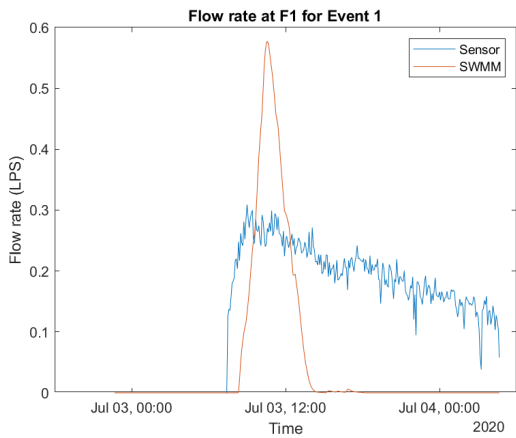
The optimum maximum infiltration ranges from 40mm to 120mm. This implies that the soil could be between clay and loam, and hence its maximum infiltration rate should roughly lie between 8 to 76mm and its minimum infiltration rate should lie between 0.2 and 1.6 mm according to the soil characteristic table (Rossman, 2015). The simulated flow rate time series of flow meter F1 and F2 under the optimum parameters are plotted and demonstrated with the observed flow rate data in the Figure 5.28. Hence the fitness of the simulated results at each flow sensor location can be visually inspected.

Event	Objectives	Optimum Maximum Infiltration Rate (mm/hr)	Optimum Minimum Infiltration Rate (mm/hr)	Optimum Decay Constant
Event 1	Minimise $E_1(X)$	50	1	6
	Minimise $E_2(X)$	40	1	5
Event 2	Minimise $E_1(X)$	110	1	7
	Minimise $E_2(X)$	120	1	6
Event 3	Minimise $E_1(X)$	80	1	7
	Minimise $E_2(X)$	75	1	6

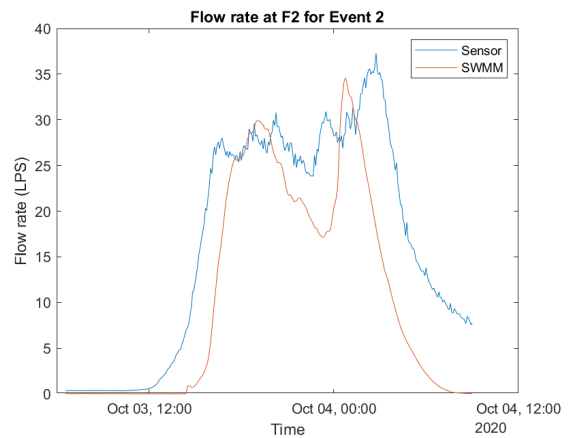
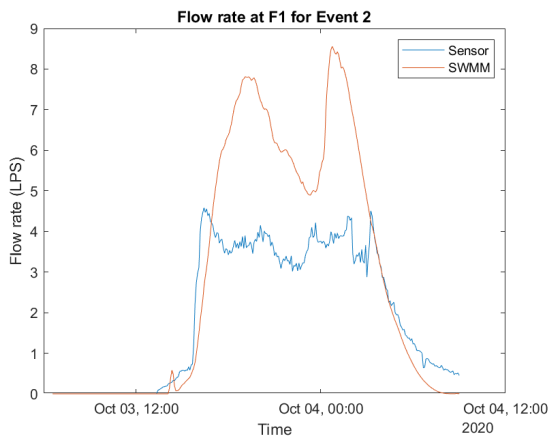
Table 5.13: Optimum hydrological parameters under different objectives for three sample events



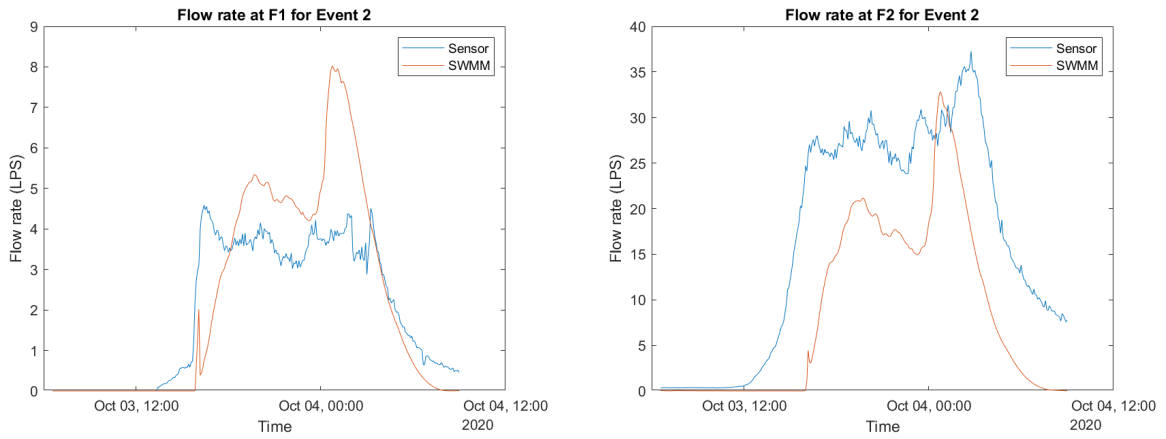
(a) Flow rate at F1 and F2 using optimum parameters under objective $E_1(X)$ for event 1



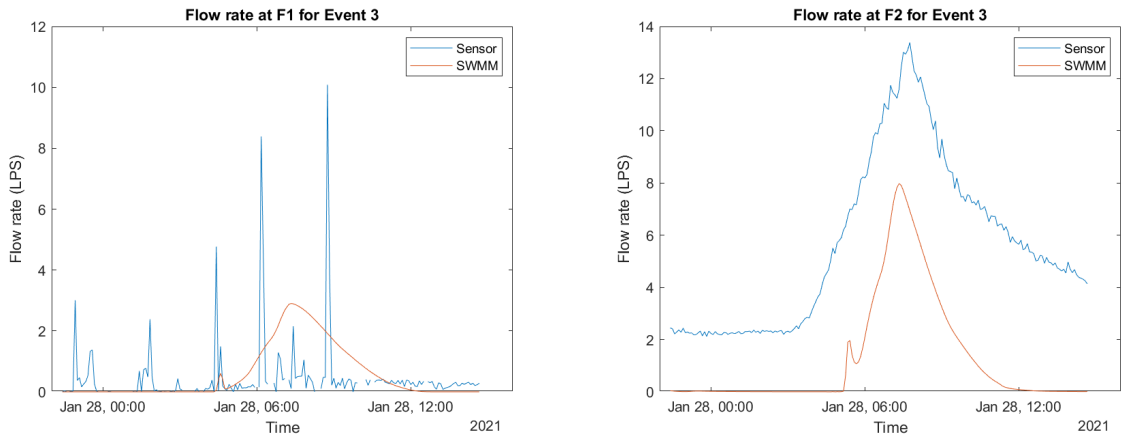
(b) Flow rate at F1 and F2 using optimum parameters under objective $E_2(X)$ for event 1



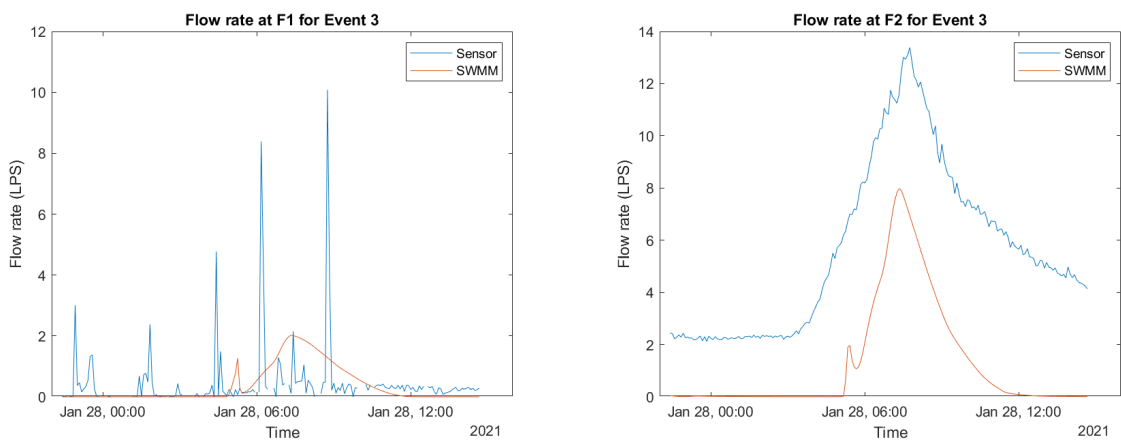
(c) Flow rate at F1 and F2 using optimum parameters under objective $E_1(X)$ for event 2



(d) Flow rate at F1 and F2 using optimum parameters under objective $E_2(X)$ for event 2



(e) Flow rate at F1 and F2 using optimum parameters under objective $E_1(X)$ for event 3



(f) Flow rate at F1 and F2 using optimum parameters under objective $E_2(X)$ for event 3

Figure 5.28: Flow rate at F1 and F2 simulated using optimum parameters

As shown in Figure 5.28, the general trend of the simulated flow rate is similar for both optimisation objectives ($E_1(X)$ and $E_2(X)$) and at both flow rate measurement location. However, it is observed that there is some trade-off between the accuracy of prediction in the two sensor locations. Especially for event 1 and 2, the flow rate at F1 is always overpredicted and the flow rate at F2 is always underpredicted. This means by matching the flow rate at F2, the flow rate at F1 will be even higher than what shown in Figure 5.28. This could be because there are less flow entering the drainage system through inlet point 4 where F1 is located assuming the total outflow (measured by F2) is measured accurately. Hence it can deduce that some of the overland flow from the catchment 41, 42 and 43 which originally assumed to enter the drainage system through inlet point 4 are actually diverted and enters the system through other inlet points. This could be due to the obstruction to overland flows caused by manmade features such as fences and roads as mentioned in catchment analysis in Section 5.2.2. Rain fall onto catchment 41, 42 and 43 could flow into the adjacent catchments 71, 72 and 73 alongside the fences before flowing towards the track. Such small changes in the runoff route cannot be detected by DTM, and can only be adjusted manually based on field inspections. However, since such changes are prone to human activities, it may change over the course of a year. As shown in event 3, such a trade-off is not so obvious compared to case 1 and 2. Hence, it is decided to keep using the current catchment layout for the remaining part of the study.

Also, for both optimisation objectives, the simulated and observed results are quite similar, although, the predicted value by optimising objective $E_1(X)$ is sometimes slightly higher than the predicted value by optimising objective $E_2(X)$. This is reasonable as rainfall estimation in a small region can be unpredictable, there may be spikes in the local rainfall time series that are not picked up by radar data. In this situation, in order to meet these peak flow values, the runoff would need to be predicted higher and hence also increase the total volume.

Based on the suggested soil type according to the calibration testing for a single event, the hydraulic performance model is then run for a longer period time. As shown in the results, the optimum infiltration rate varies for events from different seasons, hence, it is suggested to split up the dataset based on seasonality and find the best hydraulic calibration parameter values for each season. For each season, the dataset should be further divided into two subsets, one to be used to find the set of optimised infiltration parameters that could represent the soil characteristics throughout the season, and the other subset will be used to verify the parameters. Due to the fact that sensor monitoring was not implemented for a whole year, in this study, it would not be possible to calibrate the model for each season. Also, during the first three months of the data collection period, the sensors has been adjusted a few times due to inaccurate datum data logged at installation as well as several calculation setting errors. The data collected during such a period could be flawed, hence, it is decided to only calibrate the model for the autumn.

First, a set of simulations are run with a range of hydrological parameters from 01/10/2020 to 31/10/2020. The hydrological parameters tested are arithmetic sequences with range

and interval listed in Table 5.14. The result $E_1(X)$ and $E_2(X)$ are plotted in Figure 5.29.

Parameter	Range	Interval
Maximum Infiltration Rate (mm/hr)	(8,76)	1
Minimum Infiltration Rate (mm/hr)	(0.1,11.5)	0.1
Decay Constant	(4,7)	0.5

Table 5.14: The range and interval of the hydrological parameters sequence tested

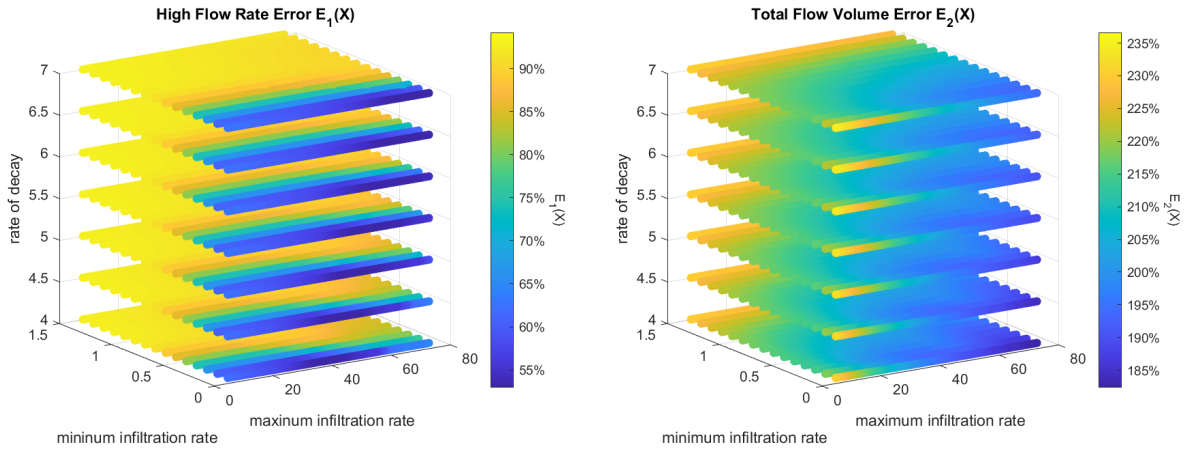


Figure 5.29: High rate flow error $E_1(X)$ and total flow volume error $E_2(X)$ for the Autumn calibration set

	Maximum infiltration rate (mm/hr)	Minimum infiltration rate (mm/hr)	Decay constant
minimising high flow rate error $E_1(X)$	39	0.1	4
minimising total flow volume error $E_2(X)$	76	0.1	4

Table 5.15: Optimum hydrological parameters for objectives $E_1(X)$ and $E_2(X)$

The optimum set of parameters under the two minimising objectives are shown in the Table 5.15. As explained in Section 5.1.5, the two objectives have a trade-off effect. As shown in the Figure 5.30, for all the tested sets of parameters, their high flow rate error $E_1(X)$ is plotted against the total flow volume error $E_2(X)$ and are displayed in blue dots; whereas the Pareto frontier is marked as a red line, which consist of a set of non-dominated solutions such that when no one criteria can be improved without making the other poorer. In this case, depending on the model user's preference, any point on the Pareto frontier can be chosen as the best fitted parameter values. As discussed earlier, if the high flow rate error $E_1(X)$ is preferred over total flow volume error $E_2(X)$, there is a possibility of overestimating flood risk. For this case study, from NR's point of view, flood risk will not only interfere with the train operation and induce financial loss,

but also damage their reputation, hence, it is better to overestimate the flood risk and get prepared beforehand than underestimate the risk which would potentially endanger passengers. Hence, the parameter values on the Pareto front with the lowest high flow rate error will be chosen as the optimal solution.

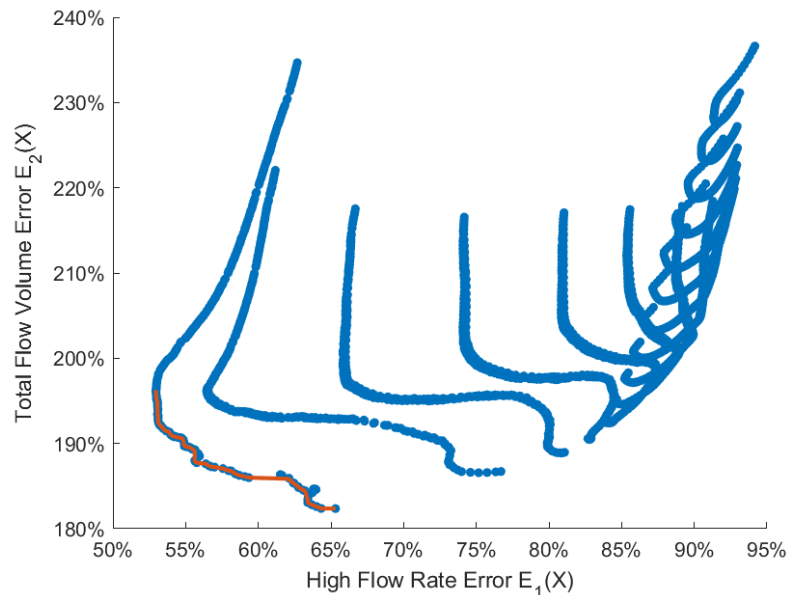


Figure 5.30: Pareto frontier of the two objectives: minimising high flow rate error $E_1(X)$ and minimising total flow volume error $E_2(X)$

After the hydrological calibration process is complete, the chosen parameter values are put back into the SWMM model to be used for the hydraulic parameter calibration. As described in the methodology section, the hydraulic parameter that will be calibrated is the roughness of the pipes, and the water depth in each monitored catchpits will be analysed to find the roughness value that minimise the water depth error $E_3(Y)$ at the monitored catchpits. The roughness coefficient in SWMM is Manning's n , and the range of roughness values tested is from 0.01 to 0.06, with a step increase of 0.005. The range of roughness is defined based on the guidance of the SWMM user's manual, as well as the Manning's n Values for Closed Conduits table in Schall et al. (2008) and table of values of roughness n in Chow (1959). All tables can be found in the Appendix G. As shown in these tables, the roughness of closed conduits can range from 0.009 to 0.03; whereas for constructed and maintained channels, the roughness ranges from 0.01 to 0.06. Although the roughness can be quite different for different types of asset made by difference material and shape, it is computationally costly to assign a specific roughness score to each asset. Hence, it is decided to use a unified roughness coefficient for all linear assets. Result shows that $E_3(Y)$ is minimal when Manning's n is equal to 0.01.

Manning's n	0.01	0.02	0.02	0.03	0.03	0.04	0.04	0.05	0.05	0.06	0.06
$E_3(Y)$	0.40	0.46	0.59	0.75	0.92	1.12	1.32	1.50	1.66	1.81	1.95

Table 5.16: Water depth error $E_3(Y)$ with various Manning's n

With both the optimum hydrological and hydraulic parameter values identified from the calibration process, the model is then validated with sensor data collected in November 2020. The simulated and observed flow rate at F1 and F2 of are shown in Figure 5.31; and the water depth level at each monitoring catchpit is shown in Figure 5.32.

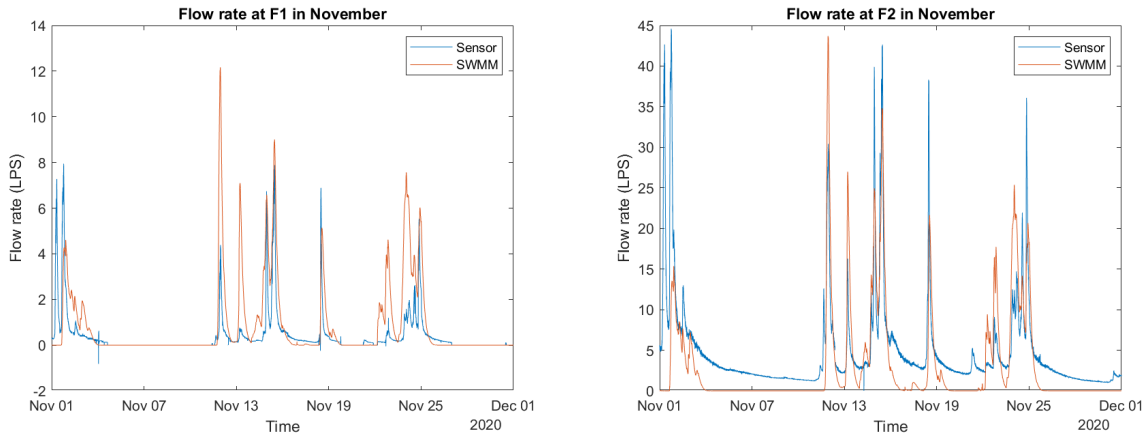
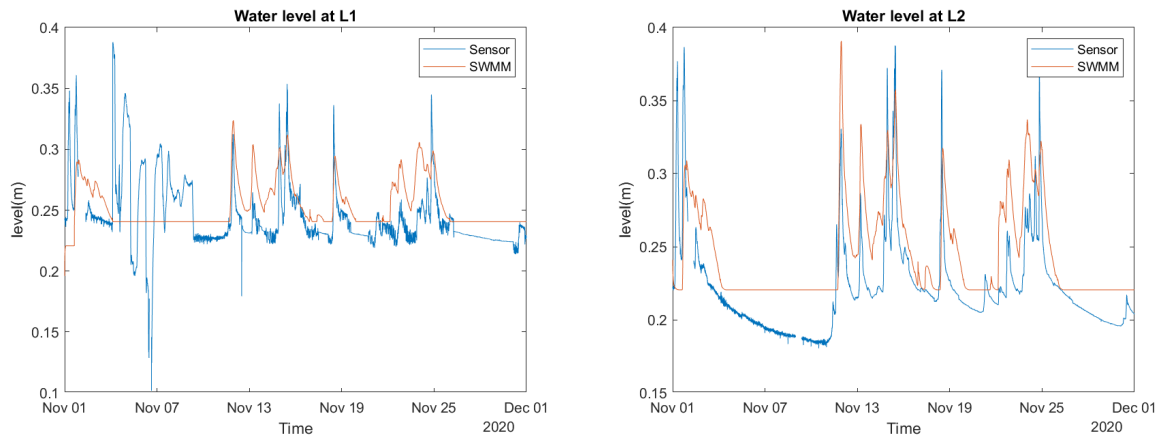


Figure 5.31: Flow rate at F1 and F2 in November 2020 using calibrated parameters



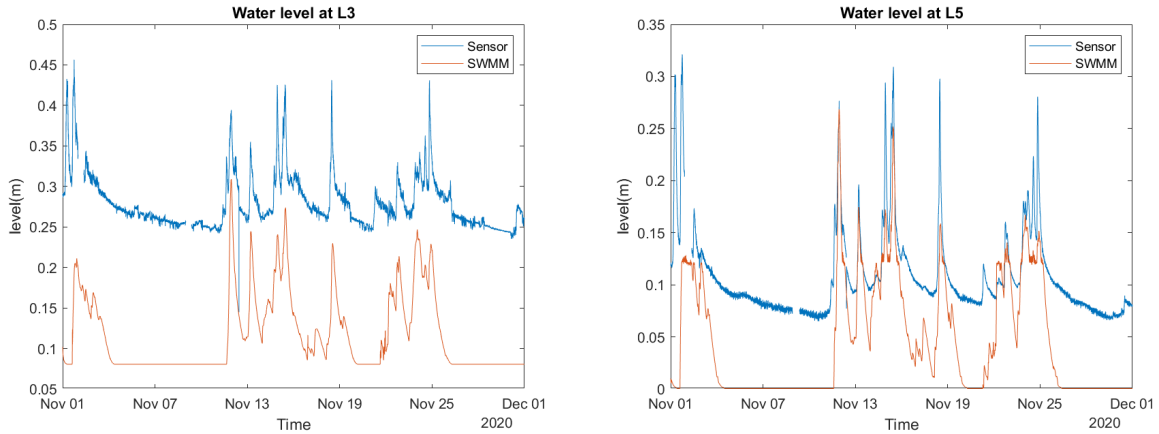


Figure 5.32: Water depth level at L1, L2, L3, L5 in November 2020 using calibrated parameters

As shown in the figures, both the flow rate and the water depth fit quite well. At least 90% of the simulated peaks occur at the same time as the sensor data and many have a reasonable correspondence in values. Though a lot of the flow in between the rainfall events are not captured well. As the focus is on the flood risk, the data fitting around the peak flow rate and highest water depth is more valued and the effect of the lower readings between rainfall events are less considered, which is already reflected by choice made when selecting parameter values on the Pareto front as the one minimises the high flow error is preferred.

It is also noted that for the water depth sensor at L1, there are some fluctuations during 4th Nov and 9th Nov 2020 that are not indicated in the simulated data. Comparing the other water depth and the flow rate sensor data, they does not show any significant movement, hence, it can be concluded that the fluctuations in L1 may be caused by some sensor malfunction. Also, for water level at L3, the plot for simulated data is lower than the sensor data, though they exhibit similar trends. Such phenomenon is also observed in the previously calibrated datasets, therefore, it can be assumed that either the datum of the sensor is set lower than the actual catchpit base level or there is error in the field survey data so that the actual catchpit is deeper than recorded.

The value of each type of error for the validation set are shown in Table 5.17. As shown in the table, the water depth error $E_3(Y)$ is the same, whereas total flow volume error $E_2(X)$ is also lower than the calibration set. However, the peak flow error is higher for the validation set. This may due to the fact that the case study hydraulic system serves a relatively small catchment area, and the radar rainfall data is processed over 1 km square, hence local variation which are expected to exist may lead to modest inaccuracy in forecasting runoff. Despite recent advances in radar technologies, it is still very challenging to accurately measure rainfall due to its highly variable nature over time and space. This type of error can be potentially reduced by installing numerous local rain gauges and comparing with the radar data to eliminate the uncertainties in the

precipitation data.

	$E_1(X)$	$E_2(X)$	$E_3(Y)$
Calibration	0.5	1.8	0.4
Validation	1.1	1.5	0.4

Table 5.17: Estimation error for the calibration set and validation set

5.3 Conclusion

This section has introduced the methodology used to evaluate the hydraulic performance of railway drainage systems for both single-event and long-term rain fall time series. The SWMM modelling software is used to build a digital replica of existing drainage systems. The model uses input rainfall time series and simulates runoff volume across the defined catchment areas which then feeds into the drainage system digital replica. The time and location of where water exits the system through nodes are recorded as system failures. This can help asset managers to understand the potential of flooding in any designed rainfall event for a particular drainage systems.

Building of the SWMM model required detailed information of the geometry of the drainage assets such as invert level and pipe diameter, as well as the surrounding catchment geology information. Hence, although ideally it is best to populate these models nationally, due to the scarcity of the existing data and the cost of field survey, it is suggested to use such models only in areas where flood risks are more severe.

The case study is in a rural area, hence the catchment geology and soil characteristics has a large influence in the runoff prediction as infiltration processes may vary during the year. For railway drainage systems in urban areas, extra consideration of the land use is needed in catchment study. Manmade features such as buildings and structures would have a bigger impact on the hydrological model. In the catchment identification process, watershed identification should be drawn not only based on the water concentration feature but also on the land cover, and extra water flow routes may need to be manually implemented such as stormwater gutters and drains.

The calibrated and validated SWMM model can also be used as a tool to identify critical assets in a system by incorporating the effect of deterioration of each asset. The asset that cause the highest amount of flooding when deteriorate to a higher roughness would be the weak link in the system. The drainage system performance would hence be more prone to asset condition changes to critical assets, as roughness changes are often lead by asset condition degradation. Following on this, the hydraulic model will be combined with the degradation model introduced in Chapter 4 to simulate the possible loss in hydraulic performance with asset degradation; this will be discussed in detail in the next chapter.

6 Integrated Model Combining Hydraulic Performance Model and Degradation Model

Drainage assets are expected to degrade over time. Both the service and structural degradation of drainage assets affect the hydraulic carrying capacity of a whole drainage system. For example, service degradation such as blockage due to debris accumulation would limit the amount of water that could flow freely towards the outlet and hence increase upstream water levels and potentially cause flooding in one of the upstream catchpits; structural degradation such as collapse of a culvert could prevent runoff from one side of the railway from flowing safely under the railway tracks, leading to water accumulation above tracks and hence obstruction to train operation. Hence, it would be in an asset manager's interest to be able to predict the effect of asset degradation on drainage system performance, in order to take proactive actions to prevent any unacceptable loss of performance.

As demonstrated in Chapter 4, asset degradation processes for railway drainage assets can be simulated using a Markov Chain model. Combining the degradation model with the hydraulic performance model shown in Chapter 5 would provide asset managers with an integrated model that could forecast the future drainage system performance whilst taking into account any estimated future asset degradation.

Nevertheless, after the tragic derailment of a passenger train at Carmont on 12 August 2020, the importance of a resilience and safe railway in a changing climate has been raised (Haines, 2020). The root cause of the incident was a poorly constructed drainage system which failed to meet design standards. Inadequate drainage capacity caused soil to be washed onto the track after a high volume rainfall event, which led to the fatal accident as the train hit the soil on the track at high speed and derailed. It is recognised that the drainage system plays a vital role in weather resilience as it is essential for the water management of all railway assets. The integrated model can also provide asset managers with a tool to simulate and forecast the resilience of the existing system using forecast precipitation projections under various climate change scenarios as well as accounting for asset degradation projections.

In the sections below, a description of the integrated model will be presented followed by a case study using data collected from the Knockenjig site.

6.1 Methodology

The hydraulic performance model is integrated with the degradation model using Matlab. The forecast drainage asset condition changes are simultaneously reflected in the hydraulic model by automatically changing the asset characteristic parameters. The service condition of the asset impacts three important factors that could affect the hydraulic carrying capacity of the drainage asset: size, gradient and roughness. For example: siltation of a pipe reduces its size; vegetation growth in a ditch increases its roughness as

well as reducing its size; severe siltation of a ditch or channel can reduce the gradient (NetworkRail, 2017). Since gradient is a very sensitive factor in the SWMM model and a minimum slope is required for the model to run, i.e. the elevation drop between the two ends of any conduit must be at least 0.00035 m, in this study only size and roughness of the drainage asset will be altered to reflect the service condition degradation. For Pipe, Channel, Culvert and Granular Drain, service condition degradation is reflected both by increase of the roughness and a decrease of the asset diameter/height/width. For Chambers, Outfall, Inflow and Syphon, reduction in depth or increase in elevation level is used to mimic physical property change that leads to worsening service condition score. However, the relation between asset service condition score and the changes that lead in an asset's physical characteristic is not fully understood yet and cannot be precisely quantified without further studies. Hence, assumptions need to be made based on expert opinions and assessments of the study area while applying the model to real life.

The structural condition degradation would affect the hydraulic capacity in a different way. With a minor defect such as a small crack, it is expected to obstruct and slow down the water flow, but such crack may only present in a small section of the pipe and does not affect the roughness of the whole pipe, so it is hard to quantify. Also, if such a crack is observed in the catchpit, it would not have any impact on the hydraulic capacity until it develops and endangers the structural integrity of the catchpit which could lead to the catchpit collapsing. Hence, it is suggested that when the structural condition of an asset degrades to 5, the asset is removed from the system. Since the effect of minor structural degradation on hydraulic performance is a much more complex problem, it will require further study to be able to reflect it in this integrated model.

The following are the steps for building an integrated model of asset degradation, drainage system performance, and climate change. Since the asset degradation process is simulated with the stochastic simulation algorithm based on the asset degradation transition rate, all the simulations rely on an element of probability, hence each simulation run will generate a different result. Therefore, multiple stochastic runs are needed to generate a distribution of the simulated performance results. The average of the simulation results is taken as the estimate of the forecasted drainage system performance.

1. Calculate asset degradation rate using a Markov Chain model as explained in Section 4.2.3.
2. Define the number of years of simulation T .
3. Generate asset degradation time series of T years for each asset in the drainage system using stochastic simulation algorithm as described in Section 4.2.4. The time series contains the asset number, condition scores that asset will transition into and the time of transitions.
4. Combine degradation time series of all assets and sort them according to the time of transition in ascending order.
5. Run simulation with hydraulic performance model (SWMM) using current asset condition data and designed/predicted rainfall time series.

6. When an asset degradation is predicted to happen according to the degradation time series, the simulation will be stopped and the corresponding asset characteristics will be altered to reflect the effect of asset degradation.
7. A temporary file is generated every time the simulation is stopped to record the full hydrologic and hydraulic state of the drainage system at the time of stopping. It can then serve as the initial conditions for the subsequent run after condition change to enable a continuous simulation process.
8. Time series of desired output such as flow rate, water depth and runoff volume are extracted from the output file for each simulation.
9. Repeat steps 3 – 8 for n times to obtain a set of stochastic simulation results.

The results were analysed, the performance related parameters such flooding volume and duration were studied, mean expected performance estimate was calculated. Such performance indicators would give asset managers a tool to predict the future performance reduction assuming asset degradation is continuous without any intervention mechanism and under the stress of defined rainfall time series.

6.1.1 Rainfall time series construction

To test the performance of the drainage system with different climate scenarios, rainfall time series needed to be constructed based on the future climate projections. There are several developed climate change models available that can provide simulated rainfall time series in the next decades, such as UK Climate Projections (UKCP18) and the sixth phase of the Coupled Model Intercomparison Project (CMIP6). However, most of the time series usually have a temporal resolution of one hour, which is longer than the 5 minute interval used in the hydraulic performance model in Chapter 5. Hence, it is required to disaggregate the existing rainfall time series data into finer temporal resolution.

Review of the rainfall disaggregation methods

Many hydrological studies require rainfall data at fine time scales that range from daily to 1-minute intervals. Due to the scarcity of sub-hourly scale data in real-world situations, stochastic disaggregation methods are proposed to generate statistically consistent rainfall events that aggregate up to the field data collected at coarser scales. Over the years, various stochastic models have been developed to address the rainfall disaggregation problem, such as Poisson-cluster models, cascade models, artificial neural network, K-nearest neighbor technique and method of fragments framework (Gyasi-agyei and Mahbub, 2007; Kossieris et al., 2018; Rafatnejad et al., 2022; Fadhel et al., 2021). However, most of the methods proposed are focusing on disaggregating of daily or longer time increment rainfall; only a few addressed the problem of disaggregation of sub-hourly rainfall data to finer resolution (Burian et al., 2000).

The Poisson-cluster models are based on point process theory developed by Rodríguez-Iturbe et al. (1987); Rodríguez-Iturbe et al. (1988), including the Neyman–Scott (Cow-

pertwait et al., 1996*b*; Cowpertwait, 2006; Fatichi et al., 2011) and Bartlett–Lewis rectangular pulses (Cowpertwait et al., 1996*a*; Onof and Wheater, 1994; Koutsoyiannis and Onof, 2001; Gyasi-agyei and Mahbub, 2007; Vanhaute et al., 2012; Villani et al., 2015). The models assumes rainfall at a finer resolution can be represented as a sequence of rectangular pulses, hence disaggregate the hourly rainfall into smaller time intervals by allocating pulses of a specified small depth at different intervals. The model parameters are estimated using historical rainfall data, and the disaggregation is achieved by sampling from the estimated parameters to generate the desired sub-hourly rainfall time series. The main difference between these two types is that Neyman–Scott models distribute rain cells from the time origin (beginning of the storm), whereas Bartlett–Lewis models distribute rain cells based on their interarrival time (Rodriguez-Iturbe et al., 1987).

The Cascade model is another major group of rainfall disaggregation models (Ormsbee, 1989; Olsson, 1998; Olsson and Berndtsson, 1998; Güntner et al., 2001; Molnar and Burlando, 2005; Sivakumar and Sharma, 2008). The approach is based on the concept of scaling in rainfall, assuming that the characteristics of different timescales are related and scale-invariant, hence finer time series can be generated according to patterns of coarser time scales. The approach is based on the concept of scaling in rainfall, or, relating the properties associated with the rainfall process at one temporal scale to a finer-resolution scale. The Cascade processes model the distribution of rainfall by partitioning the available space into smaller sections and then reassigning a corresponding value at each stage according to the cascade generator. The scaling rules are usually determined by calibrating the universal multifractal model on existing rainfall time series data.

Examples of other models include the two artificial neural network (ANNs) models introduced by Burian et al. (2000), one is trained by backpropagation/steepest-descent algorithm and the other model uses a self-organization approach. Method of fragments was used for sub-daily rainfall disaggregation by Rafatnejad et al. (2022), using historical sub-daily data to facilitate the disaggregation of future daily data by producing a series of fragments. Also, two different approaches were introduced to improve the accuracy, one is to consider weather variables in the selection process while the second one uses generalized regression neural network to simulate the sub-daily characteristics. Shahabul Alam and Elshorbagy (2015) and Uraba et al. (2019) used the K-nearest neighbour method to disaggregate future daily rainfall to hourly and sub-hourly scales using only historical rainfall as the predictor for the disaggregation.

Several software packages have been developed based on the models mentioned above, namely Hyetos, Hyetominute, Stormpac, and NetStorm.

Hyetos was developed by Koutsoyiannis and Onof (2001) based on a modified Bartlett–Lewis rectangular pulse model that disaggregates rainfall into a finer timescale while preserving the daily total rainfall. However, Hyetos can only disaggregate the daily rainfall into hourly rainfall. A few studies has proposed methods to generate sub-hourly rainfall by

creating a hybrid model of Hyetos with an additional model to enable disaggregation of the hourly rainfall output into sub-hourly time series. Laloy and Bielders (2009) applied a symmetrical double-triangular hydrograph method to hourly data from Hyetos to generate rainfall time series of 1-min interval. Whereas Anis and Rode (2015) used a micro-canonical cascade model (Onof2005, Sivakumar2008) to disaggregate the hourly depths into 10-min data.

(Kossieris et al., 2018) created HyetosMinute based on Hyetos with the following few new features: (1) generation of synthetic rainfall data at sub-hourly time scales (minimum 1-min time scale), (2) incorporate the Bartlett-Lewis model with randomised intensity parameter that assumes dependence between cell intensity and duration (Kaczmarska et al., 2014), (3) implementation of an enhanced-version of the Evolutionary Annealing-Simplex (EAS2) optimization algorithm for the estimation of model parameters.

Stormpac is a software tool designed for rainfall generation, predominantly used by water companies in the UK for design and simulation purposes (Onof et al., 2005). This software incorporates a cluster point process model to create hourly time series, which are then disaggregated to a 5-min time scale. It is built based on the rainfall disaggregation model proposed by Ormsbee (1989).

Ormsbee (1989) developed models based on a continuous distribution approach that permits disaggregation of hourly rainfall into time intervals from 1 to 30min. The model is composed by two methods; one is the deterministic method which constructs rainfall time series of refined time steps based on patterns of the previous three-hour sequence in the original dataset (i.e. pattern of the preceding, current and successive hours' rainfall data); the other is the stochastic method which distributes the volume of rainfall using a Monte Carlo approach based on the distribution deduced using the three-hour sequence. Although Ormsbee (1989)'s algorithm has demonstrated reasonable effectiveness, it exhibits a negative bias when compared to actual high-frequency data (Heineman, 2004). This could result in an underprediction of the peak rainfall intensity, and consequently, lead to an underestimation of flood risk.

NetSTORM is a software for hydrologic data analysis developed by Mitch Heineman at CDM Smith that can perform rainfall time series synthetic disaggregation (Heineman, 2004). It is also developed based on Ormsbee (1989)'s model with a choice of deterministic approach and stochastic approach. In addition, NetSTORM added an optional 'spiking' factor that increase the maximum value of the disaggregated dataset by a user-specified factor (between 0 and 1) multiplied by a random value (between 0 and 1) multiplied by the difference between the original total and the initial maximum value. The rest of the data of the hour are decreased accordingly to meet the original hourly value. This additional component is designed to reproduce sub-hourly extrema that were often not adequately replicated in the original approach.

Model choice

Although as mentioned above, there are several recently developed sub-hourly rainfall dis-

aggregation models such as the modified method of fragments (Rafatnejad et al., 2022) and K-nearest neighbour method (Uraba et al., 2019), their accuracy has not been compared with the all the other models. Also, for the simplicity of application, it is decided to use an established software for the rainfall disaggregation process.

Among the readily build software, Hyetons and HyetonsMinute would not be suitable for this study because Hyetos only disaggregate daily data into hourly data, whereas HyetosMinute only takes input as daily time series, and then disaggregates daily values into hourly or sub-hourly data. The climate change rainfall time series extracted from UKCP18 projections is hourly data that needs to be disaggregated into 5-min scale. Hyetons could not provide rainfall disaggregation of 5-min level, whereas HyetonsMinute requires aggregation of the hourly time series into daily value before it can be input into the model, hence would lose certain finer temporal features in the original rainfall projection time series. Since both Stormpac and NetStorm were build based on Ormsbee's model, and Netstorm is available software and with an extra component, compared to Stormpac to address the problem of underestimation of the peak flows, it was chosen to be used in the study.

6.1.2 Selection of simulation number

As described above, multiple simulations are required for each scenario as the degradation simulation is a stochastic process. To determine how many runs are needed to derive a reliable representative of potential outcomes, a preliminary test to find such number is suggested as described below:

1. Make a preliminary test of 100 simulation runs over a designed period.
2. Extract and calculate the performance indicator for each run.
3. Calculate the mean \bar{x}_{100} and standard deviation $\bar{\sigma}_{100}$ of the 100 run .
4. For $n = 2, 3, 4, \dots, 100$, randomly select performance indicator of n runs, calculate the sample mean \bar{x}_n and standard deviation $\bar{\sigma}_n$.
5. Use the two-sample t-test (Snedecor and Cochran, 1991) to test null hypothesis that the sample mean \bar{x}_n is equal to the total \bar{x}_{n+1} .
6. Find the maximum n such that the null hypothesis is rejected at 5% significance level.
7. $n+1$ would be the minimum simulation runs required for the model to get a reliable estimate of the system performance indicator.

6.2 Case Study

A case study was performed with the Knockenjig site, using the calibrated hydraulic performance model developed in Chapter 5. The service condition degradation rate of drainage assets at the Knockenjig site used in the simulation is the transition rate generated using the historical asset condition data of all assets nationwide. This was done as

there was insufficient data at this size of site to generate a stable transition matrix. The service condition degradation rate is analysed separately for each asset group because the results of cohort analysis in Section 4.4.2 suggests that asset condition transition rate would differentiate between asset groups.

As discussed earlier, the consequence of degrading into structural condition 2 to 4 is not clear and hard to quantify. Although the consequence of degrading into structural condition 5 is very severe and usually means complete destruction, the probability of transitioning into a structural condition 5 is very low. For example, pipes have less than 0.02% probability of degradation to condition 5 in 10 years' time. Considering the low probability of failure and uncertainties in modelling the performance loss, it was decided to not include the structural condition degradation in this case study.

Hydraulic performance of the Knockenjig railway drainage system can be simulated for any period of time. According to the historical condition data, the average duration between observations is 2.7 years. Therefore, a period of 10 years from 2022 to 2031 is chosen to be tested for this case study, as this duration would be long enough for sufficient amounts of asset degradation to be observed.

To test the resilience of the drainage system under climate change, precipitation forecasts under climate change scenarios are also tested to investigate and forecast the ability of any degrading railway drainage system to cope under future extreme weather conditions. In this case study, UK Climate Projections 2018 (UKCP18) is used to provide precipitation forecasts under several global warming scenarios. In particular, the UKCP Local model is selected, as it provides weather projections on a 2.2km scale, which gives the opportunity to analyse the risk of extreme weather events at precise geographical locations and the spatial scale is similar to most railway drainage systems. The local projections provide hourly precipitation predictions under the high-emissions 'RCP8.5' global warming scenario. RCP stands for Representative Concentration Pathway which is a greenhouse gas concentration trajectory adopted by the Intergovernmental Panel on Climate Change. These pathways describe various potential climate change futures based on the projected volume of greenhouse gases that will be emitted. RCP 8.5 refers to the concentration of carbon that delivers global warming at an average of 8.5 watts per square meter across the planet. The hourly precipitation time series are disaggregated into shorter durations of 5 minute intervals using NetSTORM. A stochastic version of the disaggregation model was selected as it adds a random component to the disaggregated time series and a spike factor of 0.5 is used.

In the case where climate conditions will not worsen, the rainfall statistics were assumed to remain the same as the previous 10 years. Historical precipitation records from 2011 to 2020 were used as the future precipitation predictions. The rainfall time series is the same as the one used in Chapter 5 case study: Met Office Rain Radar Data from the NIMROD System.

6.2.1 Assumptions

As explained in Section 6.1, the following assumptions are made based on expert opinions and assessments of the case study area, defining the effect of asset service condition changes on their physical characteristics:

- For Pipe, Channel, Culvert and Granular Drain
 - i. Service condition score changes will have the following effect on roughness:

Service Condition Score	1	2	3	4	5
Manning's n	0.010	0.012	0.020	0.035	0.055

Table 6.1: Condition score and corresponding roughness

- ii. Service condition score changes will have the following effect on asset diameter/height/width:

Service Condition Score	1	2	3	4	5
Percentage reduction	0%	0%	10%	30%	50%

Table 6.2: Condition score and effect on asset diameter/height/width

When changing the diameter/height/width of the asset, the asset's invert level will remain the same. This will result in a decrease in cross sectional area for about 20% - 75% depending on the shape

- For Chambers, Outfall, Inflow, Syphon
Service condition score changes will have the following effect on reduction in asset depth:

Service Condition Score	1	2	3	4	5
Depth reduction (m)	0	0	0.1	0.2	0.4

Table 6.3: Condition score and effect on reduction in asset depth

The depth reduction is in place to reflect the loss of storage capacity of the catchpit due to siltation and blockage.

Moreover, based on NR Drainage Policy (NetworkRail, 2017), the effect of interventions on the drainage service condition score is assumed to be as following:

Start Service Condition	1	2	3	4	5
Service Condition After Refurbishment	1	1	1	1	1
Service Condition After Maintenance	1	1	2	2	3

Table 6.4: Effect of intervention on drainage service condition scores

Since there is not enough field data to calibrate the hydraulic performance model for each season, it is assumed that the input parameters of the hydraulic performance model remain the same throughout all seasons in this case study. The parameters of the calibrated model for autumn were used, as deduced in Section 5.2.6. Making such an assumption could potentially lead to an overestimation of flood volume in summer and an underestimation of flood volume in winter. This is because the infiltration capacity usually is high in summer and low in winter Horton (1940*b*), hence, the percentage of runoff in summer predicted with autumn infiltration rate will be higher than the actual value which leads to a higher chance of flooding, whereas in winter the predicted runoff would be lower than the actual value which leads to a lower chance of flooding.

6.2.2 Scenarios

The hydraulic performance of this system was simulated under several proposed scenarios to test the effect of asset degradation and climate change on drainage system performance in the next 10 years (2022-2031). Operational intervention on degraded assets are not analysed in this modelling, in order to set a bench mark for the degradation scenarios, assets are assumed to be maintained in the current condition in Scenario 1 and 3. The scenarios investigated are listed as below:

- Scenario 1: Assets maintained in the current condition and no climate change
- Scenario 2: Assets degrade naturally and no climate change
- Scenario 3: Assets maintained in the current condition and RCP8.5 global warming scenario
- Scenario 4: Assets degrade naturally and RCP8.5 global warming scenario

For each scenario, the duration that at least one model node is flooded (i.e. water leaving catchpit) is calculated from the node depth time series. Through discussions with Network Rail engineers, it is suggested that if flooded water is ponded with a 30 cm depth above ground, it is likely to be above the rail level, which can lead to temporary speed restrictions or temporary closures of railway lines. Therefore, the duration of the possible train operation interference is also listed as an indicator of the drainage asset performance.

6.2.3 Number of simulations

For scenarios 2 and 4 where asset degradation takes place, the model needs to run multiple times to address the possible fluctuations in the behaviour of stochastic simulations of the asset degradation process. Since one single simulation run of Scenario 4 would take 5 to 6 hours to run. In order to save computational time, a test is carried out to determine the minimum number of simulations needed to get a stable result, The model was run 100 times under Scenario 4, but with a shorter duration of 5 years. Since less degradation would be observed in a shorter duration, the volatility of change in performance might also be lower, so it was suggested to use a stricter confidence level of 1%. The results

showed that the minimum number of simulations required is 23.

6.2.4 Cases study results

Hence, 30 simulations are run for scenarios 2 and 4 and the average Flooding hours of the 30 simulations is taken as being representative of the forecasted drainage system performance. The results of the proposed scenarios are shown in Table 6.5.

	Scenario 1	Scenario 2	Scenario 3	Scenario 4
Total Estimated Average Flooding Hours in 10 years	37.0	405.2	667.8	1637.1
Total Estimated Average Flooding Hours above rail in 10 years	11.6	281.4	331.4	1155.4

Table 6.5: Drainage system performance under various weather and asset condition scenarios

As shown in Table 6.5, comparing scenario 1 and 2, and scenario 3 and 4, it is noticed that the asset degradation has a significant effect on the performance of the drainage system. In both no climate change and RCP8.5 global warming scenarios, when asset degradation takes place without any human intervention, the flooding hours increased significantly. The flooding hours above rail is about 25 times more with degradation in place than the case where asset condition is maintained in original condition. This shows that if assets are left unattended, the hydraulic capacity of the existing system will be significantly reduced, hence it is important for asset managers to regularly inspect the assets and maintain the assets at serviceable condition.

By comparing scenario 1 and 3, there is a large increase of 320 hours in the hours flooded above rail. This indicates that climate change will also affect the performance of the drainage system significantly. For scenario 1 and 3 the asset conditions are assumed to be unchanged, i.e. maintained in current condition. Under current asset condition, only 11.6 hours of flooding above the rail is expected in 10 years. That is on average roughly 1 hour of flooding per year which is an acceptable value, because it is possible that this one-hour flooding won't have any effect on the train operation as there is a low chance of having a train passing by in such a short period. However, under the RCP8.5 global warming scenario, the hours flooded increased significantly, resulting in an estimated 30 times more flooding hours than the 'no climate change' scenario. This means if climate change continues the railway drainage system is expected to fail due to lack of hydraulic capacity. Hence, it is necessary to acknowledge the importance of global climate change and make efforts to account for this in any design and maintenance procedures, as well as to prepare for any potential consequences due to climate change and make drainage system upgrade decisions when needed. Also, such climate change scenario simulations should be taken into account in the drainage system design phase to help build sustainable

systems that can withstand future extreme weather circumstances.

Moreover, comparing scenario 2 and 3, the results show that the effect of asset degradation alone is almost as significant as the effect of climate change on its own, hence further emphasizing the importance of building a proactive and effective drainage asset management regime.

6.2.5 Sensitivity testing

As explained in above, due to the lack of knowledge about the corresponding physical characteristics for each asset service condition category, assumptions have to be made based on expert opinion for the integrated model to run. Several sensitivity tests have been performed to evaluate the uncertainty in the hydraulic performance prediction with variation in the assumed changes in asset condition parameters.

Roughness coefficient corresponding with degraded service condition is increased and reduced by 20% and the new set of roughness parameter values are listed in Table 6.6. The Manning’s n for condition 1 is not changed as roughness for assets in perfect condition is set to be the same as a baseline. Adjusted roughness when Pipe, Channel, Culvert and Granular Drain degrade are assumed to be:

	1	2	3	4	5
Manning’s n (reduced)	0.0100	0.0096	0.0160	0.0280	0.0440
Manning’s n (increased)	0.0100	0.0144	0.0240	0.0420	0.0660

Table 6.6: Condition score and corresponding roughness for sensitivity test

The results of estimated flooding hours are shown in the Table 6.7 below, since Scenario 1 and 3 does not involve asset degradation, only results from Scenario 2 and 4 are listed. Percentage change of the flooding results compared with results obtained the original assumptions are shown in Table 6.8.

					Scenario 2	Scenario 4
Manning’s n (reduced)	Total	Estimated	Average	Flooding	308.8	1425.6
	Hours in 10 years					
Manning’s n (increased)	Total	Estimated	Average	Flooding	507.8	1833.0
	Hours in 10 years					
Manning’s n (reduced)	Total	Estimated	Average	Flooding	205.4	965.3
	Hours above rail in 10 years					
Manning’s n (increased)	Total	Estimated	Average	Flooding	365.9	1339.2
	Hours above rail in 10 years					

Table 6.7: Drainage system performance under weather and asset condition scenarios with reduced and increased asset roughness assumption

		Scenario 2	Scenario 4
Manning's n (reduced)	Percentage change in Total Estimated Average Flooding Hours in 10 years	-23.8%	-12.9%
	Percentage change in Total Estimated Average Flooding Hours above rail in 10 years	-27.0%	-16.5%
Manning's n (increased)	Percentage change in Total Estimated Average Flooding Hours in 10 years	25.3%	12.0%
	Percentage change in Total Estimated Average Flooding Hours above rail in 10 years	30.0%	15.9%

Table 6.8: Percentage change in drainage system performance under weather and asset condition scenarios with reduced and increased asset roughness assumption compared with original assumptions

As shown in the above tables, the reduction in roughness coefficient values leads to less flooding hours, whereas the increase in roughness coefficient results in higher flooding hours. This is as expected since any increase in the Manning's number indicates a higher energy loss per length of pipe, a slower water flow velocity and a higher flow depth. Hence the ability of transporting water to the outlets is reduced which leads to higher chances of flooding. The percentage difference of the estimated average flooding hour is roughly the same as the percentage change of the Manning's n. The changes for both reduced and increased cases under scenario 2 is about 10% higher than scenario 4, though the absolute difference in flooded hours for scenario 4 is still much higher. This is because for scenario 4, besides asset degradation, climate change also made a large contribution to the resultant flooded hours. Hence, the percentage increase in flooding hours due to change in roughness scores compared with the flooding hours due to both asset degradation and climate change would be smaller than the change compared with only the flooding hours due to asset degradation.

Also, comparing the results of scenario 2 with the graph (Figure 6.1) of storm drain capacity sensitivity to the parameters in the Manning's equation from the Urban Drainage Design Manual of Federal Highway Administration (Brown et al., 2013), the percentage reduction of the performance indicator is quite similar to the changes in hydraulic capacity shown in the graph. As shown in Figure 7.1, 20% reduction in the roughness will result in 30% increase in hydraulic capacity and 20% increase in the roughness will result in 15% reduction in hydraulic capacity. This suggests that the original assumptions made linking roughness change to asset condition score appears reasonable.

Assumption on percentage reduction in asset diameter/height/width with regard to asset service condition degradation is increased and reduced by 20%, and the new set of assumptions are listed in Table 6.9. The resulting cross sectional area reduction will be about 15% - 64% in the reduced case, and 22% - 84% in the increased case.

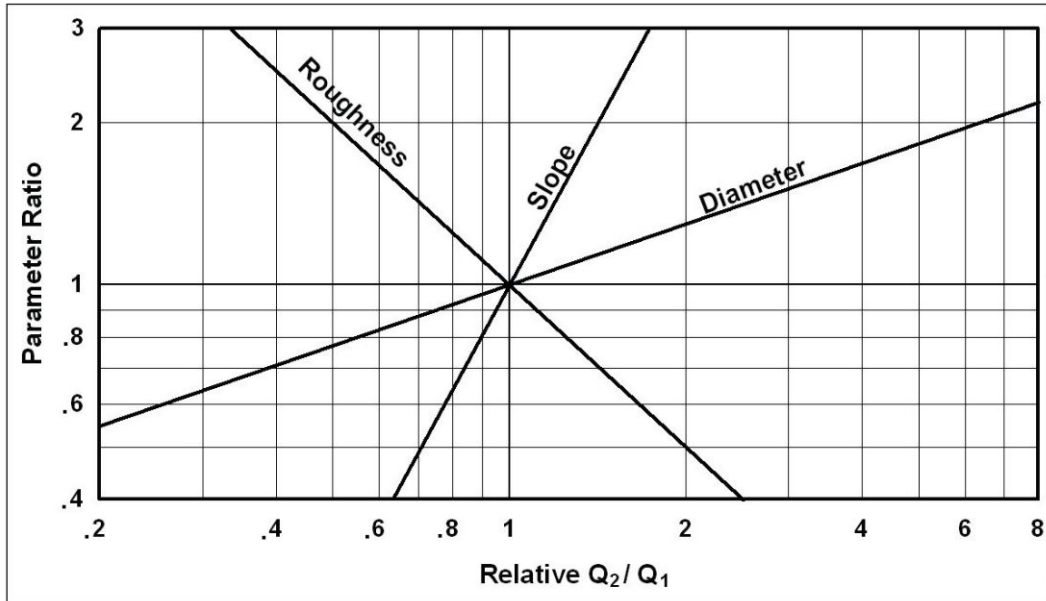


Figure 6.1: Storm drain capacity sensitivity to the parameters in the Manning's equation (Brown et al., 2013)

	1	2	3	4	5
Percentage reduction (reduced)	0%	0%	8%	24%	40%
Percentage reduction (increased)	0%	0%	12%	36%	60%

Table 6.9: Condition score and corresponding asset diameter/height/width for sensitivity test

The results are shown in the Table 6.10 below.

		Scenario 2	Scenario 4
Diameter/height/width percentage reduction (reduced)	Total Estimated Average Flooding Hours in 10 years	257.5	1314.6
	Total Estimated Average Flooding Hours above rail in 10 years	160.0	852.3
Diameter/height/width percentage reduction (increased)	Total Estimated Average Flooding Hours in 10 years	669.3	2097.9
	Total Estimated Average Flooding Hours above rail in 10 years	512.2	1609.8

Table 6.10: Drainage system performance under weather and asset condition scenarios with reduced and increased asset diameter/height/width reduction assumptions

		Scenario 2	Scenario 4
Diameter/height/ width percentage reduction (reduced)	Percentage change in Total Estimated Average Flooding Hours in 10 years	-36.5%	-19.7%
	Percentage change in Total Estimated Average Flooding Hours above rail in 10 years	-43.1%	-26.2%
Diameter/height/ width percentage reduction (increased)	Percentage change in Total Estimated Average Flooding Hours in 10 years	65.2%	28.1%
	Percentage change in Total Estimated Average Flooding Hours above rail in 10 years	82.0%	39.3%

Table 6.11: Percentage change in drainage system performance under weather and asset condition scenarios with reduced and increased asset diameter/height/width reduction assumptions

Similar to the change in the roughness assumption, the increase/decrease in diameter/height/width percentage reduction also increases/decreases the total estimated flooding hours. The percentage change in the performance indicator due to reduction in diameter/height/width is higher than the ones due to roughness changes. This indicated the predicted drainage system performance is more sensitive to the reduction in diameter/height/width. The may be due to the fact that any change in diameter/height/width will result in squared change in the cross sectional area, and hence will lead to even higher change in hydraulic capacity. Such a relationship is also shown in Figure 6.1; if the diameter of a storm drain is decreased to 60% of the original, its capacity will decrease to roughly 25%. The percentage change in the performance indicator is within the range of changes in asset cross sectional area due to changes in the diameter/height/width. The percentage changes in the “increased” case is higher than the “decreased” case, this is because the change in diameter/height/width reduction percentage will have a larger effect in the total cross sectional area change in the increased case.

Assumption on asset depth change is examined by changing this parameter by up to 20%, and the new set of assumptions are listed in Table 6.12. Depth reduction when Chambers, Outfall, Inflow, Syphon degrade are assumed to be:

	1	2	3	4	5
Depth reduction (m) (reduced)	0	0	0.08	0.16	0.32%
Depth reduction (m) (increased)	0	0	0.12	0.24	0.48%

Table 6.12: Condition score and effect on reduction in asset depth for sensitivity test

The flooding results are shown in the Table 6.13 below:

		Scenario 2	Scenario 4
Depth reduction (m) (reduced)	Total Estimated Average Flooding Hours in 10 years	404.2	1632.2
	Total Estimated Average Flooding Hours above rail in 10 years	281.3	1153.4
Depth reduction (m) (increased)	Total Estimated Average Flooding Hours in 10 years	406.2	1643.3
	Total Estimated Average Flooding Hours above rail in 10 years	281.5	1158.3

Table 6.13: Drainage system performance under weather and asset condition scenarios with reduced and increased depth reduction assumptions

The change in assumption of depth reduction is less than 0.4% for both scenarios and for both reduced and increased cases. This means the effect of this assumption with regard to the predicted system performance is very small. The system performance is least sensitive to this assumption among the three assumptions tested. This may be because by changing the depth of the node, only a limited amount of storage capacity (no more than $0.5 m^2$) will be reduced as a result, which will not have a significant effect on the hydraulic capacity of the whole system.

		Scenario 2	Scenario 4
Depth reduction (m) (reduced)	Percentage change in Total Estimated Average Flooding Hours in 10 years	-0.25%	-0.30%
	Percentage change in Total Estimated Average Flooding Hours above rail in 10 years	-0.04%	-0.17%
Depth reduction (m) (increased)	Percentage change in Total Estimated Average Flooding Hours in 10 years	0.25%	0.38%
	Percentage change in Total Estimated Average Flooding Hours above rail in 10 years	0.04%	0.25%

Table 6.14: Percentage change in drainage system performance under weather and asset condition scenarios with reduced and increased depth reduction assumptions

6.3 Conclusion

The integrated hydraulic and degradation model for a railway drainage system demonstrated a way to systematically evaluate the performance of a railway drainage system under the influence of asset degradation and climate change. It gives a way of predicting the future failure possibilities and comparing the ability of the drainage system to fulfil its designed purpose under different climate change scenarios. For the case study drainage system, the expected flooding is much more significant for the climate change scenario (RCP 8.5) than the ‘no climate change’ scenario, no matter whether asset degradation

process is taken into consideration or not. For both the ‘no climate change’ scenario and the RCP8.5 scenario, the asset degradation will bring a large increase in the flooding hours. These show that both the asset degradation and climate change will have a significant impact on the railway drainage system performance. Hence, it is important for asset managers to make proactive management decisions that can help maintain the serviceability of the drainage assets and mitigate any possible flood risk. It is also important for asset managers to consider possible effects of future climate change due to global warming, and design programs of work to increase the hydraulic capacity of existing drainage systems.

The case study is simulated under several assumptions to describe the linkage between asset condition change and asset characteristics. The sensitivity of the system performance indicator to these assumptions is tested. Result shows that the assumption on the roughness change and reduction in diameter/height/width of the linear assets has a large effect on the predicted performance, whereas the change in depth reduction has very little effect. The performance is most sensitive to the diameter/height/width changes; hence this assumption should be considered more carefully. On balance however the assumptions used to link changes in asset condition with modelled parameters appear reasonable.

The Knockenjig site is a typical rural railway section. The railway drainage system receives water from the surrounding farmland and then directs water to a nearby natural watercourse. Hence the demonstrated case study proves that the same methodology can be similarly applied to other railway sections in rural areas. For railway drainage systems in urban areas, extra analysis in the catchment area is needed, as the catchment served by the drainage system may be affected by factors other than surrounding topography. There might be extra discharges from structures and buildings, and man-made features may obstruct the rainfall runoff.

Although in this case study, only the worst global warming scenario RCP 8.5 is tested, scenarios of less severe climate change could also be tested to analyse the sensitivity of drainage system performance to different degrees of climate change. Moreover, the effect of human intervention (such as pipe renewal and maintenance) to bring drainage asset condition into a more robust state is not considered in this case study, which would be introduced in the next chapter and the results incorporated into the whole life cost model. The effect of human intervention will be reflected in the improvement of asset conditions, and the effect of various asset intervention strategies will be examined to provide asset managers with guidance to discover improved asset management regimes.

7 Whole life cost model using hydraulic performance measures

In this chapter, the degradation and hydraulic performance model explained in the previous chapters will be integrated into a whole life cost model to estimate the cost of owning the drainage assets in its service life time. By optimising the whole life cost, a decision support tool can be developed to help NR's asset managers develop a proactive asset maintenance regime that minimises the risk of asset failure.

7.1 Methodology

As shown in Chapter 5 and 6, once the hydraulic performance model is built and calibrated, it then can be implemented in the whole life cost model alongside with the degradation model so that the performance of railway drainage systems can be evaluated under the influence of worsening asset condition. The whole life cost model is then completed by introducing the decision support tool where various intervention strategies are generated to reverse or slow down the asset degradation process, and hence improve the drainage system hydraulic performance and reduce the consequences of failure.

The whole life cost model is designed to calculate the cost of an asset from 'womb' to 'tomb', ie. from the time when asset is acquired or build to its disposal. The whole life cost simulation process can be expressed in the flow chart shown in Figure 7.1. At the start of time, the asset is either constructed by the asset owner or purchased from a previous owner. Hence, a Design and Construction / Acquisition cost is calculated to reflect the price paid for owning the assets. The Penalty costs and intervention costs will then be calculated based on the performance and intervention strategies applied. At the end of the asset's life, a cost is incurred for the disposal of the asset.

Since drainage assets have a very long life-cycle, the model can be modified for short term management purposes. By disregarding the Design and Construction / Acquisition cost and Disposal Cost (shaded boxes in the diagram), the model can run not only for the whole life of an asset, but also for any appropriate accounting periods such as the 5-year Control Period in NR.

Here are the steps to run the whole life cost simulation:

1. Define the duration of the simulation T .
2. If simulating for the whole service life of the drainage assets, calculate the Design and Construction / Acquisition cost.
3. Apply the degradation model to simulate the condition degradation for each asset.
4. Whenever an asset is degraded, carry out interventions on the assets based on the intervention strategy generated by the Decision Support Tool.
5. Prepare a time series combining predicted degradation and intervention for all assets and sort them according to the time of transition in ascending order.

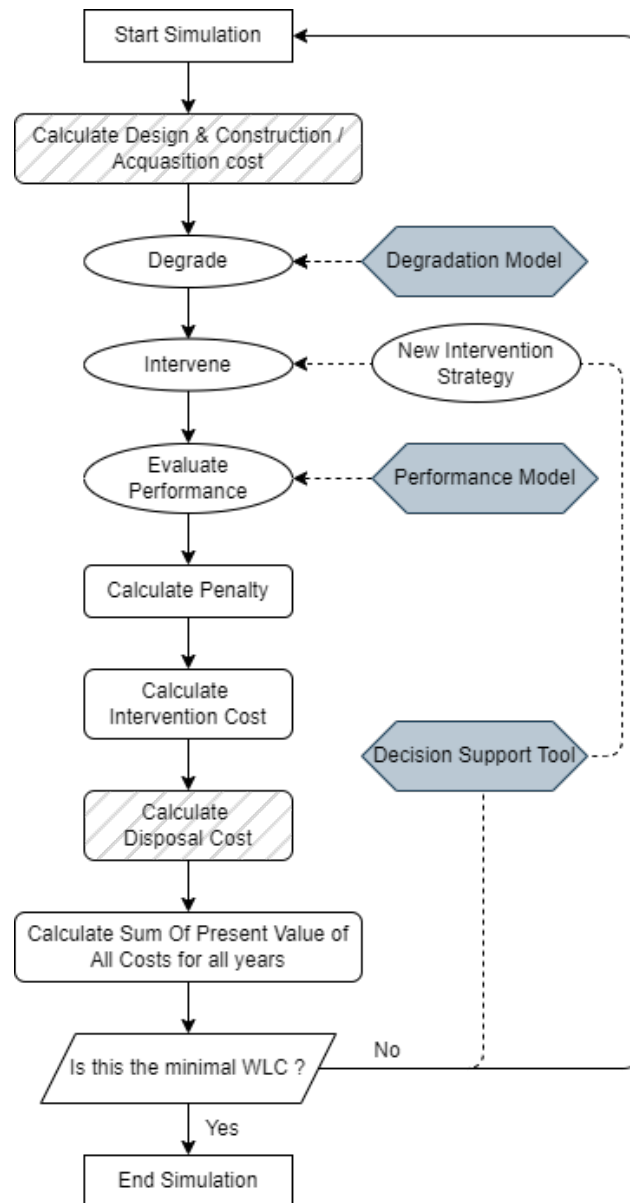


Figure 7.1: Flow chart for Whole Life Cost simulation

6. Run a calibrated hydraulic performance model with the current asset condition and modify the asset characteristics according to the condition changes due to degradation and intervention.
7. Extract the level of flooding from the performance model output and calculate the duration of water above rail level.
8. Calculate the cost of penalties based on the asset's performance.
 $\text{penalty cost} = \text{duration of flooding} \times \text{delay compensation cost per minute due to flooding}$
9. Calculate the total costs of the interventions carried out.
10. Calculate disposal cost if simulating for the whole service life of the drainage assets.

11. Aggregate the present value of all the costs.
12. Compare the total cost generated with previous simulations (compare with 0 on first iteration). If the WLC is minimal, end simulation and export the optimal intervention strategy; if not, rerun the simulation with a new set of intervention strategies generated by the decision support tool.

As explained in Chapter 6, the asset degradation process simulated is a stochastic process, hence each run will generate a different result. In order to reduce the stochasticity, for each intervention strategy, multiple stochastic simulations are needed to obtain a representative value of performance. As demonstrated in Section 6.2.3, a minimum of 23 runs is required for a 5 year simulation of drainage hydraulic performance under influence of asset degradation and climate change. Hence in this chapter, 30 simulation runs are performed for each scenario.

The Decision Support Tool is designed to generate a set of possible intervention strategies based on expert opinion and understanding of existing NR asset management policies. For each intervention strategy, two things will be defined: the proportion of interventions that will take place for each asset condition groups; the proportion of assets that will get intervened for each intervention type in each asset condition groups.

The WLC model was built using Matlab, SWMM was called and run with system command within Matlab when the hydraulic simulation has taken place, and the results are then fed back into Matlab to be analysed and used in the WLC calculation.

7.2 Case Study

A case study is performed with the Knockenjig case study site to forecast the whole life costs in the next 5 year Control Period under the influence of asset degradation and various asset intervention strategies. The strategy that costs the least will be taken to be the optimum intervention strategy. The historical rainfall data from 2015 to 2019 was used to mimic future rainfall. A few assumptions and decisions need to be made for each model and cost calculation steps before running the simulation.

7.2.1 Assumptions and model inputs

Before the starting the whole life cost simulation, several assumptions need to be made and a few input parameters need to be defined and calculated.

Assumptions

The effect of asset service condition changes on their physical characteristics needs to be defined in order to simulate the performance of the drainage system under the influence of asset degradation. Similarly, as explained and stated in Chapter 6, following assumptions are made based on data from the literature, expert opinion and preliminary investigations of the case study area:

- For Pipe, Channel, Culvert and Granular Drain
 - i. Service condition score changes will have the following effect on roughness:

Service Condition Score	1	2	3	4	5
Manning's n	0.010	0.012	0.020	0.035	0.055

Table 7.1: Condition score and corresponding roughness

- ii. Service condition score changes will have the following effect on asset diameter/height/width:

Service Condition Score	1	2	3	4	5
Percentage reduction	0%	0%	10%	30%	50%

Table 7.2: Condition score and effect on asset diameter/height/width

When changing the diameter/height/width of the asset, the asset's invert level will remain the same. This will result in a decrease in cross sectional area for about 20% - 75% depending on the shape

- For Chambers, Outfall, Inflow, Syphon
Service condition score changes will have the following effect on reduction in asset depth:

Service Condition Score	1	2	3	4	5
Depth reduction (m)	0	0	0.1	0.2	0.4

Table 7.3: Condition score and effect on reduction in asset depth

Based on NR Drainage Policy (NetworkRail, 2017), the effect of interventions on the drainage service condition score is assumed to be as following:

Start Service Condition	1	2	3	4	5
Service Condition After Refurbishment	1	1	1	1	1
Service Condition After Maintenance	1	1	2	2	3

Table 7.4: Effect of intervention on drainage service condition scores

Drainage asset condition at the start of simulation is expected to be the same as the current asset condition. However, as NR's asset database is incomplete, the current asset condition may be unknown and assumptions of the asset condition can only be made based on field survey observations. As shown in Appendix E, the service condition of many catchpits is relatively good. Hence, it is assumed that this type of asset's current condition is 1.

Model inputs

The parameters needed for the Whole Life Cost model are listed below. How they are deduced is also explained.

- Degradation generator matrix
 - Degradation matrices are calculated based on asset types.
 - All historical condition data are used to calculate the matrices.
- Unit penalty cost
 - Unit penalty cost is defined as the delay cost per minute, calculated using the delay cost due to flooding extracted from the Schedule 8 delay dataset, dated from 2015 to 2021.
 - Schedule 8 is an automatic payment scheme in the rail industry designed to protect train operators from uncontrollable risks by keeping them financially neutral during disruptions caused by other parties.

$$\begin{aligned} \text{Unit penalty cost} &= \frac{\text{Total delay cost of all incidents from 2015 to 2021}}{\text{Total delay minutes of all incidents from 2015 to 2021}} \\ &= \text{£55 per minute of flooding} \end{aligned}$$

- Unit intervention cost
 - Unit intervention cost is extracted from the Delivery Plan of CP6 for drainage maintenance and renewal cost and volume table in 2021. The Delivery Plan is a comprehensive document that outlines the strategic goals, projects, initiatives, and performance targets of Network Rail for a Control Period.
 - The average cost of refurbishment is £224 per meter and the cost of maintenance is £46 per meter.
 - Since the unit cost per meter does not differentiate between asset type, and the asset length is not recorded for all assets. The unit cost per asset is calculated based on whether an asset is a linear or a point asset. Linear assets such as pipes and culverts are assumed to be 30 meters long, whereas point assets such as culverts and inflow/outfall are assumed to be 3 meters long.

	Refurbishment	Maintenance
Linear Asset	£ 6720	£ 672
Point Asset	£ 1380	£ 138

Table 7.5: Unit intervention cost

- Interest rate
 - Interest rate is required to calculate the present value of future cash flow. The interest rate used in this study is the long-term interest rate from March 2022, which was the time when the WLC model was built. Long-term interest rates are defined by the yield on government bonds maturing in ten years. According to the forecasts generated by the Organisation for Economic Co-operation and

Development (OECD), the long-term interest rate was 1.5% in March 2022 (OECD, 2023).

7.2.2 Results

The whole life cost simulation algorithm, developed in this study through the integration of Matlab and SWMM, takes approximately three hours to execute a five-year simulation for a single intervention strategy. This was computed on a system with an Intel Core i9 processor, using 8 cores, and equipped with 16 GB of RAM. Although with Matlab Parallel Computing Toolbox™, multiple simulations can run at the same time, it is not sensible and efficient to run simulations for all possible interventions. Hence, an initial test of three strategies is performed, and a larger set of intervention strategies are selected based on the results of the initial test, and the outcomes of the set of new strategies are interpolated to estimate the whole life cost for the rest of the possible intervention strategies.

The initial three intervention strategies compared are as follows, assuming all assets are in condition 1 at the start of the simulation.

- (A) No intervention
- (B) Only intervene on an asset in condition 4 and 5
 - Intervention percentage

Service Condition Score	1	2	3	4	5
Refurbish	0%	0%	0%	50%	100%
Maintain	0%	0%	0%	50%	0%

Table 7.6: Intervention percentage for each asset condition group for Strategy B

- Intervention interval in months

Service Condition Score	1	2	3	4	5
Refurbish	6	6	6	6	6
Maintain	6	6	6	6	6

Table 7.7: Intervention interval for each asset condition group and each intervention type for Strategy B

- (C) Test with shorter Intervention interval
 - Intervention interval in months

Comparison of the results for these three strategies are listed below:

Service Condition Score	1	2	3	4	5
Refurbish	3	3	3	3	3
Maintain	1	1	1	1	1

Table 7.8: Intervention interval for each asset condition group and each intervention type for Strategy C

	Strategy A	Strategy B	Strategy C
Average Flooding Hours	95.1	72.3	64.1
Average Flooding Hours above 30cm	69.1	47.9	44.4
Penalty Cost	£191,936	£133,213	£123,226
Refurbishment – Linear Asset	0	1.8	2.2
Refurbishment – Point Asset	0	1.9	2.1
Maintenance – Linear Asset	0	0.5	0.5
Maintenance – Point Asset	0	0.6	0.4
Intervention Cost	£0	£13,255	£15,783
Total Cost	£191,936	£146,468	£139,009

Table 7.9: Results of the three initial intervention strategies

As shown in Table 7.9, compared with any intervention taken place, the amount of total costs is lower with some intervention actions. Although there is a cost paid out for intervention, the amount of penalty cost reduced is higher than the intervention cost, hence, it is more cost efficient for asset managers to maintain their assets following that strategy. Also, comparing strategy B and C, it is observed that the size of the total cost is reduced when the asset is intervened sooner after they degrade into a poorer condition. More interventions are carried out as expected as the response time to degradation is quicker which leads to a slightly higher intervention cost, however, such cost is balanced out by the improvement of drainage performance which leads to a reduction in flooding time and hence a lower penalty cost. The overall cost added up is lower for strategy C than B, this means it is always encouraged for asset managers to remedy the degraded asset as soon as possible.

However, it is not always possible at the current stage to have a response time less than 6 months for all drainage assets for various reasons: some assets may be hard to access and some intervention may need to be outsourced and require longer times to plan and arrange. Also, although the amount of flooding time is reduced when assets are intervened sooner, the difference is not as large as compared with no intervention. As shown in Table 7.9, the average flooding hours for strategy B is actually lower than strategy C, although the flooding in strategy B is more severe hence the average flooding time that will affect train operation is higher. Therefore, it is decided that in the following simulations, the intervention interval will be fixed at 6 months.

Hence a set of strategies are constructed based on the following pre-defined rules:

- Since condition 5 is the worst condition, all should be refurbished to a better state.

- For all types of intervention and for all condition classes, intervention will take place 6 months after the degradation condition state transition happens.
- The aggregate percentage of Maintenance and Refurbishment applied to one asset condition group should not exceed 100%, i.e. any asset can only be intervened with one type of intervention action.
- No intervention is applied to condition class 1 and 2, as assets with condition score 1 are in their perfect condition and do not need to be intervened; whereas assets with condition 2 are defined as ‘Superficial deposits with no loss of capacity’, interventions are also not needed.
- No refurbishment is applied to condition class 3, since maintenance is enough to bring condition 3 back to functioning state with full hydraulic capacity, as a more expensive option, refurbishment will not be performed on asset with condition 3.

The strategies are hence composed by combinations of maintaining assets at condition grade 3, maintaining assets at condition grade 4 and refurbishing assets at condition grade 4. A set of 21 combinations were tested and results were interpolated. The list of the tested strategies can be found in Appendix H. Assets conditions at the start of the simulation are assumed to be 1. The plots of the interpolated results are shown in Figure 7.2 below. The total cost value is shown as volumetric data along slice planes that are orthogonal to each axis. The colour bar indicated the scale of the cost value. The optimum intervention strategy that minimises the total cost is marked with a red dot.

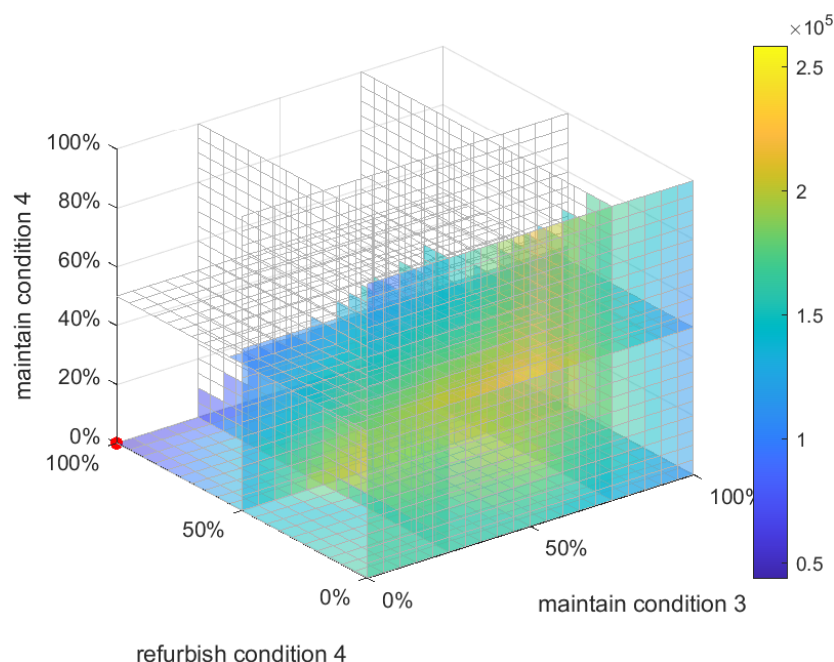


Figure 7.2: Total cost of the Knockenjig system under various intervention strategies with starting condition 1

The optimum intervention strategy in this case is refurbishing 100% of condition 4 and intervening 0% of condition 3. Although only slices of the total cost colour can be

seen in the graph, it clearly shows that the total cost increases when the amount of refurbishment for condition 4 approaches 0%. The effect of maintaining condition 3 and 4 is less significant. This could be due to the fact that the assets at the start are in a “perfect” condition, hence the degradation of assets is slower or less unlikely. Degradation to condition 4 and 5 would rarely happen, hence the overall state of the drainage system will remain in a relatively good level if all assets degraded to a condition 4 or 5 is intervened.

7.2.3 Sensitivity testing

Start condition

As explained in the assumptions, the condition of the assets at the start of the simulation is assumed since the asset condition data does not exist in the database. In Section 7.2.2, the results of 5 years’ of simulation with start condition of 1 is presented. However, the assumption of asset in condition 1 is questionable, as only new build assets (installed without error) can be qualified in such status. Since the assets have been in use for many years, in reality, their conditions are expected to be worse. To test the effect on the final result under such assumptions, a sensitivity test is performed by running similar simulations with various start condition scores. The test is done assuming assets are in a good but not perfect condition, ie. condition 2. Also, the model is tested with randomly assigned start conditions that better reflect the general population of the asset conditions; the proportion of assets in each condition class in the Knockenjig site is designed to be the same as the proportion of assets in each condition class nationwide. The results are shown in Figure 7.3 and 7.4.

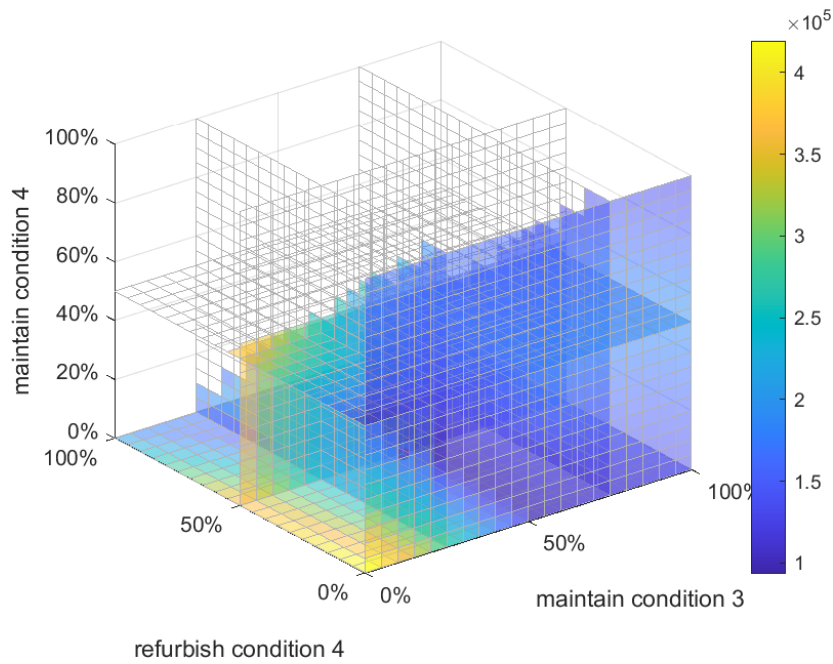


Figure 7.3: Total cost of the Knockenjig system under various intervention strategies with starting condition 2

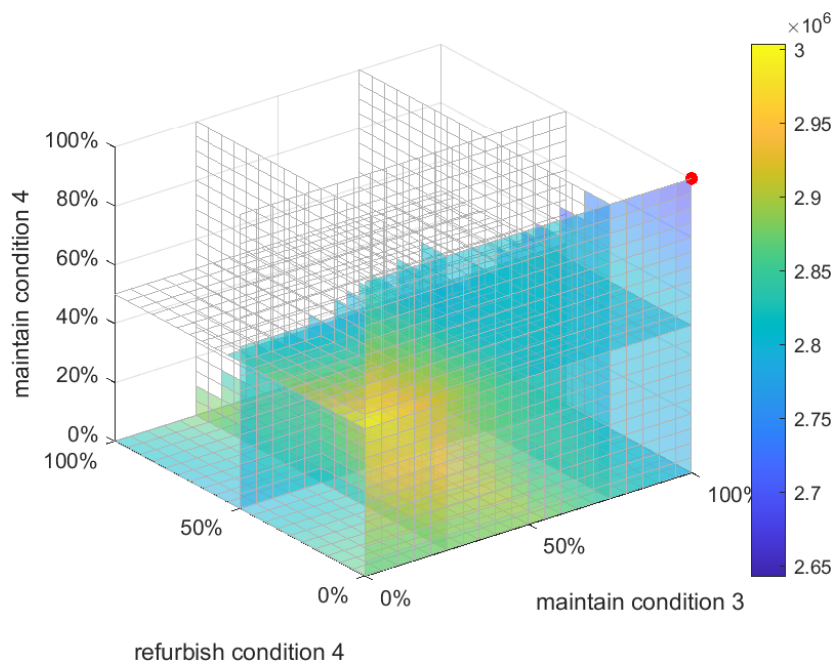


Figure 7.4: Total cost of the Knockenjig system under various intervention strategies with starting condition 3

As shown in the Figure 7.4, the optimum strategy with start condition 2 is 50% of maintenance for condition 3 and 50% of refurbishment for condition 4. There is more cost incurred on the edge where 0% of maintenance is done or both asset conditions 3 and 4. This means it is important to intervene on the poorer asset state, as a condition 4 asset left unattended can have a much worse effect. However, the optimum strategy

is not refurbishing 100% and only 50% of condition 4, this may be because the cost of refurbishment is high, the cost of refurbishing all condition 4 cannot be recovered by the savings in reducing flood risk. Since the loss of hydraulic capacity at condition 3 is less severe, the effect of maintaining condition 3 would be less significant, hence only 50% is needed to be intervened to reach the minimum overall cost.

The optimum strategy with randomly assigned start asset condition is 100% of maintenance for condition 3 and 100% of maintenance for condition 4. In this case, the average asset condition is worse than the previous two cases, and there exist some assets with the worst conditions at the beginning. It is expected that more interventions should be carried out to take the assets to a better functioning condition. Hence, all assets in both condition 3 and 4 are intervened. 100% of condition 3 assets are maintained compared to the 50% for the case with start condition 2. 100% of the condition 4 assets are maintained rather than refurbished, since refurbishment and maintenance will bring assets back into a better functioning state, but refurbishment is more costly, so maintenance would seem to be the more cost efficient option.

Therefore, it is demonstrated that the condition of the drainage assets at the start of the simulation has a significant effect on the optimum intervention strategy. Asset managers should therefore understand the importance of making frequent inspections and acquire updated asset condition when using the whole life cost model to simulate the possible future costs and finding the optimum intervention strategy. Without an up to date condition score, it is suggested that the asset manager could use a randomly selected start condition using the national asset condition score distribution. Although based on the simulation results, the overall costs for the randomly assigned condition case is the highest among all the simulation scenarios, and more interventions are expected to be planned; it is believed it is always better to overestimate than underestimate the amount of budget needed to cover the scheduled intervention costs and penalty costs.

Roughness score

As presented in the sensitivity analysis in Section 6.2.5, the assumption made as to how asset service condition change is reflected on a pipe roughness score and hence the effect of asset degradation on the hydraulic performance of the drainage system under an asset degradation trajectory. Similarly, a sensitivity test is also performed with the whole life cost model to examine how sensitive the result of the optimum intervention strategy is to the change in roughness assumption. The Manning's n in degraded assets are reduced by 20% compared to the assumption made in the above section, and the results are shown in the Table 7.10.

Service Condition Score	1	2	3	4	5
Manning's n	0.010	0.0096	0.016	0.028	0.044

Table 7.10: Condition score and corresponding assumed roughness

Simulations are run while the rest of the assumptions remain the same, the condition of

the assets at the start is 1. The graph of the resultant total costs is shown in Figure 7.5. The optimum intervention strategy is 50% maintenance for condition 3 assets and 50% of refurbishment for condition 4 assets. Compared with the original scenario, which is 100% of refurbishment for condition 4, there is less refurbishment required which could mean that assets in poorer states require less intervention as its effect on hydraulic capacity is reduced. However, for assets in less severe condition, the decrease in roughness may not reduce the risk of flooding in some situations. For example, if the upstream pipes have a lower roughness score, flow velocity may increase which is helpful in protecting the upstream railway assets; however, at the same time, it could also put more pressure on the downstream assets and cause flooding in locations where the drainage system does not have enough hydraulic capacity. Therefore, some maintenance of condition 3 is also required to bring the overall drainage system to a better state.

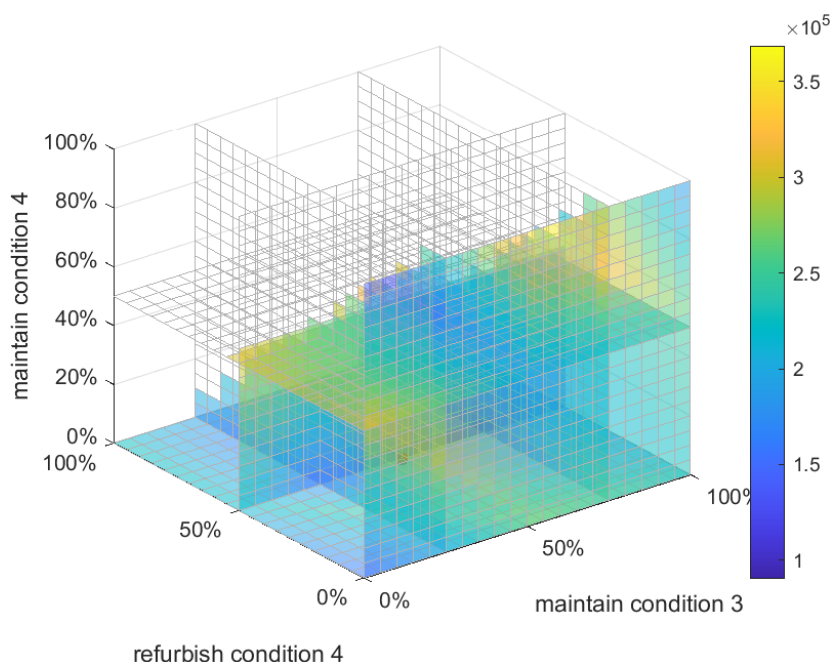


Figure 7.5: Total cost of the Knockenjig system under reduced roughness score

Asset diameter/height/width

Assumption on percentage reduction in asset diameter/height/width with regard to asset service condition degradation is increased by 20%, and the new set of assumptions are listed in Table 7.6. This will result in a reduction of 22% - 84% in pipe cross sectional area.

Service Condition Score	1	2	3	4	5
Percentage reduction	0%	0%	12%	36%	60%

Table 7.11: Condition score and corresponding asset diameter/height/width for sensitivity test

The result WLC with the increased reduction in asset diameter/height/width is shown in the Figure 7.6. The optimum solution is 100% maintenance for condition 3 and 100% refurbishment for condition 4. As shown in the sensitivity test for the integrated hydraulic model in Section 6.2.5, drainage system performance is most sensitive to the increase/reduction in asset diameter/height/width percentage reduction. With the increased percentage reduction assumption, the asset hydraulic capacity will be severely reduced and its performance will become much poorer. Hence, a much higher penalty cost would be expected as more flooding is likely to occur. Therefore, since the consequence of asset degrading is more serious, there is more incentive to intervene these assets and bring them to a better condition. Hence all of the conditions 3 and 4 are intervened, and both are improved to its highest possible performance level under the pre-defined rules.

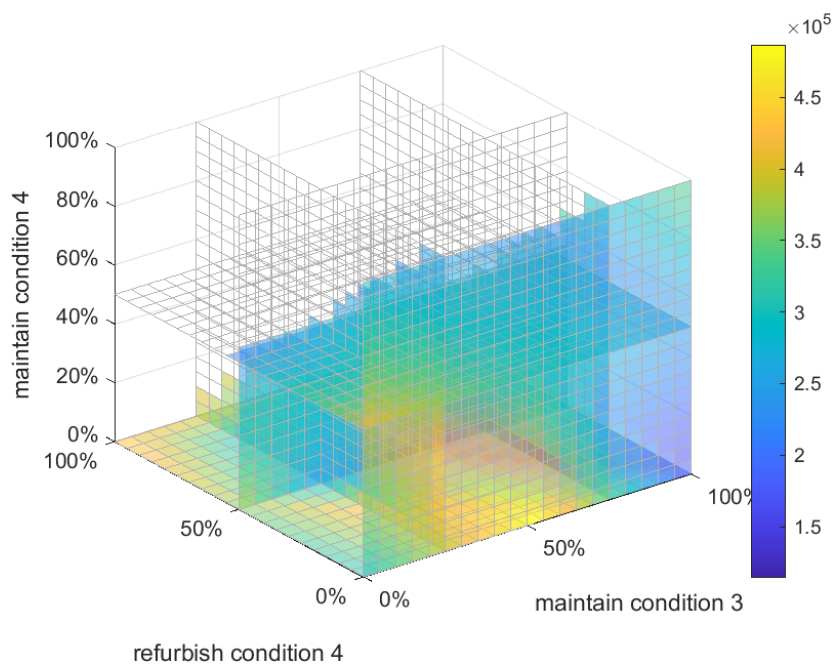


Figure 7.6: Total cost of the Knockenjig system for a 10 year simulation

Duration of simulation

For the case study, the duration of simulation is 5 years, i.e. one Control Period. In reality, simulations may be performed for a longer period of time, e.g. the useful life of the assets. Hence in this section, how the optimum intervention strategy might change with an increasing simulation period was also tested. The result is shown in Figure 7.7 and the optimum is 100% of maintenance for condition 3 and 100% of maintenance for condition 4. 100% of condition 3 is intervened compared to the 0% in the 5-year simulation, this may due to the fact that duration a longer time period, there is a higher probability of assets transitioning from condition 3 to the worse condition 4 and 5. As such transitions are less likely to be observed in a 5-year simulation, it is less likely to cause any flooding due to performance loss, and hence there is no incentive to intervene assets in condition 3. Whereas in a 10-year simulation, more asset degradation from

condition 3 is expected; and it is always ideal to intervene in all degraded assets to bring them back to a serviceable condition before it degrades into the worst state (condition 5), as assets with condition 5 may cause larger or even critical damage to the performance of the drainage system. It is noted that the optimum intervention strategy over 10 years' period with start condition 1 is the same as the optimum strategy of the random start case. This might indicate that over a longer simulation period, the effect of the start condition will become less significant, and the optimum intervention strategy will converge into one single longer term strategy. Moreover, since refurbishment cost more than maintenance, and the consequence of the two is not too different according to the assumed changes in asset characteristics (i.e. difference between condition 1 and 2 is only an increase of 0.002 in roughness); refurbishment would normally be the more cost effective way of intervening assets.

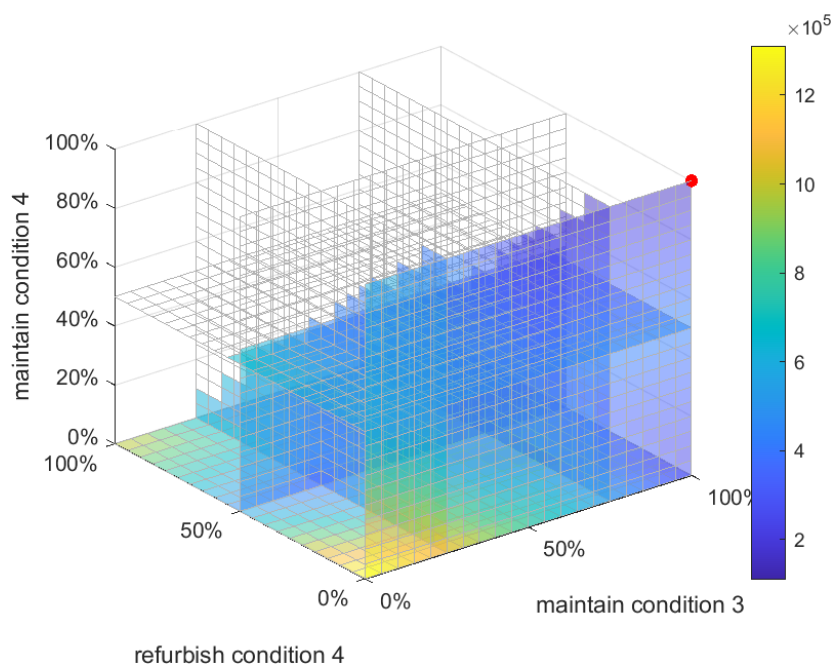


Figure 7.7: Total cost of the Knockenjig system for a 10 year simulation

7.3 Conclusion

In this chapter, Whole Life Cost model was developed using the integrated hydraulic performance model introduced in Chapter 6. A set of feasible intervention strategies were generated based on expert opinion from route engineers about the general rules of route level maintenance planning. The intervention strategies were then applied to the degradation simulation process to bring an asset's condition to a better state after the asset had significantly degraded. The asset condition trajectory simulated under the influence of both asset degradation and human intervention was then used as an input to change the asset characteristics in the integrated hydraulic performance model. The performance of the drainage system was then evaluated using the hydraulic performance model with the adjusted asset characteristic, and the output performance indicator (du-

ration of flooding) is used to calculate the penalty costs due to loss of performance. The whole life cost is calculated by adding up the present value of the intervention costs and penalty costs. The intervention strategy with the the minimal total whole life cost is proposed as the optimum strategy.

A case study is performed for the Knockenjig site, for a 5 year simulation, the optimum intervention solution is found to be refurbishing all assets with condition scores 4 and 5 while not intervening in assets in other conditions. Since several assumption has been made on the linkage between condition degradation and the asset characteristic changes, as well as the start condition of the drainage assets, sensitivity tests were performed to test their effect on the WLC simulation. Decreasing the roughness score of the degraded assets would decrease the percentage of asset need to be intervened in a worse condition. Since the effect of degradation is reduced, less intervention is required to maintain the asset's condition and performance level. On the contrary, the increase in the percentage reduction of asset's diameter/width/height would lead to a higher percentage of asset interventions. For a worse start condition, the percentage of assets intervened was increased as more intervention is required to bring the assets' performance to a desired level. For a longer simulation period of 10 years, the percentage of assets intervened also increased, and the optimum intervention strategy would converge into one strategy that intervenes all degraded assets to bring them back to a serviceable condition before it degrades into condition 5.

This model can be used on a tactical level to assist asset managers in identifying the optimum intervention strategy for a portfolio of drainage systems. Since the model is built based on a very thorough investigation of the geometric properties and hydraulic capacity of the drainage system, it can provide site-specific information that assists route engineers in prioritising their day to day maintenance plan. It can also be used during the design process of building a sustainable and climate resilient drainage system, providing justification for construction expenditure from a whole life cost perspective.

8 Whole life cost model using data driven approach

As explained in Section 3.3 and Chapter 5, two parallel models are developed to evaluate the performance of the drainage assets and which then integrated into the Whole life cost model in order to provide asset manager with a tool that can be used for decision making both on the tactical and the strategical level. The hydraulic performance model introduced in Chapter 5 can produce a thorough assessment of the hydraulic carrying capacity of any railway drainage system, however, it requires detailed asset information that are currently not available nationwide in the NR database. The WLC model that integrated with the hydraulic performance model also has its limitations. It needs a lot of computational power; it takes a day to simulate for the 1 km long drainage system in the case study. Hence it will be both too financially costly and time consuming to perform an aggregated WLC simulation nationally for all the railway drainage systems. Although it is very useful on a tactical level to help route engineer to prioritise their day to day maintenance regime, it is less practical to be used for national budget planning and workload forecasting. Therefore, a WLC model with data driven approach is presented in this chapter to assist strategic top level management planning.

8.1 Methodology

8.1.1 Failure mode analysis

As described in Section 3.3.2, railway drainage failure mechanisms have been investigated using Machine Learning (ML) algorithms in the In2track2 project. ML techniques can enable the identification of dominant failure mechanisms and empirical failure relationships in large data sets by mapping inputs to outputs without attempting to replicate assumed underlying processes, a property that has made it a useful method for various engineering applications. They are categorised into two groups: supervised learning and unsupervised learning. Supervised ML approaches such as Linear regression and Decision Trees are employed when parameters in the data set can be clearly labeled as input and output, and then the algorithm is used to “learn” the mapping function from the input to the output parameters. However, when relationships between parameters are poorly understood and prior knowledge about data is unavailable, an unsupervised clustering technique such as Principal Component Analysis (PCA) or Self-Organising Mapping (SOM) will provide a more objective tool to uncover those relationships. PCA is unable to deal with missing values in the input data and with nonlinear relationships between parameters, while SOM can easily handle both issues (Speight et al., 2019). SOM is suitable specifically for visualizing relationships within large data sets, producing a low-dimensional (typically two-dimensional) representation of a higher dimensional data set while preserving the topological structure of the data (Miljkovic, 2017).

The historical data set recorded by NR contains large numbers of samples with many variables, with a significant amount of missing values due to the incremental and devolved way in which the asset data was collected. Therefore, SOM was chosen to explore and

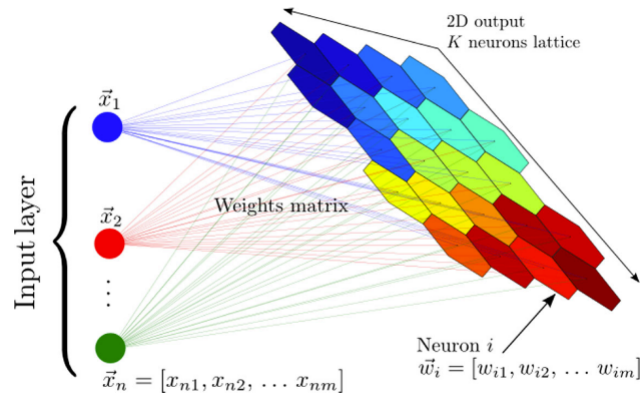


Figure 8.1: A schematic representation of a Self-Organizing Map

visualise relationships and correlations between various parameters in the data ranging from weather, drainage and other railway asset characteristics to delays, derailments and railway asset failures (Kazemi et al., 2021).

SOM does not have hidden layers, it maps the training set directly to the output network using competitive learning. The idea is illustrated in Figure 8.1, a training set of n vectors of x_1, x_2, \dots, x_n , is mapped into a lattice of K neurons. A neuron contains a vector of weights $(w_{i1}, w_{i2}, \dots, w_{im})$ associated with all the input attributes and with the same dimension of m . The colour of the map encodes the organization of groups of samples/observations with similar properties (Kazemi et al., 2021).

The SOM training process consists of the following steps:

1. Initialise the weights of neurons.
2. A vector from the input data (a sample in the data) is presented to the lattice and the weight vectors of the neurons in the output layer are compared with the input vector.
3. The neuron with the most similar weights to the input vector is selected as its ‘Best Matching Unit’ (BMU). This is done by calculating the Euclidean distance between weight vector and input vectors.
4. The weights of the neighbouring neurons of the BMU are updated to make them more like the input vector but with a smaller degree, according to their distance to the BMU.
5. The neighbourhood is defined by a circle with a certain radius which decreases gradually over the training process.
6. Repeat steps 2-5 until the change of the weight vectors falls below a certain threshold, i.e. the clusters are formed.

The failure pathways of drainage related failure incidents was derived as a result of SOM analysis. Based on the failure pathways identified in the In2Track2 project, in this study, another widely used supervised ML algorithm: linear regression model has been employed

to quantify the relationship between the identified “cause of failure” parameters and the number of failures. The linear regression is usually expressed in the form:

$$Y = \beta_0 + X_1\beta_1 + \dots + X_p\beta_p + \epsilon, \quad (22)$$

where Y is the observed failure value, and X_i is the input variables that are parameters presented with a linkage to failures, and ϵ denotes the error term that cannot be explained by the model. The model is fitted using least-squares.

8.1.2 Whole life cost optimisation

The output of failure mode analysis then was incorporated into the Whole Life Cost model to provides predictions of asset failure risk and drainage asset performance. The WLC optimisation problem is described as follows:

$$\begin{aligned} \min_x C &= \sum_{t=1}^{t=n} P_t(x, y) \frac{1}{(1+r)^t} + \sum_{t=1}^{t=n} I_t(x, y) \frac{1}{(1+r)^t} \\ \text{subject to } C &\leq \text{budget constraint} \\ P_t &\leq \text{risk constraints } \forall t \in [1, n] \\ I_t &\leq \text{manpower constraints } \forall t \in [1, n] \\ x &\text{ meets feasibility constraints} \end{aligned} \quad (23)$$

C is the whole life cost account, P_t is the penalty cost at time step t , I_t is the intervention cost at time step t , x is the intervention strategy, y is the a set of user defined input parameters, n is number of time steps simulated, and r is the interest rate of one time step.

The WLC cost is the sum of the aggregated present value of the penalty costs and the aggregated present value of the intervention costs. The objective of the WLC optimisation problem is to find the optimum intervention strategy x that minimise C and comply with the constraints.

Several constraints have been proposed to meet operational requirement as well as assisting asset managers with intelligent decision making which could limit the risks they are willing to take.

- The WLC account is set to meet the budget constraints, i.e. the total amount of cost must not exceed the amount of budget set for each year, no matter whether the cost is contributed by penalty cost due to asset degradation and performance loss, or contributed by intervention costs to bring assets into a better condition state.
- At each time step, penalty costs are restricted by the risk constraints. This prevents the algorithm from allocating too much cost into the penalty rather than intervention, even though it may yield a lower total cost when no constraints are set. This constraint is put in place since one of the main purpose of the model is to mitigate failures while minimising the WLC cost. By adjusting this constraint, asset managers can then alter the model based on their risk appetite.

- In NR, many interventions are done in-house, but there may be limited amount of manpower in NR, i.e. a limited amount of intervention can be carried out each year. Hence, the intervention cost is restricted by the manpower at each time step.
- The intervention strategy needs to be feasible, for example, it cannot exceed 100% and one asset should not be intervened with different intervention action in the same time step.

Matlab function ‘fmincon’ was used to solve the optimisation problem. ‘fmincon’ is a nonlinear programming solver that finds the minimum of a problem specified by:

$$\min_x f(x) \text{ such that } \begin{cases} c(x) \leq 0 \\ ceq(x) = 0 \\ A \cdot x \leq b \\ Aeq \cdot x = beq \\ lb \leq x \leq ub. \end{cases}$$

The first two equation define the non-linear inequality and equality constraints, and next two equation defines the linear inequality and equality constraints, and the last equation defines the lower and upper boundary of the minimiser x . ‘fmincon’ solves the optimisation problem with gradient-based method by finding local minima through iterations. The process of ‘fmincon’ begins with a selected initial point, follows a predetermined update mechanism, and concludes when a specified stopping condition is satisfied. A local optimum is found if the first-order necessary and second-order sufficient conditions are both satisfied.

Normally, multiple runs with different initial starting points would be performed manually with ‘fmincon’ to look for a global optimum. However, with the Matlab ‘GlobalSearch’ algorithm, such a process can be automated. ‘GlobalSearch’ attempts to find the global minimum of a problem by performing a search over the entire problem space. The function is typically used when the problem has multiple local minima and the goal is to find the absolute minimum, not just a local one. The algorithm is developed based on methodology in Ugray et al. (2011), detailed description can be found at (*How GlobalSearch and MultiStart Work*, n.d.). The simulation process is shown in the Figure 8.2 and the basic steps of the algorithm as stated below:

1. Randomly select a set of different starting points in the problem space using the scatter-search method.
2. From each starting point, a local search algorithm (‘fmincon’) is run to find a local minimum.
3. Keep track of the optimum solution found from all of the local searches.
4. After all local searches are completed, the best solution is returned as the global minimum.

GlobalSearch Algorithm

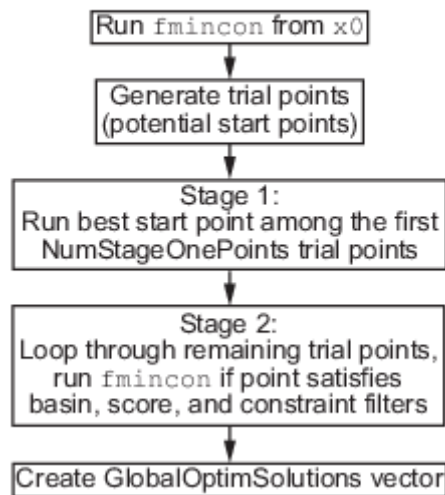


Figure 8.2: Matlab GlobalSearch Algorithm Overview (source:(*How GlobalSearch and MultiStart Work*, n.d.))

8.2 Case Study

A case study is conducted on a national scale to demonstrate the use of whole life cost algorithm with the data driven approach. A failure mode analysis was carried out in the In2track2

8.2.1 Failure Mode Analysis

Two failure types were under investigating in the In2track2 project: Track Flooding and Earthwork Failure. Track Flooding is defined as the incidents recorded when train is under speed restriction or stopped due to excess of water present above the railway track. Earthwork Failure is defined as damage of an earthwork asset due to underperforming drainage. Track Flooding incidents are the result of short term drainage failures, whereas the Earthwork Failures are the result of a combination of short term and long term drainage failure, i.e. it can happen due to long term water erosion and short term excessive water flows. Since the failure mechanism of Earthwork failures is more complex and is related to some earthwork specific parameters that requires further investigation, in this case study, only the Track Flooding failures are taken into consideration as part of the WLC simulation.

Several parameters has been investigated using SOMs to test for linkage to Track Flooding failures, such as drainage structural and service asset condition, precipitation and local geology. The result shows that the following parameters are identified to be important:

- Total precipitation (mm) in the last 5 days before the failure and non-failure events
- Average service condition score of all assets 100 m of the location of failures and non-failures

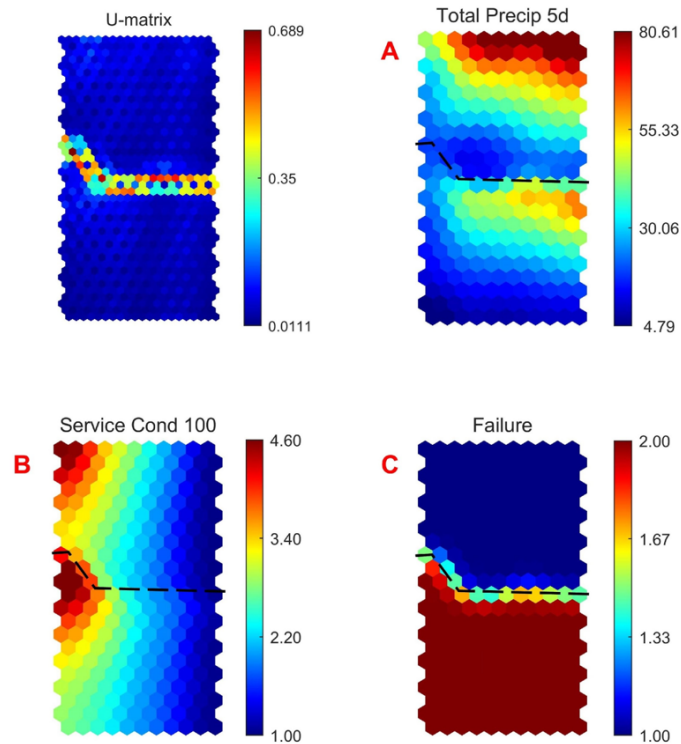


Figure 8.3: Relationships between Failure, total precipitation in the last 5 days, and average service condition score

The SOMs graph is presented in Figure 8.3. On the maps, each cell (colored hexagon) represents a group of observations; the spatial location of a cell in a topographic map corresponds to a particular domain or feature drawn from the input space. Colour of the cell represents the value of the variables where red is high and blue is low. Each cell in the same position on different maps corresponds to the same group of observations/samples. As shown in the Figure 8.3, two clusters are formed due to the Failure map (lattice C), which is marked by the dashed lines. The number in the Failure map indicates whether a failure occurred, where 1 means failure happened and 2 means there is no failure. As expected, the failure is linked to a higher precipitation level as there are lots more red cells in the upper cluster in the 5 day total precipitation map (lattice A). The linkage between asset service condition is less obvious, however, in the service condition map (lattice B), there is slightly less cells with a low condition score (better condition) in the cluster corresponding to failure.

Following the result of SOMs analysis, linear regression is performed to model the relationship between Track Flooding failures and the average service condition score and total precipitation nationwide. Number of failure per year is calculated using historical failure records. Service condition for each drainage asset at the end of each year is extracted from the historical asset condition records in Ellipse database, and the average service condition is calculated. Annual precipitation in the UK is obtained from the UK Meteorological Office. The model was simulation with a time step of one year, due to the fact that inspection of the drainage asset is likely to be only carried out once per year;

with a shorter time steps, there is not enough asset condition information to generate an accurate prediction of the number of failures. The analysis was performed using failure data from 2017-2021, and the result are as follows:

Estimated Coefficients:

	Estimate	SE	tStat	pValue
(Intercept)	-3301.5	639.88	-5.16	0.036
x1	1360.5	313.94	4.33	0.049
x2	1.02	0.45	2.15	0.164

Number of observations: 5, Error degrees of freedom: 2

Root Mean Squared Error: 97.8

R-squared: 0.95, Adjusted R-Squared: 0.899

F-statistic vs. constant model: 18.8, p-value = 0.05

Table 8.1: Linear regression results for Track Flooding failure analysis

x1 is the average service condition score and x2 is the annual precipitation. The p-value for the F-test on the model is 0.05, means this null hypothesis of each independent variable has no effect on the dependent variable is rejected at 5% significance level. The R-squared is 0.95 suggests that the model explains approximately 95% of the variability in the dependent variable. The added variable plot is shown in Figure 8.4, demonstrating a partial correlation between the independent variables and the dependent variable. The dotted line shows a confidence interval that indicates how precisely the sample data fit that correlation.

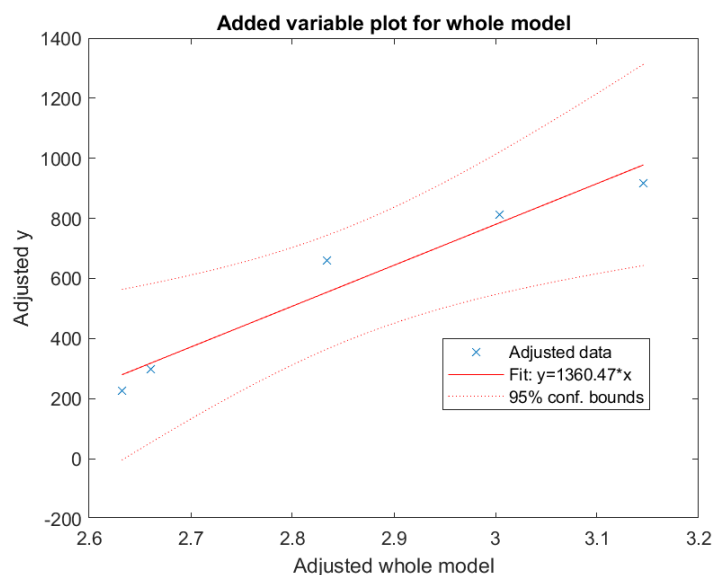


Figure 8.4: Added variable plot for Track Flooding failure analysis

The slope of the regression line in the Figure 8.4 indicates that there is a positive correlation between the independent variables (asset service condition and annual precipitation)

and the depend variable (number of failures). The graph also demonstrated that the adjusted data are all in the 95% confidence bounds and most of them are quite close to the best fitted line. This indicates that the model gives a sound prediction for the number of failures.

It is noted that this prediction model could pass origin when $x_1 > 1$. This means the predicted of failures could reduced to 0 even when the asset service condition is not at its minimum value 1. This is sensible as once the average service condition reaches a low value, even though it is not at its best performance, the existing hydraulic performance is enough to direct water away from railway assets and mitigate any flood risks. Hence, in cases when predicted number of failures is negative, it is assumed to be 0.

8.2.2 Whole life cost optimisation

The WLC optimisation problem is described in Section 8.1.2 as:

$$\begin{aligned} \min_x C &= \sum_{t=1}^{t=n} P_t(x, y) \frac{1}{(1+r)^t} + \sum_{t=1}^{t=n} I_t(x, y) \frac{1}{(1+r)^t} \\ \text{subject to } C &\leq \text{budget constraint} \\ P_t &\leq \text{risk constraints } \forall t \in [1, n] \\ I_t &\leq \text{manpower constraints } \forall t \in [1, n] \\ x &\text{ meets feasibility constraints} \end{aligned} \quad (24)$$

The minimizer x represents the intervention strategy. Two types of intervention can be carried out to remedy the drainage service condition: Refurbishment and Maintenance. Hence x is constructed as a matrix that represents the percentage of each condition category get intervened by each type of intervention action.

$$x = \begin{pmatrix} r_1 & r_2 & r_3 & r_4 & r_5 \\ m_1 & m_2 & m_3 & m_4 & m_5 \end{pmatrix} \quad (25)$$

r_i is the percentage of assets in service condition i get refurbished. m_i is the percentage of assets in service condition i get maintained. As condition 1 represents the perfect performance, no intervention is needed for this condition category, hence, r_1 and m_i are set to equal to 0.

The constraints of the optimisation problem are listed as follows:

- Total cost \leq budget constraint
- Expected failures \leq risk constraint
- Total refurbish work done \leq Maximum refurbish manpower
- Total maintenance work done \leq Maximum maintenance man hour
- Lower boundary of intervention matrix element is 0%
- Upper boundary of intervention matrix element is 100%
- Asset can not be both refurbished and maintained

8.2.2.1 Inputs and assumptions

Similarly as Chapter 6 and Chapter 7, the effect of interventions on the drainage service condition score is assumed to be as following based on NR Drainage Policy (NetworkRail, 2017):

Start Service Condition	1	2	3	4	5
Service Condition After Refurbishment	1	1	1	1	1
Service Condition After Maintenance	1	1	2	2	3

Table 8.2: Effect of intervention on drainage service condition scores

Hence, the refurbishment and maintenance effect can be calculated using the matrix:

$$E = \begin{pmatrix} r_1 + m_1 & 0 & 0 & 0 & 0 \\ r_2 + m_2 & 1 - r_2 - m_2 & 0 & 0 & 0 \\ r_3 & m_3 & 1 - r_3 - m_3 & 0 & 0 \\ r_4 & m_4 & 0 & 1 - r_4 - m_4 & 0 \\ r_5 & 0 & m_5 & 0 & 1 - r_5 - m_5 \end{pmatrix} \quad (26)$$

Input parameters generated from the asset degradation model and the failure mode analysis, as well as several user defined parameters are listed and explained below. Assumptions are made when required information is not available or uncertain.

Precipitation

Precipitation is used as one of the independent variable to predict the number of failures. Hence, future annual precipitation in the simulated time period needs to be predicted. In cases where precipitation is assumed to be similar to the precipitation in the past, the annual precipitation is randomly picked from past 100 year's record. In cases when climate changes are considered, annual precipitation from the UK Climate Projections (UKCP18) global projections (60km) and regional projections (12km) is used as the future precipitation prediction. Two climate change scenarios provided by the model: RCP2.6 and RCP8.5. The predicted annual precipitation at time t is denoted as H_t .

Service Condition degradation transition matrices

Service condition degradation transition matrix is calculated with the methodology stated in Section 4.2.3 using historical asset condition records. For better accuracy of prediction, transition rate is calculated and applied individually for each asset groups. In cases when an asset has no asset group information record or the asset group does not have enough asset samples to generate a stable transition matrix, the transition rate matrix produced with all drainage assets is used as a proxy. Q_k represents transition rate matrix for asset type k .

Asset Start Condition

The amount of assets in each service condition category for each asset type is calculated from the drainage database, and recorded in matrix $N_{k,1} = [n_{1,k,1}, n_{2,k,1}, n_{3,k,1}, n_{4,k,1}, n_{5,k,1}]$, where $n_{i,k,1}$ is number of assets in condition i with asset type k at time $t = 1$.

Simulation Duration and Time steps

The length of the time steps l and number of iterations n need to be defined for the simulation process. l is presented as a fraction of years, hence the number of years simulated would be $l \times n$.

Unit Penalty Cost

The average penalty cost of the Track Flooding incidents is calculated and used as the unit penalty cost pc .

Unit Intervention Cost

Similarly to Section 7, unit intervention cost per meter is extracted from the Delivery Plan Table, unit cost per asset is calculated for linear and point assets and is shown in Table 8.3.

	Refurbishment	Maintenance
Linear Asset	£ 6720	£ 672
Point Asset	£ 1380	£ 138

Table 8.3: Unit intervention cost

The unit intervention cost is hence denoted as: $uc = \begin{bmatrix} 6720 & 672 \\ 1380 & 138 \end{bmatrix}$.

Interest rate

Interest rate is required to calculate the present value of future cash flow. The interest rate used in this study is the long-term interest rate from March 2022, which was the time when the WLC model was built. Long-term interest rates are defined by the yield on government bonds maturing in ten years. According to the forecasts generated by the Organisation for Economic Co-operation and Development (OECD), the long-term interest rate was 1.5% in March 2022 (OECD, 2023).

Budget Constraints

As the budget for drainage interventions are historically accounts as part of the expenditures of other railway assets such as track and earthwork, it is hard to obtain the exact total budget allocated to drainage. Hence, a budget constraint of £30,000,000 per year is estimated based the historical drainage related work done in track/ earthwork and average compensation cost due to flooding.

Risk Constraints

The average number of historical annual failures of 600 is used as the maximum number of failures allowed to happen in a year.

Manpower Constraints

The manpower constraints are unclear as no information can be found from NR. Hence, an assumption is made: no more than 3% of all the assets can be refurbished and no more than 5% of all the assets can be maintained in a year, which is 14,019 and 23,365 respectively.

8.2.2.2 Calculations steps

At each time step, the following calculations are performed to calculate the penalty cost P_t and intervention cost I_t .

1. Use transition rate matrices Q_k and intervention strategy matrix x to calculate the amount of number of interventions at time t . $T_{r,t}$ is the amount of refurbishment carried out at time t , whereas $T_{m,t}$ the amount of maintenance carried out.

$$T_{r,t} = \left(\sum_k N_{k,t} \times Q_k \right) \cdot [r_1, r_2, r_3, r_4, r_5] \quad (27)$$

$$T_{m,t} = \left(\sum_k N_{k,t} \times Q_k \right) \cdot [m_1, m_2, m_3, m_4, m_5] \quad (28)$$

$N_{k,t}$ is the start condition of asset group k at time t .

2. Calculate the Intervention cost I_t .

$$I_t = \begin{bmatrix} T_{r,t} \\ T_{m,t} \end{bmatrix} \odot uc \quad (29)$$

3. Use degradation matrices and intervention effect matrices to calculate the amount assets in each condition category for each asset type at the end of the time step.

$$N_{k,t+1} = N_{k,t} \times Q_k \times E \quad (30)$$

4. Calculate the national mean service condition M_t .

$$M_t = \frac{\sum_k N_{k,t+1} \cdot [1, 2, 3, 4, 5]}{\sum_{i=1}^{i=5} n_{i,k,t+1}} \quad (31)$$

5. Predict number of failure F_t using the result of the linear regression model.

$$F_t = -3301.49 + 1360.46 \times M_t + 1.02 \times H_t; \quad (32)$$

6. Calculate the penalty cost.

$$P_t = F_t \times pc \quad (33)$$

8.2.2.3 Optimisation problem summary

The optimisation problem hence can be expressed in the more detailed format:

$$\begin{aligned}
 \min_{\mathbf{x}} C = & \sum_{t=1}^{t=n} \sum_{\forall \text{ Asset type } k} P_t(\mathbf{x}, H_t, Q_k, N_{k,1}, pc, uc) \frac{1}{(1+r)^t} \\
 & + \sum_{t=1}^{t=n} \sum_{\forall \text{ Asset type } k} I_t(\mathbf{x}, H_t, Q_k, N_{k,1}, pc, uc) \frac{1}{(1+r)^t} \\
 \text{subject to } & C \leq 30000000 \times n \\
 & F_t \leq 900 \forall t \in [1, n] \\
 & T_{r,t} \leq 14019 \forall t \in [1, n] \\
 & T_{m,t} \leq 23365 \forall t \in [1, n] \\
 & r_i \geq 0\% \forall i \in [1, 5] \\
 & m_i \geq 0\% \forall i \in [1, 5] \\
 & r_i \leq 100\% \forall i \in [1, 5] \\
 & m_i \leq 100\% \forall i \in [1, 5] \\
 & r_i + m_i \leq 100\% \forall i \in [1, 5]
 \end{aligned} \tag{34}$$

Definition of each term in the equation is listed below.

x : Intervention strategy matrix.

C : Total whole life cost account.

P_t : Penalty cost at time step t .

I_t : Intervention cost at time step t .

H_t : Annual precipitation predicted at time step t .

Q_k : Transition matrix for asset type k .

$N_{k,1}$: Number of asset in each condition state for asset type k at start of the simulation.

n : Number of time steps simulated.

pc : Unit penalty cost.

uc : Unit intervention cost.

r : Interest rate of one time step.

8.2.3 Results

5 year simulation

The test was firstly run for 5 years period as it is the duration of one Control Period (CP) in NR, and their budget planning is carried out at beginning of every CP. The time step was defined as one year, and it was assumed that the precipitation would not be affected by climate change. The optimum intervention strategy is presented in Table 8.4, showing

the percentage of asset get intervened in each condition category. The present value of the aggregated costs are shown in Table 8.5.

Asset Condition	1	2	3	4	5
Refurbishment	0.0%	0.0%	0.0%	0.0%	40.0%
Maintenance	0.0%	0.0%	6.6%	77.9%	52.2%

Table 8.4: Optimum intervention strategy for 5 year simulation period

Penalty cost	£70,959,579
Intervention cost	£52,984,409
Total	£123,943,988

Table 8.5: Present value of penalty, intervention and total cost for 5 year's simulation

The optimum intervention strategy focus on intervening assets in worst conditions: 77.9% of asset condition 4 is and 92.2% of condition 5 is intervened. All intervention on condition 4 is maintenance. This is because the difference between condition 1 and 2 is very small, also the regression model shows that the predicted failure falls to zero between an average condition 1 and 2. Refurbishing condition 4 will bring it to 2 whereas maintaining condition 4 will bring it to 1, but the cost of maintenance is 10 times lower than refurbishment; hence maintenance would be the more cost efficient choice when intervening condition 4. For condition 5, the percentage of refurbishment and maintenance does not differ too much, this may because due to limited budget or manpower, not all assets can be refurbished, hence maintenance are performed to bring them from completely ruined to a condition level with partial hydraulic capacity.

Also, some of the condition 3 are also maintained to bring the overall condition into a better state and slow down the degradation process to prevent them from degrading into condition 4 and 5, as the hydraulic capacity of asset in condition 4 and 5 will be severally reduced.

The breakdown of the forecasted average service condition score, failures and intervention as well as the calculated penalty and intervention costs are shown in Table 8.6.

Simulation Step	Forecasted Average Service Condition Score	Forecasted Number of Failures	Penalty Cost	Number of Refurbishment	Number of Maintenance	Intervention Cost
1	1.87	409	£11,573,525	7355	23365	£30,443,778
2	1.88	600	£16,969,202	1232	9614	£7,621,180
3	1.91	600	£16,969,201	745	7913	£5,566,968
4	1.94	425	£12,006,816	709	7849	£5,446,103
5	1.97	592	£16,746,562	711	8045	£5,535,013

Table 8.6: Number of forecasted average service condition score, failures and intervention; and penalty and intervention costs for a simulation of 5 year duration

As shown in Table 8.6, although the forecasted average service condition is increasing over the 5 year period, the predicted amount of failures varies from 400 to 600, and does not follow the trend of the asset condition changes. This is because the predicted failure is also affected by the forecasted precipitation level. Although in time step 4, average service condition is poorer than year 3, the amount of failures is actually lower, this is because in year 4, the forecasted precipitation is 1057.5 mm whereas in year 3 it is 1269.6 mm. In addition, the increment in average service condition is at a maximum of 0.03, which might be too small to have an effect on the predicted number of failures. Annual results provide an insight into the impact of rainfall variability; increased failure risk in a year may be due to the rainfall volume in that year and not the level of asset degradation. Aggregating results over a 5 year period aligns with the expected performance over a 5 year control period.

The number of interventions shows a downward trend, the number of assets intervened in the first time step is 3.5 times to the ones in the last year. This is because drainage assets have a long life time and degrade relatively slowly, an asset is very unlikely to degrade from a condition 1 or 2 to the worst states of 4 or 5 in a short time period. Also, as most of the assets in condition 4 and 5 are intervened in time step 1, there is only a few left to be addressed in the following time steps. Given the limited number of assets degrading into conditions 4 and 5, and the fact that almost all of these will be improved to a better state, the majority of assets will have a condition score of 1 to 3 which means they will provide an acceptable level of hydraulic performance, assuming their designed hydraulic capacity is sufficient. Hence, the amount of assets need to be intervened will decrease over the years which leads to an decrease in the expected intervention cost.

The upward trend in the asset condition score indicates that under this strategy the intervention actions can not offset the degradation effect completely. Although such effect is minimal in a short time period, it could accumulate in the long term and increase the risk of failure to a point that the risk constraint could not be meet. Hence, a simulation over a longer period of 50 years will be performed to analyse the long-term optimum intervention strategy.

50 year simulation

The model was tested for a longer time period of 50 years while all other inputs and constraints remains the same, however, no feasible solution was found. This is probably because in a longer period, more intervention are needed to maintain the asset in a acceptable service condition and hence keeps the number of predicted failures is below the risk constraint. As explained above, the optimum intervention strategy for a 5-year period could not offset the degradation effect completely. Such difference between the rate of degradation and the rate of remediation would become more significant over time. Hence, it is possible that the optimum solution can only exist beyond the boundary of the current manpower constraints or risk constraint. As risk mitigation would be a major concern to the asset manager, it is decided to only relax the manpower constraint and encourage more interventions to improve the asset service condition. The manpower constraint was lifted by 1%, so a maximum of 4% of all assets can be refurbished and a maximum of 6% of all assets can be refurbished (18,692 and 28,038 receptively). A solution was found under the new constraint. The optimum intervention strategy is shown in the Table 8.7 and the present value of the aggregated costs are shown in Table 8.8.

Asset Condition	1	2	3	4	5
Refurbishment	0.0%	0.0%	0.0%	0.0%	100%
Maintenance	0.0%	8.4%	20.4%	40.1%	0.0%

Table 8.7: Optimum intervention strategy for 50 year's simulation

Penalty cost	£91,111,218
Intervention cost	£557,735,988
Total	£648,847,206

Table 8.8: Present value of penalty, intervention and total cost for 50 year's simulation

As shown in Table 8.7, comparing with the optimum strategy of the 5 year simulation, the percentage of intervention for all asset condition categories except condition 4 has increased. Although less assets in condition 4 is intervened, more assets are intervened for condition 2 and 3. As improvement of asset condition in 2 and 3 will prevent asset from degrading to the worst state, this will consequently reduce the number of asset in condition 4 and hence improve the overall condition of drainage assets. Also, 100% of the condition 5 is refurbished, which is as expected since they are the ones that can leads the most significant reduction in performance. The result indicates that adopting a more active intervention strategy would prove to be more cost-effective in the long run. Initially, it may entail high costs to intervene in a large proportion of assets. However, once the asset condition is brought down to a desirable level, both the intervention and penalty costs are expected to remain low. Over time, the asset condition level should stabilise, since any degradation of assets can be offset by the high proportion of intervention. Even

with a high proportion of intervention, fewer interventions would be required as less degradation is expected. Furthermore, asset performance would be optimised once assets reaches the stable level, which would lead to fewer failures and significant reduction in penalty costs.

Climate change scenarios

Tests was run under RCP 2.6 and RCP 8.5 climate change scenarios to examine potential effect of the climate change on the performance of the drainage assets and the influence on the choices of the optimum intervention strategy. The result optimum strategy are shown in Table 8.9 and 8.11 and the present value of the aggregated costs are shown in Table 8.10 and 8.12.

Asset Condition	1	2	3	4	5
Refurbishment	0.0%	0.0%	0.0%	0.0%	0.0%
Maintenance	0.0%	7.2%	18.7%	26.4%	24.6%

Table 8.9: Optimum intervention strategy for 50 year's simulation under RCP 2.6 climate change scenario

Penalty cost	£223,456,867
Intervention cost	£332,909,223
Total	£556,366,090

Table 8.10: Present value of penalty, intervention and total cost for 50 year's simulation under RCP 2.6 climate change scenario

Asset Condition	1	2	3	4	5
Refurbishment	0.0%	0.0%	0.0%	0.0%	95.7%
Maintenance	0.0%	7.8%	20.2%	40.7%	4.3%

Table 8.11: Optimum intervention strategy for 50 year's simulation under RCP 8.5 climate change scenario

Penalty cost	£57,656,721
Intervention cost	£542,845,844
Total	£600,502,575

Table 8.12: Present value of penalty, intervention and total cost for 50 year's simulation under RCP 8.5 climate change scenario

Comparing the two climate change scenarios (RCP 2.6 and RCP 8.5), the optimum intervention strategies were found to be quite different. For the RCP 2.6 scenario, the optimum intervention strategy is formed by maintenance interventions only. For all assets not in perfect condition (i.e., those in conditions 2-4), a certain percentage is maintained, while the percentage of assets intervened is slightly higher for the worst conditions (i.e., conditions 4 and 5). This may be because with a milder climate change scenario, the volume of expected precipitation is less than in the RCP 8.5 scenario, hence, assets are not required to be maintained at such a high condition standard in order to cope with the failure risks expected to be caused by the higher rainfall volume. This is also reflected

by the smaller amount of whole life cost and intervention cost. However, the penalty cost of the RCP 2.6 scenario is higher than the RCP 8.5 scenario despite the fact that its precipitation level is lower. This may be because with a less proactive intervention regime, assets will experience more degradation, as long as the loss in performance does not lead to excess amount of failures that will violate the risk constraint. In this case, asset managers may wish to adjust the model when their risk expectation has changed, i.e. fewer failures will be expected if precipitation is lower than in the RCP 8.5 scenario.

In the optimum intervention strategy for the RCP 8.5, almost all assets scored at condition grade 5 are intervened with 95.7% refurbished and 4.3% maintained. Higher failure risk is induced by the high precipitation prediction, this then motivates the model to generate a strategy that can better maintain or improve an asset's current service condition. Hence, a higher number of interventions is performed which is reflected by the high intervention cost compared to the RCP 2.6 scenario. As a result, the asset condition is improved and the failure risk is mitigated and the penalty cost is reduced.

It is noted that, compared with the optimum intervention strategy for 50 year's simulation assuming no climate change, although the optimum intervention strategy under RCP 8.5 climate change scenario is quite similar, the total cost is still lower. This is due to the fact that the rainfall prediction generated using the UKCP18 RCP 8.5 global projections (60km) has a lower mean value than the randomly selected historical rainfall time series that has been used for the non-climate change scenario, hence, fewer failures are expected to occur.

The RCP 8.5 climate change scenario is then tested again with precipitation simulated in the UKCP18 regional projections (12km), which provides data with higher spatial resolution. The predicted annual precipitation in the next 50 years using UKCP18 regional projections (12km) is generally higher than the one using UKCP18 global projections (60km). No feasible solution was found probably due to the fact that under a higher predicted rainfall volume, inevitably more failures will be expected to happen, and with the current budget and manpower constraints, the asset conditions were not able to be maintained to a level that could keep the number of predicted failures below the risk constraint. This implies that more resources are needed in order to cope with the increasing precipitation expected under this climate change scenario. In order to find a feasible solution, it is decided to increase the manpower constraint by another 1%, so a maximum of 5% of all assets can be refurbished and a maximum of 7% of all assets can be maintained (23,365 and 32,711 respectively). A solution was found under the new constraint. The optimum intervention strategy is shown in Table 8.13 and the present value of the aggregated costs is shown in Table 8.14.

Asset Condition	1	2	3	4	5
Refurbishment	0.0%	0.0%	0.0%	0.0%	100.0%
Maintenance	0.0%	11.0%	22.3%	37.8%	0.0%

Table 8.13: Optimum intervention strategy for 50 year’s simulation under RCP 8.5 climate change scenario using UKCP18 regional projections (12km)

Penalty cost	£146,845,275
Intervention cost	£590,466,238
Total	£737,311,513

Table 8.14: Present value of penalty, intervention and total cost for 50 year’s simulation under RCP 8.5 climate change scenario using UKCP18 regional projections (12km)

As shown in Table 8.13, the optimum intervention strategy is similar to the one using historical precipitation data. However, both the penalty and intervention costs have increased, with the intervention cost rising by 6%, while the penalty cost increased by 60%. This could be due to the fact that even though assets are maintained at a similar or slightly better condition, high precipitation levels will lead to more failures as the hydraulic capacity of many assets has been exceeded and this cannot be eliminated due to current budget and manpower limitations.

8.3 Conclusion

In this chapter, a whole life cost model is developed using data drive approach to analysis the risk of failure. In the failure mode analysis, machine learning algorithms are used to determine the linkages between between parameters that can affect drainage asset performance and hence cause damage to railway assets and obstruction to rail operations. After the failure mechanism has been identified using the unsupervised machine learning model SOMs, such linkage is further investigated and quantified using Linear Regression. The analysis is performed using historical Track Flooding record and asset condition data from NR as well as precipitation data from Met Office. As a outcome of the failure mode analysis, the amount of Track Flooding Failures can be predicted using average service condition of drainage assets and national precipitation. This is then build into the Whole Life Cost model to provide asset manager a tool that can help them with asset maintenance planning and expenditure projection calculation. An optimum intervention strategy can be found by minimizing the total costs of owning the drainage asset, while complying with any operational requirements and controlling the amount of risks they are willing to take.

Several scenarios has been test in Section 8.2 as a demonstration of possible ways to use the model. The model was run both with a short period of 5 year and a longer period of 50 year. The results shown that, in the long term, a more proactive maintenance regime is required to mitigate the risk caused by loss in performance as a result of asset

degradation. Also, two climate change scenarios of RCP 2.6 and RCP 8.5 were tested. The result shows that the amount of precipitation will have a clear effect on the expected failures and hence affect the intervention strategy. When less precipitation is expected, the expected failure risk will also be lower, and hence less intervention is required to adapt to the changing climate. Also, climate change projections of different Spatial resolutions were tested and compared. The results showed that the WLC simulation is sensitive to the choice of climate projections. Under the same climate change scenario (RCP 8.5), the rainfall predictions generated from the UKCP18 Regional (12km) projections were higher than the Global(60km) projections, which led to a higher prediction of the WLC and a need for a more active intervention regime.

This model can be used on a strategic level to help asset manager make top-level budgetary plans that provide asset degradation prediction and performance estimation as well as work volumes and expenditures projections for a portfolio of assets. The portfolio of asset could both be all asset nationwide or assets in a particular route. This model can also be used with the Whole Life Cost model with hydraulic performance, as this model only provide high level intervention instructions. The detailed hydraulic model can help local engineer to prioritise asset based on their criticality in the local drainage system.

9 Discussion

In this study, new models were developed: degradation model, strategic and tactical performance models, and WLC models with decision support tools. These models were designed for the UK railway drainage assets to help NR's managers gain a better understanding of their assets and assist them to develop proactive management regimes by considering the whole life cost of the drainage assets throughout their lifetime. The whole life cost accounting incorporates not only the costs of acquiring and disposing of the assets, but also the operational costs incurred between the time of construction and disposal. There are two main types of operational costs identified by the model: penalty costs and intervention costs. Penalty costs are caused by the loss of performance of the drainage assets. The performance level is affected by the asset condition and hence is prone to any changes due to asset deterioration or changing environmental pressures. The intervention costs are those incurred to improve or rectify the performance level through the intervention actions that can remedy deteriorated assets.

A condition degradation model was developed using the Continuous Time Markov Chain concept to simulate asset service and structural condition degradation. Two types of system performance model were examined, each operated at a tactical and a strategic level. A hydraulic performance model was constructed for individual drainage systems, using the SWMM hydrological/hydrodynamic models to evaluate the drainage asset performance based on both current and forecasted asset conditions and rainfall time series. In parallel to this hydraulic performance model, a data driven failure mode analysis was also carried out to examine failure mechanisms and quantify the failure risks due to loss of asset performance at a national (strategic) scale using data from NR's national asset databases. The above models are incorporated into the WLC simulation algorithm alongside a decision support tool; the whole life cost of the drainage assets can then be calculated under the influence of asset degradation, rainfall under climate change and the intervention strategies generated by the decision support tool. By solving the optimisation problem with the objective of minimising the whole life cost, an optimum intervention strategy can be found. Asset managers could hence use the simulated results to build objective, more cost efficient and sustainable management plans to mitigate undesired risks to the operation of the railway due to drainage related asset failures.

Several case studies were presented to demonstrate the practical use of the models. For the degradation model, both the service and structural condition of the 300 mm diameter pipe (the most common type of pipe asset group) have been studied in detail. The transition rate matrices for both service and structural condition were calculated using the historical NR asset condition records collected from 2012. The minimal number of sample data needed to obtain a stable matrix was found, where a stable matrix is defined as the transition matrix that varies within 5% of the matrix deduced using all assets in a particular asset cohort. The results show that the asset degradation model can provide a sensible prediction of the service and structural degradation process with 21% and 94% randomly selected samples from all 300 mm diameter pipes respectively. The

transition matrices can help asset managers better understand the magnitude of the asset degradation processes for railway drainage assets; the construction and analysis of stable transition matrices can be used to justify NR's asset inspection volume and costs, as well as contributing to the decision making process of potential intervention schemes. As requested by NR, this model has been applied to a wide set of asset groups and asset types, and the results have been implemented as part of their asset management tools.

The hydraulic performance model was demonstrated with a case study of a drainage system on an operational railway line near Knockenjig, Scotland. A digital replica of the drainage system was built in the SWMM hydrological/hydrodynamic software tool. A catchment study was conducted to identify the catchment area served by the Knockenjig drainage system. Several water flow and water depth sensors were installed in the system at locations that are more likely to fail according to critical asset testing performed using the hydraulic performance model. Several critical hydrological and hydraulic model parameters were calibrated using the collected sensor data, so that the model can more accurately simulate the catchment run-off and drainage system hydraulic performance. The hydraulic performance of the drainage system is quantified by the duration of flooding. When there is not enough hydraulic capacity in the system, excess water will leave the drainage system through drainage nodes (catchpits) and cause flooding onto the railway. The hydraulic performance of the Knockenjig site was analysed both with the current assets' conditions and with degraded conditions that were simulated using the degradation model described above. Also, the resilience of the drainage system is tested with current rainfall time series and rainfall times series adjusted using climate change projection RCP 8.5. Results show that both asset degradation and climate change will affect the flood risk performance of this drainage system significantly. The estimated flooding hours under either the effect of degradation or climate change is 25-30 times more than the baseline scenario of no condition change and rainfall time series with no climate change. The combined effect of asset degradation and climate change is even higher and causes 100 times more flooding hours than the baseline scenario. These results indicate the scale of the challenge facing NR's drainage assets might face over the next few decades. This model provides asset managers with a useful tool that can quantify the current asset performance and forecast future performance levels under the influence of asset degradation and climate change projections, which can help asset managers make proactive management decisions to mitigate current and future potential flood risks. The model can also be used during the design phase for any new railway drainage system to help build a sustainable and resilient drainage system that can withstand future extreme rainfall conditions.

The quality of the output from the hydraulic model is subject to the accuracy of the asset information and the assumptions made during the calibration process. Accurate and detailed asset information is required to build the model. Gathering such detailed asset information and building individual system models will be costly, so this modelling approach would not be suitable for national rollout. Furthermore, the linkage between asset condition degradation and parameters that could affect asset performance is unclear.

Assumptions, such as the change in roughness parameter values when pipes degrade, have been made based on values reported in literature and expert opinion in this study. Any further experimental studies to identify and quantify such linkages would be beneficial. Sensitivity tests were carried out to analyse the effect of these assumptions on the performance of the drainage system model. The performance was proven to be more sensitive to changes in assumptions on roughness and diameter/width/height of degraded conduits; the percentage changes in the performance indicator (flooding duration) are similar but slightly higher than the percentage change in roughness scores due to roughness and cross sectional area changes due to diameter/width/height reduction.

On the tactical level, the developed Whole Life Cost model incorporated the hydraulic performance model and the asset degradation model, and was tested with data from the Knockenjig drainage system. A set of feasible intervention strategies was generated based on expert knowledge of the general rules in route level maintenance planning. It was then applied to the degradation model to estimate the improvement in condition of degrading drainage assets during the asset condition simulation. The forecasted asset condition scores were then input into the hydraulic performance model and the resulting performance indicator (i.e. flooding hours) is used to calculate the penalty cost. The aggregated present value of the intervention costs and penalty costs were compared among the tested intervention strategies, and the one with the minimal total whole life cost is proposed as the optimum strategy. For a 5 year simulation at the Knockenjig site, the optimum intervention solution is found to be refurbishing all assets with condition scores 4 and 5 while not intervening assets with other condition grades. Sensitivity tests were performed for a set of parameters that could affect the WLC simulation: the asset start condition, asset roughness, asset diameter/width/height and the duration of simulation. Changing the assumptions of how asset condition score affects asset roughness and asset diameter/width/height reduction will lead to a larger/smaller percentage of assets interventions. For a longer simulation period of 10 years or a worse start condition, the percentage of assets intervened was also increased. As this model is built based on a very thorough investigation of the geometric properties and hydraulic capacity of the study drainage system, it can provide site specific information that helps route engineers to prioritise their short-term maintenance schedule, as well as assist asset managers to make maintenance planning on a long-term tactical level.

The case studies of the hydraulic performance based WLC model indicated that carrying out maintenance/refurbishment within one/three months after the observation of degradation is more cost beneficial compared to 6 months. Also, in this study, interventions were assumed to be carried out at a fixed interval after asset degradation. In real life practice, routine (cyclical) maintenance might be the norm rather than the condition-based approach proposed here. Routine maintenance could lead to delays in restoring asset condition back to a satisfactory state, consequently increasing the failure risk. The benefit of prompt intervention includes not only mitigating the immediate risks posed by the degrading assets, but also preventing more severe risks that could emerge as assets degrade into the worst condition state. However, implementing a condition-based

intervention approach presents practical challenges. For instance, scheduling intervention within the desired time frame might be difficult for some assets, as they are located on a busy railway line, making site access hard to arrange.

Although it has demonstrated that the WLC model based on hydraulic performance measures was able to identify an optimum intervention strategy for individual drainage system over a 5 and 10 year period, the cost and time required to develop the underlying models was high and therefore this approach could not be applied at a strategic level. On a strategic level, when considering a WLC approach of a large portfolio of drainage assets in conjunction with regional and national level budgeting, operational and risk requirements, a performance model with data driven approach was built to provide predictions of performance that could be input into a national WLC modelling approach. The data driven performance model incorporated knowledge from failure mode analysis developed in the In2track2 project, where self-organising maps were used to identify the causal mechanisms of failures caused by drainage performance loss. Based on historical failure records, it is found that the average drainage condition score and precipitation volume exhibit a linkage with the likelihood of track flooding failure. This finding is implemented into a linear regression model to quantify these linkages, and the estimated number of failures can be expressed as a function of average asset condition score and annual precipitation. Optimum intervention strategies can then be found by solving the optimisation problem that minimises the total present value of the simulated interventions and penalty cost, while complying with budget, risk and manpower constraints. This WLC approach was tested on a national scale over a 5 year and a 10 year period, and the result shows that for a longer period, a more proactive intervention strategy is needed to maintain the asset condition at an adequate level so that the performance under such condition level stays within the boundary of the risk constraint. The WLC model was also tested with different climate change scenarios: RCP 2.6 and RCP 8.5, the results shows that under the more severe climate change scenario RCP 8.5, more interventions need to be carried out to maintain the asset condition in a level that can withstand the climate change effect and meet the risk constraint set in place. When comparing the results of the RCP 2.6 and RCP 8.5 scenarios tested with UKCP18 global climate projections, it is found that the optimal strategy for the RCP 8.5 scenario requires interventions for an additional 16% of assets in condition 4 and 75% more assets in condition 5 compared to the RCP 2.6 scenario. Simulation of the RCP 8.5 climate change scenario was performed with rainfall data from both the UKCP18 regional and global climate change projections. The results indicated that the model is sensitive to the choice of climate change projections. The total cost of the optimum strategy using regional projection is 23% higher than the one using global projection. Also, a higher percentage of assets in condition 5 needs to be refurbished instead of maintained with the regional projection. Hence, it is essential to carefully choose the climate change projections for future simulations. This model is suitable to be used as a tool to develop top-level asset management regimes. It can help asset managers to make decisions on budgeting and work volume planning on a national scale, and provide long term intervention strategies that minimise the whole

life cost while mitigating failure risks and complying with operational limitations. Given that the data-driven performance model was implemented on a large scale (i.e., at the national level), it might be limited when applied on a smaller scale for risk identification and management decisions pertaining to an individual asset.

The two WLC models can be used jointly to provide management solutions on both strategic and tactical levels. While a WLC model with a data driven performance modelling approach can provide justifications for top-level management decisions, the WLC model with hydraulic approach can assist route engineers to make localised daily work planning decisions. Together they will offer a robust solution to the problem faced by NR of improving knowledge of the drainage assets' condition and performance and maintaining assets economically and efficiently.

It can be considered that all the objectives of the study have been met.

- A framework of WLC that can be applied across the railway drainage network were developed as stated in Section 3.1.1.
- To analyse the residual asset life and deterioration patterns of existing assets, a degradation was developed as shown in Chapter 4.
- Drainage system performance assessment regimes were developed in Chapter 5 based on drainage system's hydraulic capacity and in Chapter 8 using data-driven machine learning techniques, which can help asset managers gain a thorough appreciation of the impact of poor drainage.
- The high risk / critical drainage assets can be identified using the asset performance models as stated Chapter 5 and Chapter 8. This will provide the foundation for a more robust and economic intervention regime.
- In Chapter 7 and Chapter 8, decision support tool were developed using the WLC models. They can help asset manager prioritise drainage maintenance works based on budgets and risks both on a tactical and strategical level.

The applicability of the WLC approach to railway infrastructure outside the UK has been explored via the In2tack2 and In2track3 projects. Presentations have been made and discussions have taken place with several European railway drainage asset owners/operators. Two of these operators have agreed that the model has the potential to be applied to their railway systems if there is sufficient asset condition and failure data available. However, asset condition data is recorded in different ways, and like NR asset databases are often incomplete, especially for assets built before drawings were digitized. However, these operators have also noted that there are areas where railway infrastructure was constructed in recent years, and they tend to have better records, making them potentially suitable for model testing. Also, both countries have national rainfall databases. There is therefore the potential to apply the WLC framework described above to the railway systems of these two European operators.

10 Conclusion

This study established a comprehensive whole life cost framework for railway drainage assets, providing valuable insights to Network Rail’s railway drainage asset managers regarding asset deterioration, system performance, and costs associated with penalties and interventions. This framework can enhance the managers’ understanding of both the current and evolving conditions and performance of the drainage assets, and hence assist asset managers in building cost-effective, proactive maintenance strategies to mitigate the risks associated with drainage asset failures.

A degradation model was created using Continuous Time Markov Chains to analyse the service and structural condition degradation process for a range of railway drainage asset groups and types. A case study was conducted on 300mm diameter pipes, demonstrating that the model can predict condition grade transitions with less than 0.2% error. A journal paper of the degradation model was published in the *Journal of Infrastructure Systems* in 2021 (Wu et al., 2021). This modelling approach has been used to obtain transition rate matrices of all drainage asset groups and these have been implemented in NR’s asset management tools to help simulate the future condition of NR’s drainage assets.

A hydraulic performance model was constructed using SWMM to assess the hydraulic capacity of a railway drainage system. A case study was performed on a single drainage system located on an operational railway line near Knockenjig, Scotland. This model was built and calibrated using field-collected water depth and water flow sensor data. This performance model was integrated with the asset degradation model to evaluate drainage asset performance based on forecast asset condition grades and rainfall projections. The use of the integrated model was demonstrated through a case study at the Knockenjig site. Flooding hours are calculated for various climate change and asset degradation scenarios. This demonstrated that both climate change and asset deterioration increased flooding duration by between one and two orders of magnitude.

The hydraulic performance modelling approach requires detailed information on drainage assets that are not available nationally. Hence, a data-driven failure mode analysis method was developed to analyse failure risks using machine learning techniques that could be applied nationally with current asset data.

Whole life cost models were developed using both the hydraulic performance model and the data-driven approach to support asset management decision-making at tactical and strategic levels, respectively. Decision support tools were developed through the optimization of whole life cost accounts, enabling the identification of the most robust and cost effective intervention strategy for railway drainage systems.

For the WLC model using hydraulic performance analysis, a case study was conducted at the Knockenjig site to find the optimum strategy for the next 5 years assuming all assets are in perfect condition. The optimum strategy is refurbishing all assets with condition

scores of 4 and 5 and not intervening assets in other conditions, resulting in the lowest total cost of £43,704, whereas the highest total cost from the poorest strategy tested was £258,623. Sensitivity tests were carried out to evaluate the effect of the starting condition assumption and duration of simulation.

While for the WLC model using the data-driven approach, a case study was conducted for all drainage assets nationwide to determine the optimal strategy based on given budget and risk constraints in a 5-year and a 50-year simulation, as well as 50-year simulations under various climate change scenarios. Results showed that the optimum strategy of 50-year simulation promotes a higher number of interventions for assets in lower condition scores. This suggests that implementing a more proactive intervention strategy could result in greater cost-effectiveness in the long run. Results also showed that the model is sensitive to rainfall prediction in climate change scenarios and hence the choice of climate change projections is important in further simulation process.

The combination of the two WLC models allows for comprehensive management solutions at both strategic and tactical levels. The data-driven WLC model offers justifications for high-level management decisions, while the hydraulic-based WLC model aids route engineers in making localized daily work planning decisions.

Although different intervention strategies have been investigated under a number of climate change scenarios, more scenarios should be examined in addition to the ‘best’ and ‘worst’ RCP cases tested in this study, to enable better understanding of the impact of climate change uncertainty in long term WLC optimisations. Also, the effect of changes in constraints and inputs on the optimum intervention strategies was not fully examined in this study. Further studies could be conducted to study the impact of these parameters on the WLC model; investigating how optimum interventions will be affected by the changes in budget, manpower and risk constraint, as well as other inputs such as interest rate and unit cost. Also, as that level of resource and cost of goods are expected to change over time, for simulations of a longer period, model should be developed to incorporate dynamic changes in the constraints and input parameters over every 5 year control periods.

Reference

- Alegre, H., Baptista, J. M., Cabrera, Enrique, J., Cubillo, F., Duarte, P., Hirner, W., Merkel, W. and Parena, R. (2016), *Performance Indicators for Water Supply Services: Third Edition*, IWA Publishing.
- Alegre, H. and Coelho, S. T. (1995), Hydraulic performance and rehabilitation strategies, in E. Cabrera and A. Vela, eds, 'Improving Efficiency and Reliability in Water Distribution Systems', Kluwer Academic Press.
- Aljafari, N., Burrow, M., Ph, D., Ghataora, G., Ph, D., Torbaghan, M. E., Ph, D. and Raja, J. (2022), 'Condition Modeling of Railway Drainage Pipes', *Journal of infrastructure systems* **28**(4).
- Allouche, E. N. and Freure, P. (2002), *Management and maintenance practices of storm and sanitary sewers in Canadian municipalities*, Institute for Catastrophic Loss Reduction.
- Altarabsheh, A., Kandil, A. and Ventresca, M. (2016), Multi-Objective Optimization Algorithm for Sewer Network Rehabilitation Using Life Cycle Cost Analysis and Semi-Markov Deterioration Models, in 'Construction Research Congress 2016', American Society of Civil Engineers, Reston, VA, pp. 2089–2099.
- Ambrose, M., Burn, S., DeSilva, D. and Rahilly, M. (2008), Life cycle analysis of water networks, in '14th Plastics Pipes Conference, PXIV', Budapest, Hungary.
- Ana, E. and Bauwens, W. (2007), Sewer network asset management decision-support tools: a review, in 'International Symposium on New Directions in Urban Water Management', Citeseer, 12-14 September 2007, UNESCO Paris.
- Ana, E. and Bauwens, W. (2010), 'Modeling the structural deterioration of urban drainage pipes: the state-of-the-art in statistical methods', *Urban Water Journal* **7**(1), 47–59.
- Ana, E., Bauwens, W., Pessemier, M., Thoeye, C., Smolders, S., Boonen, I. and de Guelde, G. (2009), 'An investigation of the factors influencing sewer structural deterioration', *Urban Water Journal* **6**(4), 303–312.
- Andreou, S. A., Marks, D. H. and Clark, R. M. (1987), 'A new methodology for modelling break failure patterns in deteriorating water distribution systems: Theory', *Advances in Water Resources* **10**(1), 2–10.
- Anis, M. R. and Rode, M. (2015), 'A new magnitude category disaggregation approach for temporal high-resolution rainfall intensities', *Hydrological Processes* **29**, 1119–1125.
- Arriero Shinma, T. and Ribeiro Reis, L. F. (2014), 'Incorporating multi-event and multi-site data in the calibration of SWMM', *Procedia Engineering* **70**, 75–84.

- Ashley, R. and Hopkinson, P. (2002), ‘Sewer systems and performance indicators—into the 21st century’, *Urban Water* **4**(2), 123–135.
- Awol, F. S., Coulibaly, P. and Tolson, B. A. (2018), ‘Event-based model calibration approaches for selecting representative distributed parameters in semi-urban watersheds’, *Advances in Water Resources* **118**, 12–27.
- Baffaut, C. and Delleur, J. W. (1989), ‘Expert System for Calibrating Swmm’, *Journal of Water Resources Planning and Management* **115**(3), 278–298.
- Bai, L., Liu, R., Sun, Q., Wang, F. and Xu, P. (2015), ‘Markov-based model for the prediction of railway track irregularities’, *Proceedings of the Institution of Mechanical Engineers, Part F: Journal of Rail and Rapid Transit* **229**(2), 150–159.
- Baik, H.-s. S., Seok, H., Jeong, D., Abraham, D. M., Jeong, H. S. and Abraham, D. M. (2006), ‘Estimating transition probabilities in markov chain-based deterioration models for management of wastewater systems’, *Journal of Water Resources Planning and Management* **132**(1), 15–24.
- Balekelayi, N. and Tesfamariam, S. (2021), ‘Operational Risk-Based Decision Making for Wastewater Pipe Management’, *Journal of Infrastructure Systems* **27**(1), 1–16.
- Banks, H. T., Broido, A., Canter, B., Gayvert, K., Hu, S., Joyner, M. and Link, K. (2011), ‘Simulation Algorithms for Continuous Time Markov Chain Models’, *Studies in Applied Electromagnetics & Mechanics* pp. 1–18.
- Baur, R. and Herz, R. (2002), ‘Selective inspection planning with ageing forecast for sewer types’, *Water Science and Technology* **46**(6-7), 389–396.
- Beven, K. (2004), ‘Robert E. Horton’s perceptual model of infiltration processes’, *Hydrological Processes* **18**(17), 3447–3460.
- Boddice, D., Metje, N. and Chapman, D. (2017), ‘Unique insight into the seasonal variability of geophysical properties of field soils: Practical implications for near-surface investigations’, *Near Surface Geophysics* **15**(5), 515–526.
- Brown, S. A., Schall, J. D., Morris, J. L., Doherty, C. L., Stein, S. M. and Warner, J. C. (2013), ‘Urban Drainage Design Manual’, *Hydraulic Engineering Circular* **22**(22), 478.
- Bruaset, S., Sægrov, S. and Ugarelli, R. (2018), ‘Performance-based modelling of long-term deterioration to support rehabilitation and investment decisions in drinking water distribution systems’, *Urban Water Journal* **15**(1), 46–52.
- Burian, S. J., Durrans, S. R., Tomić, S., Pimmel, R. L. and Wai, C. N. (2000), ‘Rainfall Disaggregation Using Artificial Neural Networks’, *Journal of Hydrologic Engineering* **5**(3), 299–307.

- Burrough, P. A. and McDonnell, R. A. (1998), 'Principles of Geographical Information Systems', *Principles of Geographical Information Systems* **75**(4), 422.
- Cardoso, M. A., Coelho, S. T., Praça, P., Brito, R. S. and Matos, J. (2005), 'Technical performance assessment of urban sewer systems', *Journal of performance of constructed facilities* **19**(4), 339–346.
- Cardoso, M., Coelho, S., Matos, R. and Alegre, H. (2004), 'Performance assessment of water supply and wastewater systems', *Urban Water Journal* **1**(1), 55–67.
- Cerdà, A. (1999), 'Seasonal and spatial variations in infiltration rates in badland surfaces under Mediterranean climatic conditions', *Water Resources Research* **35**(1), 319–328.
- Cerdà, A. (1996), 'Seasonal variability of infiltration rates under contrasting slope conditions in southeast Spain', *Geoderma* **69**(3), 217–232.
- Cerdà, A. (1997), 'Seasonal changes of the infiltration rates in a Mediterranean scrubland on limestone', *Journal of Hydrology* **198**(1), 209–225.
- Chamani, R., Rajaratnam, N., Beirami, M. K. and Sakhalkar, S. V. (2011), 'Automatic Calibration of the U.S. EPA SWMM Model for a Large Urban Catchment', *Journal of Hydraulic Engineering* **134**(10), 15321535.
- Chow, V. (1959), *Open-channel Hydraulics*, Civil engineering series, McGraw-Hill.
- Clark, R. M., Stafford, C. L. and Goodrich, J. A. (1982), 'Water distribution systems: a spatial and cost evaluation', *Journal of the Water Resources Planning & Management Division, ASCE*, **108**(3), 243–256.
- Constantine, A. G. and Darroch, J. N. (1993), *Pipeline reliability: stochastic models in engineering technology and management*, World Scientific Publishing Co.
- Cowpertwait, P., O'Connell, P., Metcalfe, A. and Mawdsley, J. (1996a), 'Stochastic point process modelling of rainfall . I . Single-site fitting and validation', **175**, 17–46.
- Cowpertwait, P., O'Connell, P., Metcalfe, A. and Mawdsley, J. (1996b), 'Stochastic point process modelling of rainfall . II . Regionalisation and disaggregation', **175**, 47–65.
- Cowpertwait, P. S. P. (2006), 'A spatial – temporal point process model of rainfall for the Thames catchment , UK', *Journal of Hydrology* **330**, 586–595.
- Davis, P. Ñ., Burn, S., Moglia, M. and Gould, S. (2007), 'A physical probabilistic model to predict failure rates in buried PVC pipelines', **92**, 1258–1266.
- Deb, A. K. and Foundation, A. R. (1998), *Quantifying Future Rehabilitation and Replacement Needs of Water Mains*, AWWA Research Foundation.

- Duchesne, S., Beardsell, G., Villeneuve, J. P., Toumbou, B. and Bouchard, K. (2013), ‘A Survival Analysis Model for Sewer Pipe Structural Deterioration’, *Computer-Aided Civil and Infrastructure Engineering* **28**(2), 146–160.
- El-Haram, M. A., Marenjak, S. and Horner, M. W. (2002), ‘Development of a generic framework for collecting whole life cost data for the building industry’, *Journal of Quality in Maintenance Engineering* **8**(2), 144–151.
- Emblemsvag, J. (2001), ‘Activity-based life-cycle costing’, *Managerial Auditing Journal* **16**(1), 17–27.
- Engelhardt, M., Savic, D., Skipworth, P., Cashman, A., Saul, A. and Walters, G. (2003), ‘Whole life costing: Application to water distribution network’, *Water Science and Technology: Water Supply* **3**(1-2), 87–93.
- Fabrycky, W. and Blanchard, B. (1991), *Life-cycle Cost and Economic Analysis*, Prentice-Hall international series in industrial and systems engineering, Prentice Hall.
- Fadhel, S., Al Aukidy, M. and Saleh, M. S. (2021), ‘Uncertainty of intensity-duration-frequency curves due to adoption or otherwise of the temperature climate variable in rainfall disaggregation’, *Water* **13**(17).
- Fatichi, S., Ivanov, V. Y. and Caporali, E. (2011), ‘Simulation of future climate scenarios with a weather generator’, *Advances in Water Resources* **34**(4), 448–467.
- Fuchs-Hanusch, D., Kornberger, B., Friedl, F. and Scheucher, R. (2011), Whole of life cost calculations for water supply pipes, in ‘Water Asset Management International’, Vol. 8, pp. S7, 1–11.
- Greenlee, D. D. (1987), ‘Raster and vector processing for scanned linework’, *Photogrammetric Engineering and Remote Sensing* **53**(10), 1383–1387.
- Gueldre, G., F, V., I, B., C, T. and B, V. (2007), ‘Hydroplan-EU: An integrated approach for sewer asset management’.
- Gyasi-agyei, Y. and Mahbub, S. M. P. B. (2007), ‘A stochastic model for daily rainfall disaggregation into fine time scale for a large region’, *Journal of Hydrology* **347**, 358–370.
- Güntner, A., Olsson, J., Calver, A. and Gannon, B. (2001), ‘Cascade-based disaggregation of continuous rainfall time series : the influence of climate’.
- Haines, A. (2020), Resilience of rail infrastructure following the derailment at Carmont, near Stonehaven, Technical report, Network Rail and Department for Transport.
- Harvey, R. R. and McBean, E. A. (2014), ‘Predicting the structural condition of individual sanitary sewer pipes with random forests’, *Canadian Journal of Civil Engineering* **41**(4), 294–303.

- Heineman, M. C. (2004), Netstorm-a computer program for rainfall-runoff simulation and precipitation analysis, *in* ‘Critical Transitions in Water and Environmental Resources Management’, pp. 1–14.
- Herrera, M., Heathcote, I., James, W. and Bradford, A. (2006), ‘Multi-Objective Calibration of SWMM for Improved Simulation of the Hydrologic Regime’, *Journal of Water Management Modeling* .
- Herz, R. K. (1996), ‘Ageing processes and rehabilitation needs of drinking water’, *J Water SRT – Aqua* **45**(5), 221–231.
- Horton, R. E. (1933), ‘The role of infiltration in the hydrologic cycle’, *Hydrology* .
- Horton, R. E. (1940a), ‘An Approach Toward a Physical Interpretation of Infiltration-Capacity’, *Soil Science Society of America Journal* **5**(C), 399–417.
- Horton, R. E. (1940b), ‘An Approach Toward a Physical Interpretation of Infiltration-Capacity’, *Soil Science Society of America Journal* **5**(C), 399–417.
- How Fill works—ArcGIS Pro* (n.d.). Accessed: 17/06/2021.
URL: <https://pro.arcgis.com/en/pro-app/latest/tool-reference/spatial-analyst/how-fill-works.htm>
- How Flow Accumulation works—ArcGIS Pro* (n.d.). Accessed: 28/06/2021.
URL: <https://pro.arcgis.com/en/pro-app/2.7/tool-reference/spatial-analyst/how-flow-accumulation-works.htm>
- How GlobalSearch and MultiStart Work* (n.d.), MATLAB & Simulink. Accessed: 28/09/2022.
URL: <https://uk.mathworks.com/help/gads/how-globalsearch-and-multistart-work.html>
- How Slope works* (n.d.). Accessed: 28/06/2021.
URL: <https://pro.arcgis.com/en/pro-app/2.7/tool-reference/3d-analyst/how-slope-works.htm>
- IEC (2004), ‘Dependability management - Part 3-3: Application guide - Life cycle costing. IEC 60300-3-3.’.
- In2Track2* (2018), Horizon 2020. Grant agreement ID: 826255. doi: 10.3030/826255.
- Inamura, Y. (2006), ‘Estimating Continuous Time Transition Matrices From Discretely Observed Data’.
- ISO 15686-5:2008 - Buildings and constructed assets — Service-life planning — Part 5: Life-cycle costing* (2008), Technical report, Geneva, Switzerland: International Organization for Standardization.

- Jarrett, R., Hussain, O. and Van Der Touw, J. (2003), Reliability assessment of water pipelines using limited data, *in* ‘Proceedings of OzWater 2003 : 19th AWA Convention’, OzWater, Perth, Australia.
- Jeffrey, L. (1985), ‘Predicting urban water distribution maintenance strategies: a case study of New Haven, Connecticut’, *Dissertation, Massachusetts Institute of Technology, Department of Civil Engineering, USA* .
- Jenson, S. K. and Domingue, J. O. (1988), ‘Extracting topographic structure from digital elevation data for geographic information system analysis’, *Photogrammetric Engineering and Remote Sensing* **54**(11), 1593–1600.
- Jung, I. S., Garrett, J. H., Soibelman, L. and Lipkin, K. (2012), ‘Application of classification models and spatial clustering analysis to a sewage collection system of a mid-sized city’, *Congress on Computing in Civil Engineering, Proceedings* pp. 537–544.
- Kaczmarska, J., Isham, V. and Onof, C. (2014), ‘Point process models for fine-resolution rainfall’, *Hydrological sciences journal* **59**(11), 1972–1991.
- Kazemi, E., Wu, Y., Liu, F., Tait, S. and Nichols, A. (2021), In2track2 3.4.2: Efficient drainage management systems: Data driven failure prediction, Technical report.
- Khan, Z., Zayed, T. and Moselhi, O. (2010), ‘Structural Condition Assessment of Sewer Pipelines’, *Journal of Performance of Constructed Facilities* **24**(2), 170–179.
- Kimutai, E., Betrie, G., Brander, R., Sadiq, R. and Tesfamariam, S. (2015), ‘Comparison of statistical models for predicting pipe failures: Illustrative example with the city of calgary water main failure’, *Journal of Pipeline Systems Engineering and Practice* **6**(4).
- Kirkwood, L., Giuntini, L., Shehab, E. and Baguley, P. (2016), ‘Development of a Whole Life Cycle Cost Model for Electrification options on the UK Rail System’, *Procedia CIRP* **47**, 1–5.
- Kleiner, Y. (2001), ‘Scheduling inspection and renewal of large infrastructure assets’, *Journal of Infrastructure Systems, ASCE* **7**(December), 136–143.
- Kleiner, Y. and Rajani, B. (2001), ‘Comprehensive review of structural deterioration of water mains: statistical models’, *Urban Water* **3**(3), 131–150.
- Kleiner, Y. and Rajani, B. (2010), ‘I-WARP: Individual Water main Renewal Planner’, *Drinking Water Engineering and Science* **3**(1), 71–77.
- Kleiner, Y., Sadiq, R. and Rajani, B. (2006), ‘Modelling the deterioration of buried infrastructure as a fuzzy Markov process’, *Journal of Water Supply: Research and Technology - AQUA* **55**(2), 67–80.
- Kolsky, P. and Butler, D. (2002), ‘Performance indicators for urban storm drainage in developing countries’, *Urban Water* **4**(2), 137–144.

- König, A. (2005), CARE-S WP2 External corrosion model description, Technical report, SINTEF Technology and Society.
- Korpi, E. and Ala-Risku, T. (2008), ‘Life cycle costing: a review of published case studies’, *Managerial Auditing Journal* **23**(3), 240–261.
- Korving, H. and van Noordwijk, J. M. (2008), ‘Bayesian updating of a prediction model for sewer degradation’, *Urban Water Journal* **5**(1), 51–57.
- Kossieris, P., Makropoulos, C., Onof, C. and Koutsoyiannis, D. (2018), ‘A rainfall disaggregation scheme for sub-hourly time scales: Coupling a Bartlett-Lewis based model with adjusting procedures’, *Journal of Hydrology* **556**, 980–992.
- Koutsoyiannis, D. and Onof, C. (2001), ‘Rainfall disaggregation using adjusting procedures on a poisson cluster model’, *Journal of Hydrology* **246**(1), 109–122.
- Laloy, E. and Biielders, C. (2009), ‘Modelling intercrop management impact on runoff and erosion in a continuous maize cropping system: Part ii. model pareto multi-objective calibration and long-term scenario analysis using disaggregated rainfall’, *European journal of soil science* **60**, 1022–1037.
- Le, B. and Andrews, J. (2013), ‘Modelling railway bridge asset management’, *Proceedings of the Institution of Mechanical Engineers, Part F: Journal of Rail and Rapid Transit* **227**(6), 644–656.
- Le Gat, Y. (2008), ‘Modelling the deterioration process of drainage pipelines’, *Urban Water Journal* **5**(2), 97–106.
- Le Gat, Y. and Eisenbeis, P. (2000), ‘Using maintenance records to forecast failures in water networks’, *Urban Water* **2**(3), 173–181.
- Li, M. F., Tang, X. P., Wu, W. and Liu, H. B. (2013), ‘General models for estimating daily global solar radiation for different solar radiation zones in mainland China’, *Energy Conversion and Management* **70**, 139–148.
- Liang, Q., Peng, C. and Li, X. (2023), ‘A multi-state semi-markov model for nuclear power plants piping systems subject to fatigue damage and random shocks under dynamic environments’, *International Journal of Fatigue* **168**, 107448.
- Liong, S. Y., Chan, W. T. and Lum, L. H. (1991), ‘Knowledge-based system for SWMM runoff component calibration’, **17**(1), 10–23.
- Liong, S.-Y., Chan, W. T. and ShreeRam, J. (1995), ‘Peak-Flow Forecasting with Genetic Algorithm and SWMM’, *Journal of Hydraulic Engineering* **121**(8), 613–617.
- Luque, J. and Straub, D. (2019), ‘Risk-based optimal inspection strategies for structural systems using dynamic bayesian networks’, *Structural Safety* **76**, 68–80.

- Macro, K., Matott, L. S., Rabideau, A., Ghodsi, S. H. and Zhu, Z. (2019), ‘OSTRICH-SWMM: A new multi-objective optimization tool for green infrastructure planning with SWMM’, *Environmental Modelling & Software* **113**, 42–47.
- Maharjan, M., Pathirana, A., Gersonius, B. and Vairavamoorthy, K. (2009), ‘Staged cost optimization of urban storm drainage systems based on hydraulic performance in a changing environment’, *Hydrol. Earth Syst. Sci* **13**, 481–489.
- Mashford, J., Marlow, D., Tran, D. and May, R. (2011), ‘Prediction of Sewer Condition Grade Using Support Vector Machines’, *Journal of Computing in Civil Engineering* **25**(4), 283–290.
- Matos, R., Cardoso, A., Duarte, P., Ashley, R., Molinari, A. and Schulz, A. (2003), ‘Performance indicators for wastewater services - Towards a manual of best practice’, *Water Science and Technology: Water Supply* **3**(1-2), 365–371.
- Meegoda, J. N., Juliano, T. M., Ayoola, M. and Dhar, S. (2004), ‘A Methodology to Predict the Remaining Service Life of CSCPs’, *International Conference on Case Histories in Geotechnical Engineering* .
- Meijer, D., van Bijnen, M., Langeveld, J., Korving, H., Post, J. and Clemens, F. (2018), ‘Identifying critical elements in sewer networks using graph-theory’, *Water (Switzerland)* **10**(2).
- Met Office (2003): Met Office Rain Radar Data from the NIMROD System* (n.d.), NCAS British Atmospheric Data Centre. Accessed: 30/06/2018.
URL: <http://catalogue.ceda.ac.uk/uuid/82adec1f896af6169112d09cc1174499>
- Micevski, T., Kuczera, G. and Coombes, P. (2002), ‘Markov model for storm water pipe deterioration’, *Journal of infrastructure systems* **8**(2), 49–56.
- Miljkovic, D. (2017), ‘Brief review of self-organizing maps’, *2017 40th International Convention on Information and Communication Technology, Electronics and Microelectronics, MIPRO 2017 - Proceedings* pp. 1061–1066.
- Moghtadernejad, S., Huber, G., Hackl, J. and Adey, B. T. (2021), ‘Data-driven estimation of deterioration curves: A railway supporting structures case study’, *Infrastructure Asset Management* **9**(1), 3–17.
- Molnar, P. and Burlando, P. (2005), ‘Preservation of rainfall properties in stochastic disaggregation by a simple random cascade model’, *Atmospheric Research* .
- Najafi, M. and Kulandaivel, G. (2005), Pipeline Condition Prediction Using Neural Network Models, in ‘Pipelines 2005’, American Society of Civil Engineers, Reston, VA, pp. 767–781.
- NetworkRail (2011), ‘Railway Drainage Systems Manual Part 2A: General design requirements’. Internal document.

- NetworkRail (2017), ‘Drainage Asset Policy’. Internal document.
- Ng, S. K. and Moses, F. (1998), Bridge deterioration modeling using semi-Markov theory, *in* ‘Structural Safety and Reliability: Proceedings of ICOSSAR’97, the 7th International Conference on Structural Safety and Reliability, Kyoto, 24-28 November 1997’, p. 113.
- OECD (2023), ‘Long-term interest rates (indicator)’, doi: 10.1787/662d712c-en. Accessed: 05/06/2023.
- Olsson, J. (1998), ‘Evaluation of a scaling cascade model for temporal rainfall disaggregation’.
- Olsson, J. and Berndtsson, R. (1998), ‘Temporal rainfall disaggregation based on scaling properties’, *Water Science and Technology* .
- Onof, C., Townend, J. and Kee, R. (2005), ‘Comparison of two hourly to 5-min rainfall disaggregators’, **77**, 176–187.
- Onof, C. and Wheeler, H. (1994), ‘Improvements to the modelling of british rainfall using a modified random parameter bartlett-lewis rectangular pulse model’, *Journal of Hydrology* .
- Ormsbee, L. E. (1989), ‘Rainfall Disaggregation Model for Continuous Hydrologic Modeling’, *Journal of Hydraulic Engineering* **115**(4), 507–525.
- Our routes - Network Rail* (n.d.). Accessed: 02/10/2022.
URL: <https://www.networkrail.co.uk/running-the-railway/our-routes/>
- Rafatnejad, A., Tavakolifar, H. and Nazif, S. (2022), ‘Evaluation of the climate change impact on the extreme rainfall amounts using modified method of fragments for sub-daily rainfall disaggregation’, *International Journal of Climatology* **42**(2), 908–927.
- Rahman, S. and Vanier, D. (2004), ‘Life cycle cost analysis as a decision support tool for managing municipal infrastructure’, *CIB 2004 Triennial Congress* .
- Rajani, B. and Kleiner, Y. (2001), ‘Comprehensive review of structural deterioration of water mains: physically based models’, *Urban Water* **3**(3), 151–164.
- Rajani, B. and Makar, J. (2000), ‘A methodology to estimate remaining service life of grey cast iron water mains’, *Canadian Journal of Civil Engineering* **27**(6), 1259–1272.
- Rajasekhar, M., Umabai, D., Krupavathi, K., Navyasai, I. and Gopi, R. (2018), ‘Development and Comparison of Infiltration Models and Their Field Validation’, *International Journal of Current Microbiology and Applied Sciences* **7**(10), 2691–2701.
- Rama, D. and Andrews, J. D. (2016), Railway infrastructure asset management: The whole-system life cost analysis, *in* ‘IET Intelligent Transport Systems’, Vol. 10, pp. 58–64.

- Randall-Smith, M., Russell, A., Oliphant, R. and Britain), W. R. C. G. (1992), *Guidance Manual for the Structural Condition Assessment of Trunk Mains*, WRC.
- Rodriguez-Iturbe, I., Cox, D. and Isham, V. (1988), ‘A point process model for rainfall: further developments’, *Proceedings of The Royal Society A: Mathematical, Physical and Engineering Sciences* .
- Rodriguez-Iturbe, I., Cox, D. R. and Isham, V. (1987), ‘Some Models for Rainfall Based on Stochastic Point Processes’, **410**(1839), 269–288.
- Rodríguez-Iturbe, I., Cox, D. R. and Isham, V. (1987), ‘Some models for rainfall based on stochastic point processes’, *Proceedings of the Royal Society of London. A. Mathematical and Physical Sciences* .
- Rokstad, M. M. and Ugarelli, R. M. (2015), ‘Evaluating the role of deterioration models for condition assessment of sewers’, *Journal of Hydroinformatics* **17**(5), 789–804.
- Ross, S. (2014), *Introduction to Probability Models*, Elsevier Science.
- Rossmann, L. a. (2015), *Storm Water Management Model User’s Manual Version 5.1*, United States Environment Protection Agency.
- Rossum, J. R. (1969), ‘Prediction of pitting rates in ferrous metals from soil parameters’, *Journal - American Water Works Association* **61**(6), 305–310.
- Sægrov, S. and Schilling, W. (2002), CARE-S: Computer aided rehabilitation of sewer and storm water networks, *in* ‘Global Solutions for Urban Drainage’, Vol. 40644, pp. 1–14.
- Sasidharan, M., Burrow, M. and Ghataora, G. (2020a), ‘A whole life cycle approach under uncertainty for economically justifiable ballasted railway track maintenance’, *Research in Transportation Economics* **80**, 100815.
- Sasidharan, M., Burrow, M. P. and Ghataora, G. S. (2020b), ‘A whole life cycle approach under uncertainty for economically justifiable ballasted railway track maintenance’, *Research in Transportation Economics* **80**, 100815.
- Sasidharan, M., Burrow, M. P. N., Ghataora, G. S. and Marathu, R. (2022), ‘A risk-informed decision support tool for the strategic asset management of railway track infrastructure’, *Proceedings of the Institution of Mechanical Engineers, Part F: Journal of Rail and Rapid Transit* **236**(2), 183–197.
- Savic, D. A., Djordjevic, S. and Dorini, G. (2005), ‘COST-S: a new methodology and tools for sewerage asset management based on whole life costs’, *Water Asset Management International* **1**(4), 20–24.
- Schall, J., Richardson, E. and Morris, L. (2008), HDS 4 - Introduction to Highway Hydraulics, Technical report, U.S. Department of Transport and National Highway Institute.

- Schleiss, M., Olsson, J., Berg, P., Niemi, T., Kokkonen, T., Thorndahl, S., Nielsen, R., Ellerbæk Nielsen, J., Bozhinova, D. and Pulkkinen, S. (2020), ‘The accuracy of weather radar in heavy rain: a comparative study for denmark, the netherlands, finland and sweden’, *Hydrology and Earth System Sciences* **24**(6), 3157–3188.
- Sempewo, J. I. and Kyokaali, L. (2016), ‘Prediction of the Future Condition of a Water Distribution Network Using a Markov Based Approach: A Case Study of Kampala Water’, *Procedia Engineering* **154**, 374–383.
- Shahabul Alam, M. and Elshorbagy, A. (2015), ‘Quantification of the climate change-induced variations in intensity–duration–frequency curves in the canadian prairies’, *Journal of hydrology (Amsterdam)* **527**, 990–1005.
- Shahed Behrouz, M., Sample, D. J. and Nayeb Yazdi, M. (2023), ‘Robustness of storm water management model parameter sets for dry and wet hydroclimatic conditions’, *Journal of Cleaner Production* **411**, 137328.
- Shahed Behrouz, M., Zhu, Z., Matott, L. S. and Rabideau, A. J. (2020), ‘A new tool for automatic calibration of the Storm Water Management Model (SWMM)’, *Journal of Hydrology* **581**, 124436.
- Shamir, U., Howard, C. D. D., Shamir, U. and Howard, C. D. D. (1979), ‘An Analytic Approach to Scheduling Pipe Replacement’, **71**(5), 248–258.
- Shepherd, W., Cashman, A., Djordjevic, S., Dorini, G., Saul, A., Savic, D. and Lewis, L. (2004), ‘Whole life costing of sewer systems’, *Proceedings of WaPUG Autumn Meeting 2004* pp. 1–6.
- Sivakumar, B. and Sharma, A. (2008), ‘A cascade approach to continuous rainfall data generation at point locations’, *Stochastic Environmental Research and Risk Assessment* **22**, 451–459.
- Skinne, M., Kirwan, A. and William, J. (2011), Challenges of developing whole life cycle cost models for network rail’s top 30 assets, in ‘IET and IAM Asset Management Conference 2011’, pp. 1–6.
- Skipworth, P. (2002), *Whole life costing for water distribution network management*, Thomas Telford.
- Snedecor, G. and Cochran, W. (1991), *Statistical Methods*, Wiley.
- Sobanjo, J. O. (2009), ‘State transition probabilities in bridge deterioration based on weibull sojourn times’, *Structure and Infrastructure Engineering* **7**(10), 747–764.
- Speight, V. L., Mounce, S. R. and Boxall, J. B. (2019), ‘Identification of the causes of drinking water discolouration from machine learning analysis of historical datasets’, *Environmental science water research & technology* **5**(4), 747–755.

- Spink, T., Duncan, I., Lawrance, A. and Todd, A. (2014), Transport infrastructure drainage: condition appraisal and remedial treatment, Technical report, CIRIA.
- Surendrakumar, K., Prashant, N. and Mayuresh, P. (2013), ‘Application Of Markovian Probabilistic Process To Develop A Decision Support System For Pavement Maintenance Management’, *International Journal of Scientific and Technology Research* **2**(8), 295–303.
- Tavakoli, R., Sharifara, A. and Najafi, M. (2019), ‘Prediction of Sewer Pipe Deterioration Using Random Forest Classification’.
- Thomas, O. and Sobanjo, J. (2013), ‘Comparison of Markov Chain and Semi-Markov Models for Crack Deterioration on Flexible Pavements’, *Journal of Infrastructure Systems* **19**(2), 186–195.
- Tran, D. H., Ng, A. W. M. and Perera, B. J. C. (2007), ‘Neural networks deterioration models for serviceability condition of buried stormwater pipes’, *Engineering Applications of Artificial Intelligence* **20**(8), 1144–1151.
- Tran, D. H., Ng, A. W. M., Perera, B. J. C., Burn, S. and Davis, P. (2006), ‘Application of probabilistic neural networks in modelling structural deterioration of stormwater pipes’, *Urban Water Journal* **3**(3), 175–184.
- Tran, D. H., Perera, B. J. C. and Ng, A. W. M. (2009a), ‘Comparison of structural deterioration models for stormwater drainage pipes’, *Computer-Aided Civil and Infrastructure Engineering* **24**(2), 145–156.
- Tran, H. D., Marlow, D. and May, R. (2010), ‘Application of decision support models in asset management of sewer networks: Framework and case study’, *Pipelines 2010: Climbing New Peaks to Infrastructure Reliability - Renew, Rehab, and Reinvest - Proc. of the Pipelines 2010 Conference* **386**, 846–856.
- Tran, H. D., Perera, B. J. C. and Ng, A. W. M. (2009b), ‘Predicting Structural Deterioration Condition of Individual Storm-Water Pipes Using Probabilistic Neural Networks and Multiple Logistic Regression Models’, *Journal of Water Resources Planning and Management* **135**(6), 553–557.
- Ugray, Z., Lasdon, L., Plummer, J., Glover, F., Kelly, J. and Marti, R. (2011), ‘Scatter Search and Local Nlp Solvers: A Multistart Framework for Global Optimization’, *SSRN Electronic Journal* .
- Uraba, M. B., Gunawardhana, L. N., Al-Rawas, G. A. and Baawain, M. S. (2019), ‘A downscaling-disaggregation approach for developing idf curves in arid regions’, *Environmental monitoring and assessment* **191**(4), 245–17.
- Vanhaute, W., Vandenberghe, S., Scheerlinck, K., Baets, B. and Verhoest, N. (2012), ‘Calibration of the modified bartlett-lewis model using global optimization techniques and alternative objective functions’.

- Villani, V., Serafino, D. d., Guido, R. and Mercogliano, P. (2015), ‘Stochastic models for the disaggregation of precipitation time series on sub-daily scale: Identification of parameters by global optimization’.
- Walski, T. M. and Pelliccia, A. (1982), ‘Economic analysis of water main breaks’, *Journal - American Water Works Association* **74**(3), 140–147.
- Wang, Y., Xia, A., Zhang, P. and Qin, G. (2022), ‘Probabilistic physical modeling of randomly corroded surface and its use in reliability analysis of corroded pipelines under spatiotemporal vibration’, *Ocean engineering* **262**, 112219.
- Water Research Centre (Great Britain) (2001), *Sewerage Rehabilitation Manual*, WRC Publications.
- Wellalage, N. K. W., Zhang, T. and Dwight, R. (2015), ‘Calibrating Markov Chain–Based Deterioration Models for Predicting Future Conditions of Railway Bridge Elements’, *Journal of Bridge Engineering* **20**(2), 1–13.
- Whole Life Costing for Sustainable Drainage* (2004), Technical report, H R Wallingford.
- Wieczorek, D., Plebankiewicz, E. and Zima, K. (2019), ‘Model estimation of the whole life cost of a building with respect to risk factors’, **25**(1), 20–38.
- Wilson, D., Filion, Y. and Moore, I. (2017), ‘State-of-the-art review of water pipe failure prediction models and applicability to large-diameter mains’, *Urban Water Journal* **14**(2), 173–184.
- Wirahadikusumah, R., Abraham, D. and Iseley, T. (2001), ‘Challenging issues in modeling deterioration of combined sewers’, *Journal of infrastructure systems* **7**(2), 77–84.
- Wu, Y., Tait, S., Nichols, A. and Raja, J. (2021), ‘Simulation of Railway Drainage Asset Service Condition Degradation in the UK Using a Markov Chain–Based Approach’, *Journal of Infrastructure Systems* **27**(3), 04021023.
- Xie, Q., Bharat, C., Nazim Khan, R., Best, A. and Hodkiewicz, M. (2017), ‘Cox proportional hazards modelling of blockage risk in vitrified clay wastewater pipes’, *Urban Water Journal* **14**(7), 669–675.
- Xu, H. and Sinha, S. K. (2020), Applying Survival Analysis to Pipeline Data: Gaps and Challenges, in ‘Pipelines 2020’, American Society of Civil Engineers (ASCE), pp. 148–158.
- Yamijala, S., Guikema, S. D. and Brumbelow, K. (2009), ‘Statistical models for the analysis of water distribution system pipe break data’, **94**, 282–293.
- Zaghloul, N. A. and Kiefa, M. A. A. (2001), ‘Neural network solution of inverse parameters used in the sensitivity-calibration analysis of the swmm model simulations’, *Advances in Engineering Software* .

Zhao, J., Chan, A. H. C., Stirling, A. B., Madelin, K. B. and Zhao, J. (2006), 'Optimizing Policies of Railway Ballast Tamping and Renewal', **1943**(1), 50–56.

Appendix

A Designed return period

Route Classification	Return period of design event(years)
Primary	50
London & South East commuter	
Secondary	25
Rural	10
Freight	

Table A.1: Rainfall event return period

B Asset groups and asset types

Asset Group	Asset Type
Chamber	Chamber - Catchpit
	Chamber - Manhole
	Chamber - Interceptor
	Chamber - Pumping Station
Outfall	Outfall - Public Sewer
	Outfall - Watercourse (Natural)
	Outfall - Watercourse (Artificial)
	Outfall - Soakaway
	Outfall - Sea Or Estuary
Inflow	Inflow - Land Drainage (Farm)
	Inflow - Land Drainage (Garden)
	Inflow - Surface Water Drain
	Inflow - Foul Water Drain
	Inflow - Combined Water Drain
	Inflow - Trade Effluent Drain
	Inflow - Unknown
	Inflow - Watercourse
	Inflow - Groundwater
Point	Point Drainage Node
Ghost	Intermediate Drainage Node
	Boundary Drainage Node
	Unable to Locate Drainage Node
	Point of Interest Drainage Node
Channel	Channel - Natural Ditch
	Channel - Artificial Ditch
	Channel - Flume
	Channel - Aqueduct
	Channel - Cascade
Culvert	Culvert
Granular Drain	Granular Drain - French Drain
	Granular Drain - Counterfort
Pipe	Pipe - Surface Water
	Pipe - Foul Water
	Pipe - Combined
Syphon	Syphon
Covered Channel	Covered Channel - Collector
	Covered Channel - Other
Pond	Pond
Structure	Inlet or Outlet Structure

Table B.1: Asset groups and asset types

C Chi-squared Test Contingency Table

Outfall				Inflow			
sequence	$X_t = i$	$X_t \neq i$	χ^2	sequence	$X_t = i$	$X_t \neq i$	χ^2
(4, 3 1)	5	22	0.98	(4, 3 1)	4	29	0.77
(4, 3 2)	11	48		(4, 3 2)	10	87	
(5, 3 1)	1	26	0.94	(5, 3 1)	0	33	0.56
(5, 3 2)	2	57		(5, 3 2)	1	96	
(5, 4 1)	0	2	0.79	(5, 4 1)	0	1	0.68
(5, 4 2)	2	8		(5, 4 2)	0	4	
(5, 4 3)	3	14		(5, 4 3)	1	6	

Structure				Covered Channel			
sequence	$X_t = i$	$X_t \neq i$	χ^2	sequence	$X_t = i$	$X_t \neq i$	χ^2
(4, 3 1)	30	111	0.01	(4, 3 1)	0	2	0.57
(4, 3 2)	21	172		(4, 3 2)	1	6	
(5, 3 1)	4	137	0.89	(5, 3 1)	0	2	N/A
(5, 3 2)	5	188		(5, 3 2)	0	7	
(5, 4 1)	3	9	0.79	(5, 4 1)	0	0	N/A
(5, 4 2)	5	26		(5, 4 2)	0	0	
(5, 4 3)	7	33		(5, 4 3)	1	2	

Table C.1: Chi-squared test contingency table for Outfall, Inflow, Structure and Covered Channel service condition

Outfall				Inflow			
sequence	$X_t = i$	$X_t \neq i$	χ^2	sequence	$X_t = i$	$X_t \neq i$	χ^2
(4, 3 1)	1	10	0.96	(4, 3 1)	1	12	0.19
(4, 3 2)	4	38		(4, 3 2)	2	108	
(5, 3 1)	0	11	N/A	(5, 3 1)	0	13	N/A
(5, 3 2)	0	42		(5, 3 2)	0	110	
(5, 4 1)	0	0	N/A	(5, 4 1)	0	0	N/A
(5, 4 2)	0	3		(5, 4 2)	0	2	
(5, 4 3)	0	1		(5, 4 3)	0	3	

Structure				Covered Channel			
sequence	$X_t = i$	$X_t \neq i$	χ^2	sequence	$X_t = i$	$X_t \neq i$	χ^2
(4, 3 1)	9	71	0.10	(4, 3 1)	0	2	N/A
(4, 3 2)	16	255		(4, 3 2)	0	30	
(5, 3 1)	0	80	N/A	(5, 3 1)	0	2	N/A
(5, 3 2)	0	271		(5, 3 2)	0	30	
(5, 4 1)	0	7	N/A	(5, 4 1)	0	0	N/A
(5, 4 2)	0	12		(5, 4 2)	0	0	
(5, 4 3)	0	12		(5, 4 3)	0	0	

Table C.2: Chi-squared test contingency table for Outfall, Inflow, Structure and Covered Channel structural condition

D Asset criticality test – total flooding volume and duration

Pipe	Total Flooding Volume ($10^3 m^3$)	Duration of Flooding Occurred (Hour)
C1	21.072	127.42
C2	21.063	126.92
C3	21.061	127.25
C4	23.462	162.25
C5	24.059	170.75
C6	23.599	163.00
C7	33.818	221.50
C8	35.781	173.92
C9	36.313	174.00
C10	37.139	173.92
C11	35.682	172.08
C12	36.535	172.08
C13	40.041	173.50
C14	21.091	127.42
C15	21.078	127.17
C16	21.076	127.25
C17	21.080	127.17
C18	21.080	127.33
C19	21.076	127.25
C20	21.073	127.33
C21	21.074	127.17
C22	21.074	127.33
C23	21.073	127.33
C24	21.072	127.17
C25	21.072	127.25

Table D.1: Total flooding volume and duration of the asset criticality test for each pipe

E Sensor installation photos



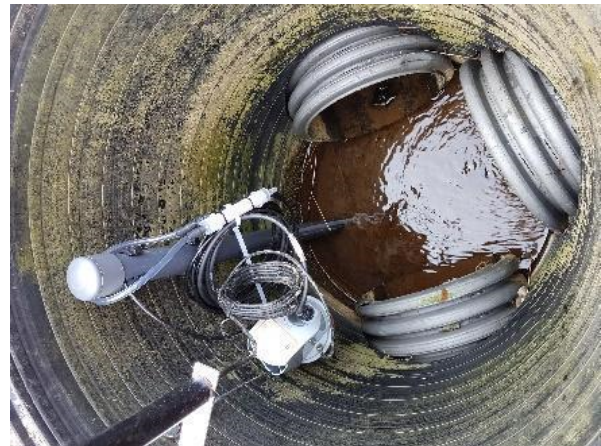
(a) Water depth sensor at catchpit 4



(b) Flow meter between catchpit 4 and 5



(c) Water depth sensor at catchpit 5



(d) Water depth sensor at cathpit 7



(e) Water depth sensor at culvert entry D1



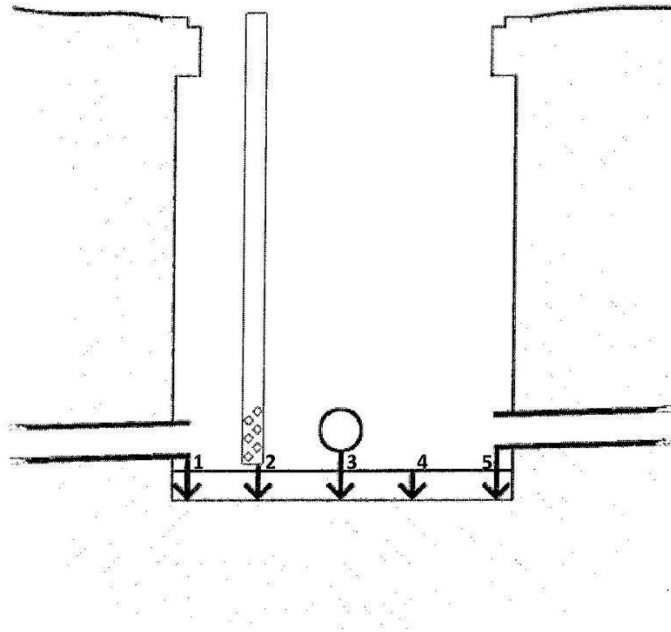
(f) Flow meter at outlet point

Figure E.1: Photos of sensors installed at Knockenjig site

F Installation sheets for the level monitoring locations

University of Sheffield/Network Rail – Knockenjig Level and Flow Monitoring
Installation Survey

Catchpit 4



1. Base of chamber to bottom of outgoing 'X' pipe

220mm

2. Base of chamber to bottom of pressure transducer

~ 35mm

3. Base of chamber to bottom of incoming 'A' pipe (if applicable)

215mm

4. Depth of silt (measured from base of chamber)

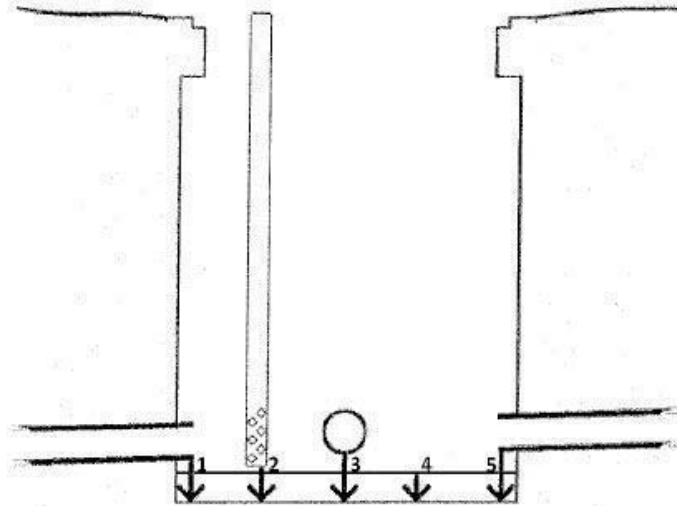
~ 15mm, firm - rock, stone. Uneven

5. Base of chamber to bottom of incoming 'B' pipe (or 'A' pipe depending on configuration)

230mm

Figure F.1: Installation sheets for catchpit 4

Catchpit 5



1. Base of chamber to bottom of outgoing 'X' pipe

210mm

2. Base of chamber to bottom of pressure transducer

~ 35mm

3. Base of chamber to bottom of incoming 'A' pipe (if applicable)

4. Depth of silt (measured from base of chamber)

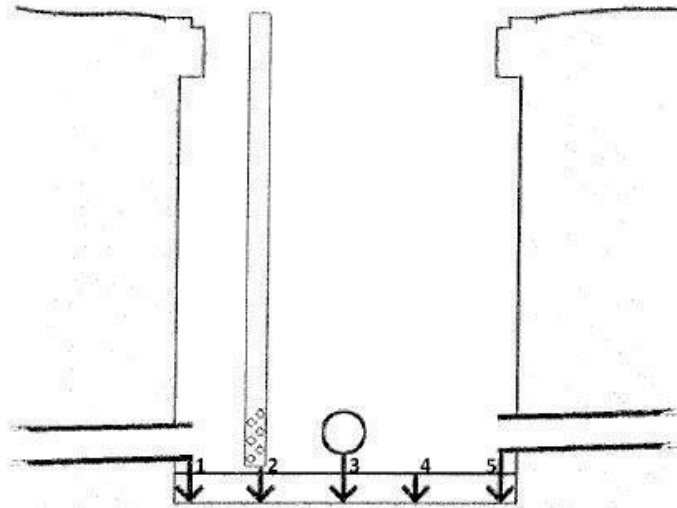
~ 70mm

5. Base of chamber to bottom of incoming 'B' pipe (or 'A' pipe depending on configuration)

240mm

Figure F.2: Installation sheets for catchpit 5

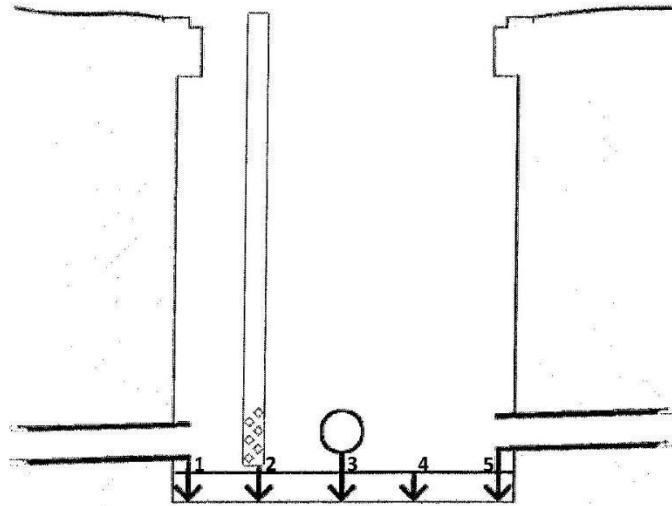
Catchpit 7



1. Base of chamber to bottom of outgoing 'X' pipe
100mm
2. Base of chamber to bottom of pressure transducer
~20mm
3. Base of chamber to bottom of incoming 'A' pipe (if applicable)
110mm
4. Depth of silt (measured from base of chamber)
~ 50-60mm , rocky - Stone , uneven .
5. Base of chamber to bottom of incoming 'B' pipe (or 'A' pipe depending on configuration)
120mm

Figure F.3: Installation sheets for catchpit 7

Catchpit 11



1. Base of chamber to bottom of outgoing 'X' pipe

220mm

2. Base of chamber to bottom of pressure transducer

~20mm (heavy silting around PT).

3. Base of chamber to bottom of incoming 'A' pipe (if applicable)

4. Depth of silt (measured from base of chamber)

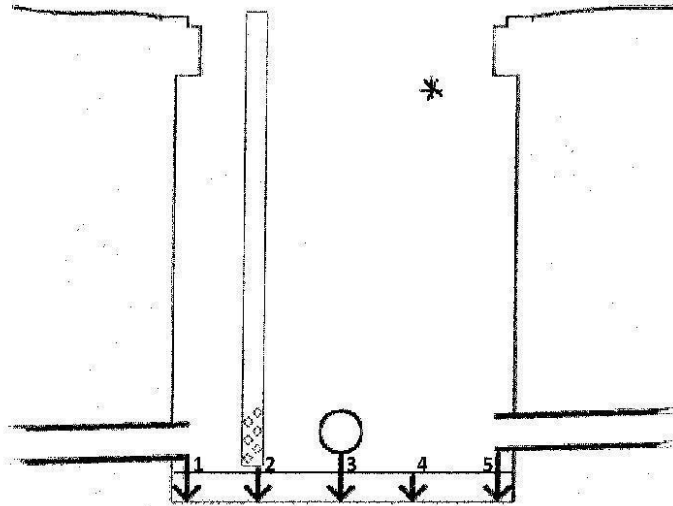
210mm

5. Base of chamber to bottom of incoming 'B' pipe (or 'A' pipe depending on configuration)

235mm

Figure F.4: Installation sheets for catchpit 11

Culvert nr. Catchpit 14



1. Base of chamber to bottom of outgoing 'X' pipe

~ 50mm

2. Base of chamber to bottom of pressure transducer

~ 15mm

3. Base of chamber to bottom of incoming 'A' pipe (if applicable)

4. Depth of silt (measured from base of chamber)

5. Base of chamber to bottom of incoming 'B' pipe (or 'A' pipe depending on configuration)

150mm

* diagram not representative of Culvert/Channel.

Figure F.5: Installation sheets for culvert at outfall

G Table of Manning's n

Manning's n - Closed Conduits		Manning's n - Open Channels	
Conduit Material	Manning n	Channel Type	Manning n
Asbestos-cement pipe	0.011 - 0.015	Lined Channels	
Brick	0.013 - 0.017	- Asphalt	0.013 - 0.017
Cast iron pipe		- Brick	0.012 - 0.018
- Cement-lined & seal coated	0.011 - 0.015	- Concrete	0.011 - 0.020
Concrete (monolithic)		- Rubble or riprap	0.020 - 0.035
- Smooth forms	0.012 - 0.014	- Vegetal	0.030 - 0.40
- Rough forms	0.015 - 0.017	Excavated or dredged	
Concrete pipe	0.011 - 0.015	- Earth, straight and uniform	0.020 - 0.030
Corrugated-metal pipe (1/2-in. x 2-2/3-in. corrugations)		- Earth, winding, fairly uniform	0.025 - 0.040
- Plain	0.022 - 0.026	- Rock	0.030 - 0.045
- Paved invert	0.018 - 0.022	- Unmaintained	0.050 - 0.140
- Spun asphalt lined	0.011 - 0.015	Natural channels (minor streams, top width at flood stage < 100 ft)	
Plastic pipe (smooth)	0.011 - 0.015	- Fairly regular section	0.030 - 0.070
Vitrified clay		- Irregular section with pools	0.040 - 0.100
- Pipes	0.011 - 0.015		
- Liner plates	0.013 - 0.017		

Figure G.1: Table of Manning's n in SWMM user's manual (Rossman, 2015)

Manning's n for Channels (Chow, 1959).

Type of Channel and Description	Minimum	Normal	Maximum
Natural streams - minor streams (top width at floodstage < 100 ft)			
1. Main Channels			
a. clean, straight, full stage, no rifts or deep pools	0.025	0.030	0.033
b. same as above, but more stones and weeds	0.030	0.035	0.040
c. clean, winding, some pools and shoals	0.033	0.040	0.045
d. same as above, but some weeds and stones	0.035	0.045	0.050
e. same as above, lower stages, more ineffective slopes and sections	0.040	0.048	0.055
f. same as "d" with more stones	0.045	0.050	0.060
g. sluggish reaches, weedy, deep pools	0.050	0.070	0.080
h. very weedy reaches, deep pools, or floodways with heavy stand of timber and underbrush	0.075	0.100	0.150
2. Mountain streams, no vegetation in channel, banks usually steep, trees and brush along banks submerged at high stages			
a. bottom: gravels, cobbles, and few boulders	0.030	0.040	0.050
b. bottom: cobbles with large boulders	0.040	0.050	0.070
3. Floodplains			
a. Pasture, no brush			
1. short grass	0.025	0.030	0.035
2. high grass	0.030	0.035	0.050
b. Cultivated areas			
1. no crop	0.020	0.030	0.040
2. mature row crops	0.025	0.035	0.045
3. mature field crops	0.030	0.040	0.050
c. Brush			
1. scattered brush, heavy weeds	0.035	0.050	0.070
2. light brush and trees, in winter	0.035	0.050	0.060
3. light brush and trees, in summer	0.040	0.060	0.080
4. medium to dense brush, in winter	0.045	0.070	0.110
5. medium to dense brush, in summer	0.070	0.100	0.160
d. Trees			
1. dense willows, summer, straight	0.110	0.150	0.200
2. cleared land with tree stumps, no sprouts	0.030	0.040	0.050
3. same as above, but with heavy growth of sprouts	0.050	0.060	0.080
4. heavy stand of timber, a few down trees, little undergrowth, flood stage below branches	0.080	0.100	0.120
5. same as 4. with flood stage reaching branches	0.100	0.120	0.160

4. Excavated or Dredged Channels			
a. Earth, straight, and uniform			
1. clean, recently completed	0.016	0.018	0.020
2. clean, after weathering	0.018	0.022	0.025
3. gravel, uniform section, clean	0.022	0.025	0.030
4. with short grass, few weeds	0.022	0.027	0.033
b. Earth winding and sluggish			
1. no vegetation	0.023	0.025	0.030
2. grass, some weeds	0.025	0.030	0.033
3. dense weeds or aquatic plants in deep channels	0.030	0.035	0.040
4. earth bottom and rubble sides	0.028	0.030	0.035
5. stony bottom and weedy banks	0.025	0.035	0.040
6. cobble bottom and clean sides	0.030	0.040	0.050
c. Dragline-excavated or dredged			
1. no vegetation	0.025	0.028	0.033
2. light brush on banks	0.035	0.050	0.060
d. Rock cuts			
1. smooth and uniform	0.025	0.035	0.040
2. jagged and irregular	0.035	0.040	0.050
e. Channels not maintained, weeds and brush uncut			
1. dense weeds, high as flow depth	0.050	0.080	0.120
2. clean bottom, brush on sides	0.040	0.050	0.080
3. same as above, highest stage of flow	0.045	0.070	0.110
4. dense brush, high stage	0.080	0.100	0.140
5. Lined or Constructed Channels			
a. Cement			
1. neat surface	0.010	0.011	0.013
2. mortar	0.011	0.013	0.015
b. Wood			
1. planed, untreated	0.010	0.012	0.014
2. planed, creosoted	0.011	0.012	0.015
3. unplaned	0.011	0.013	0.015
4. plank with battens	0.012	0.015	0.018
5. lined with roofing paper	0.010	0.014	0.017
c. Concrete			
1. trowel finish	0.011	0.013	0.015
2. float finish	0.013	0.015	0.016
3. finished, with gravel on bottom	0.015	0.017	0.020
4. unfinished	0.014	0.017	0.020
5. gunite, good section	0.016	0.019	0.023

6. gunite, wavy section	0.018	0.022	0.025
7. on good excavated rock	0.017	0.020	
8. on irregular excavated rock	0.022	0.027	
d. Concrete bottom float finish with sides of:			
1. dressed stone in mortar	0.015	0.017	0.020
2. random stone in mortar	0.017	0.020	0.024
3. cement rubble masonry, plastered	0.016	0.020	0.024
4. cement rubble masonry	0.020	0.025	0.030
5. dry rubble or riprap	0.020	0.030	0.035
e. Gravel bottom with sides of:			
1. formed concrete	0.017	0.020	0.025
2. random stone mortar	0.020	0.023	0.026
3. dry rubble or riprap	0.023	0.033	0.036
f. Brick			
1. glazed	0.011	0.013	0.015
2. in cement mortar	0.012	0.015	0.018
g. Masonry			
1. cemented rubble	0.017	0.025	0.030
2. dry rubble	0.023	0.032	0.035
h. Dressed ashlar/stone paving	0.013	0.015	0.017
i. Asphalt			
1. smooth	0.013	0.013	
2. rough	0.016	0.016	
j. Vegetal lining	0.030		0.500

Figure G.2: Manning' n for channels (Chow, 1959)

Manning's n for Closed Conduits Flowing Partly Full (Chow, 1959).

Type of Conduit and Description	Minimum	Normal	Maximum
1. Brass, smooth:	0.009	0.010	0.013
2. Steel:			
Lockbar and welded	0.010	0.012	0.014
Riveted and spiral	0.013	0.016	0.017
3. Cast Iron:			
Coated	0.010	0.013	0.014
Uncoated	0.011	0.014	0.016
4. Wrought Iron:			
Black	0.012	0.014	0.015
Galvanized	0.013	0.016	0.017
5. Corrugated Metal:			
Subdrain	0.017	0.019	0.021
Stormdrain	0.021	0.024	0.030
6. Cement:			
Neat Surface	0.010	0.011	0.013
Mortar	0.011	0.013	0.015
7. Concrete:			
Culvert, straight and free of debris	0.010	0.011	0.013
Culvert with bends, connections, and some debris	0.011	0.013	0.014
Finished	0.011	0.012	0.014
Sewer with manholes, inlet, etc., straight	0.013	0.015	0.017
Unfinished, steel form	0.012	0.013	0.014
Unfinished, smooth wood form	0.012	0.014	0.016
Unfinished, rough wood form	0.015	0.017	0.020
8. Wood:			
Stave	0.010	0.012	0.014
Laminated, treated	0.015	0.017	0.020
9. Clay:			
Common drainage tile	0.011	0.013	0.017
Vitrified sewer	0.011	0.014	0.017
Vitrified sewer with manholes, inlet, etc.	0.013	0.015	0.017
Vitrified Subdrain with open joint	0.014	0.016	0.018
10. Brickwork:			
Glazed	0.011	0.013	0.015
Lined with cement mortar	0.012	0.015	0.017
Sanitary sewers coated with sewage slime with bends and connections	0.012	0.013	0.016
Paved invert, sewer, smooth bottom	0.016	0.019	0.020
Rubble masonry, cemented	0.018	0.025	0.030

Figure G.3: Manning' n for close conduits flowing partly full (Chow, 1959)

Description		Manning's n Range
Concrete pipe		0.011-0.013
Corrugated metal pipe or pipe-arch:		
Corrugated Metal Pipes and Boxes, Annular or Helical Pipe (Manning's n varies with barrel size)	68 by 13 mm (2-2/3 x 1/2 in.) corrugations	0.022-0.027
	150 by 25 mm (6 x 1 in.) corrugations	0.022-0.025
	125 by 25 mm (5 x 1 in.) corrugations	0.025-0.026
	75 by 25 mm (3 x 1 in) corrugations	0.027-0.028
	150 by 50 mm (6 x 2 in.) structural plate corrugations	0.033-0.035
	230 by 64 mm (9 x 2-1/2 in.) structural plate corrugations	0.033-0.037
Corrugated Metal Pipes Helical Corrugations, Full Circular Flow	68 by 13 mm (2-2/3 x 1/2 in.) corrugations	0.012-0.024
Spiral Rib Metal Pipe	Smooth walls	0.012-0.013
Vitrified clay pipe		0.012-0.014
Cast-iron pipe, uncoated		0.013
Steel pipe		0.009-0.013
Brick		0.014-0.017
Monolithic concrete:		
1.	Wood forms, rough	0.015-0.017
2.	Wood forms, smooth	0.012-0.014
3.	Steel forms	0.012-0.013
Cemented rubble masonry walls:		
1.	Concrete floor and top	0.017-0.022
2.	Natural floor	0.019-0.025
Laminated treated wood		0.015-0.017
Vitrified clay liner plates		0.015
<p>NOTE: The values indicated in this table are recommended Manning's n design values. Actual field values for older existing pipelines may vary depending on the effects of abrasion, corrosion, deflection, and joint conditions. Concrete pipe with poor joints and deteriorated walls may have n values of 0.014 to 0.018. Corrugated metal pipe with joint and wall problems may also have higher n values, and in addition, may experience shape changes which could adversely effect the general hydraulic characteristics of the pipeline.</p>		

Figure G.4: Manning's n values for closed conduits table (Schall et al., 2008)

